The central role of the transcriptional regulator IκBζ in psoriasis

Dissertation

der Mathematisch-Naturwissenschaftlichen Fakultät

der Eberhard Karls Universität Tübingen

zur Erlangung des Grades eines

Doktors der Naturwissenschaften

(Dr. rer. nat.)

vorgelegt von

Anne Müller

aus Finsterwalde

Tübingen

2020

Gedruckt mit Genehmigung der Mathematisch-Naturwissenschaftlichen Fakultät der Eberhard Karls Universität Tübingen.

Tag der mündlichen Qualifikation:	10.11.2020
Stellvertretender Dekan:	Prof. Dr. József Fortágh
1. Berichterstatter:	Prof. Dr. Klaus Schulze-Osthoff
2. Berichterstatter:	Prof. Dr. Alexander N.R. Weber

Table of Content

Abbreviations

AMP	Antimicrobial peptide
ATP	Adenosine triphosphate
BAFFR	B-cell activating factor receptor
BCL-2	B-cell lymphoma 2
CAK	CDK-activating kinase
cAMP	Cyclic adenosine monophosphate
CARD	Caspase recruitment domain
CBX	Chromobox
CCL	CC-chemokine ligand
CCL20	CC-chemokine ligand 20
CD40	Cluster of differentiation 40
CDK	Cyclin-dependent kinase
CpG	Cytosine-phosphatidyl-guanine
CXCL	C-X-C motif chemokine
DNA	Deoxyribonucleic acid
EED	embryonic ectoderm development
ERα	Estrogen receptor alpha
EZH2	Enhancer of zeste homolog 2
GWAS	Genome-wide association study
H3	Histone 3
HAT	Histone acetyltransferase
HDAC	Histone deacetylase
ICAM	Intercellular adhesion molecule
IKK	IκB kinase
IL	Interleukin
IMQ	Imiquimod
INK	inhibitor of CDK
IRAK	Interleukin-1 receptor-associated kinase
IκB	Inhibitor of NF-κB
JAK	Janus kinase
KO	Knockout
LCN2	Lipocalin-2
LPS	Lipopolysaccharide
LTβR	Lymphotoxin β receptor
MALT	Mucosa-associated lymphoid tissue
MAPK	Mitogen-activated protein kinase
mDC	Myeloid dendritic cells
MHC	Major histocompatibility complex
mRNA	Messenger ribonucleic acid
MyD88	Myeloid differentiation primary response 88
NEMO	NF-kappa-B essential modulator
NF-κB	Nuclear factor of kappa light chain gene enhancer in B cells
NIK	NF-κB inducing kinase

NLS	Nuclear localisation sequence
PCGF	Polycomb group RING finger protein
pDC	Plasmacytoid dendritic cells
PHC	Polyhomeotic-like protein
PRC	Polycomb repressive complex
RANK	Receptor activator of NF-κB
Rb	Retinoblastoma
RbAp	Retinoblastoma protein associated protein
RHD	Rel homology domain
RNF2	Ring finger protein 2
ROR	RAR-related orphan receptor
SNP	Single nucleotide polymorphism
STAT	Signal transducers and activator of transcription
SWI/SNF	Switch/sucrose nonfermenting
TAD	Transactivating domain
TCF	T-cell factor
Th17	T-helper cells 17
TLR	Toll-like receptor
TNF	Tumor necrosis factor
TRAF	TNF receptor associated factor
VCAM	Vascular cell adhesion molecule
VEGF	Vascular endothelial growth factor

Zusammenfassung

IκBζ gehört zur Gruppe der atypischen NF-κB Inhibitoren (IκBs). Im Gegensatz zu klassischen IκBs wird IκBζ fast ausschließlich induzierbar im Zellkern exprimiert, wo es die Expression von bestimmten Targetgenen nicht nur inhibieren, sondern auch aktivieren kann. Das Gen *NFKBIZ,* welches für IκBζ kodiert, wurde als Risikogen in der Psoriasis identifiziert.

Ebenso sind IκBζ-Knockout-Mäuse in bestimmten Modellen gegenüber einer experimentellen Psoriasis geschützt. Ziel dieser Dissertation war es, die Rolle von IκBζ in der Psoriasis näher zu beleuchten, um daran anknüpfend neue Therapieoptionen zu entwickeln. Es konnte gezeigt werden, dass IκBζ neben dem IL-17 Signalweg auch den IL-36 Signalweg reguliert, welcher bei bestimmten Formen der Psoriasis eine wichtige Rolle spielt. Die IL-36-vermittelte Induktion von IκBζ wird von NF-κB und STAT3 gesteuert und führt zur Expression von bestimmten pro-inflammatorischen Genen, welche die Pathogenese der Psoriasis initiieren. *Vice versa* sind IκBζ-Knockout-Mäuse gänzlich vor einer IL-36-vermittelten experimentellen Psoriasis geschützt. Demnach stellt IκBζ einen zentralen Regulator in der Psoriasis dar, welcher unabhängig von der Art des Stimulus die Inflammation fördert. Darauf aufbauend folgten Screenings für pharmakologische Inhibitoren, welche die Induktion von IκBζ unterdrücken. Dabei konnte ein neuer proinflammatorischer Signalweg identifiziert werden, bei dem EZH2, eine Methyltransferase, durch CDK4/6 phosphoryliert wird und ihrerseits STAT3 methyliert, welches die IκBζ-Expression induziert. Die pharmakologische Hemmung von CDK4/6 oder EZH2 hemmte die Pathogenese von Psoriasis *in vitro* und *in vivo*.

Zusammenfassend konnte diese Arbeit IκBζ nicht nur als verantwortlichen Mediator in der Psoriasis näher charakterisieren, sondern mit dem CDK4/6-EZH2-vermittelten Signalweg auch einen neuen Mechanismus identifizieren, dessen Inhibition eine mögliche Therapieoption in der Psoriasis darstellt.

Abstract

IκBζ belongs to the group of atypical NF-κB inhibitors (IκBs). In contrast to classical IκBs, IκBζ is only inducibly expressed in the cell nucleus, where it can inhibit, but more importantly, also activate the expression of a particular subset of target genes. *NFKBIZ*, the gene encoding IκBζ, has been identified as new risk gene in psoriasis. Moreover, IκBζ knockout mice are protected in certain models of experimental psoriasis. The aim of this thesis was to examine the global role of IκBζ in psoriasis in order to find a new therapy approach. It could be shown that IκBζ is a regulator not only of IL-17 but also of IL-36 signaling, which plays a major role in certain forms of psoriasis. The IL-36-mediated induction of IκBζ was driven by NF-κB and STAT3, and led to the expression of pro-inflammatory genes that initiate the development of psoriasis. Accordingly, IκBζ knockout mice were completely protected from IL-36-mediated experimental psoriasis. Thus, IκBζ represents a central regulator in psoriasis, which promotes inflammation regardless of the type of stimulus. Based on this finding, screenings for small-molecule inhibitors were performed that are able to repress the induction of IκBζ. Thereby, I could identify a new pro-inflammatory signal pathway in keratinocytes. In this pathway, CDK4/6 phosphorylated the methyltransferase EZH2, which in turn methylated and activated STAT3, which transcriptionally induced IκBζ. The pharmacological inhibition of CDK4/6 or EZH2 inhibited the pathogenesis of psoriasis *in vitro* and *in vivo*.

In conclusion, this thesis not only validates IκBζ as an essential mediator of psoriasis, but also identifies the CDK4/6-EZH2 axis as a novel mechanism whose inhibition could provide a potential therapeutic option for the treatment of psoriasis.

1 Introduction

1.1 The pathogenesis of psoriasis

Psoriasis is a mixed autoinflammatory and autoimmune disease of the skin which partially develops due to genetic predispositions, but also due to a variety of environmental factors. It is characterized by scaly, erythematous patches, papules, and plaques that are often pruritic [1]. Around 2-3% of the worldwide population suffer from psoriasis, which affects statistically more women [2]. The most severe forms of psoriasis are psoriasis vulgaris (also named plaque psoriasis), inverse psoriasis, guttate psoriasis, erythrodermic psoriasis, and pustular psoriasis. Psoriasis is often associated with further co-morbidities such as metabolic syndrome, cardiovascular disease, psoriatic arthritis or inflammatory bowel disease like Crohn's disease [3]. Moreover, psoriasis also represents a possible risk factor for the onset of coronary artery disease [4], stroke [5], myocardial infarct [6] hypertension and obesity [7].

The strongest genetic risk factor for psoriasis constitutes a single-nucleotide polymorphism (SNP) in the class I major histocompatibility complex (MHC I) human leukocyte antigen HLA-Cw*06 [8]. Other genetic risk factors have been identified which are involved in controlling epidermal barrier integrity (*LCE3B*, *LCE3D*), antigen presentation (*ERAP1*) and genes of the innate (*NFKBIA*) and adaptive immune systems (*IL12B, IL23R*) [9]. Furthermore, mutations in interleukin 36RA (IL-36RA), an endogenously expressed antagonist of IL-36 signaling, is associated with pustular psoriasis [10]. So far, few genetic variants have been analyzed, although more than 60 SNPs are known to be associated with psoriasis [11].

Generally, keratinocyte hyperproliferation and infiltration of immune cells, such as neutrophils, T helper 17 cells (Th17) and macrophages, are key features of psoriatic skin lesions [12]. Subsequently, psoriasis is a disorder of the innate and the adaptive immune systems. In genetically susceptible patients, the triggers for psoriatic lesions mostly arise from an injury, trauma, infection (e.g. *Streptococcus*) or drug (e.g. β-blocker), followed by the release of antimicrobial peptides (AMP) such as LL-37, β-defensins, and S100 proteins from keratinocytes, which complex with free DNA or RNA (Figure 1). In general, AMPs are absent in healthy keratinocytes and were upregulated during epithelial damage [13]. Furthermore, these AMP-DNA/RNA-complexes get recognized by Toll-like receptor 7 and 9 (TLR7 and 9) in antigen presenting cells,

especially plasmacytoid dendritic cells (pDC) but also myeloid dendritic cells (mDC) and a defined subpopulation of monocytes [14]. This initial event starting the development of the psoriatic plaque.

Furthermore, the activation of pDCs leads to the MHC-dependent activation of CD8+ T cells and their clonal expansion. This process takes place in the dermis or in lymph nodes [13]. Subsequently, this activated CD8+ T cells migrate into the epidermis and trigger keratinocytes, in MHC-dependent manner, to secret proinflammatory mediators and initiate keratinocyte hyperproliferation. Additionally, activated pDCs produce type 1 interferons (IFNα and IFNβ), which in turn activate mDC. Furthermore, mDCs drain into the lymph nodes to activate the adaptive immune system, especially T cell differentiation. This include the maturation to T helper 1 (Th1), Th17 and Th22 cells, followed by their infiltration and activation into psoriatic skin lesions [13]. Subsequently, the activation of T cell differentiation drives the maintenance phase of psoriatic inflammation [14].

Additionally, the mDC-mediated secretion of tumor necrosis factor α (TNFα), IL-1, IL-23, and IL-12 leading to the activation of the innate immune system, including the recruitment of neutrophils and macrophages into the affect skin area. In turn, Th17 cells release cytokines such as TNFα, IL-17, IL-22 and IL-23 to drive keratinocyte proliferation, impair their differentiation, and promote an inflammatory response by activating nuclear factor of kappa B (NF-κB), signal transducer and activator of transcription 1 and 3 (STAT1 and 3), CCAAT-enhancer-binding proteins β and δ (C/EBPβ and δ). This leads to the expression of pro-inflammatory molecules, including AMP (e.g. S100A7-9 and DEFB4), chemokines (e.g. CCL20, CXCL8 and CXCL2), cytokines (TNF, IL-1, IL-6, and IL-36), vascular endothelial growth factor (VEGF) and adhesion molecules (e.g. intercellular adhesion molecule 1 (ICAM-1) and vascular cell adhesion molecule 1 (VCAM-1)), which promote immune cell extravasation and migration at the site of inflammation [13]. Particularly noteworthy here is the IL-1 family cytokines. This family also includes IL-36γ, which is induced by keratinocytes in paracrine and autocrine loops, leading to the secretion of CXC-motif-chemokine ligand 8 (CXCL8) and CXCL1 via the IL-36 receptor (IL36R) and consequently to the recruitment of neutrophils into lesional skin [15]. In addition, overexpression of IL-36γ enhances the response of Th17-driven cytokines in keratinocytes [16, 17]. Finally, a circle of inflammation is established.

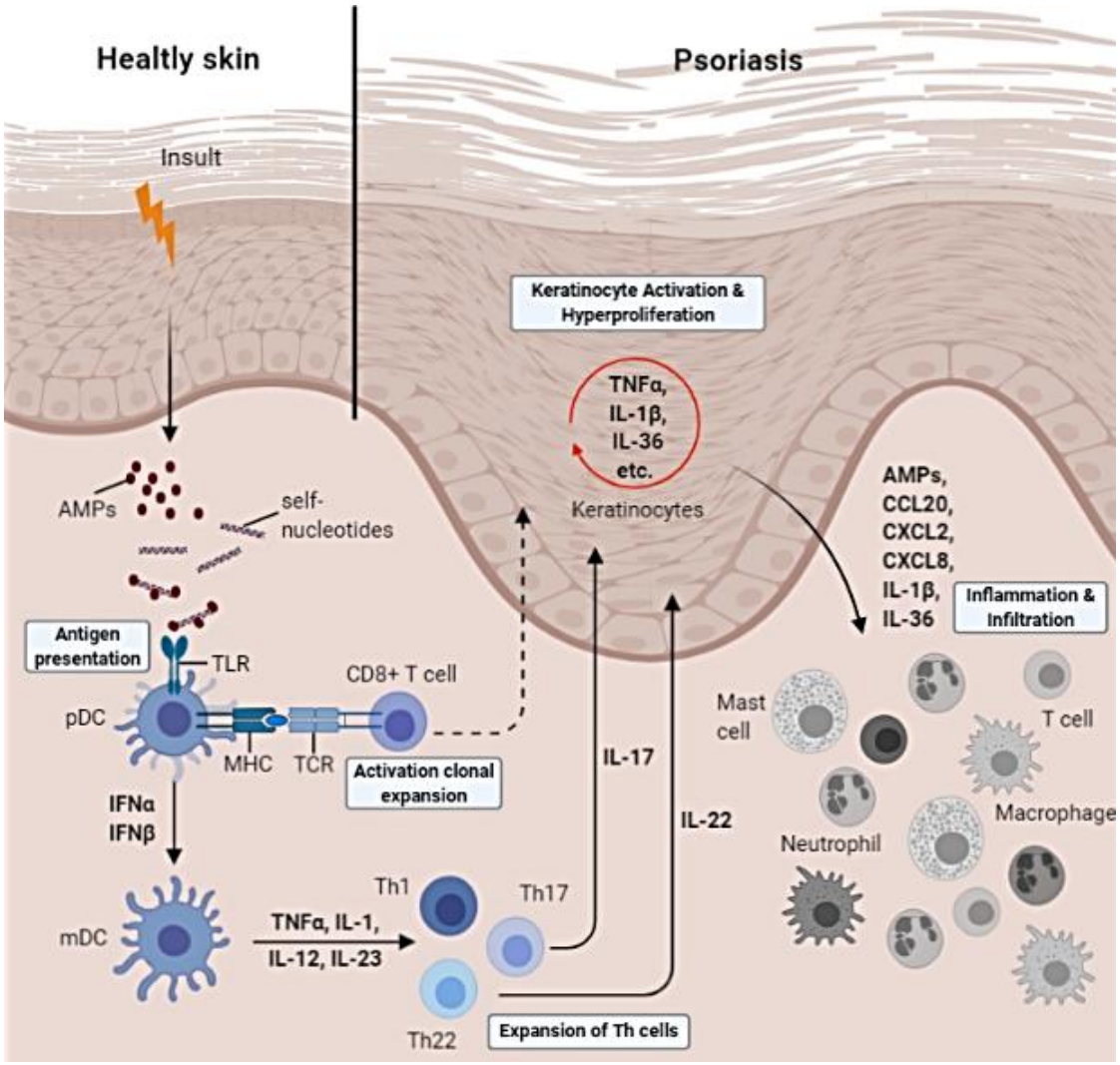

Figure 1: Pathogenic Mechanisms of Psoriasis (Created with BioRender.com). External insults can cause the release of self-nucleotides and keratinocytes-derived antimicrobial peptides (AMPs). These components form complexes, which can bind to receptors (TLRs) on plasmacytoid dendritic cells (pDCs). This binding trigger MHC-dependent antigen presentation to antigen-specific CD8+ T cells, which were activated and initiate their clonal expansion. This activated CD8+ T cells migrate into the epidermis. There they trigger keratinocytes to release soluble factors. This initiate the local inflammation and the keratinocyte proliferation. In parallel, activated pDCs release interferons, which stimulate myeloid DCs (mDCs) to secrete IL-12, IL-23 and tumor necrosis factor (TNF). These proinflammatory factors stimulate different T cell populations, such as T helper 1 (Th1), Th17 and Th22 cells to secret further cytokines. The combination of IL-17, IL-22, IL-23 and TNF drives the proinflammatory cascade in different cell types. Finally, keratinocytes release a variety of chemokines, cytokines and AMPs to enhance the migration of immune cells and the inflammation in the psoriatic skin. The figure was adapted from [13].

Current standard therapies against psoriatic lesions constitute glucocorticoids, which suppress keratinocyte inflammation, proliferation, and promote differentiation; methotrexate, cyclosporin A, fumarate, phototherapy or neutralizing antibodies acting along the IL-23/IL-17/IL-22 axis, such as ustekinumab, infliximab, secukinumab,

ixekizumab and brodalumab [18]. In addition, antibodies against the IL-36R are currently being tested in clinical trials [19]. Numerous topical and systemic therapies are available for the treatment of psoriasis. The choice of the appropriate therapy is based on various parameters, such as disease severity, relevant comorbidities, costs, efficacy, and evaluation of individual patient responses [18]. However, none of the treatments effectively addresses the mechanism of the pathogenesis of psoriasis; only symptoms are treated or pro-inflammatory cytokines are blocked. Accordingly, novel therapies are necessary that act more specifically, thus limiting unwanted site-effects.

At the moment, there is no mouse model available that fully recapitulates human psoriasis. This might be partially due to the fact that mouse and human skin differ in their immune cell composition or because psoriasis is a disease arising from multiple triggers, that cannot be completely modelled in mice. Therefore, treatment of mouse skin with the TLR7/8 agonist imiquimod (IMQ) represents the standard mouse model for preclinical investigations of psoriasis at the moment, as most signs of a psoriasis pathogenesis are induced, including keratinocyte hyperproliferation and immune cell infiltration especially from Th17 cells. However, Th17 cells represent a minority in IL-17A secretion in mice, whereas γδ-T cells, that are absent in human skin, are the major IL-17A-producing population [20]. The importance of the IL-23/IL-17 axis in skin inflammation was demonstrated using knockout mice for IL-23p19 or the IL-17A receptor (IL-17RA), as these mice are protected from IMQ-mediated psoriasis [21]. However, recent studies showed that IL-36R-deficient mice are also completely protected in IMQ-mediated psoriasis [22]. This suggests that the IL-36 signaling pathway also appears to be a regulator of the IL-23/IL-17/IL-22 axis and disease development [22]. This finding is also reflected in a subtype of psoriasis called pustular psoriasis, in which a mutation in the IL-36 antagonist IL-36Ra has been frequently detected [23]. In contrast to T cell-mediated plaque psoriasis, the innate immune system plays a greater role in this subtype [24], including elevated levels of IL-1β, IL-36α, and IL-36γ [25]. Nevertheless, patients with pustular psoriasis without IL-36R mutation show a response to anti-IL-17 treatments [26]. In conclusion, IL-17/IL-23 and IL-36 are major cytokines in psoriasis, while these cytokines can also cross-regulate each other [17].

The key transcription factors that have been identified in psoriasis include the STAT family and NF-κB and additionally, cyclic adenosine monophosphate (cAMP). In

agreement, elevated expression levels of activated STAT3 are detected in the epidermis of psoriatic lesions [27], while an epidermal overexpression of a constitutively active STAT3 mutant (STAT3C) leads to the development of psoriasis-like skin lesions in mice [28]. Furthermore, genome-wide association studies (GWAS) identified genes of the JAK-STAT signaling pathway as psoriasis susceptibility loci: SNPs at rs744166 in *STAT3* and rs10758669 in *JAK2*, rs367569 in suppressor of cytokine signaling 1 (*SOCS1*), rs34536443 in *TYK2*, which are involved in STAT-mediated signaling [9, 29].

Beside STAT3, lesional psoriatic skin was shown to contain elevated levels of active NF-κB compared to non-psoriatic skin [30, 31]. Additionally, GWAS demonstrated that several components or pathways, which are regulated by NF-κB, are up-regulated in psoriasis: innate immune responses involving TLR2 [32] and caspase-5 [33], apoptosis inhibitors such as Bcl-xL and cyclins [34], which lead to an increase of keratinocyte survival and epidermal hyperproliferation [35-37]; keratinocyte-derived chemokines, CCL20 and CCL27, which recruit DC and Th17 cells [38, 39], adhesion molecules (E-selectin, ICAM-1, and VCAM-1) to support leukocyte adhesion and migration [40]; and pro-inflammatory genes such as cytokines and chemokines in several cell types [41, 42]. Moreover, CARD14, a member of the caspase recruiting domain family, represents the psoriasis susceptibility gene PSORS-2 [43], which is sometimes found to be mutated in psoriasis. These mutations in CARD14 result in its hyperactivation leading to the onset of a Th17-mediated psoriasis-like skin disease in mice [44]. In detail, CARD14 forms a complex with Bcl10 and MALT1 to recruit downstream signaling components, leading to the activation of MAPK and NF-κB signaling [43]. Furthermore, CARD14, predominantly restricted to keratinocytes [44], is involved in the activation of pro-inflammatory cytokines and chemokines, including IL-36γ, IL-8, and CCL20 [45]. Further SNPs in the NF-κB signaling pathway were found for *NFKB1* (rs230526), *NFKBIA* (rs7152376), and *NFKBIZ* (rs3217713), which are associated with the development of psoriatic lesions [46].

1.2 The NF-κB pathway

The pleiotropic transcription factor NF-κB is involved in a variety of biological processes such as inflammation, immunity, cell proliferation, cell differentiation and apoptosis [47]. Consequently, beside its involvement in psoriasis, deregulated NF-κB activity is also frequently found in various other inflammatory diseases, such as rheumatoid arthritis, inflammatory bowel disease, multiple sclerosis, systemic lupus erythematosus, type I diabetes and asthma [48].

NF-κB is a DNA-binding complex consisting of homo- and heterodimers of the Rel family, including: RelA (also named p65), RelB, p50 (also named NF-κB1), p52 (also named NF-κB2) and c-Rel, that bind with their Rel homology domain (RHD) to the κB binding motif 5´GGGPuNNPyPyCC-3´ [49] at the promoter region of their target genes upon stimulation [50]. The stimulus-dependent activation and regulation of NF-κB is closely linked to the nuclear factor of kappa light polypeptide gene enhancer in B-cells inhibitor (IκB) cofactor family (Figure 2), which is characterized by ankyrin repeats [51]. IκB proteins can be divided into two subgroups: classical IκBs (e.g. IκBα, IκBβ, IκBε, p100 and p105), which are constitutively expressed in the cytoplasm, and so-called atypical IκBs (e.g. BCL3, IκBζ, $IκB_{NS}$), which are mostly inducibly expressed and mainly localize to the nucleus.

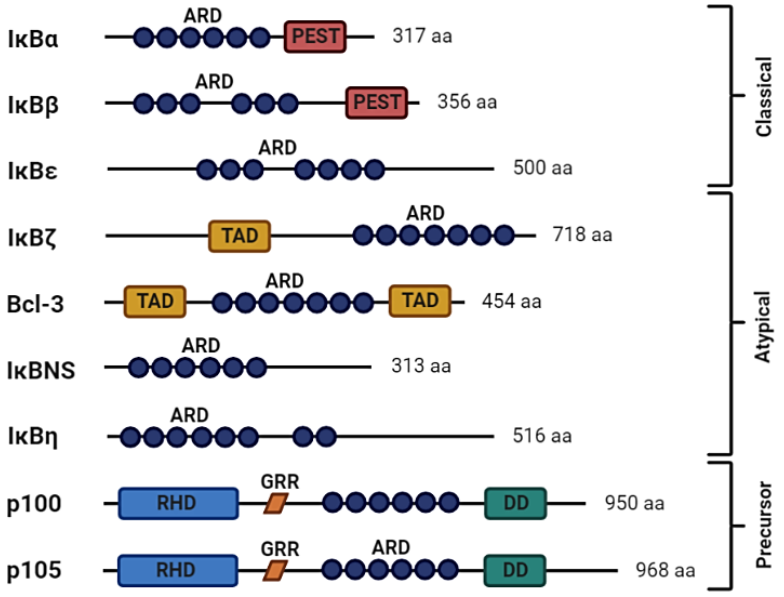

Figure 2: IκB family members (Created with BioRender.com). The IκB family can be subdivided in classical or cytoplasmic IκBs (IκBα, IκBβ and IκBε), the atypical or nuclear IκB (IκBζ, Bcl-3, $IκB_{NS}$ and IκBη) and the precursors which can act as inhibitors in the cytoplasm (p100 and p105). ARD - ankyrin repeat domain; DD - death domain; GRR - glycine-rich region; PEST – proline (P), glutamic acid (E),

serine (S) and threonine (T)-rich region; RHD - REL homology domain; TAD - transactivation domain. The figure was adapted from [52, 53].

In general, classical IκBs repress NF-κB activation by preventing its nuclear localization and DNA binding, whereas the atypical IκBs can act as activating or repressing co-factors of NF-κB-mediated target gene expression [47].

The activation of NF-κB can be divided into a canonical and a noncanonical (or alternative) pathway. The activation of the noncanonical pathway is triggered by specific stimuli, such as the binding of LTβR, BAFFR, CD40 and RANK. Subsequently, NF-κB-inducing kinase (NIK) interacts and activates inhibitor of NF-κB kinase α (IKKα) to phosphorylate p100, which is the precursor of p52. The phosphorylation of p100 triggers its own processing into mature p52, which translocates into the nucleus as a heterodimer complex with RelB. The canonical signaling pathway is activated upon stimulation of various receptors such as cytokine receptors (IL-1R), pattern-recognition receptors, (TLR), T-cell receptor and TNFR [54]. In unstimulated cells, NF-κB is inactive due to its interaction with the ankyrin repeat domains of classical IκBs, like IκBα, leading to a cytoplasmic localization and masking of the DNA binding domain [51]. Upon canonical activation of NF-κB, the IKK complex, consisting of IKKα, IKKβ and IKKγ (NEMO), phosphorylates IκBα at serine 32 [55]. Subsequently, phosphorylated IκBα gets polyubiquitinated and proteasomal degraded. Consequently NF-κB gets released and translocates into the nucleus to induce or to repress NF-κB target genes [56]. Of note, IκBα encoded by *NFKBIA*, is also transcriptionally induced by NF-κB. Newly synthesized IκBα therefore binds NF-κB again, masking the NLS and exports it back to the cytoplasm, thereby inactivating NF-κB [57]. Thus, activation of NF-κB and therefore induction of NF-κB-dependent target gene expression is oscillating and exists in multiple waves.

NF-κB-dependent target genes can be divided into early or primary response genes and late or secondary response genes based on the accessibility of their promoter regions [58]. Primary response genes are rapidly activated, do not require any additional chromatin modifications and can be induced without *de novo* protein synthesis. In contrast, secondary response genes of NF-κB are activated more slowly and require *de novo* protein synthesis and nucleosome remodeling prior to their

induction [58]. In detail, nucleosome remodeling makes genomic DNA more accessible to transcription factor binding [59]. Lysine acetylation and methylation are the most common histone modifications that regulate transcription. Moreover, the SWI/SNF complex decondenses the chromatin at low CpG content or directly remodel the nucleosome and thus, increases the accessibility of the promoter [60, 61]. Furthermore, the SWI/SNF complex also cooperates with transcriptional coactivators of NF-κB, which comprise the nuclear IκB proteins such as IκBζ, IκBNS and BCL3 [62]. Histone acetyltransferase complexes (HATs), such as the CREB-binding protein (CBP)/p300 complex, acetylate histones to activate transcription such as the acetylation of p65 at lysine 310 [63], and histone deacetylases (HDACs) remove this residue [47]. However, lysine methylation can activate or repress transcription, this depends on the specific modified residue [64]. Moreover, in addition to nucleosome remodeling there are further ways to regulate the NF-κB-mediated gene expression, as for example by transcriptional coactivators, post-translational modifications [65] and proteasomal degradation [66].

Post-translational modifications, such as phosphorylation, ubiquitination, acetylation, and methylation, control the nuclear translocation and influence the functions of NF-κB subunits including protein degradation, DNA binding, and transcriptional activity [67-69]. This includes protein kinase A (PKA) or mitogen- and stress-activated protein kinase 1 and 2 (MSK1 and 2) mediated phosphorylation at serine 276 of p65 [70, 71], IKKα and IKKβ or casein kinase II (CKII) phosphorylation at serine 536 [63, 72, 73] and protein kinase C ζ (PKCζ)-dependent phosphorylation of p65 at serine 311 [74].

1.3 The atypical IκB member IκBζ

IκBζ, encoded by *NFKBIZ* on chromosome 3q12.3, constitutes an important cofactor for NF-κB target gene regulation, as already mentioned before [75]. IκBζ is highly conserved in a variety of species such as human, chimpanzee, rhesus monkey, dog, cow, mouse, rat, chicken and zebrafish [76]. In addition to a nuclear translocation signal (NLS) and transactivating domain (TAD), multiple ankyrin repeats characterize the structure of IκBζ, which mainly mediate the interaction with other proteins, such as the NF-κB subunits p50 or p52. Proven triggers of IκBζ expression comprise ligands of TLR 2, 4, 5, 7 and 9, such as peptidoglycan, flagellin, CpG oligonucleotides or

lipopolysaccharide (LPS). Moreover pro-inflammatory cytokines such as IL-1β via its receptor IL-1R and IL-17A via a heterodimeric IL-17R complex can induce IκBζ expression in different cell types [76]. Upon stimulation of TLRs or IL-1R, myeloid differentiation primary response 88 (MyD88) is activated and recruits the serine-threonine kinases IL-1 receptor-associated kinase 1 and 4 (IRAK1 and 4) to induce autophosphorylation of both proteins [77]. Subsequently, phosphorylated IRAK1 associates with TNF receptor-associated factor 6 (TRAF6), leading to activation of NF-κB and mitogen-activated protein kinases (MAPK), which then trigger the expression IκBζ [78]. Beside a transcription-mediated induction of IκBζ, stabilization of its mRNA and post-translational modifications regulate the expression levels of IκBζ. For example, translation of *NFKBIZ* mRNA is regulated via a translation silencing element (TSE) at the 3`UTR, which is the target of RNA binding proteins such as monocyte chemotactic protein-induced protein 1 (MCPIP1)/Regnase-1. Consequently, binding of MCPIP1 via stem-loop structures at the 3`UTR of *NFKBIZ* results in the degradation and therefore suppression of IκBζ expression [79]. Interestingly, however, IL-17 stimulation via the IL-17R complex triggers the degradation of MCPIP1, leading to an increase in NFKBIZ mRNA stability and translation into IκBζ protein. Thus, stimulation with TNFα and IL-17 is sufficient to induce IκBζ [53, 80].

How IκBζ regulates NF-κB target genes is not fully understood yet. NF-κB-dependent, primary response genes, such as *Cxcl1* and *Il23a*, are not directly regulated by IκBζ, whereas the expression of a subset of secondary response genes, including *Il12b*, *Il6*, *Ccl2* and *Lcn2*, is fully dependent on IκBζ expression [81, 82]. Interestingly, IκBζ can repress or activate NF-κB target genes, based on its interaction with different NF-κB homo- and heterodimers [82, 83]. A complex consisting of IκBζ- and a p50-p50 homodimer can activate the expression of e.g. *Ccl2* and *Lcn2* in LPS- or IL-1-stimulated macrophages [81, 82]. *Vice versa*, interaction of IκBζ with p65-p50 heterodimers mostly results in suppression of gene expression through the recruitment of histone-deacetylating proteins (HDAC) [84]. Moreover, IκBζ can interact with p52 in ABC- diffuse large B-cell lymphoma (DLBCL) to mediate tumor cell survival [85], whereas interaction with STAT3 via its coiled-coiled domain seem to inhibit the DNA binding capability of STAT3 [86]. Furthermore, IκBζ cooperates with retinoic acid-related orphan receptors α and γ (RORα and γ) to induce IL-17A expression inTh17 cells [87].

Mechanistically, it has been shown that epigenetic modifiers are recruited by IκBζ to certain gene promoters that are characterized by a high content of CpG islands. Consequently, cofactors that are recruited by IκBζ, such as Tet2 or the SWI/SNF complex alter DNA methylation and remodel nucleosome composition, respectively, in order to make promoter regions assessable for transcription factors [62, 88]. Moreover, IκBζ can also co-localize with HDAC4 and HDAC5 in matrix-associated deacetylase nuclear bodies leading to deacetylation of p65 and therefore repression of target gene expression [84]. Additionally, IκBζ is involved in the regulation of histone 3 lysine 4 trimethylation (H3K4me3) after nucleosome remodeling, which seems to be important for the regulation of gene expression [89].

Therefore, IκBζ-dependent target genes such as IL-17 in Crohn's disease [90] or LCN2 in inflammatory bowel disease [91] represent key factors in various inflammatory and autoimmune diseases. Moreover, mutations in the *NFKBIZ* gene locus have been implicated in ulcerative colitis [92] and cancer [76].

1.4 IκBζ in psoriasis

In psoriasis, a SNP (rs7637230) adjacent to the *NFKBIZ* gene locus was found to be overrepresented in psoriasis patients [93]. Furthermore, elevated mRNA levels of *NFKBIZ* could be detected in psoriatic skin lesions compared to non-lesional controls [94]. Therefore *NFKBIZ*/ IκBζ constitutes a risk gene for the development of psoriasis. In agreement, global IκBζ knockout mice are fully protected against experimental induced psoriasis-like skin inflammation induced by IMQ or IL-23 treatment. This might be due to the fact that IκBζ regulates the expression of IL-17A in Th17 cells, a key cytokine in psoriasis [87]. Alternatively, keratinocyte-derived IκBζ might also contribute to the development of psoriasis and its associated systemic inflammation, as it promotes the expression of psoriasis-associated chemokines and cytokines, leading to the recruitment of neutrophils and macrophages [95].

Generally, global IκBζ-deficient mice develop severe skin irritations in the face, neck and periocular regions in adulthood [82]. Furthermore, global knockout leads to chronic inflammation of the submucosa due to massive infiltration of immune cells. This phenotype corresponds to a Sjögren syndrome-like inflammation of the eye [96]. Additionally, these mice are difficult to breed because of high embryonic lethality [97].

What causes this autoinflammatory phenotype in these mice is under debate. In detail, a goblet cell disappearance [98] and autoreactive T cells, which attack the keratinocytes [99], are discussed.

1.5 Project objectives

IκBζ is known as a risk factor for psoriasis [46, 93]. Furthermore, global IκBζ knockout mice are completely protected against IMQ-induced psoriasis-like skin inflammation as opposed to a *Tnfa*- or *Il17a*-KO mice, which show only partial protection against IMQ-mediated skin inflammation. Moreover, IκBζ levels remain elevated in *Tnfa* or *Il17a*-KO mice [94], thereby suggesting alternative signaling pathways that promote IκBζ expression in psoriasis. Interestingly, IL-36α and IL-36γ, two cytokines of the IL-1 family, are upregulated in psoriatic lesions. Moreover, it was shown before that IL-1b can also induced IκBζ expression in various cell types [82]. Furthermore, an inactivating mutation of *IL36RN* leads to the establishment of pustular psoriasis [23], whereas *IL-36R* KO mice are fully protected against IMQ-induced psoriasis [22]. Therefore, we hypothesized that IL-36, beside of IL-17 can induce IκBζ expression in psoriatic lesions, thereby promoting pro-inflammatory gene expression. Accordingly, it should be investigated whether IκBζ and IκBζ target genes are regulated under IL-36 in keratinocytes. Following, the *in vivo* role of IκBζ in IL-36-driven psoriasis should be examined in more detail (Müller et al. 2018). Moreover, we revealed that keratinocyte-derived IκBζ drives the onset of psoriasis and following, represents an attractive target for psoriasis therapy. However, IκBζ cannot be directly targeted, as it lacks any enzymatic activity [88]. Finally, a better understanding of the induction of IκBζ should find an inhibitor that prevents the expression of IκBζ (Müller et al. 2020).

2 Results & Discussion

In previous studies, IκBζ was identified as a major mediator of IL-17A-mediated proinflammatory signaling in keratinocytes [94, 100]. Furthermore, pro-inflammatory signaling in keratinocytes is also triggered by IL-36 [101]. Our studies implicate that IκBζ bridges IL-36 or IL-17 signaling and psoriasis-associated inflammatory gene expression in keratinocytes, as the stimulation with both cytokines triggers similar IκBζ induction kinetics. Thus, we hypothesize that IκBζ represents a central player in the regulation of the pathogenesis of psoriasis and would be a new target of a small-molecular inhibitor therapy for the global induction of inflammation.

2.1 STAT3 and NF-κB mediate the induction of IκBζ in keratinocytes

IκBζ occurs in two functional isoforms: the long IκBζ(L) variant (encoded by 14 exons) and the short IκBζ(S) variant, which is N-terminally truncated [76]. By analyzing published ChIPseq data [102], we identified that the two isoforms have different promoter regions with distinct transcriptional start sites (Figure 2, Müller et al. 2018). The isoforms are expressed differently in the respective cell types. Our RNAseq data identified the long isoform as the primary IκBζ isoform in keratinocytes. In previous analyses, only the promoter of the short isoform was considered [75, 80]. By analyzing the promoter region of the long isoform, we identified several putative binding sites for transcription factors including NF-κB, STAT3, CEBPβ, AP1, KLF4 and a shared binding site of STAT1 and STAT3 (Figure 2, Müller et al. 2018). Further analysis has shown that, in addition to NF-κB [84], also STAT3 transcriptionally induced IκBζ in IL-36- and IL-17/TNFα-stimulated keratinocytes (Figure 2, Müller et al. 2018). This observation has already been validated in *STAT3*-depleted CD4-positive T cells, which lack inducible expression of IκBζ [87]. However, activation of the STAT3 signaling pathway alone does not seem to be sufficient to induce IκBζ because classical STAT3 stimuli such as IL-6 or IL-22 do not induce IκBζ expression [87, 103]. This is also true for NF-κB-exclusive stimulations such as TNFα [76]. Consequently, these observations suggest that activation of IκBζ requires a cooperation between STAT3 and NF-κB, either directly on the chromatin, or by supporting the activation of each other.

A cooperation of STAT3 and NF-κB, especially the subunits p65 and p50, has already been revealed for a variety of target genes. These genes are mainly involved in anti-apoptotic pathways, cell cycle control and proliferation, such as *BCL3* and *SOCS3*, but also encode cytokines and chemokines like *IL6* [104]. An example of the mutual activation is the link between unphosphorylated STAT3 and the NF-κB/IκBα complex upon IL-6 stimulation. This interaction displaces IκBα and thereby facilitates the nuclear translocation and activation of NF-κB [104]. As revealed by our ChIP data (Figure 2, Müller et al. 2018) it can be assumed that there is a direct interaction between NF-κB and STAT3 at the *NFKBIZ* promoter, which might result in the recruitment of additional transcription factors or co-factors. Grivennikov and Karin described an interaction of STAT3 with other transcription factors, such as androgen receptor and c-Jun, which may further modulate the STAT3-NF-κB interaction [104]. In contrast our experiments showed, that different MAPK inhibitors did not alter the expression of IκBζ (Suppl. Figure 2, Müller et al. 2018), indicating that STAT3 does not recruit transcription factors such as c-Jun to the promoter which might stabilize the complex with NF-κB and promote gene expression.

Possible co-factors of STAT3 and NF-κB are HATs, such as p300, CBP and PCAF, or HDACs [105-107]. For example, p300 can acetylate p65 and increases its nuclear retention and transcriptional activity [104]. This results in the release of cytokines such as IL-6, which by itself activates STAT3 [108]. Additionally, histone acetylation is associated with an open chromatin structure to support gene expression. Generally, HDACs de-acetylate histones or non-histone targets such as STAT3 and NF-κB to repress their activity. For HDAC3, however, it was shown that de-acetylation at different NF-κB sites can also positively regulate pro-inflammatory gene expression [106]. It is thus tempting to speculate that co-factors may stabilize STAT3-NF-κB at the *NFKBIZ* promoter in order to induce IκBζ.

Taken together, our experimental results indicate that STAT3 and NF-κB induce the IκBζ expression upon IL-36 and IL-17/TNFα stimulation in a cooperative and synergized manner. Therefore, it might be speculated that IκBζ is generally induced through NF-κB and STAT3, which are directly activated upon stimulation with cytokines or TLR ligands. This hypothesis is supported by the fact that both transcription factors are activated by different stimuli in various cell types e.g. by LPS in macrophages or through IL-1 in fibroblasts [80]. Other stimuli are TLR ligands such as poly(I:C) and

flagellin which activate both, STAT3 and NF-κB, and as a consequence induce IκBζ expression (Suppl. Figure 1, Müller et al. 2020).

2.2 IκBζ regulates a subset of IL-36-dependent target genes in two waves

As we identified the IL-36-mediated induction of IκBζ in keratinocytes, it was also of interest to identify the IL-36 response genes, which are regulated by IκBζ. By analyzing IL-36 responses in IκBζ knockdown keratinocytes, we could demonstrate that the IL-36-mediated, IκBζ-dependent gene expression occurs in two waves – one 1.5 h and the other 24 h after stimulation (Figure 3, Müller et al. 2018). Noteworthy, IκBζ-dependent gene expression seems to be highly conserved, as we found similar changes in the IκBζ-related proinflammatory target gene expression in keratinocytes e.g. *DEFB4, CCL20, S100A9* and *LCN2* upon different stimuli such as IL-36α, IL-36γ, IL-1β or IL-17A/TNFα (Figure 3/S4, Müller et al. 2018).

The proinflammatory gene expression 24 h upon IL-36 stimulation has also been described in a variety of ways in keratinocytes [101]. Only about 10% of these genes are regulated by IκBζ, all genes that drive inflammation. This set of genes includes in particular genes encoding AMPs such as *LCN2*, *S100A* genes and *DEFB4*, which are upregulated after 24 h (Figure 3, Müller et al. 2018). These genes indirectly trigger the adaptive immune response by dendritic cells to recruit T cells as well as neutrophils and macrophages and ultimately activate them. Additionally, proinflammatory chemo- and cytokines such as *CXCL8*, *IL23* and *IL36G,* potentiated the inflammation system at 24 h. *Vice versa*, little is known about the early response genes of the IL-36 mediated immune response (1.5 h). We found that in particular chemokines such as *CXCL5* and *CXCL6* are upregulated by IκBζ, which are supposed to respond to the innate immune response in order to recruit neutrophils and macrophages into the tissue and proceed the inflammation (Figure 3, Müller et al. 2018). Since the IκBζ-mediated gene response runs in two waves, it can be assumed that the regulation of the genes differs at the two time points. It needs to be clarified whether the two waves are interdependent. Following, it can be supposed that the AMP expression after 24 h could be driven indirectly by early IL-17C secretion, as already described for *S100A* and *DEFB4* [109]. This would coincide with our data that keratinocytes expressed *IL17C* 1 h upon IL-36 stimulation (Figure S3, Müller et al. 2018). In addition to the possible partial

dependence of the late response genes (24 h) on the early response genes (1.5 h), another major difference is the various regulatory mechanisms of the target genes. Remarkably, early effects of IL-36 stimulation on gene expression have not been investigated before in keratinocytes. We validated defined IL-36 target genes [101] and new IL-36-dependent genes (e.g. *IL17C, CSF2, CSF3*) that encode important psoriasis-promoting cytokines [110, 111].

The regulatory mechanism of IκBζ at the early point of gene expression (1.5 h) could be the direct interaction with transcription factors like NF-κB to activate or repress genes. For example, the interaction of IκBζ with p65-p50 heterodimers leads to the downregulation of genes like *IL6* in monocytes; on the other hand, the interaction with p50 homodimers enhances gene expression such as *DEFB4* in bronchial epithelial cells. Otherwise, IκBζ can also inhibit the DNA binding of STAT3 to regulate cell proliferation and apoptosis by interacting with STAT3 [76]. It should be noticed that many of the IL-36-mediated target genes are downregulated by IκBζ at the early time point (Figure 3, Müller et al. 2018). This could be a hint for repressive interactions of IκBζ with e.g. STAT3 or p65-p50 NF-κB heterodimers.

Genes are also downregulated at the late expression point (24 h). For the repression of these genes, the recruitment of histone deacetylases (HDACs) to DNA would be possible. Interactions between IκBζ and HDAC4 and HDAC5 have already been shown, which lead to de-acetylation of p65 and therefore repression of target gene expression [84]. A subsequent HDAC1 interaction and thus limited target gene expression was also observed based on a specific phosphorylation of IκBζ [112]. This hypothesis can be supported by the fact that HDAC inhibitors are able to reduce proinflammatory gene expression in LPS-stimulated human peripheral blood mononuclear cells, and especially in keratinocytes to inhibit proinflammatory target genes such as *IL6*, *IL20* and *S100A9* [112, 113]. The overall role of HDACs in inflammation was demonstrated by *HDAC3*-lacking macrophages upon LPS treatment, which were unable to activate almost half of the inflammatory gene expression program [114]. Moreover, it was recently shown that IκBζ targeted Tet methyl-cytosine dioxygenase 2 (Tet2), which mediates DNA de-methylation. Tet2 in turn recruited HDAC2, which repressed *Il6* expression by histone de-acetylation to resolve the inflammation [115]. This indicates that not only IκBζ regulates gene expression at later time points but possibly in a complex with other co-factors such as HDACs to modulate

the gene expression. Additionally, to histone modifications mediated e.g. by HDACs, general mechanisms like nucleosome remodeling are possible mechanisms for the second IκBζ-mediated gene response at 24 h. An IκBζ-dependent transcription-enhancing H3K4 trimethylation at the *CCL2* promoter has already been shown in macrophages [81]. In addition, chromatin remodeling factors e.g. the SWI/SNF complex may be recruited by IκBζ, which alter DNA methylation and remodel nucleosome composition to open the chromatin for transcription [59, 88]. In accordance, it was shown that Akirin2 bridges NF-κB and the chromatin remodeling SWI/SNF complex by interacting with IκBζ. These mechanisms drive the TLR-mediated proinflammatory gene expression (*Il6* and *Il12b)* in macrophages during the innate immune response to viral or bacterial infection [62]. Additionally, it was observed that the SWI/SNF complex is mainly required for the activation of secondary response genes (*Il12b, Il6*, and *Nos2)*, and late primary response genes (*Ccl5)*, but not for rapidly induced primary response genes (*Cxcl2)* in LPS-stimulated macrophages. Furthermore, the Mi-2β complex was selectively recruited in addition to the SWI/SNF complexes to temper the induction of these secondary response genes [116].

Consequently, IκBζ plays a crucial role in the early as well as in the late IL-36 or IL-17/TNFα-mediated immune response, both as a direct mediator by interacting with e.g. NF-κB or STAT3, and as an indirect factor, which can adjust the gene expression by recruiting various factors such as nucleosome remodeling (SWI/SNF) and post-translational modifications-mediating co-factors (HDACs).

2.3 IL-36-mediated dermatitis: IκBζ function *in vivo*

A common psoriasis mouse model is the topical application of imiquimod (IMQ), which triggers the IL-23/Th17 immune axis. For this model, it has already been shown that a global IκBζ KO mouse is completely protected against a psoriasis-like skin disorder, whereas an *Il17* KO mouse and a *Tnf* KO mouse show continuously weak effects in preventing disease. Furthermore, the mRNA levels of *NFKBIZ* in *Il17* and *Tnf* KO mice are still upregulated [94]. Remarkably, IL-17 and TNFα play an essential role in psoriatic inflammation and drugs that target these cytokines have been used in the treatment of psoriasis for several years [117, 118]. This suggests that, in addition to the IL-17 pathway, there must be another factor that drives the IMQ-mediated

psoriasis-like skin disease and thus the pathogenesis of psoriasis. Moreover, it should be emphasized that IκBζ might act downstream from both pathways. Furthermore, it has already been described that a subtype of psoriasis, the pustular psoriasis, is driven by a genetic defect in the natural antagonist of the IL-36 signaling, IL-36Ra [10]. Accordingly, the phenotype of an *Il36ra* KO mouse is aggravated in an IMQ-mediated psoriasis-like skin disease, while IL-36 receptor-deficient mice (*Il36r* KO) were protected [22]. Noteworthy, *Il36r* KO mice showed stronger protection in the IMQ-mediated psoriasis-like skin disorder than *Il17a* KO mice [22]. These data imply that, regardless of IL-17, IL-36 plays an essential role in the pathogenesis of psoriasis. In accordance, expression data from psoriasis patients validated upregulated *NFKBIZ* and *IL36G* levels in psoriatic lesions (Figure 4, Müller et al. 2018). The correlation of the expression of *IL36G* and *NFKBIZ* was even stronger compared to the correlation of the expression of *IL17A* with *NFKBIZ*.

As already described, IMQ triggers the IL-23/IL-17 cytokine axis by activating TLR7/8 primarily on APCs including DCs, monocytes/macrophages and B cells [119]. Thus, the induction of the pathogenesis of psoriasis is not based on keratinocytes and does not take place directly via a single cytokine such as IL-17 or IL-36. Consequently, to investigate the function of IκBζ of an IL-36-driven immune response *in vivo*, we established an IL-36 model with intradermal injection. The application of IL-36, like IMQ, led to a psoriasis-like skin disease that is completely IκBζ dependent, as the IκBζ KO mice data suggests (Figure 4, Müller et al. 2018). This data implicated that IκBζ is both the driver of the IL-17- and IL-36-mediated gene response in psoriasis. Furthermore, the involvement of IκBζ in both pathways suggests that IκBζ is an interesting target/factor for various subtypes of psoriasis e.g. pustular psoriasis and psoriasis vulgaris, thus the inhibition of IκBζ might be a possible approach for a global therapy.

Following this hypothesis, it is also possible that IκBζ plays a role in other IL-36- or IL-17-driven diseases. For example, it has already been shown that IL-36 plays a driving role in the clearance of *Candida albicans* or *Staphylococcus aureus* infections or the pathogenesis of atopic dermatitis [120, 121]. In addition, IκBζ can also act as an important co-factor for the expression of proinflammatory genes in the regulation of fungal and bacterial infections [112]. Thus, IκBζ might play a global role in the context of an IL-36/IL-17-mediated gene expression in various diseases.

2.4 Targeting IκBζ in keratinocytes as a new therapy approach for psoriasis

As we identified IκBζ as attractive psoriasis target downstream of IL-36 and IL-17/TNFα, we screened for potential inhibitors. Since IκBζ has no enzymatic activity, it is difficult to find or design an inhibitor directly targeting IκBζ [88]. However, we have already shown that IκBζ is regulated transcriptionally below IL-36 and IL-17 (Suppl. Figure 1, Müller et al. 2018), thus inhibition of IκBζ expression using small molecule inhibitors that target the induction pathway can be implemented. Since NF-κB and STAT3 are known to regulate the expression of IκBζ (Figure 2, Müller et al. 2018), common co-factors of these transcription factors could be possible targets for the inhibitors. However, not all co-factor inhibitors are useful. For example, the specificity of p300 or HDAC inhibitors is not sufficient, as they would not only inhibit the induction of IκBζ, but also any gene expression. Moreover, they are too toxic [122]. Interestingly, we found that CDK4/6 and EZH2 inhibitors regulate the induction of IκBζ by regulating STAT3 activity (Figure 3, Müller et al. 2020).

CDK4/6, which belong to the serine/threonine kinase protein family, are traditionally necessary for the transition from G1 to S phase of the cell cycle. Upon activation of CDK4/6 through their D-type cyclins and CDK activating kinase (CAK), they are able to regulate transcription, differentiation or apoptosis by specifically phosphorylating proteins including the retinoblastoma (RB) signaling pathway, which regulates the E2F activity of the cell cycle [123, 124]. However, our data implicated that CDK4/6 acts in a cell-cycle-independent manner, as *RB* KO had no impact on IκBζ induction and IκBζ is induced in all cell cycle stages (Suppl. Figure 1, Müller et al. 2020). As a consequence, CDK4/6 does not only seem to play a role in the cell cycle. This has already been shown for proinflammatory gene expression by the direct association and regulation of proinflammatory transcription factors such as NF-κB, STAT3 and AP1 [125]. In detail, CDK4/6 is able to modulate transcription factors in a kinase-dependent and -independent manner [126-128]. Especially the interaction of CDK6 and p65, a subunit of NF-κB, in human tumors was observed to upregulate NF-κB target gene expression which can contribute to chronic inflammation and neoplasia [125, 126]. Moreover, it was shown that CDK6 can be recruited to distinct chromatin regions of inflammatory genes upon IL-1 stimulation [125]. We propose that IL-36, which belongs to the IL-1 family, can also activate CDK6. In accordance, we observed a direct interaction of CDK4/6 with STAT3 upon IL-36 treatment (Figure 3, Müller et al. 2020),

which is chromatin-bound (Figure 4, Müller et al. 2020). The complex of STAT3 and CDK6 was previously detected at the *INK4a* promoter (inducible CDK4/6 inhibitor of the cell cycle) as autoregulatory feedback loop to limit the growth or proliferation [129].

In addition to the interaction of STAT3 and CDK6, the presence of EZH2 in this complex was also demonstrated (Figure 4, Müller et al. 2020). Furthermore, a correlation of EZH2 and CDK6 was shown to regulate angiogenesis in melanoma [130]. EZH2 as a part of the polycomb repressive complex 2 (PRC2) generally catalyzes the methylation of H3K27 which is a transcriptionally repressive mark by chromatin condensation and following, suppression of gene expression [131-133]. Gene silencing is associated with increased cell proliferation and survival, as well as decreased senescence and differentiation [134, 135]. It was shown that EZH2 is frequently mutated or deregulated in various malignancies, including various cancer [136-138]. Moreover, EZH2 also plays an important role in differentiation of keratinocytes by repressing *Ink4A* and *Ink4B* expression and preventing the recruitment of the transcription factor AP1 to structural genes of epidermal differentiation [139]. Hence it is not surprising that EZH2 is upregulated in lesions of psoriasis patients (Figure 5, Müller et al. 2020), as EZH2 has already been identified as a mediator of inflammation in inflammatory bowel disease [140].

In conclusion, CDK4/6 and EZH2 seem to act independently in inflammation in addition to their classically described roles. Moreover, there are first indications that EZH2 and the CDK4/6 pathway can interact with each other [139].

2.5 Initiation of the CDK4/6-EZH2-STAT3 pathway

As described above, CDK4/6 and EZH2 regulated the expression of IκBζ in keratinocytes upon IL-36 or IL-17/TNFα treatment. This arised the question how this pathway, especially CDK4/6, is activated.

With regard to the activation of CDK4/6, we were able to confirm the classical activation via the associated D-cyclins. However, not all cyclin D proteins contribute to the activation of IκBζ. We found that cyclin D1 seem to repress CDK4/6-STAT3-mediated *NFKBIZ* promoter activation, whereas cyclin D2 and D3 promoted its activation by CDK4/6 and STAT3 (Suppl. Figure 2, Müller et al. 2020). The repressive role of cyclin

D1 has already been shown combined with STAT3 activation as a part of feedback network controlling of STAT3 activity. In detail, cyclin D1 is associated with the activation domain of STAT3 upon IL-6 stimulation and reduced the STAT3 nuclear level [141]. In addition, the cyclin D1 levels in psoriatic lesions are down-regulated (Figure 5, Müller et al. 2018), which indicates the lack of a repressive pathway in terms of IκBζ induction. In contrast, the cyclin D2 and D3 level are increased in psoriatic lesions (Figure 5, Müller et al. 2018). Consistent with this, a functional difference between cyclin D1 and D2 was observed in the regulation of RB [142]. This underlines the diversity of the individual D-type cyclins [143]. Only 52–64% of the sequence between cyclin D1, D2 and D3 is conserved [144]. Additionally, the individual D-type cyclins have been shown tissue-specific expression levels like the specific dependence of embryonal retina and breast epithelia on cyclin D1 or the unique function of cyclin D3 in lymphocyte development [145-147]. For D-type cyclins it is known that their expression is regulated by NF-κB [148, 149]. In accordance, we detected the binding of the NF-κB subunit p65 to the promoter regions of *CCND2* and *CCND3* upon stimulation of primary keratinocytes. We were also able to determine a p65-dependent gene expression of the D-type cyclins at early timepoints upon stimulation (Suppl. Figure 2, Müller et al. 2020). This rapid activation of p65 could already be associated with pre-bound transcription factors and/or epigenetic marks, which enable the specific recruitment of p65 [150]. In addition to NF-κB, other transcription factors could be involved in the induction of D-type cyclins in a stimulus- and cell type-specific manner, such as STAT3, AP1 and NFAT [151-153]. For example, STAT3 enhanced *CCND2* expression in colorectal cancer [154].

Conclusively, D-type cyclins seem to act as an adjusting screw for the CDK4/6-mediated signaling, as cyclin D1 has a negative and cyclin D2 and D3 have a positive effect on the induction of IκBζ and finally on the IκBζ-mediated gene expression, which leads to the establishment of psoriasis. Figure 3 summarizes our present working thesis for activation of CDK4/6 upon IL-36 or IL-17/TNFα treatment.

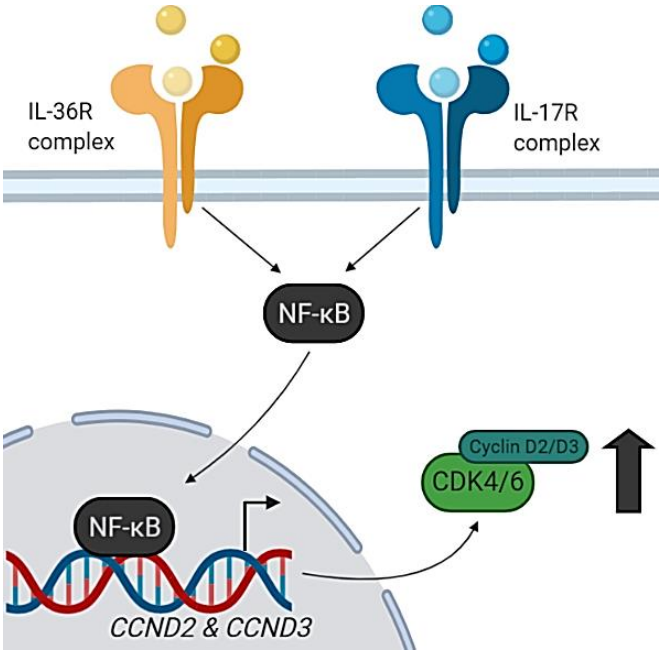

Figure 3: NF-κB regulates CDK4/6 activity (Created with BioRender.com). The binding of IL-36 or IL-17 activates the NF-κB signaling pathway to rapidly induce the *CCND2* and *CCND3* gene expression. The upregulation of the cyclin D2 and D3 expression activates CDK4/6 in a cyclin D-dependent manner.

2.6 Does CDK4/6 regulate PRC2-independent functions of EZH2?

EZH2 classically acts in a complex with the PRC2 components EED and Suz12 to mediate H3K27 trimethylation and therefore gene repression [131-133]. Interestingly, we showed that CDK4/6 phosphorylation of EZH2 at T345 leads to a non-classical EZH2-dependent methylation of STAT3 and therefore its activation (Figure 3/4, Müller et al. 2020). It was remarkable, that the PRC2-independent, non-classical function of EZH2 was found to induce gene expression by interacting with β-catenin or the SWI/SNF complex [155, 156]. In the PRC2 complex, EED classically serves as a bridging factor between histone H3 and EZH2. As a consequence, this linker (EED) is missing, histone-mediated methylation is no longer possible. Therefore, the question arises, if EED and Suz12 are needed for EZH2-mediated methylation of STAT3 in keratinocytes, or did the CDK4/6-dependent phosphorylation of EZH2 lead to the abrogation of EZH2 and EED/Suz12 interaction? It has already been shown that EZH2 can be phosphorylated by CDK1/2 at the CDK phosphorylation sites threonine 345 (T345) and T487 to modulate its function. The CDK1/2-mediated EZH2 phosphorylation results in the de-stabilization of the PRC2 complex at target gene promoters, following of epigenetic silencing of genes at G2 phase [157, 158]. However, we examined both sites and identified T345 as essential for the interaction with STAT3,

since an EZH2 mutant lacking the CDK4/6-directed phosphorylation site is unable to induce IκBζ via STAT3 methylation (Figure 3, Müller et al. 2020). Interestingly, previous reports have already been shown that in glioblastoma cells EZH2-directed methylation of STAT3 at lysine 180 (K180) is triggered by an Akt-dependent phosphorylation of EZH2 at serine 21, leading to the abrogation of EZH2 and EED interaction. Thus, it would be possible that the PRC2 complex is dissolved under our conditions in order to methylate STAT3 by EZH2. Additionally, we observed that the EZH2-mediated methylation of STAT3 leads to an increased STAT3 activity, which is triggered by the phosphorylation at tyrosine 705 (Y705) (Figure 3/4, Müller et al. 2020). This non-classical activation of STAT3 by EZH2 was already described in glioblastoma stem-like cells [159].

Finally, phosphorylation of EZH2 might induce a switch in EZH2 function from classical function of H3K27 methylation and following transcriptional repression to non-canonical functions, including STAT3 methylation and gene activation. Therefore, we hypothesize that CDK4/6 phosphorylation might induce similar effects in keratinocytes. However, it remains open, why EZH2 needs to get phosphorylated at different sites (T345 or T487) leading to similar effects. One explanation could be that the CDK4/6-mediated phosphorylation of EZH2 does not only abrogate its interaction with EED, while inducing its interaction with STAT3. Moreover, this might trigger an EZH2-mediated recruitment of other epigenetic modulators to STAT3 such as HDACs to de-acetylate STAT3. Corresponding, it was found that inhibition of HDAC activity enhanced p300-mediated STAT3 acetylation and supported nuclear export of STAT3 in B cell lymphoma. Furthermore, HDAC inhibition abolished phosphorylation of STAT3 at Y705 [105]. Especially with regard to the phosphorylation of STAT3 at Y705, it would be possible that HDACs in this pathway contribute to the stabilization of STAT3 in the nucleus.

In summary, there appears to be a functional switch in EZH2 triggered by its phosphorylation, which leads either to the methylation of transcription factors (phosphorylated EZH2) or to its classical function of histone modification (non-phosphorylated EZH2). Whether this function is also PCR2-independent requires further investigation.

2.7 CDK4/6- or EZH2-mediated inhibition of pSTAT3 at Y705

We could show that inhibitors against CDK4/6 and EZH2, as well as a knockdown of the respective genes, reduced not only the methylation of STAT3 at K180 but also the phosphorylation of STAT3 at Y705 (Figure 3/4, Müller et al. 2020). These data are indicative to a previous report describing that methylation of STAT3 at K180 enhances Y705-phosphorylation by protecting STAT3 from de-phosphorylation [159]. Furthermore, it seems that CDK4/6 and EZH2 do not only regulate the methylation of STAT3, but also alter phosphorylation of STAT3 at Y705 in a K180-methylation-independent manner. Nevertheless, how does inhibition of CDK4/6 and EZH2 abrogate the phosphorylation of STAT3 at Y705? STAT3 phosphorylation at this position is traditionally mediated by the JAK family. Interestingly, activation of all JAKs – JAK1, JAK2, JAK3 and TYK2 – have been implicated in stimulated keratinocytes before [160]. JAKs are induced by type I and type II cytokine receptors. The type I cytokine receptor superfamily contains the common γ chain (γc) which recognizes IL-2, IL-4, IL-7, IL-9, and IL-15 via JAK1/JAK3 heterodimers [161]. Further cytokines like IL-3 and IL-6 are recognized by type I cytokine receptors acting through JAK1/JAK2 heterodimers or JAK2 homodimers. The type II cytokine receptor family is activated by interferons (IFNs) and IL-10 utilizing heterodimers of JAK1/JAK2 or JAK1/TYK2 [162]. Which JAKs are activated in IL-36- or IL-17/TNFα-treated keratinocytes is not clear yet. Moreover, as IL-36 or IL-17/TNFα do not directly activate the type I or type II cytokine receptors, stimulation with these cytokines needs to trigger an auto-secretion of other JAK-activating cytokines.

Since our experiments were carried out exclusively in keratinocytes, it can be assumed that it affects cytokines that are secreted in an autocrine manner. It has already been shown that keratinocytes constitutively express IL-15 [163] and IL-7 [164], which can be recognized by JAKs. Our RNAseq data (Table S1-2, Müller et al. 2018) included deregulation of *IL7* upon IL-36 stimulation in an IκBζ-dependent manner. Accordingly, it would be possible for CDK4/6-EZH2 to regulate the expression of IL-7 and IL-15. In agreement, increased and accelerated expression levels of IL-15R were detected in EZH2-inhibited NKp cells [165]. However, as IκBζ is expressed after just 1 hour of stimulation, it is unlikely that cytokines will be generated and further secreted to activate STAT3 in an autocrine loop. As an alternative it is possible that pre-synthesized cytokines are stored in Golgi vesicles, which are released upon

stimulation. This “pre-stored” cytokines can activate STAT3 signaling and then mediate IκBζ expression in an autocrine loop. This mechanism is similar to the release of inflammatory compounds from secretory granules in mast cells [166]. Moreover it was shown for IL-6 in skin and other tissues that there is a release of pre-stored cytokines in systemic inflammatory response syndrome [167]. There is also an evidence of STAT3 activation with non-classical stimulants e.g. by IL-1β in *IL6* KO MEF cells [167]. This supports the previous hypothesis that STAT3 can be induced indirectly by IL-36 via pre-stored cytokines such as keratinocyte-derived IL-7 and IL-15, as a parallel pathway to the CDK4/6-EZH2 axis in order to activate IκBζ and its target genes in keratinocytes.

2.8 Prevention of psoriasis and therapeutic application of novel inhibitors

Some psoriatic studies provide indications for the pathological regulation/expression of IκBζ and herein involved pathways. These include that IκBζ has already been identified as the driver of inflammation in murine psoriasis model [94]. Furthermore, increased *NFKBIZ* levels have been detected in human psoriatic lesions [95] (Figure S5, Müller et al. 2018). In addition, we showed an increased nuclear accumulation of EZH2 and elevated cyclin D2 and D3 levels in mouse models of psoriasis (IMQ and IL-36 intradermal injection) and in human psoriatic skin lesions (Figure 5, Müller et al. 2020). Moreover, STAT3 mutations are risk factors for the development of psoriasis [168] and constitutively active STAT3 was detected in the epidermis of human psoriatic lesions [169]. Finally, this collection suggests that the CDK4/6-EZH2-STAT3 pathway is hyperactive in psoriatic skin lesions, especially in keratinocytes. Consequently, the CDK4/6 inhibitors, abemaciclib and palbociclib, and the EZH2 inhibitor block IL-36- and IL-17/TNFα-mediated induction of IκBζ including psoriasis-related genes (Figure 1/3 and Suppl. Figure 1/3, Müller et al. 2020) and following the whole development of psoriasis (Figure 6/7, Müller et al. 2020). The advantage here is the high specificity of the inflammatory pathway and the early block in the initiation process of the pathogenesis of psoriasis in keratinocytes.

In contrast, the common forms of therapy such as anti-IL-23 or anti-IL-17 antibodies or currently in clinical testing anti-IL-36 antibodies, are directed only against one arm of the inflammation and not against the origin of the pathogenesis. Not to mention,

psoriasis contains various subtypes that are associated with certain expression patterns or mutations, for example, in contrast to psoriasis vulgaris, pustular psoriasis is strongly characterized by an imbalance in IL-36 signaling [120]. Accordingly, neutralizing antibody therapy that can be used for all subtypes of psoriasis is rather ineffective. Supporting this statement, some of the biologics such as anti-TNFα antibodies show no effect in the treatment of patients with pustular psoriasis [170]. In addition, IL-17 or IL-36 can cross-regulate each other [171], which cannot be prevented with monotherapy. It is therefore important to find a therapy that targets the origin of the psoriatic inflammation.

Further clinical tests are carried out with a pan-JAK1/3 inhibitor (tofacitinib), which diminished overactive STAT3 signaling in psoriatic lesions [172] and thus for the first time does not block a specific cytokine but an entire pathway. In detail, pharmacological inhibition of STAT3 ameliorated psoriasis-like skin lesions in mice [169, 173]. Furthermore, STAT3 is instrumentally involved in Th17 cell differentiation, activation, proliferation, and survival through the regulation of key genes such as *RORγT, RORα, BATF, IRF4, AHR, IL-6Rα*, and *C-MAF*, as well as in direct IL-17A and IL-17F expression. *Vice versa*, an overexpression of constitutively active STAT3 upregulates the number of IL-17 producing cells [168]. Nevertheless, a complete block of the STAT3 pathway is not advisable due to its involvement in the proliferation, proinflammatory gene expression, activation and survival of cells as it is the case with treatment of tofacitinib. Moreover side effects of tofacitinib like an increased risk of infection, particularly viral (herpetic) infections, elevated level of low-density and high-density lipoprotein (LDL and HDL), and anemia have already been identified upon oral application [174].

However, we were able to show that the new (discovered) pro-inflammatory CDK4/6-EZH2 pathway only works specifically below IL-36 or IL-17/TNFα and that pro-survival functions from STAT3 to IL-6 remain intact (Suppl. Figure 4, Müller et al. 2020). Furthermore, our results suggest that all main characteristics of psoriasis are suppressed: immune cell recruitment, skin inflammation and additionally the cytokine-mediated induction of IκBζ and pro-inflammatory target gene expression (Figure 6/7, Müller et al. 2020). We thus provide a specific target for inflammation in psoriasis, where functions like activation and survival are not affected. A welcome side effect of a topical application in psoriasis is the proliferation block of keratinocytes by a CDK4/6

inhibitor [175]. Beside the cell cycle control, it was found that CDK4/6 also regulates immune cell differentiation and function [176-178].

The advantage of the described pathway and the used inhibitors is the high specificity, for example, EZH2 is not expressed in normal skin [139]. Furthermore, a topical application almost exclusively addresses keratinocytes, which are regarded as one of the key players in psoriasis in addition to T cells [179]. In general, the ATP-competitive CDK4/6 inhibitors, such as palbociclib, ribociclib or abemaciclib, are already widely used in cancer therapy, especially in breast and lung cancer [180], and therefore already tested for their effectiveness and side effects. In this context, CDK4/6 have been implicated as transcriptional co-factors that activate a subset of NF-κB or STAT3 target genes [126-128]. Moreover, it was shown that they block the keratinocyte hyperproliferation [175]. Thus, an inhibition of EZH2 by small molecular inhibitors to diminished trimethylation of H3K27 and upregulation of the silenced transcription, is another promising therapeutic approach. As a result, cancer cell growth and tumor formation is reduced in EZH2 inhibitor-treated patients with B-cell lymphomas and advanced solid tumor [181]. The use of both inhibitors has already been tested for various diseases.

Furthermore, the mode of application is another important point. For example, tofacitinib (pan-JAK inhibitor) is administered orally and therefore acts systemically and not only locally on the skin. Side effects that are toxic to the liver and kidneys have already been identified [168]. Local application, such as topical administration, which showed efficacies in our mouse models (Figure 6/7, Müller et al. 2020), would be advantageous and would prevent systemic toxicity. Furthermore, topical treatment using a cream would no longer require a doctor's visit, like in the case of anti-IL-23 or anti-IL-17 therapy, which are administered by intradermal injections. In addition, the production costs of monoclonal antibodies for human therapy are very expensive [168]. Thus, small molecule drugs such as palbociclib and abemaciclib (CDK4/6 inhibitors) have lower costs, and a reduced risk of eliciting adverse immune responses in topical application. In addition, neutralizing antibody therapy show rising resistance by anti-drug antibodies, which diminished the clinical responses over the duration of treatment. This phenomenon is not uncommon in psoriasis patients, e.g. infliximab (anti-TNFα antibodies) up to 43.6%, adalimumab (anti-TNFα antibodies) up to 44.8% or ustekinumab (anti-IL-12/IL-23 antibodies) up to 5.4% [182].

Next to psoriasis, this pathway could play a role in other inflammatory diseases or autoimmune diseases in which elevated *NFKBIZ* levels can be detected, such as ulcerative colitis [92] and multiple sclerosis [87].

2.9 Working model: IκBζ induction in psoriasis

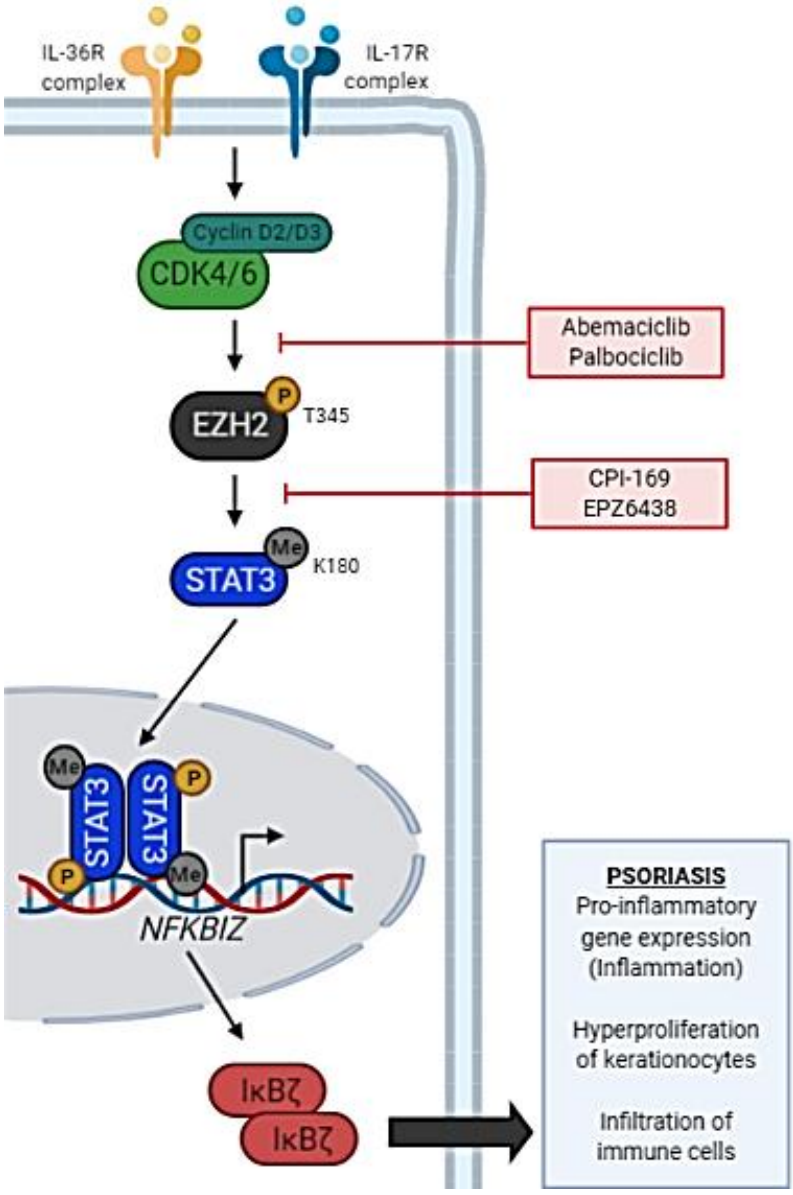

Figure 4: CDK4/6-EZH2-STAT3 signaling pathway to induce IκBζ and following psoriasis (Created with BioRender.com). The IL-36- or IL-17-mediated activation of CDK4/6 via cyclin D2 and D3 leads to the phosphorylation of EZH2 at T345, which in turn methylate STAT3 at K180. This methylation leads to the stabilization and further activation of STAT3 (phosphorylation at Y705) whereby STAT3 translocate into the nucleus and induce IκBζ expression. IκBζ and its target genes are the main driver of the pathogenesis of psoriasis including the proinflammatory gene expression, the hyperproliferation

of keratinocytes and the migration of immune cells to the inflammation site. The small-molecule inhibitors for CDK4/6 (abemaciclib and palbociclib) and EZH2 (CPI-169 and EPZ6438) can inhibit this specific proinflammatory pathway to block the induction of IκBζ in keratinocytes and further the onset of psoriasis.

3 References

1. Menter, A., et al., *Guidelines of care for the management of psoriasis and psoriatic arthritis: Section 1. Overview of psoriasis and guidelines of care for the treatment of psoriasis with biologics.* J Am Acad Dermatol, 2008. 58(5): p. 826-50.
2. Levine, D. and A. Gottlieb, *Evaluation and management of psoriasis: an internist's guide.* Med Clin North Am, 2009. 93(6): p. 1291-303.
3. Ogdie, A., et al., *Prevalence and treatment patterns of psoriatic arthritis in the UK.* Rheumatology (Oxford), 2013. 52(3): p. 568-75.
4. Ludwig, R.J., et al., *Psoriasis: a possible risk factor for development of coronary artery calcification.* Br J Dermatol, 2007. 156(2): p. 271-6.
5. Gelfand, J.M., et al., *Risk of myocardial infarction in patients with psoriasis.* JAMA, 2006. 296(14): p. 1735-41.
6. Gelfand, J.M., et al., *The risk of stroke in patients with psoriasis.* J Invest Dermatol, 2009. 129(10): p. 2411-8.
7. Kimball, A.B., et al., *Economic burden of comorbidities in patients with psoriasis is substantial.* J Eur Acad Dermatol Venereol, 2011. 25(2): p. 157-63.
8. Chen, L. and T.F. Tsai, *HLA-Cw6 and psoriasis.* Br J Dermatol, 2018. 178(4): p. 854-862.
9. Tsoi, L.C., et al., *Identification of 15 new psoriasis susceptibility loci highlights the role of innate immunity.* Nat Genet, 2012. 44(12): p. 1341-8.
10. Marrakchi, S., et al., *Interleukin-36-receptor antagonist deficiency and generalized pustular psoriasis.* N Engl J Med, 2011. 365(7): p. 620-8.
11. Tsoi, L.C., et al., *Large scale meta-analysis characterizes genetic architecture for common psoriasis associated variants.* Nat Commun, 2017. 8: p. 15382.
12. Nestle, F.O., D.H. Kaplan, and J. Barker, *Psoriasis.* N Engl J Med, 2009. 361(5): p. 496-509.
13. Greb, J.E., et al., *Psoriasis.* Nat Rev Dis Primers, 2016. 2: p. 16082.
14. Rendon, A. and K. Schäkel, *Psoriasis Pathogenesis and Treatment.* Int J Mol Sci, 2019. 20(6).
15. Li, B., et al., *Transcriptome analysis of psoriasis in a large case-control sample: RNA-seq provides insights into disease mechanisms.* J Invest Dermatol, 2014. 134(7): p. 1828-1838.
16. Bassoy, E.Y., J.E. Towne, and C. Gabay, *Regulation and function of interleukin-36 cytokines.* Immunol Rev, 2018. 281(1): p. 169-178.
17. Carrier, Y., et al., *Inter-regulation of Th17 cytokines and the IL-36 cytokines in vitro and in vivo: implications in psoriasis pathogenesis.* J Invest Dermatol, 2011. 131(12): p. 2428-37.
18. SR., F. *Treatment of psoriasis in adults*. UpToDate Dec 2019 [cited 2019; Available from: https://www.uptodate.com/contents/treatment-of-psoriasis-in-adults#H45.
19. Wolf, J. and L.K. Ferris, *Anti-IL-36R antibodies, potentially useful for the treatment of psoriasis: a patent evaluation of WO2013074569.* Expert Opin Ther Pat, 2014. 24(4): p. 477-9.
20. Cai, Y., et al., *Pivotal role of dermal IL-17-producing gammadelta T cells in skin inflammation.* Immunity, 2011. 35(4): p. 596-610.
21. van der Fits, L., et al., *Imiquimod-induced psoriasis-like skin inflammation in mice is mediated via the IL-23/IL-17 axis.* J Immunol, 2009. 182(9): p. 5836-45.
22. Tortola, L., et al., *Psoriasiform dermatitis is driven by IL-36-mediated DC-keratinocyte crosstalk.* J Clin Invest, 2012. 122(11): p. 3965-76.
23. Onoufriadis, A., et al., *Mutations in IL36RN/IL1F5 are associated with the severe episodic inflammatory skin disease known as generalized pustular psoriasis.* Am J Hum Genet, 2011. 89(3): p. 432-7.
24. Liang, Y., et al., *Psoriasis: a mixed autoimmune and autoinflammatory disease.* Curr Opin Immunol, 2017. 49: p. 1-8.
25. Johnston, A., et al., *IL-1 and IL-36 are dominant cytokines in generalized pustular psoriasis.* J Allergy Clin Immunol, 2017. 140(1): p. 109-120.

26. Wilsmann-Theis, D., et al., *Successful treatment with interleukin-17A antagonists of generalized pustular psoriasis in patients without IL36RN mutations.* J Dermatol, 2018. 45(7): p. 850-854.
27. Ghoreschi, K., et al., *Fumarates improve psoriasis and multiple sclerosis by inducing type II dendritic cells.* J Exp Med, 2011. 208(11): p. 2291-303.
28. Sano, S., et al., *Stat3 links activated keratinocytes and immunocytes required for development of psoriasis in a novel transgenic mouse model.* Nat Med, 2005. 11(1): p. 43-9.
29. Ellinghaus, D., et al., *Combined analysis of genome-wide association studies for Crohn disease and psoriasis identifies seven shared susceptibility loci.* Am J Hum Genet, 2012. 90(4): p. 636-47.
30. Goldminz, A.M., et al., *Prevalence of the metabolic syndrome in children with psoriatic disease.* Pediatr Dermatol, 2013. 30(6): p. 700-5.
31. Lizzul, P.F., et al., *Differential expression of phosphorylated NF-kappaB/RelA in normal and psoriatic epidermis and downregulation of NF-kappaB in response to treatment with etanercept.* J Invest Dermatol, 2005. 124(6): p. 1275-83.
32. Begon, E., et al., *Expression, subcellular localization and cytokinic modulation of Toll-like receptors (TLRs) in normal human keratinocytes: TLR2 up-regulation in psoriatic skin.* Eur J Dermatol, 2007. 17(6): p. 497-506.
33. Salskov-Iversen, M.L., et al., *Caspase-5 expression is upregulated in lesional psoriatic skin.* J Invest Dermatol, 2011. 131(3): p. 670-6.
34. Ghosh, S. and M.S. Hayden, *Celebrating 25 years of NF-kappaB research.* Immunol Rev, 2012. 246(1): p. 5-13.
35. Moorchung, N., et al., *Role of NF-kappaB in the pathogenesis of psoriasis elucidated by its staining in skin biopsy specimens.* Int J Dermatol, 2014. 53(5): p. 570-4.
36. Takada, Y., S. Singh, and B.B. Aggarwal, *Identification of a p65 peptide that selectively inhibits NF-kappa B activation induced by various inflammatory stimuli and its role in down-regulation of NF-kappaB-mediated gene expression and up-regulation of apoptosis.* J Biol Chem, 2004. 279(15): p. 15096-104.
37. Doger, F.K., et al., *Nature of cell kinetics in psoriatic epidermis.* J Cutan Pathol, 2007. 34(3): p. 257-63.
38. Liu, Y., et al., *Regulation of the psoriatic chemokine CCL20 by E3 ligases Trim32 and Piasy in keratinocytes.* J Invest Dermatol, 2010. 130(5): p. 1384-90.
39. Vestergaard, C., et al., *Tumor necrosis factor-alpha-induced CTACK/CCL27 (cutaneous T-cell-attracting chemokine) production in keratinocytes is controlled by nuclear factor kappaB.* Cytokine, 2005. 29(2): p. 49-55.
40. Chen, F., et al., *New insights into the role of nuclear factor-kappaB, a ubiquitous transcription factor in the initiation of diseases.* Clin Chem, 1999. 45(1): p. 7-17.
41. Barnes, P.J. and M. Karin, *Nuclear factor-kappaB: a pivotal transcription factor in chronic inflammatory diseases.* N Engl J Med, 1997. 336(15): p. 1066-71.
42. Siebenlist, U., G. Franzoso, and K. Brown, *Structure, regulation and function of NF-kappa B.* Annu Rev Cell Biol, 1994. 10: p. 405-55.
43. Wang, M., et al., *Gain-of-Function Mutation of Card14 Leads to Spontaneous Psoriasis-like Skin Inflammation through Enhanced Keratinocyte Response to IL-17A.* Immunity, 2018. 49(1): p. 66-79 e5.
44. Mellett, M., et al., *CARD14 Gain-of-Function Mutation Alone Is Sufficient to Drive IL-23/IL-17-Mediated Psoriasiform Skin Inflammation In Vivo.* J Invest Dermatol, 2018. 138(9): p. 2010-2023.
45. Jordan, C.T., et al., *Rare and common variants in CARD14, encoding an epidermal regulator of NF-kappaB, in psoriasis.* Am J Hum Genet, 2012. 90(5): p. 796-808.

46. Coto-Segura, P., et al., *Gene Variant in the NF-kappaB Pathway Inhibitor NFKBIA Distinguishes Patients with Psoriatic Arthritis within the Spectrum of Psoriatic Disease.* Biomed Res Int, 2019. 2019: p. 1030256.
47. Ghosh, S. and M.S. Hayden, *New regulators of NF-kappaB in inflammation.* Nat Rev Immunol, 2008. 8(11): p. 837-48.
48. Pai, S. and R. Thomas, *Immune deficiency or hyperactivity-Nf-kappab illuminates autoimmunity.* J Autoimmun, 2008. 31(3): p. 245-51.
49. Chen, F.E., et al., *Crystal structure of p50/p65 heterodimer of transcription factor NF-kappaB bound to DNA.* Nature, 1998. 391(6665): p. 410-3.
50. Rothwarf, D.M. and M. Karin, *The NF-kappa B activation pathway: a paradigm in information transfer from membrane to nucleus.* Sci STKE, 1999. 1999(5): p. RE1.
51. Li, Q. and I.M. Verma, *NF-kappaB regulation in the immune system.* Nat Rev Immunol, 2002. 2(10): p. 725-34.
52. Hayden, M.S. and S. Ghosh, *NF-kappaB in immunobiology.* Cell Res, 2011. 21(2): p. 223-44.
53. Schuster, M., et al., *Atypical IkappaB proteins - nuclear modulators of NF-kappaB signaling.* Cell Commun Signal, 2013. 11(1): p. 23.
54. Lawrence, T., *The nuclear factor NF-kappaB pathway in inflammation.* Cold Spring Harb Perspect Biol, 2009. 1(6): p. a001651.
55. Brown, K., et al., *Control of I kappa B-alpha proteolysis by site-specific, signal-induced phosphorylation.* Science, 1995. 267(5203): p. 1485-8.
56. Heissmeyer, V., et al., *Shared pathways of IkappaB kinase-induced SCF(betaTrCP)-mediated ubiquitination and degradation for the NF-kappaB precursor p105 and IkappaBalpha.* Mol Cell Biol, 2001. 21(4): p. 1024-35.
57. Pahl, H.L., *Activators and target genes of Rel/NF-kappaB transcription factors.* Oncogene, 1999. 18(49): p. 6853-66.
58. Saccani, S., S. Pantano, and G. Natoli, *Two waves of nuclear factor kappaB recruitment to target promoters.* J Exp Med, 2001. 193(12): p. 1351-9.
59. Clapier, C.R. and B.R. Cairns, *The biology of chromatin remodeling complexes.* Annu Rev Biochem, 2009. 78: p. 273-304.
60. Ramirez-Carrozzi, V.R., et al., *A unifying model for the selective regulation of inducible transcription by CpG islands and nucleosome remodeling.* Cell, 2009. 138(1): p. 114-28.
61. Zhao, K., et al., *Rapid and phosphoinositol-dependent binding of the SWI/SNF-like BAF complex to chromatin after T lymphocyte receptor signaling.* Cell, 1998. 95(5): p. 625-36.
62. Tartey, S., et al., *Akirin2 is critical for inducing inflammatory genes by bridging IkappaB-zeta and the SWI/SNF complex.* EMBO J, 2014. 33(20): p. 2332-48.
63. Chen, L.F. and W.C. Greene, *Shaping the nuclear action of NF-kappaB.* Nat Rev Mol Cell Biol, 2004. 5(5): p. 392-401.
64. Bhatt, D. and S. Ghosh, *Regulation of the NF-kappaB-Mediated Transcription of Inflammatory Genes.* Front Immunol, 2014. 5: p. 71.
65. Kiernan, R., et al., *Post-activation turn-off of NF-kappa B-dependent transcription is regulated by acetylation of p65.* J Biol Chem, 2003. 278(4): p. 2758-66.
66. Saccani, S., et al., *Degradation of promoter-bound p65/RelA is essential for the prompt termination of the nuclear factor kappaB response.* J Exp Med, 2004. 200(1): p. 107-13.
67. Viatour, P., et al., *Phosphorylation of NF-kappaB and IkappaB proteins: implications in cancer and inflammation.* Trends Biochem Sci, 2005. 30(1): p. 43-52.
68. Perkins, N.D., *Post-translational modifications regulating the activity and function of the nuclear factor kappa B pathway.* Oncogene, 2006. 25(51): p. 6717-30.
69. Won, M., et al., *Post-translational control of NF-kappaB signaling by ubiquitination.* Arch Pharm Res, 2016. 39(8): p. 1075-84.

70. Zhong, H., R.E. Voll, and S. Ghosh, *Phosphorylation of NF-kappa B p65 by PKA stimulates transcriptional activity by promoting a novel bivalent interaction with the coactivator CBP/p300.* Mol Cell, 1998. 1(5): p. 661-71.
71. Vermeulen, L., et al., *Transcriptional activation of the NF-kappaB p65 subunit by mitogen- and stress-activated protein kinase-1 (MSK1).* EMBO J, 2003. 22(6): p. 1313-24.
72. Bird, T.A., et al., *Activation of nuclear transcription factor NF-kappaB by interleukin-1 is accompanied by casein kinase II-mediated phosphorylation of the p65 subunit.* J Biol Chem, 1997. 272(51): p. 32606-12.
73. Wang, D., et al., *Tumor necrosis factor alpha-induced phosphorylation of RelA/p65 on Ser529 is controlled by casein kinase II.* J Biol Chem, 2000. 275(42): p. 32592-7.
74. Duran, A., M.T. Diaz-Meco, and J. Moscat, *Essential role of RelA Ser311 phosphorylation by zetaPKC in NF-kappaB transcriptional activation.* EMBO J, 2003. 22(15): p. 3910-8.
75. Shiina, T., et al., *Genomic organization, chromosomal localization, and promoter analysis of the mouse Mail gene.* Immunogenetics, 2001. 53(8): p. 649-55.
76. Willems, M., et al., *IkappaBzeta: an emerging player in cancer.* Oncotarget, 2016. 7(40): p. 66310-66322.
77. Wesche, H., et al., *MyD88: an adapter that recruits IRAK to the IL-1 receptor complex.* Immunity, 1997. 7(6): p. 837-47.
78. Irie, T., T. Muta, and K. Takeshige, *TAK1 mediates an activation signal from toll-like receptor(s) to nuclear factor-kappaB in lipopolysaccharide-stimulated macrophages.* FEBS Lett, 2000. 467(2-3): p. 160-4.
79. Behrens, G., et al., *A translational silencing function of MCPIP1/Regnase-1 specified by the target site context.* Nucleic Acids Res, 2018. 46(8): p. 4256-4270.
80. Yamazaki, S., et al., *Stimulus-specific induction of a novel nuclear factor-kappaB regulator, IkappaB-zeta, via Toll/Interleukin-1 receptor is mediated by mRNA stabilization.* J Biol Chem, 2005. 280(2): p. 1678-87.
81. Hildebrand, D.G., et al., *IkappaBzeta is a transcriptional key regulator of CCL2/MCP-1.* J Immunol, 2013. 190(9): p. 4812-20.
82. Yamamoto, M., et al., *Regulation of Toll/IL-1-receptor-mediated gene expression by the inducible nuclear protein IkappaBzeta.* Nature, 2004. 430(6996): p. 218-22.
83. Motoyama, M., et al., *Positive and negative regulation of nuclear factor-kappaB-mediated transcription by IkappaB-zeta, an inducible nuclear protein.* J Biol Chem, 2005. 280(9): p. 7444-51.
84. Totzke, G., et al., *A novel member of the IkappaB family, human IkappaB-zeta, inhibits transactivation of p65 and its DNA binding.* J Biol Chem, 2006. 281(18): p. 12645-54.
85. Nogai, H., et al., *IkappaB-zeta controls the constitutive NF-kappaB target gene network and survival of ABC DLBCL.* Blood, 2013. 122(13): p. 2242-50.
86. Wu, Z., et al., *Nuclear protein IkappaB-zeta inhibits the activity of STAT3.* Biochem Biophys Res Commun, 2009. 387(2): p. 348-52.
87. Okamoto, K., et al., *IkappaBzeta regulates T(H)17 development by cooperating with ROR nuclear receptors.* Nature, 2010. 464(7293): p. 1381-5.
88. Annemann, M., et al., *Atypical IkappaB proteins in immune cell differentiation and function.* Immunol Lett, 2016. 171: p. 26-35.
89. Kayama, H., et al., *Class-specific regulation of pro-inflammatory genes by MyD88 pathways and IkappaBzeta.* J Biol Chem, 2008. 283(18): p. 12468-77.
90. Kerami, Z., et al., *Effect of interleukin-17 on gene expression profile of fibroblasts from Crohn's disease patients.* J Crohns Colitis, 2014. 8(10): p. 1208-16.
91. Stallhofer, J., et al., *Lipocalin-2 Is a Disease Activity Marker in Inflammatory Bowel Disease Regulated by IL-17A, IL-22, and TNF-alpha and Modulated by IL23R Genotype Status.* Inflamm Bowel Dis, 2015. 21(10): p. 2327-40.

92. Kakiuchi, N., et al., *Frequent mutations that converge on the NFKBIZ pathway in ulcerative colitis.* Nature, 2020. 577(7789): p. 260-265.
93. Tsoi, L.C., et al., *Enhanced meta-analysis and replication studies identify five new psoriasis susceptibility loci.* Nat Commun, 2015. 6: p. 7001.
94. Johansen, C., et al., *IkappaBzeta is a key driver in the development of psoriasis.* Proc Natl Acad Sci U S A, 2015. 112(43): p. E5825-33.
95. Lorscheid, S., et al., *Keratinocyte-derived IkappaBzeta drives psoriasis and associated systemic inflammation.* JCI Insight, 2019. 4(22).
96. Okuma, A., et al., *Enhanced apoptosis by disruption of the STAT3-IkappaB-zeta signaling pathway in epithelial cells induces Sjogren's syndrome-like autoimmune disease.* Immunity, 2013. 38(3): p. 450-60.
97. Shiina, T., et al., *Targeted disruption of MAIL, a nuclear IkappaB protein, leads to severe atopic dermatitis-like disease.* J Biol Chem, 2004. 279(53): p. 55493-8.
98. Ueta, M., et al., *Spontaneous ocular surface inflammation and goblet cell disappearance in I kappa B zeta gene-disrupted mice.* Invest Ophthalmol Vis Sci, 2005. 46(2): p. 579-88.
99. Singh, N. and P.L. Cohen, *The T cell in Sjogren's syndrome: force majeure, not spectateur.* J Autoimmun, 2012. 39(3): p. 229-33.
100. Muromoto, R., et al., *IL-17A plays a central role in the expression of psoriasis signature genes through the induction of IkappaB-zeta in keratinocytes.* Int Immunol, 2016. 28(9): p. 443-52.
101. Mahil, S.K., et al., *An analysis of IL-36 signature genes and individuals with IL1RL2 knockout mutations validates IL-36 as a psoriasis therapeutic target.* Sci Transl Med, 2017. 9(411).
102. Bernstein, B.E., et al., *The NIH Roadmap Epigenomics Mapping Consortium.* Nat Biotechnol, 2010. 28(10): p. 1045-8.
103. Nagalakshmi, M.L., et al., *Interleukin-22 activates STAT3 and induces IL-10 by colon epithelial cells.* Int Immunopharmacol, 2004. 4(5): p. 679-91.
104. Grivennikov, S.I. and M. Karin, *Dangerous liaisons: STAT3 and NF-kappaB collaboration and crosstalk in cancer.* Cytokine Growth Factor Rev, 2010. 21(1): p. 11-9.
105. Gupta, M., et al., *Regulation of STAT3 by histone deacetylase-3 in diffuse large B-cell lymphoma: implications for therapy.* Leukemia, 2012. 26(6): p. 1356-64.
106. Leus, N.G., M.R. Zwinderman, and F.J. Dekker, *Histone deacetylase 3 (HDAC 3) as emerging drug target in NF-kappaB-mediated inflammation.* Curr Opin Chem Biol, 2016. 33: p. 160-8.
107. Nan, J., et al., *TNFR2 Stimulation Promotes Mitochondrial Fusion via Stat3- and NF-kB-Dependent Activation of OPA1 Expression.* Circ Res, 2017. 121(4): p. 392-410.
108. Hoesel, B. and J.A. Schmid, *The complexity of NF-kappaB signaling in inflammation and cancer.* Mol Cancer, 2013. 12: p. 86.
109. Wilson, N.J., et al., *Development, cytokine profile and function of human interleukin 17-producing helper T cells.* Nat Immunol, 2007. 8(9): p. 950-7.
110. Johnston, A., et al., *Keratinocyte overexpression of IL-17C promotes psoriasiform skin inflammation.* J Immunol, 2013. 190(5): p. 2252-62.
111. Scholz, T., et al., *GM-CSF in murine psoriasiform dermatitis: Redundant and pathogenic roles uncovered by antibody-induced neutralization and genetic deficiency.* PLoS One, 2017. 12(8): p. e0182646.
112. Grondona, P., et al., *Threonine Phosphorylation of IkappaBzeta Mediates Inhibition of Selective Proinflammatory Target Genes.* J Invest Dermatol, 2020.
113. Leoni, F., et al., *The histone deacetylase inhibitor ITF2357 reduces production of pro-inflammatory cytokines in vitro and systemic inflammation in vivo.* Mol Med, 2005. 11(1-12): p. 1-15.
114. Chen, X., et al., *Requirement for the histone deacetylase Hdac3 for the inflammatory gene expression program in macrophages.* Proc Natl Acad Sci U S A, 2012. 109(42): p. E2865-74.
115. Zhang, Q., et al., *Tet2 is required to resolve inflammation by recruiting Hdac2 to specifically repress IL-6.* Nature, 2015. 525(7569): p. 389-393.

116. Ramirez-Carrozzi, V.R., et al., *Selective and antagonistic functions of SWI/SNF and Mi-2beta nucleosome remodeling complexes during an inflammatory response.* Genes Dev, 2006. 20(3): p. 282-96.
117. Leonardi, C.L., et al., *Etanercept as Monotherapy in Patients with Psoriasis.* New England Journal of Medicine, 2003. 349(21): p. 2014-2022.
118. Sanford, M. and K. McKeage, *Secukinumab: First Global Approval.* Drugs, 2015. 75(3): p. 329-338.
119. Cervantes, J.L., et al., *TLR8: the forgotten relative revindicated.* Cellular & Molecular Immunology, 2012. 9(6): p. 434-438.
120. Buhl, A.L. and J. Wenzel, *Interleukin-36 in Infectious and Inflammatory Skin Diseases.* Front Immunol, 2019. 10: p. 1162.
121. Verma, A.H., et al., *IL-36 and IL-1/IL-17 Drive Immunity to Oral Candidiasis via Parallel Mechanisms.* J Immunol, 2018. 201(2): p. 627-634.
122. Subramanian, S., et al., *Clinical Toxicities of Histone Deacetylase Inhibitors.* Pharmaceuticals (Basel), 2010. 3(9): p. 2751-2767.
123. Malumbres, M. and M. Barbacid, *Mammalian cyclin-dependent kinases.* Trends Biochem Sci, 2005. 30(11): p. 630-41.
124. Malumbres, M., et al., *Cyclin-dependent kinases: a family portrait.* Nat Cell Biol, 2009. 11(11): p. 1275-6.
125. Schmitz, M.L. and M. Kracht, *Cyclin-Dependent Kinases as Coregulators of Inflammatory Gene Expression.* Trends Pharmacol Sci, 2016. 37(2): p. 101-113.
126. Buss, H., et al., *Cyclin-dependent kinase 6 phosphorylates NF-kappaB P65 at serine 536 and contributes to the regulation of inflammatory gene expression.* PLoS One, 2012. 7(12): p. e51847.
127. Handschick, K., et al., *Cyclin-dependent kinase 6 is a chromatin-bound cofactor for NF-kappaB-dependent gene expression.* Mol Cell, 2014. 53(2): p. 193-208.
128. Kollmann, K., et al., *A kinase-independent function of CDK6 links the cell cycle to tumor angiogenesis.* Cancer Cell, 2013. 24(2): p. 167-81.
129. Tigan, A.S., et al., *CDK6—a review of the past and a glimpse into the future: from cell-cycle control to transcriptional regulation.* Oncogene, 2016. 35(24): p. 3083-3091.
130. Kollmann, K., et al., *The interplay of CDK4 and CDK6 in melanoma.* Oncotarget, 2019. 10(14): p. 1346-1359.
131. Cao, R., et al., *Role of histone H3 lysine 27 methylation in Polycomb-group silencing.* Science, 2002. 298(5595): p. 1039-43.
132. Esteller, M., *Epigenetics in cancer.* N Engl J Med, 2008. 358(11): p. 1148-59.
133. Simon, J.A. and C.A. Lange, *Roles of the EZH2 histone methyltransferase in cancer epigenetics.* Mutat Res, 2008. 647(1-2): p. 21-9.
134. Jacobs, J.J. and M. van Lohuizen, *Polycomb repression: from cellular memory to cellular proliferation and cancer.* Biochim Biophys Acta, 2002. 1602(2): p. 151-61.
135. Orlando, V., *Polycomb, epigenomes, and control of cell identity.* Cell, 2003. 112(5): p. 599-606.
136. Kleer, C.G., et al., *EZH2 is a marker of aggressive breast cancer and promotes neoplastic transformation of breast epithelial cells.* Proc Natl Acad Sci U S A, 2003. 100(20): p. 11606-11.
137. Pasini, D. and L. Di Croce, *Emerging roles for Polycomb proteins in cancer.* Curr Opin Genet Dev, 2016. 36: p. 50-8.
138. Wang, C., et al., *EZH2 Mediates epigenetic silencing of neuroblastoma suppressor genes CASZ1, CLU, RUNX3, and NGFR.* Cancer Res, 2012. 72(1): p. 315-24.
139. Ezhkova, E., et al., *Ezh2 orchestrates gene expression for the stepwise differentiation of tissue-specific stem cells.* Cell, 2009. 136(6): p. 1122-35.
140. Zhou, J., et al., *Targeting EZH2 histone methyltransferase activity alleviates experimental intestinal inflammation.* Nat Commun, 2019. 10(1): p. 2427.

141. Bienvenu, F., H. Gascan, and O. Coqueret, *Cyclin D1 represses STAT3 activation through a Cdk4-independent mechanism.* J Biol Chem, 2001. 276(20): p. 16840-7.
142. Baker, G.L., M.W. Landis, and P.W. Hinds, *Multiple functions of D-type cyclins can antagonize pRb-mediated suppression of proliferation.* Cell Cycle, 2005. 4(2): p. 330-8.
143. Sherr, C.J., *Mammalian G1 cyclins.* Cell, 1993. 73(6): p. 1059-65.
144. Li, Y., et al., *Structural basis of the phosphorylation-independent recognition of cyclin D1 by the SCF(FBXO31) ubiquitin ligase.* Proc Natl Acad Sci U S A, 2018. 115(2): p. 319-324.
145. Sicinska, E., et al., *Requirement for cyclin D3 in lymphocyte development and T cell leukemias.* Cancer Cell, 2003. 4(6): p. 451-61.
146. Sicinski, P., et al., *Cyclin D2 is an FSH-responsive gene involved in gonadal cell proliferation and oncogenesis.* Nature, 1996. 384(6608): p. 470-4.
147. Sicinski, P., et al., *Cyclin D1 provides a link between development and oncogenesis in the retina and breast.* Cell, 1995. 82(4): p. 621-30.
148. Wang, Z., et al., *Characterization of the mouse cyclin D3 gene: exon/intron organization and promoter activity.* Genomics, 1996. 35(1): p. 156-63.
149. Iwanaga, R., et al., *Activation of the cyclin D2 and cdk6 genes through NF-kappaB is critical for cell-cycle progression induced by HTLV-I Tax.* Oncogene, 2008. 27(42): p. 5635-42.
150. Cieslik, M. and S. Bekiranov, *Genome-wide predictors of NF-kappaB recruitment and transcriptional activity.* BioData Min, 2015. 8: p. 37.
151. Baumgart, S., V. Ellenrieder, and M.E. Fernandez-Zapico, *Oncogenic transcription factors: cornerstones of inflammation-linked pancreatic carcinogenesis.* Gut, 2013. 62(2): p. 310-6.
152. Bisteau, X., M.J. Caldez, and P. Kaldis, *The Complex Relationship between Liver Cancer and the Cell Cycle: A Story of Multiple Regulations.* Cancers (Basel), 2014. 6(1): p. 79-111.
153. Piatelli, M.J., C. Doughty, and T.C. Chiles, *Requirement for a hsp90 chaperone-dependent MEK1/2-ERK pathway for B cell antigen receptor-induced cyclin D2 expression in mature B lymphocytes.* J Biol Chem, 2002. 277(14): p. 12144-50.
154. Park, S.Y., et al., *The JAK2/STAT3/CCND2 Axis promotes colorectal Cancer stem cell persistence and radioresistance.* J Exp Clin Cancer Res, 2019. 38(1): p. 399.
155. Li, J., et al., *TRIM28 interacts with EZH2 and SWI/SNF to activate genes that promote mammosphere formation.* Oncogene, 2017. 36(21): p. 2991-3001.
156. Shi, B., et al., *Integration of estrogen and Wnt signaling circuits by the polycomb group protein EZH2 in breast cancer cells.* Mol Cell Biol, 2007. 27(14): p. 5105-19.
157. Chen, S., et al., *Cyclin-dependent kinases regulate epigenetic gene silencing through phosphorylation of EZH2.* Nat Cell Biol, 2010. 12(11): p. 1108-14.
158. Wei, Y., et al., *CDK1-dependent phosphorylation of EZH2 suppresses methylation of H3K27 and promotes osteogenic differentiation of human mesenchymal stem cells.* Nat Cell Biol, 2011. 13(1): p. 87-94.
159. Kim, E., et al., *Phosphorylation of EZH2 activates STAT3 signaling via STAT3 methylation and promotes tumorigenicity of glioblastoma stem-like cells.* Cancer Cell, 2013. 23(6): p. 839-52.
160. Alves de Medeiros, A.K., et al., *JAK3 as an Emerging Target for Topical Treatment of Inflammatory Skin Diseases.* PLoS One, 2016. 11(10): p. e0164080.
161. Wang, X., et al., *Structural biology of shared cytokine receptors.* Annu Rev Immunol, 2009. 27: p. 29-60.
162. Schwartz, D.M., et al., *Type I/II cytokines, JAKs, and new strategies for treating autoimmune diseases.* Nat Rev Rheumatol, 2016. 12(1): p. 25-36.
163. Blauvelt, A., et al., *Interleukin-15 mRNA is expressed by human keratinocytes Langerhans cells, and blood-derived dendritic cells and is downregulated by ultraviolet B radiation.* J Invest Dermatol, 1996. 106(5): p. 1047-52.
164. Heufler, C., et al., *Interleukin 7 is produced by murine and human keratinocytes.* J Exp Med, 1993. 178(3): p. 1109-14.

165. Yin, J., et al., *Ezh2 regulates differentiation and function of natural killer cells through histone methyltransferase activity.* Proc Natl Acad Sci U S A, 2015. 112(52): p. 15988-93.
166. Blank, U., et al., *Vesicular trafficking and signaling for cytokine and chemokine secretion in mast cells.* Front Immunol, 2014. 5: p. 453.
167. Mori, T., et al., *IL-1beta and TNFalpha-initiated IL-6-STAT3 pathway is critical in mediating inflammatory cytokines and RANKL expression in inflammatory arthritis.* Int Immunol, 2011. 23(11): p. 701-12.
168. Calautti, E., L. Avalle, and V. Poli, *Psoriasis: A STAT3-Centric View.* Int J Mol Sci, 2018. 19(1).
169. Miyoshi, K., et al., *Stat3 as a therapeutic target for the treatment of psoriasis: a clinical feasibility study with STA-21, a Stat3 inhibitor.* J Invest Dermatol, 2011. 131(1): p. 108-17.
170. Robinson, A., et al., *Treatment of pustular psoriasis: from the Medical Board of the National Psoriasis Foundation.* J Am Acad Dermatol, 2012. 67(2): p. 279-88.
171. Pfaff, C.M., et al., *The psoriasis-associated IL-17A induces and cooperates with IL-36 cytokines to control keratinocyte differentiation and function.* Sci Rep, 2017. 7(1): p. 15631.
172. Papp, K.A., et al., *Tofacitinib, an oral Janus kinase inhibitor, for the treatment of chronic plaque psoriasis: Long-term efficacy and safety results from 2 randomized phase-III studies and 1 open-label long-term extension study.* J Am Acad Dermatol, 2016. 74(5): p. 841-50.
173. Andres, R.M., et al., *NF-kappaB and STAT3 inhibition as a therapeutic strategy in psoriasis: in vitro and in vivo effects of BTH.* J Invest Dermatol, 2013. 133(10): p. 2362-2371.
174. Sandborn, W.J., et al., *Tofacitinib, an oral Janus kinase inhibitor, in active ulcerative colitis.* N Engl J Med, 2012. 367(7): p. 616-24.
175. Lowes, M.A., M. Suarez-Farinas, and J.G. Krueger, *Immunology of psoriasis.* Annu Rev Immunol, 2014. 32: p. 227-55.
176. Laphanuwat, P. and S. Jirawatnotai, *Immunomodulatory Roles of Cell Cycle Regulators.* Front Cell Dev Biol, 2019. 7: p. 23.
177. Schaer, D.A., et al., *The CDK4/6 Inhibitor Abemaciclib Induces a T Cell Inflamed Tumor Microenvironment and Enhances the Efficacy of PD-L1 Checkpoint Blockade.* Cell Rep, 2018. 22(11): p. 2978-2994.
178. Scheicher, R., et al., *CDK6 as a key regulator of hematopoietic and leukemic stem cell activation.* Blood, 2015. 125(1): p. 90-101.
179. Garzorz-Stark, N. and K. Eyerich, *Psoriasis Pathogenesis: Keratinocytes Are Back in the Spotlight.* J Invest Dermatol, 2019. 139(5): p. 995-996.
180. Vidula, N. and H.S. Rugo, *Cyclin-Dependent Kinase 4/6 Inhibitors for the Treatment of Breast Cancer: A Review of Preclinical and Clinical Data.* Clin Breast Cancer, 2016. 16(1): p. 8-17.
181. Yamagishi, M. and K. Uchimaru, *Targeting EZH2 in cancer therapy.* Curr Opin Oncol, 2017. 29(5): p. 375-381.
182. Hsu, L. and A.W. Armstrong, *Anti-drug antibodies in psoriasis: a critical evaluation of clinical significance and impact on treatment response.* Expert Rev Clin Immunol, 2013. 9(10): p. 949-58.

4 Appendix

Müller A, Dickmanns A, Resch C, Schäkel K, Hailfinger S, Dobbelstein M, Schulze-Osthoff K, and Kramer D. The CDK4/6-EZH2 pathway is a potential therapeutic target for psoriasis. JCI. 2020; doi: 10.1172/JCI134217 (In-Press Preview)

Muller A, Hennig A, Lorscheid S, Grondona P, Schulze-Osthoff K, Hailfinger S and Kramer D. IkappaBzeta is a key transcriptional regulator of IL-36-driven psoriasis-related gene expression in keratinocytes. Proc Natl Acad Sci U S A. 2018;115(40): 10088-93.

IκBζ is a key transcriptional regulator of IL-36–driven psoriasis-related gene expression in keratinocytes

Anne Müller[a], André Hennig[b], Sebastian Lorscheid[a], Paula Grondona[a], Klaus Schulze-Osthoff[a,c], Stephan Hailfinger[a], and Daniela Kramer[a,1]

[a]Interfaculty Institute for Biochemistry, University of Tübingen, 72076 Tübingen, Germany; [b]Center for Bioinformatics, University of Tübingen, 72076 Tübingen, Germany; and [c]German Cancer Consortium, German Cancer Research Center, 69120 Heidelberg, Germany

Edited by Sankar Ghosh, College of Physicians and Surgeons, Columbia University, New York, NY, and accepted by Editorial Board Member Tadatsugu Taniguchi August 17, 2018 (received for review January 24, 2018)

Proinflammatory cytokine signaling in keratinocytes plays a crucial role in the pathogenesis of psoriasis, a skin disease characterized by hyperproliferation and abnormal differentiation of keratinocytes and infiltration of inflammatory cells. Although IL-17A and TNFα are effective therapeutic targets in psoriasis, IL-36 has recently emerged as a proinflammatory cytokine. However, little is known about IL-36 signaling and its downstream transcriptional responses. Here, we found that exposure of keratinocytes to IL-36 induced the expression of IκBζ, an atypical IκB member and a specific transcriptional regulator of selective NF-κB target genes. Induction of IκBζ by IL-36 was mediated by NF-κB and STAT3. In agreement, IL-36–mediated induction of IκBζ was found to be required for the expression of various psoriasis-related genes involved in inflammatory signaling, neutrophil chemotaxis, and leukocyte activation. Importantly, IκBζ-knockout mice were protected against IL-36–mediated dermatitis, accompanied by reduced proinflammatory gene expression, decreased immune cell infiltration, and a lack of keratinocyte hyperproliferation. Moreover, expression of IκBζ mRNA was highly up-regulated in biopsies of psoriasis patients where it coincided with *IL36G* levels. Thus our results uncover an important role for IκBζ in IL-36 signaling and validate IκBζ as an attractive target for psoriasis therapy.

NFKBIZ | IκBζ | IL-36 | keratinocytes | psoriasis

Transcription factor NF-κB has been implicated in several inflammatory diseases, including psoriasis, by activating various proinflammatory target genes (1). The classical activation of NF-κB is controlled by cytoplasmic inhibitory proteins, such as IκBα, which sequester NF-κB in the cytoplasm (2). Inflammatory stimulation of cells results in the rapid activation of IκB kinase (IKK), which triggers the phosphorylation-induced degradation of IκBα, leading to NF-κB's nuclear translocation and transcriptional activation. Recent evidence, however, suggests that the activation of NF-κB target genes is more complex and is dependent on the particular gene context or stimulus, which is thought to facilitate selective gene regulation in distinct physiological settings (3). Whereas the rapid activation of primary response genes is directly induced by the classical NF-κB pathway, expression of so-called "secondary-response genes" requires prior protein synthesis of additional NF-κB regulators (4). In this context, we and others have identified IκBζ, an atypical nuclear IκB protein, which functions not only as a repressor but, more importantly, also as an activator of a selective subset of NF-κB target genes (5–8). The mechanisms of this differential gene regulation by IκBζ remain largely unknown, but increasing evidence suggests that the transcriptional activity of IκBζ is mainly mediated at the level of chromatin remodeling (6, 9, 10).

In keratinocytes (KCs), IL-17A and, more potently, its combination with TNFα induce IκBζ expression (11). Subsequently, IκBζ mediates the induction of important psoriasis-related gene products, including chemokines (e.g., *CXCL8* and *CCL20*), cytokines (e.g., *IL22* and *IL17C*), and antimicrobial proteins, such as S100 calcium-binding proteins (e.g., *S100A9*), β-defensin-2 (*DEFB4A*), or lipocalin-2 (*LCN2*). Antagonists of TNFα and IL-17A have therefore been approved for the treatment of psoriasis (12). Moreover, *NFKBIZ*, the gene encoding IκBζ, has been identified as a psoriasis-susceptibility locus (13). Global *Nfkbiz*-KO mice are resistant to imiquimod (IMQ)- or IL-23–induced psoriasis-like skin inflammation (11). In contrast, *Tnfa*- or *Il17a*-KO mice, which are only partially protected against IMQ-induced psoriasis, still show elevated IκBζ mRNA levels in inflamed skin areas (11). These observations imply an additional IL-17A/TNFα–independent pathway which drives IκBζ expression and thereby contributes to inflammatory gene expression in psoriasis.

Recently, IL-36 cytokines have received attention as therapeutic targets for psoriasis (14). This subfamily of IL-1–related cytokines consists of three proinflammatory members, IL-36α (encoded by *IL1F6*/*IL36A*), IL-36β (encoded by *IL1F8*/*IL36B*), and IL-36γ (encoded by *IL1F9*/*IL36G*) (15–17). All family members bind to a common heterodimeric receptor, composed of IL-36R (also termed "IL-1RL2") and IL-1RAcP, leading to the recruitment of the adapter MyD88 and subsequent activation of NF-κB and MAPK (18). A fourth IL-36 member, IL-36RN, acts as a natural antagonist of IL-36 signaling, as it binds to IL-36R but does not recruit the coreceptor IL-1RAcP (19, 20).

Significance

Psoriasis is an autoinflammatory disease characterized by cytokine-driven keratinocyte proliferation and infiltration of immune cells. While IL-17A and TNFα are established targets in psoriasis therapy, IL-36 is emerging as an important cytokine in this disease. The mechanisms of IL-36–driven proinflammatory responses are largely unknown. Here we identified IκBζ, a transcriptional regulator of selective NF-κB target genes, as a crucial mediator of IL-36 action. In keratinocytes, IκBζ was required for the expression of several psoriasis-related cytokines and chemokines. Moreover, genetic deletion of IκBζ prevented IL-36–mediated dermatitis induction in mice. Since IκBζ is essential not only for IL-36 but also for IL-17 signaling, our results suggest that inhibition of IκBζ function could be a future strategy in psoriasis therapy.

Author contributions: K.S.-O., S.H., and D.K. designed research; A.M., A.H., S.L., P.G., and D.K. performed research; A.M., A.H., S.L., and D.K. analyzed data; and K.S.-O., S.H., and D.K. wrote the paper.

The authors declare no conflict of interest.

This article is a PNAS Direct Submission. S.G. is a guest editor invited by the Editorial Board.

Data deposition: RNA-sequencing data have been deposited in the National Center for Biotechnology Information BioProject database (ID PRJNA465504; Sequence Read Archive accession no. SRP144926).

[1]To whom correspondence should be addressed. Email: daniela.kramer@uni-tuebingen.de.

This article contains supporting information online at www.pnas.org/lookup/suppl/doi:10.1073/pnas.1801377115/-/DCSupplemental.

Published online September 17, 2018.

Importantly, while full-length IL-36 proteins seem to be biologically inactive, activation of IL-36 signaling requires their N-terminal proteolytic processing (19, 21).

IL-36 contributes to skin inflammation by acting on KCs and immune cells. Interestingly, IL-36 can induce a subset of proinflammatory target genes similar to those induced by IL-17A in KCs, including *CXCL8*, *IL23A*, *DEFB4*, or *LCN2* (22–24). Vice versa, IL-17, which is typically expressed by immune cells, induces IL-36γ expression in KCs (25, 26). Therefore, IL-36 appears to have a central position in the interplay between immune cells and KCs. In patients with psoriasis vulgaris, IL-36α and IL-36γ are overexpressed, whereas inactivating mutations of *IL36RN* are enriched in a psoriasis subtype, called "generalized pustular psoriasis" (22, 23, 27, 28). In agreement, mice overexpressing IL-36α in basal KCs exert skin inflammation at 3 wk of age, which is augmented in an *IL36RN*-deficient background (20, 29). In contrast, mice deficient for the IL-36R are fully protected against IMQ-induced psoriasis (30).

Despite its involvement in psoriasis, little is known about IL-36 signaling and its transcriptional responses. In the present study, we found that IL-36α and IL-36γ are potent inducers of IκBζ expression. Moreover, we identified MyD88, NF-κB and STAT3 as crucial components for IL-36–induced IκBζ expression. Silencing of IκBζ in primary human KCs prevented IL-36–mediated up-regulation of multiple psoriasis-associated genes, while a global knockout of IκBζ protected against IL-36–mediated psoriasis-like dermatitis in mice. These results and our finding of a strong correlation of *NFKBIZ* and *IL36G* expression in psoriatic lesions uncover an important role for IκBζ in IL-36 signaling and thus validate IκBζ as an attractive target for psoriasis therapy.

Results

IL-36 Induces IκBζ Expression in KCs. To investigate the relationship between IL-36 and IκBζ, we treated the keratinocyte cell line HaCaT and primary human KCs with recombinant IL-36α for 1–24 h. Whereas untreated KCs lacked IκBζ expression, 1 h of stimulation with IL-36α was sufficient to induce sustained IκBζ expression on the mRNA and protein level (Fig. 1*A*). As revealed by the addition of actinomycin D to IL-36α–treated cells, the increased *NFKBIZ* mRNA levels resulted from transcriptional up-regulation of *NFKBIZ* rather than from mRNA stabilization (*SI Appendix*, Fig. S1*A*). Importantly, full-length IL-36α, which supposedly lacks biological activity, failed to induce IκBζ expression, whereas IL-17A, either alone or combined with TNFα, induced IκBζ expression with kinetics similar to those of truncated IL-36α (Fig. 1*A* and *SI Appendix*, Fig. S1 *B* and *C*). As some reports implied distinct target gene regulation by the different IL-36 members (14, 24, 25), we also stimulated HaCaT cells and primary KCs with IL-36γ. IL-36γ induced *NFKBIZ* mRNA and protein expression with kinetics and potency similar to that of IL-36α (Fig. 1*B*).

We next investigated whether other psoriasis-associated cytokines, such as IL-1β, IL-17A, TNFα, or IFNγ, could potentiate the effect of IL-36α on IκBζ protein expression (Fig. 1*C*). Although certain differences were noted between HaCaT cells and primary KCs, most of the tested cytokines enhanced IL-36α–mediated IκBζ expression. Importantly, the combination of IL-17A and IL-36α was clearly more effective in triggering IκBζ expression than were the single cytokines alone.

Induction of IκBζ by IL-36 Is Mediated by MyD88, NF-κB, and STAT3. As IκBζ is also induced by IL-17A, we further dissected the mechanism of IκBζ expression induced by IL-36 compared to IL-17A. IL-17A binds and activates the IL-17RA/IL-17RC receptor, followed by the recruitment of the adapter protein Act1 and the activation of MAPK and NF-κB (31). In contrast, IL-36 utilizes a divergent proximal signaling cascade by binding to the IL-36

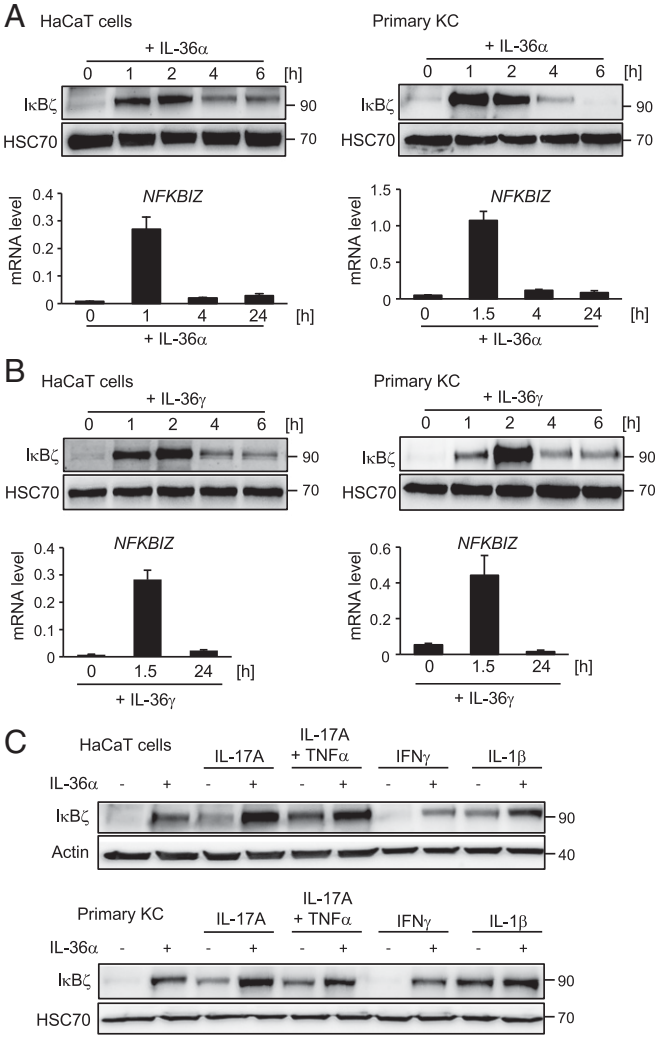

Fig. 1. IL-36 induces IκBζ expression in KCs. (*A* and *B*) HaCaT cells (*Left*) or human primary KCs (*Right*) were treated with 100 ng/mL IL-36α (amino acids 6–158) (*A*) or 100 ng/mL IL-36γ (amino acids 18–169) (*B*) for the indicated times. IκBζ protein was analyzed by Western blotting. Relative mRNA levels of *NFKBIZ* were measured in parallel and normalized to the reference *RPL37A*. (*C*) HaCaT cells (*Upper*) and primary KCs (*Lower*) were treated for 2 h with 100 ng/mL IL-36α alone or in combination with 100 ng/mL IL-17A, 10 ng/mL TNFα, 100 ng/mL IFNγ, or 100 ng/mL IL-1β. IκBζ was detected by Western blotting. HSC70 or β-actin served as loading controls.

receptor complex, composed of IL1RL2 and its coreceptor IL1RAP, leading to the recruitment of MyD88 and activation of MAPK and NF-κB (17). Indeed, knockdown of MyD88 revealed that it was indispensable for IκBζ expression upon IL-36α stimulation, while it had no effect in IL-17A–treated cells (Fig. 2*A* and *SI Appendix*, Fig. S2*A*).

As IκBζ is transcriptionally induced by IL-36, we explored the *NFKBIZ* promoter region to identify relevant transcription factors. Two major IκBζ isoforms have been described, including a long isoform ($IκBζ_L$) of 718 aa and a N-terminally truncated isoform ($IκBζ_{SS}$) of 618 aa that is thought to be generated by alternative splicing (8, 32). By analyzing published DNase I and Pol II ChIP-sequencing (ChIP-seq) data (33), we identified that the two isoforms arise not only from alternative splicing but also from two different promoter regions with distinct transcriptional start sites (Fig. 2*B*). Moreover, our own RNA-sequencing (RNA-seq) data revealed that KCs use only the proximal promoter 2 that is translated into the $IκBζ_L$ isoform. Previous promoter

IMMUNOLOGY AND INFLAMMATION

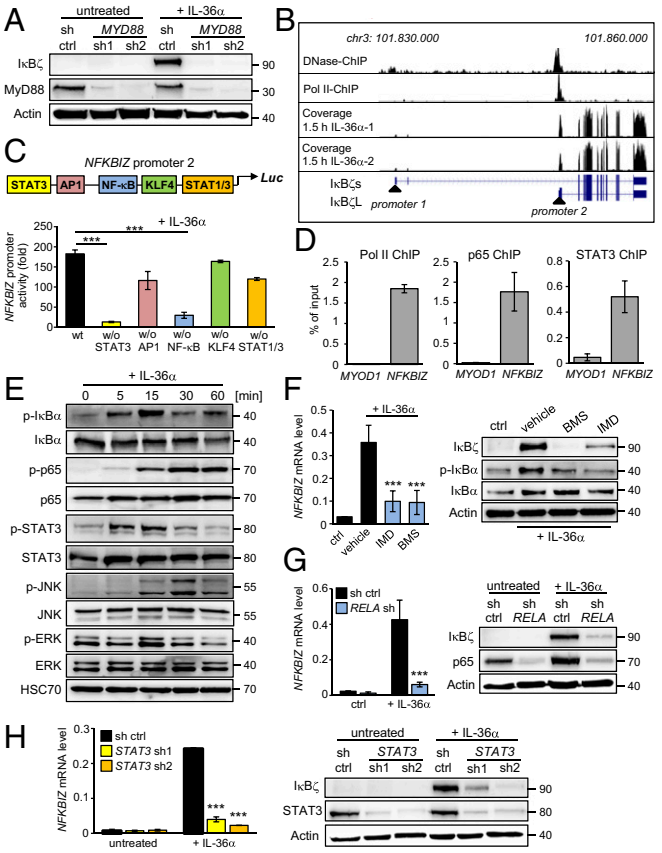

Fig. 2. Molecular dissection of IκBζ induction by IL-36. HaCaT cells were stimulated for the indicated times with 100 ng/mL IL-36α. (*A*) Cells stably expressing a control (sh ctrl) or two different shRNAs targeting *MyD88* were treated for 2 h with IL-36α and were analyzed by Western blotting. (*B*) Analysis of *NFKBIZ* promoter accessibility and structure. The genomic region around *NFKBIZ* was analyzed from a published DNase I dataset and a polymerase II ChIP-seq track (33). Exon reads of *NFKBIZ* were derived from our own RNA-seq data of HaCaT cells stimulated for 1.5 h with IL-36α. (*C*) Analysis of the *NFKBIZ* promoter 2 region in IL-36α–stimulated HaCaT cells using luciferase reporter constructs harboring deletions of transcription factor-binding sites. (*D*) P65, STAT3, and RNA polymerase II (Pol II) bind to *NFKBIZ* promoter region 2 in IL-36α–treated cells. ChIP was performed from HaCaT cells treated for 30 min with IL-36α. The promoter region of the muscle-specific gene *MYOD1* represents a negative control. (*E*) Immunoblot analysis of IL-36α–induced signaling pathways. Active NF-κB and STAT3 were detected by the phosphorylated forms of IκBα (p-IκBα at Ser32), p65 (p-p65 at Ser536), and STAT3 (p-STAT3 at Tyr705). MAPK activation was detected by phosphorylated JNK (p-JNK at Thr183/Tyr185) and ERK (p-p44/42 at Thr202/Thr204). (*F*) Cells were treated for 1 h with IL-36α in the presence or absence of the vehicle DMSO or 10 μM of the IKK inhibitors BMS-345541 or IMD0354. *NFKBIZ* mRNA and IκBζ protein levels were measured after 2 h of IL-36α stimulation. Detection of p-IκBα served as a control for NF-κB inhibition. (*G* and *H*) Gene expression and Western blot analysis of IκBζ in control and *RELA* (p65)-knockdown (*G*) or *STAT3*-knockdown (*H*) cells after 1 h of IL-36α treatment. Knockdown was controlled by detection of p65 or STAT3. ***$P < 0.001$.

analyses, however, had examined only promoter 1, which is located ∼20 kb upstream of promoter 2 (32, 34, 35). This distal promoter is used in several cell types for transcription of *NFKBIZ* variant 2, which lacks exon 3 and thus is translated to the IκBζS variant.

Bioinformatic analysis of the *NFKBIZ* promoter 2 revealed putative binding sites for STAT3, NF-κB, AP1, KLF4, and STAT1. To uncover the contribution of these sites to *NFKBIZ* induction, we cloned the promoter region (∼1.5 kb upstream of the transcription start site of IκBζL) into a luciferase construct and generated deletions lacking one of the predicted binding sites. Expression of the constructs was analyzed after transfection of HaCaT cells followed by stimulation with IL-36α. Indeed, expression of the *NFKBIZ* promoter 2 was significantly increased by IL-36α, whereas deletion of the STAT3- or the NF-κB–binding site inhibited *NFKBIZ* promoter expression (Fig. 2*C*). In accordance, ChIP identified a direct physical binding of NF-κB p65 and STAT3 to *NFKBIZ* promoter 2, along with the binding of phosphorylated RNA polymerase II as a marker for active transcription (Fig. 2*D*). IL-36α also triggered the early activation of STAT3, NF-κB, and MAPK in HaCaT cells or primary KCs (Fig. 2*E* and *SI Appendix*, Fig. S2*B*). Interestingly, a similar activation of STAT3 and NF-κB was detected in IL-17A–treated cells (*SI Appendix*, Fig. S2*C*). Whereas inhibition of MAPK did not affect IκBζ expression in IL-36α–treated HaCaT cells (*SI Appendix*, Fig. S2*D*), the blocking of NF-κB activation by IKK inhibition or knockdown of p65 efficiently prevented IκBζ expression upon IL-36α stimulation (Fig. 2 *F* and *G*). Moreover, depletion of STAT3 by two different shRNAs strongly inhibited IκBζ mRNA and protein expression (Fig. 2*H*). Similarly, depletion of p65 or STAT3 impaired IκBζ induction after stimulation with IL-17A (*SI Appendix*, Fig. S2 *E* and *F*). Thus, IL-36α and IL-17A both employ NF-κB and STAT3 for IκBζ induction.

IκBζ Is a Key Mediator of IL-36–Induced Gene Expression in KCs. Next, we investigated the function of IκBζ in IL-36 signaling and therefore first explored the time course of IκBζ-modulated gene expression. We stimulated control and *NFKBIZ*-knockdown HaCaT cells for 0–24 h with IL-36α and analyzed selected IL-36 target genes. IL-36α stimulation led to the induction of *IL36G*, *IL17C*, *CXCL5*, or *S100A9* with different kinetics (*SI Appendix*, Fig. S3*A*). Surprisingly, *NFKBIZ* silencing not only prevented the induction of late-responsive genes such as *S100A9* but also affected early gene induction, e.g., of *IL36G* or *IL17C*.

To reveal a global picture of IL-36–driven gene expression by IκBζ, we generated control and *NFKBIZ*-depleted primary KCs and performed transcriptome analyses after 1.5 and 24 h of IL-36α stimulation (Fig. 3 *A* and *B*). Silencing of IκBζ resulted in the deregulation of several hundred target genes in IL-36α–stimulated primary human KCs (*SI Appendix*, Tables S1 and S2). Interestingly, early after IL-36α stimulation most genes were down-regulated by IκBζ, including genes for antiinflammatory phosphatases (*DUSP2* and *DUSP9*). In contrast, after 24 h most IκBζ-modulated genes were positively regulated and hence were down-regulated by the *NFKBIZ* knockdown. Many of these IκBζ-inducible genes are typically overexpressed in psoriasis, including genes for antimicrobial proteins (*DEFB4* and *LCN2*), S100 proteins (*S100A7*, *S100A8*, and *S100A9*), and chemo- and cytokines (*CSF2*, *CSF3*, *CXCL8*, *IL23A*, and *IL36A*).

Principal component analysis (PCA) revealed that the gene-expression profile not only differed between untreated and IL-36α–stimulated cells but was also divergent after 1.5 and 24 h of IL-36α stimulation (*SI Appendix*, Fig. S3*B*). Moreover, as shown in the Venn diagrams in Fig. 3 *C* and *D*, only a subset of the IL-36α–regulated genes was IκBζ-dependent (83 of 607 genes after 1.5 h and 86 of 800 genes after 24 h of IL-36α stimulation). Gene ontology (GO) term analysis of the affected genes uncovered that IκBζ mostly regulated inflammatory responses, neutrophil chemotaxis, and leukocyte function downstream of IL-36 (Fig. 3*D*). We also compared our RNA-seq analyses with a previously defined IL-36 core signature comprising 182 genes that were regulated by IL-36 after 24 h in human KCs (14). The comparison not only revealed a high overlap with our RNA-seq analyses but also identified 39 of the 182 IL-36 core target genes as IκBζ-dependent (*SI Appendix*, Fig. S3 *C* and *D*).

The IκBζ-dependent gene regulation by IL-36α in primary KCs at early and late time points was confirmed by qPCR of

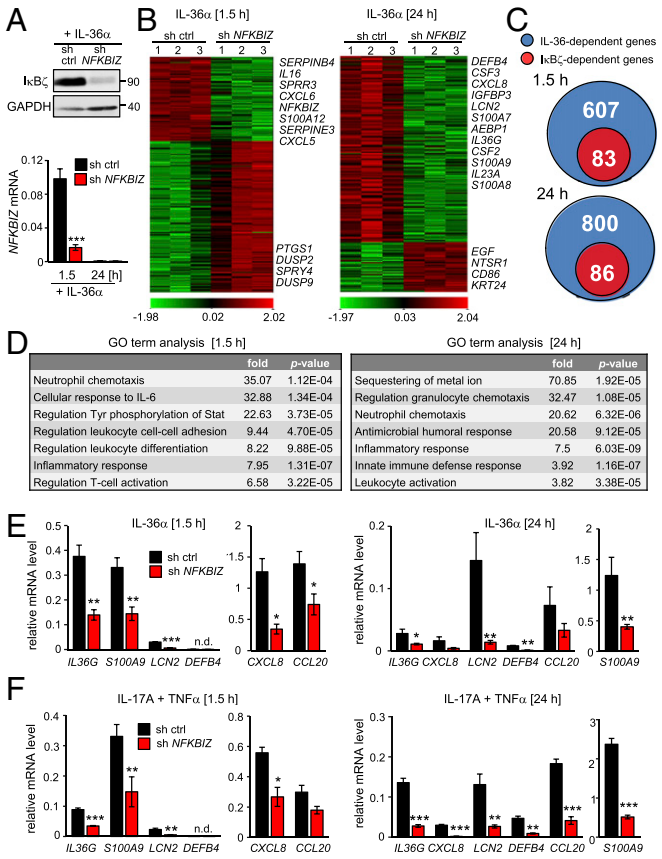

GO term analysis [1.5 h]	fold	p-value
Neutrophil chemotaxis	35.07	1.12E-04
Cellular response to IL-6	32.88	1.34E-04
Regulation Tyr phosphorylation of Stat	22.63	3.73E-05
Regulation leukocyte cell-cell adhesion	9.44	4.70E-05
Regulation leukocyte differentiation	8.22	9.88E-05
Inflammatory response	7.95	1.31E-07
Regulation T-cell activation	6.58	3.22E-05

GO term analysis [24 h]	fold	p-value
Sequestering of metal ion	70.85	1.92E-05
Regulation granulocyte chemotaxis	32.47	1.08E-05
Neutrophil chemotaxis	20.62	6.32E-06
Antimicrobial humoral response	20.58	9.12E-05
Inflammatory response	7.5	6.03E-09
Innate immune defense response	3.92	1.16E-07
Leukocyte activation	3.82	3.38E-05

Fig. 3. IκBζ regulates a subset of psoriasis-related IL-36 target genes. Primary KCs or HaCaT cells were transduced with a control or *NFKBIZ*-specific shRNA. Triplicates of each time point and shRNA were analyzed by RNA-seq or qPCR and were normalized to the reference gene *RPL37A*. (*A*) Control of *NFKBIZ*-knockdown efficiency. (*Upper*) IκBζ protein was detected in primary KCs treated for 1 h with 100 ng/mL IL-36α. (*Lower*) *NFKBIZ* mRNA levels were measured after 1.5 h and 24 h of IL-36α stimulation. (*B*) After library preparation from total RNA, primary KC samples were sequenced, and reads were aligned to the human genome hg19. Depicted are two separate heatmaps with normalized z-scores of IκBζ target genes after 1.5 h and 24 h of IL-36α treatment. As a cutoff, genes with a minimum fold change of 1 and a *P* value < 0.05 were considered. (*C*) Venn diagrams showing the fraction of IκBζ target genes among IL-36α–regulated genes 1.5 and 24 h after stimulation of primary KCs. (*D*) GO term analysis of significantly enriched IκBζ-dependent gene sets after 1.5 and 24 h of IL-36α treatment. (*E*) Validation of selected IκBζ target genes by qPCR in primary KCs after 1.5 and 24 h of incubation with 100 ng/mL IL-36α. (*F*) Gene-expression analysis of IκBζ target genes in primary KCs stimulated with 100 ng/mL IL-17A and 10 ng/mL TNFα for 1.5 and 24 h. **P* < 0.05; ***P* < 0.01; ****P* < 0.001.

selected genes, such as *IL36G*, *S100A9*, *LCN2*, *DEFB4*, *CXCL8*, and *CCL20* (Fig. 3*E*). Importantly, regulation of these IκBζ target genes was conserved in IL-17A– and TNFα–treated primary KCs as well as in IL-36α–, IL-36γ–, and IL-1β–treated HaCaT cells (Fig. 3*F* and *SI Appendix*, Fig. S4 *A–C*). These findings thus implicate IκBζ as a master regulator of proinflammatory gene expression not only in IL-36–stimulated but also in IL-17A–,TNFα–, or IL-1β–treated KCs.

IκBζ Promotes IL-36–Driven Psoriasis-Like Disease in Vivo. Global *Nfkbiz*-KO mice are protected against IMQ-induced psoriasis-like skin inflammation (11). Since the TLR7 agonist IMQ directly activates the innate immune response, it is difficult to discriminate between the contribution of IL-17 and IL-36 to the disease onset. Moreover, global *Nfkbiz*-KO mice develop an autoinflammatory phenotype in adulthood (36, 37), which could influence the skin inflammation of IMQ-treated mice. We therefore generated a mouse model using tamoxifen-inducible *Nfkbiz*-KO mice that received intradermal injections of active IL-36α into the ears. Tamoxifen-induced Cre recombinase activation just before IL-36α application led to an effective KO of IκBζ, thereby preventing potential congenital off-target effects (Fig. 4*A*). Intradermal injection of IL-36α into the ears of control animals induced *Nfkbiz* transcription (Fig. 4*A*) and, moreover, triggered ear swelling, scaling, epidermal thickening, KC hyperproliferation and increased infiltration of immune cells (Fig. 4 *B*

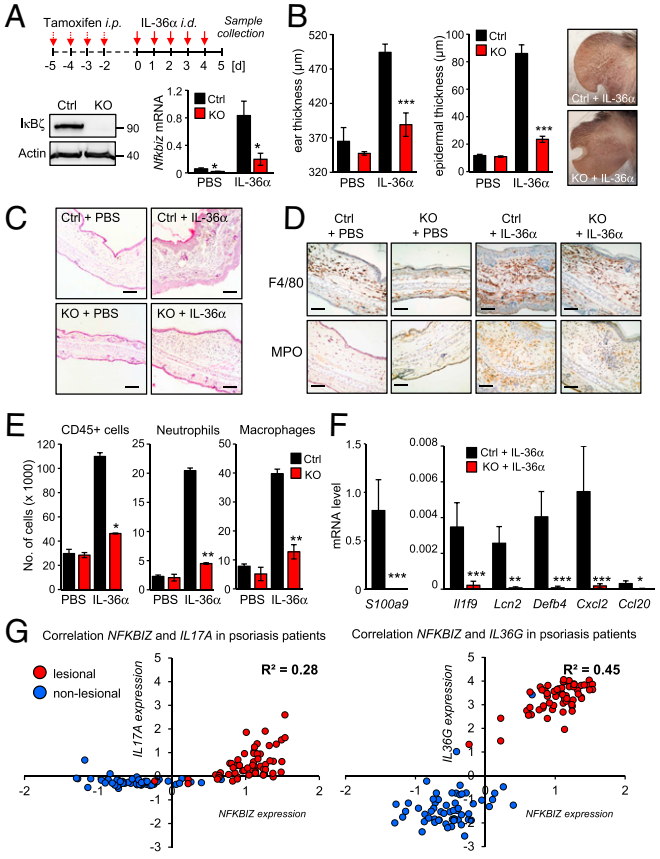

Fig. 4. Characterization of the IL-36/IκBζ axis in vivo. (*A*, *Upper*) Scheme of tamoxifen and IL-36α treatment of control and inducible *Nfkbiz*-KO mice. (*Lower*) Verification of *Nfkbiz* deletion at the protein and mRNA level. For induction of IκBζ KO, *Nfkbiz* flox/flox (Ctrl) and Rosa-creERT2 *Nfkbiz* flox/flox (KO) mice received i.p. injections of tamoxifen (75 mg/kg) for four consecutive days to induce activation of Cre recombinase. Afterward, 1 μg murine IL-36α or PBS control was intradermally injected into one ear of the mice for five consecutive days. (*B*) Ear and epidermal thickness (± SEM) of PBS- and IL-36α–treated mice at day 5 from two (for PBS) or six (for IL-36α) animals per group. Pictures were taken at day 5 to show scaling at the treatment area. (*C*) H&E staining of ears from PBS- and IL-36α–treated control and KO mice. (Scale bars: 140 μM.) (*D*) Immunohistochemistry for the macrophage marker F4/80 and the neutrophil marker MPO. (Scale bars: 80 μM) (*E*) Characterization of $CD45^+$ immune cell infiltrates by flow cytometry. Neutrophils were characterized as $CD45^+$ $Ly6G^+$ and macrophages as $CD45^+$, $CD11b^{hi}$ and $F4/80^+$. Error bars indicate results from two independent experiments. (*F*) Psoriasis-related gene expression in ears from IL-36α–treated mice. Results are shown as means ± SEM; *n* = 6 animals per group. (*G*) Expression data from skin biopsies of 64 healthy individuals and 58 psoriasis patients were analyzed from the Gene Expression Omnibus profile dataset GDS4602. Shown are normalized expression values of *NFKBIZ* and *IL17A* or *NFKBIZ* and *IL36G*, which were plotted against each other in every single nonlesional and lesional biopsy. Depicted is the regression coefficient (R^2) from the expression values of the psoriatic skin biopsies. **P* < 0.05; ***P* < 0.01; ****P* < 0.001.

and *C* and *SI Appendix*, Fig. S5*A*). These alterations were nearly absent in the IL-36α–treated KO mice. Histological and flow cytometric analyses revealed a marked increase in infiltrating $CD45^+$ immune cells, macrophages, and neutrophils in the IL-36α–treated control animals, which was significantly blocked in the KO mice (Fig. 4 *D* and *E*). T cell infiltration was reduced in the KO animals as well, although the degree of T cell infiltration was generally low in the ears of IL-36α–treated mice (*SI Appendix*, Fig. S5*B*). Importantly, expression of several psoriasis-associated target genes, similar to those identified by transcriptome analysis of IL-36α–treated KCs (Fig. 3), was up-regulated in the ears of IL-36a-treated control but not in IL-36α–treated KO mice (Fig. 4*E*). Likewise, the expression of IκBζ-dependent proteins involved in granulocyte and leukocyte chemotaxis was also decreased in the KO mice (*SI Appendix*, Fig. S5*C*). Thus, IκBζ KO strongly protected against IL-36–driven psoriasis-like disease in vivo, which could be mediated by effects of *Nfkbiz* deficiency in KCs as well as in immune cells.

As previously reported (11, 13), we validated increased *NFKBIZ* expression in lesions from psoriasis patients, as compared with nonlesional skin areas or unaffected individuals (*SI Appendix*, Fig. S5*D*). Expression of *IL17A* and especially *IL36G* was elevated in psoriatic lesions. We then correlated the expression of *NFKBIZ*, *IL36G*, and *IL17A* in nonlesional and lesional samples in the individual patients to obtain an idea of the relevance of the two cytokines in driving *NFKBIZ* expression in psoriatic tissue. The correlation of *IL36G* and *NFKBIZ* was stronger than the link between *IL17A* and *NFKBIZ*, implicating IL-36 as an important driver of *NFKBIZ* expression in psoriasis (Fig. 4*G*). Moreover, as IL-36–mediated *NFKBIZ* induction could account for increased expression of psoriasis-related cytokines, we correlated the expression of *LCN2*, a bona fide IκBζ target gene (38), to *IL36G*, *NFKBIZ*, and *IL17A* expression. Indeed, the expression level of *LCN2* matched strongly *IL36G* and *NFKBIZ* expression, whereas it was only weakly correlated to *IL17A* expression patterns in psoriatic lesions (*SI Appendix*, Fig. S5*E*). These findings support a major role of IκBζ in IL-36 signaling in KCs and psoriasis and suggest IκBζ as an attractive therapeutic target which mediates proinflammatory signaling downstream of IL-17A and IL-36.

Discussion

Previous studies by us and others found that IκBζ is overexpressed in psoriatic lesions, whereas *Nfkbiz* KO mice are protected against IMQ-induced psoriatic skin inflammation (11, 13). In these and follow-up studies, IκBζ was identified as a major mediator of IL-17A signaling, leading to the induction of proinflammatory signaling in KCs (11, 39). Interestingly, in *Il17a*- or *Il17ra*- KO mice neither induction of *Nfkbiz* nor skin inflammation were fully blocked after IMQ treatment (11, 40), implying additional pathways of *NFKBIZ* induction and promotion of psoriasis.

Recently, IL-36α and IL-36γ have been identified as being overexpressed in psoriatic lesions (22, 23). In agreement, IL-36 treatment of KCs induced proinflammatory signaling (14), whereas KO of the IL-36 receptor inhibited IMQ-induced skin inflammation in mice. Our results show that IκBζ provides an important link between IL-36 signaling and psoriasis-associated inflammatory gene expression. We revealed that IL-36 mediates IκBζ expression in HaCaT cells and primary KCs, which followed kinetics similar to those seen with IL-17A/TNFα treatment, implying similar signaling pathways in IκBζ induction.

By ChIP-seq data and our own RNA-seq analyses we identified that KCs induce transcription of *NFKBIZ* from the yet uncharacterized proximal promoter 2, which contains several conserved binding sites for proinflammatory transcription factors. Indeed, IL-36 and IL-17A stimulation led to the activation of NF-κB, whereas knockdown of the NF-κB subunit p65 prevented IκBζ induction.

Besides NF-κB, we identified STAT3 as a regulator of IκBζ expression, as its depletion was sufficient to block IL-36– and IL-17A–mediated induction of IκBζ. These findings are intriguing, as STAT3 itself can drive proinflammatory gene expression in psoriasis (41). Constitutively active STAT3 in the epidermis of psoriatic lesions is often detectable, whereas pharmacological inhibition of STAT3 ameliorated psoriasis-like skin lesions in mice (42, 43). Moreover, STAT3 was proposed to control IκBζ expression in T cells (44). As STAT3 is especially involved in IL-36–driven induction of IκBζ expression, STAT3 inhibitors could be promising agents for the effective treatment of general pustular psoriasis, which is caused by mutations of IL36RN and hyperactivation of the IL-36 pathway (27, 28).

Our gene-expression profiling revealed that IL-36 affected the expression of hundreds of genes at early and late stimulation time points. As early effects of IL-36 stimulation on gene expression have not been investigated before in KCs, we could not only validate defined IL-36 target genes (14) but also identify previously unknown IL-36 dependent genes (e.g., *IL17C*, *CSF2, CSF3*) that encode important psoriasis-promoting cytokines (45–46). Of note, *NFKBIZ* knockdown led to the deregulation of a specific subset of IL-36 target genes at early and late stimulation time points. Most of these IκBζ-dependent IL-36 target genes regulate antimicrobial and proinflammatory responses, neutrophil chemotaxis, and leukocyte activation and hence have been implicated in the pathogenesis of psoriasis. Moreover, IκBζ-dependent gene expression seems to be highly conserved, as we found similar changes in the expression of IκBζ-dependent genes (e.g., *DEFB4*, *CCL20*, *S100A7*, *S100A9*, and *LCN2*) in HaCaT cells and primary KCs as well as upon IL-36α, IL-36γ, or IL-17A/TNFα stimulation.

Employing an inducible *Nfkbiz*-KO model, we further demonstrate that the absence of IκBζ also impaired psoriasis-related gene expression under in vivo conditions of IL-36α stimulation. *Nfkbiz*-KO mice exhibited significantly reduced skin pathology, including less ear swelling and KC proliferation, and a strongly reduced infiltration of immune cells, in particular neutrophils. The results are consistent with findings in *Il36r*-deficient mice that are also protected in the IMQ psoriasis model (30). Notably, our previous study demonstrated that *Nfkbiz*-KO mice were even more protected than *Il17a*-deficient mice (11), supporting the idea that IκBζ might also be involved in IL-17–independent effects of psoriasis development. Of note, *Il36r*-deficient mice also showed stronger protection in the IMQ model than *Il17a*-KO mice (30).

In agreement with our findings in cultured KCs and *Nfkbiz*-KO mice, expression data from psoriasis patients validated elevated *NFKBIZ* and *IL36G* levels in psoriatic lesions as compared with nonaffected skin areas or skin from unaffected healthy individuals. Moreover, the expression of *IL36G* and *NFKBIZ* was strongly correlated with the IκBζ target gene *LCN2* compared with a much weaker correlation of *IL17A* with *NFKBIZ* and *LCN2* expression levels. These data strengthen the hypothesis that IL-36 is an initial driver for *NFKBIZ* expression in psoriasis.

While our results clearly position IκBζ downstream of IL-36, IL-17A and IL-36, in turn, are also transcriptional targets downstream of IκBζ (*SI Appendix*, Fig. S4*D*). Likewise, IL-17A, especially in combination with TNF, is a strong inducer of IκBζ expression but can be also induced downstream of IκBζ. Thus, the strong expression of *NFKBIZ* in psoriasis patients might be caused not only by elevated IL-36 expression but also by increased IL-17–type responses. The exact contribution of each cytokine is complicated by the existence of multiple members of the IL-17 and IL-36 families. Because IL-17 and IL-36 can mutually reinforce each other (25, 26), the two cytokines drive

complex autoamplification loops in which IκBζ seems to have an integral role in promoting skin inflammation (for a scheme see *SI Appendix*, Fig. S6). In fact, our present and previous results (11) suggest a dual requirement for IκBζ in IL-36 signaling of innate epithelial cells, such as KCs, as well as in IL-17A signaling of T cells, both of which might be necessary to drive full-blown psoriasis.

In conclusion, our findings reveal that two major cytokines, IL-36 and IL-17A, promote psoriasis by inducing IκBζ expression. While IL-17A antibodies have proven therapeutic efficacy, blocking of IL-36 might represent an alternative for patients resistant to anti–IL-17A therapy. Moreover, targeting their common mediator IκBζ might lead to future approaches for efficient long-term treatment of psoriasis patients.

Materials and Methods

Detailed information on cell culture experiments, generation of knockdown cells, luciferase reporter assays, ChIP, analyses of RNA and protein expression, RNA-seq, cytokine antibody arrays, generation of *Nfkbiz*-KO mice, flow cytometry, histology, and analysis of patient data is provided in *SI Appendix*.

ACKNOWLEDGMENTS. We thank C. Schönfeld, C. Resch, and J. Loeffler for assistance and A. Witten and M. Stoll (University of Münster) for transcriptome profiling. Murine IL-36α was generously provided by Amgen. This work was supported by the grants Sonderforschungsbereich/Transregio SFB/TR 156 (to S.H. and D.K.), SFB/TR 209 (to K.S.-O. and S.H.), the Emmy-Noether program of the Deutsche Forschungsgemeinschaft (to S.H.), and the German Ministry for Education and Research Grant of the Network for Autoinflammatory Disorders in Children and Adolescents 01FP09104B (to K.S.-O.).

1. Vallabhapurapu S, Karin M (2009) Regulation and function of NF-kappaB transcription factors in the immune system. *Annu Rev Immunol* 27:693–733.
2. Renner F, Schmitz ML (2009) Autoregulatory feedback loops terminating the NF-kappaB response. *Trends Biochem Sci* 34:128–135.
3. Smale ST (2011) Hierarchies of NF-κB target-gene regulation. *Nat Immunol* 12: 689–694.
4. Annemann M, et al. (2016) Atypical IκB proteins in immune cell differentiation and function. *Immunol Lett* 171:26–35.
5. Totzke G, et al. (2006) A novel member of the IkappaB family, human IkappaB-zeta, inhibits transactivation of p65 and its DNA binding. *J Biol Chem* 281:12645–12654.
6. Hildebrand DG, et al. (2013) IκBζ is a transcriptional key regulator of CCL2/MCP-1. *J Immunol* 190:4812–4820.
7. Yamamoto M, et al. (2004) Regulation of Toll/IL-1-receptor-mediated gene expression by the inducible nuclear protein IkappaBzeta. *Nature* 430:218–222.
8. Kitamura H, Kanehira K, Okita K, Morimatsu M, Saito M (2000) MAIL, a novel nuclear I kappa B protein that potentiates LPS-induced IL-6 production. *FEBS Lett* 485:53–56.
9. Kayama H, et al. (2008) Class-specific regulation of pro-inflammatory genes by MyD88 pathways and IkappaBzeta. *J Biol Chem* 283:12468–12477.
10. Tartey S, et al. (2014) Akirin2 is critical for inducing inflammatory genes by bridging IκB-ζ and the SWI/SNF complex. *EMBO J* 33:2332–2348.
11. Johansen C, et al. (2015) IκBζ is a key driver in the development of psoriasis. *Proc Natl Acad Sci USA* 112:E5825–E5833.
12. Lowes MA, Suárez-Fariñas M, Krueger JG (2014) Immunology of psoriasis. *Annu Rev Immunol* 32:227–255.
13. Tsoi LC, et al. (2015) Enhanced meta-analysis and replication studies identify five new psoriasis susceptibility loci. *Nat Commun* 6:7001.
14. Mahil SK, et al. (2017) An analysis of IL-36 signature genes and individuals with *IL1RL2* knockout mutations validates IL-36 as a psoriasis therapeutic target. *Sci Transl Med* 9: eaan2514, and erratum (2017) 9:eaar6600.
15. Dunn E, Sims JE, Nicklin MJ, O'Neill LA (2001) Annotating genes with potential roles in the immune system: Six new members of the IL-1 family. *Trends Immunol* 22:533–536.
16. Dinarello CA (2018) Overview of the IL-1 family in innate inflammation and acquired immunity. *Immunol Rev* 281:8–27.
17. Bassoy EY, Towne JE, Gabay C (2018) Regulation and function of interleukin-36 cytokines. *Immunol Rev* 281:169–178.
18. Towne JE, Garka KE, Renshaw BR, Virca GD, Sims JE (2004) Interleukin (IL)-1F6, IL-1F8, and IL-1F9 signal through IL-1Rrp2 and IL-1RAcP to activate the pathway leading to NF-kappaB and MAPKs. *J Biol Chem* 279:13677–13688.
19. Towne JE, et al. (2011) Interleukin-36 (IL-36) ligands require processing for full agonist (IL-36α, IL-36β, and IL-36γ) or antagonist (IL-36Ra) activity. *J Biol Chem* 286: 42594–42602.
20. Blumberg H, et al. (2007) Opposing activities of two novel members of the IL-1 ligand family regulate skin inflammation. *J Exp Med* 204:2603–2614.
21. Afonina IS, Müller C, Martin SJ, Beyaert R (2015) Proteolytic processing of interleukin-1 family cytokines: Variations on a common theme. *Immunity* 42:991–1004.
22. D'Erme AM, et al. (2015) IL-36γ (IL-1F9) is a biomarker for psoriasis skin lesions. *J Invest Dermatol* 135:1025–1032.
23. Boutet MA, et al. (2016) Distinct expression of interleukin (IL)-36α, β and γ, their antagonist IL-36Ra and IL-38 in psoriasis, rheumatoid arthritis and Crohn's disease. *Clin Exp Immunol* 184:159–173.
24. Johnston A, et al. (2011) IL-1F5, -F6, -F8, and -F9: A novel IL-1 family signaling system that is active in psoriasis and promotes keratinocyte antimicrobial peptide expression. *J Immunol* 186:2613–2622.
25. Carrier Y, et al. (2011) Inter-regulation of Th17 cytokines and the IL-36 cytokines in vitro and in vivo: Implications in psoriasis pathogenesis. *J Invest Dermatol* 131: 2428–2437.
26. Pfaff CM, Marquardt Y, Fietkau K, Baron JM, Lüscher B (2017) The psoriasis-associated IL-17A induces and cooperates with IL-36 cytokines to control keratinocyte differentiation and function. *Sci Rep* 7:15631.
27. Marrakchi S, et al. (2011) Interleukin-36-receptor antagonist deficiency and generalized pustular psoriasis. *N Engl J Med* 365:620–628.
28. Onoufriadis A, et al. (2011) Mutations in IL36RN/IL1F5 are associated with the severe episodic inflammatory skin disease known as generalized pustular psoriasis. *Am J Hum Genet* 89:432–437.
29. Blumberg H, et al. (2010) IL-1RL2 and its ligands contribute to the cytokine network in psoriasis. *J Immunol* 185:4354–4362.
30. Tortola L, et al. (2012) Psoriasiform dermatitis is driven by IL-36-mediated DC-keratinocyte crosstalk. *J Clin Invest* 122:3965–3976.
31. Gaffen SL (2009) Structure and signalling in the IL-17 receptor family. *Nat Rev Immunol* 9:556–567.
32. Yamazaki S, Muta T, Matsuo S, Takeshige K (2005) Stimulus-specific induction of a novel nuclear factor-kappaB regulator, IkappaB-zeta, via toll/interleukin-1 receptor is mediated by mRNA stabilization. *J Biol Chem* 280:1678–1687.
33. Bernstein BE, et al. (2010) The NIH roadmap epigenomics mapping consortium. *Nat Biotechnol* 28:1045–1048.
34. Shiina T, et al. (2001) Genomic organization, chromosomal localization, and promoter analysis of the mouse Mail gene. *Immunogenetics* 53:649–655.
35. Ishiguro-Oonuma T, Ochiai K, Hashizume K, Morimatsu M (2015) The role of IFN-γ in regulating Nfkbiz expression in epidermal keratinocytes. *Biomed Res* 36:103–107.
36. Okuma A, et al. (2013) Enhanced apoptosis by disruption of the STAT3-IκB-ζ signaling pathway in epithelial cells induces Sjögren's syndrome-like autoimmune disease. *Immunity* 38:450–460.
37. Ueta M, et al. (2008) Stat6-independent tissue inflammation occurs selectively on the ocular surface and perioral skin of IkappaBzeta-/- mice. *Invest Ophthalmol Vis Sci* 49: 3387–3394.
38. Karlsen JR, Borregaard N, Cowland JB (2010) Induction of neutrophil gelatinase-associated lipocalin expression by co-stimulation with interleukin-17 and tumor necrosis factor-alpha is controlled by IkappaB-zeta but neither by C/EBP-beta nor C/EBP-delta. *J Biol Chem* 285:14088–14100.
39. Muromoto R, et al. (2016) IL-17A plays a central role in the expression of psoriasis signature genes through the induction of IκB-ζ in keratinocytes. *Int Immunol* 28: 443–452.
40. El Malki K, et al. (2013) An alternative pathway of imiquimod-induced psoriasis-like skin inflammation in the absence of interleukin-17 receptor a signaling. *J Invest Dermatol* 133:441–451.
41. Sano S, et al. (2005) Stat3 links activated keratinocytes and immunocytes required for development of psoriasis in a novel transgenic mouse model. *Nat Med* 11:43–49.
42. Andrés RM, Montesinos MC, Navalón P, Payá M, Terencio MC (2013) NF-κB and STAT3 inhibition as a therapeutic strategy in psoriasis: In vitro and in vivo effects of BTH. *J Invest Dermatol* 133:2362–2371.
43. Miyoshi K, et al. (2011) Stat3 as a therapeutic target for the treatment of psoriasis: A clinical feasibility study with STA-21, a Stat3 inhibitor. *J Invest Dermatol* 131:108–117.
44. Okamoto K, et al. (2010) IkappaBzeta regulates T(H)17 development by cooperating with ROR nuclear receptors. *Nature* 464:1381–1385.
45. Johnston A, et al. (2013) Keratinocyte overexpression of IL-17C promotes psoriasiform skin inflammation. *J Immunol* 190:2252–2262.
46. Scholz T, et al. (2017) GM-CSF in murine psoriasiform dermatitis: Redundant and pathogenic roles uncovered by antibody-induced neutralization and genetic deficiency. *PLoS One* 12:e0182646.

PNAS
www.pnas.org

Supplementary Information for

IκBζ is a key transcriptional regulator of IL-36-driven psoriasis-related gene expression in keratinocytes

Anne Müller, Andre Hennig, Sebastian Lorscheid, Paula Grondona,
Klaus Schulze-Osthoff, Stephan Hailfinger, Daniela Kramer

Daniela Kramer
Email: daniela.kramer@uni-tuebingen.de

This PDF file includes:

Supplementary text
Figs. S1 to S6
Tables S1 to S4
References for SI reference citations

www.pnas.org/cgi/doi/10.1073/pnas.1801377115

Supplementary Information Text

SI Materials and Methods

Cell culture and treatment. HaCaT cells were maintained in DMEM with 10% FCS and antibiotics. Human primary KC were freshly isolated from foreskin and maintained in CnT-07S medium with gentamycin (CELLnTEC). Recombinant human IL-36α (aa 6-158), full-length IL-36α (aa 1-158), IL-36γ (aa 18-169) or mouse human IL-36α (aa 6-160) were purchased from R&D or kindly provided by Amgen. Recombinant IL-17A (11340174), TNFα (11343013), IFNγ (11343536) and IL-1β (11340013) were from Immunotools. The following inhibitors were purchased from Selleckchem: Trametinib (MEK1/2 inhibition), SCH772984 (ERK1/2 inhibition), BMS-345541 (IKK1/2 inhibition) SP600125 (JNK inhibition), IMD0354 (IKK2 inhibition).

Generation of knockdown cells. Lentiviral particles were produced in HEK293T cells using the lentiviral vector pMD2.G and a second-generation packaging system (psPAX2, Addgene). HaCaT cells or primary KC were transduced in the presence of 8 µg/mL polybrene, packaging plasmids and 5 µg of the respective shRNA construct: pLKO.1-puro (sh ctrl); pLKO.1-TRCN0000147551 (sh NFKBIZ); pLKO.1-TRCN0000014686 (sh RELA); pLKO.1-TRCN0000008025 (sh1 MyD88); pLKO.1-TRCN0000011223 (sh2 MyD88); pLKO.1-TRCN0000020840 (sh1 STAT3); pLKO.1-TRCN0000020843 (sh2 STAT3), followed by puromycin selection (1 ng/mL, Invitrogen).

Luciferase constructs and reporter assays. The promoter 2 region of *NFKBIZ* (chr3: 101848459-101850067) containing the binding sites for STAT3 (CTTCCAGGAC), NFκB (CGGGGTTTCCC), AP1 (TGACTCC), KLF4 (TGGGCGGAGCCGGGCGGGCGGGGC) and STAT1/STAT3 (ATTTTACTGGAAATC) was cloned into a pGL3 basic construct. For deletion of transcription factor-binding sites a double PCR was performed using specific forward and reverse primers (Table S4). Successful generation of the constructs was checked by sequencing. For transfection 10^5 HaCaT cells were transfected with 5 µg luciferase construct and 1.25 µg TK-Renilla-expressing construct using Lipofectamine 3000 reagent (Life Technologies). 24 h later, cells were stimulated for 24 h with 100 ng/mL IL-36α or 200 ng/mL IL-17A, before luciferase activity was measured with the Firefly Luciferase Assay Kit (Promega). Expression of the reporter constructs was calculated as fold induction over unstimulated transfected cells from data of three independent experiments.

Western blot analysis. Cells were washed in PBS and resuspended in lysis buffer containing 20 mM TRIS-HCl pH 7.5, 150 mM NaCl, 1% Triton X-100, 1 mM Na_2EDTA, 1 mM EGTA, 1 mM β-glycerophosphate, 2 M urea and 1x protease inhibitor cocktail (Roche). After 10 min on ice, samples were briefly sonicated to disrupt DNA–protein complexes. Afterwards, samples were separated by SDS-PAGE and transferred to a nitrocellulose membrane. The following antibodies were used for Western blot analysis and purchased from Cell Signaling: anti-IκBζ (9244), anti-p-STAT3 (phospho-STAT3 at Tyr705; 9145), anti-STAT3 (12640), anti-p65 (8242), anti-p-p65 (phospho-p65 at Ser536, 3031), anti-p-JNK (phospho-JNK at Thr183/Tyr185, 4668), anti-JNK (9252), anti-p-p44/42 MAPK (phospho-Erk1/2 at Thr202/Tyr204, 4370), anti-p44/42 MAPK (4695), anti-p-IκBα (phospho-IκBα at Ser32, 2859), anti-IκBα (4814), anti-MyD88 (4283), anti-GAPDH (2118) and anti-β-actin (3700). Anti-HSC70 (sc-7298) was obtained from Santa Cruz Biotechnology. For detection of mouse IκBζ, a self-made antibody was used.

Chromatin immunoprecipitation. ChIP assays were performed as described (1). After sonification, chromatin was incubated with protein G-coupled Dynabeads (Invitrogen) and 2 µg of p65 (Diagenode, C15310256), STAT3 (Thermo Fisher, MA1-13042), RNA-polymerase II (Abcam, ab5095) or IgG control antibodies (Abcam, ab46540) overnight at 4°C. The promoter

region of *MYOD1* served as an internal negative control (forward: 5´-CTCTGCTCCTTTGCCACAAC-3´, reverse: 5´-GAGTGCTCTTCGGGTTTCAG-3´). ChIP primers corresponding to the promoter region 2 of *NFKBIZ* variant 1 were self-designed (primer for readout of STAT3 ChIP: forward 5´-GCCTTAACTGGGCTAACAGC-3´, reverse 5´-CTGGCAAGTCCTGGAAGGAG-3´; primer for readout p65 and Pol II ChIP: forward 5´-GAAGGGCAGGCAAACAAC-3´, reverse 5´-GATGCGTCCGATTTCCAG-3´). Data are presented as the percentage of input from 2 independent experiments.

Gene expression analysis by qPCR. Total RNA was isolated using Qiazol (Qiagen). After digestion of genomic DNA with DNase I, cDNA synthesis was performed using M-MuLV reverse transcriptase and random hexamer primers (Thermo Fisher Scientific). Relative gene expression was quantified by real-time PCR using Maxima SYBR Green master mix (Thermo Fisher Scientific) and self-designed primers (Suppl. Table S3). PCR conditions were as follows: initial denaturation 15 min at 95°C, followed by 40 cycles of 95°C for 15 s and 60°C for 45 s. Relative mRNA levels were calculated by normalization to the reference genes *RPL37A* or *ACTB* using the $2^{-\Delta\Delta CT}$ method.

RNAseq. For RNAseq analysis, libraries were constructed with the Ultra RNA Library Prep Kit at the Core Facility Genomics in Münster, Germany. Sequencing was performed using the Illumina NextSeq High Output kit. Mapping against the human reference genome hg19 was performed by HISAT2 (2). From raw gene counts, differentially expressed genes between wild-type and knockdown cells were computed using the Bioconductor R package DESeq2. Genes were called differentially expressed if their adjusted p-value (false discovery rate) was < 0.05 and the absolute fold change > 1.

Mice. Experiments were conducted in accordance with the German law guidelines of animal care. Tamoxifen-inducible IκBζ knockout mice were generated by crossing B6.Cg-Nfkbiz<tm1.1Muta> mice (RIKEN) to B6.129-*Gt(ROSA)26Sor*$^{tm1(cre/ERT2)Tyj}$/J mice (Jackson Laboratory). IκBζ deletion was induced by intraperitoneal injection of 75 mg/kg tamoxifen (T5648, Sigma-Aldrich) for 4 consecutive days. As control, *Nfkbiz* flox/flox mice (B6.Cg-Nfkbiz<tm1.1Muta>) received tamoxifen injections in parallel. Three days after the last tamoxifen injection, mice received for 5 consecutive days intradermal injections to the ear, containing 1 µg murine IL-36α or PBS vehicle alone. At day 6, mice were sacrificed and analyzed.

Flow cytometry. Three ears per group were chopped and digested with 300 µg/ml Liberase (Roche) and 50 U/ml DNase I (Thermo Fisher) in 5% FCS in RPMI for 2 h at 37°C. For generation of single cell suspensions, cells were passed through a cell strainer (100 µm). After cell counting, 10^5 cells were treated with Fc-Block (BioRad, BUF041) and surface-stained with the following antibodies from BioLegend: anti-CD45 FITC (103107), anti-CD3 PerCP (100325), anti-CD4 PE (100407), anti-CD8 APC (100711), anti-CD11b PacificBlue (101223), anti-Ly6G PE (127607), anti-F4/80 APC (123115). Anti-γδ-TCR APC was from Thermo Fisher. Data were acquired on a LSRII flow cytometer (Becton Dickson) and gates were set based on the respective isotype controls.

Histology. After fixation in formaldehyde and paraffin-embedding, 5-µm sections were prepared and incubated with the following antibodies: MPO (AF3667, R&D, 1:200), F4/80 (70076, Cell Signaling, 1:400) or Ki67 (ab15580, Abcam, 1:1000). Antigen retrieval was performed in 1 mM EDTA pH 8.0 for MPO, and in 10 mM citrate pH 6.0 for F4/80 and Ki67. After incubation with peroxidase-coupled secondary antibodies, sections were stained with DAB substrate.

Cytokine antibody array. For detection cytokine secretion, protein lysates from 2 mouse ears per group were pooled. 600 µg total protein lysate was analyzed with a cytokine array (R&D Systems, ARY006). Mean pixel density of each spot was quantified using the dot blot analyzer (ImageJ).

Analysis of patient data. Gene expression data originated from GEO data set GSE13355 (3, 4). Pre-normalized gene expression values from each sample was directly taken from the GEO profile data set GDS4602. The following reporters were taken for analysis: *NFKBIZ*: ID 223218_s_at, *IL17A*: ID 216876_s_at, *IL36G*: ID 220322_at and *LCN2*: ID 212531_at.

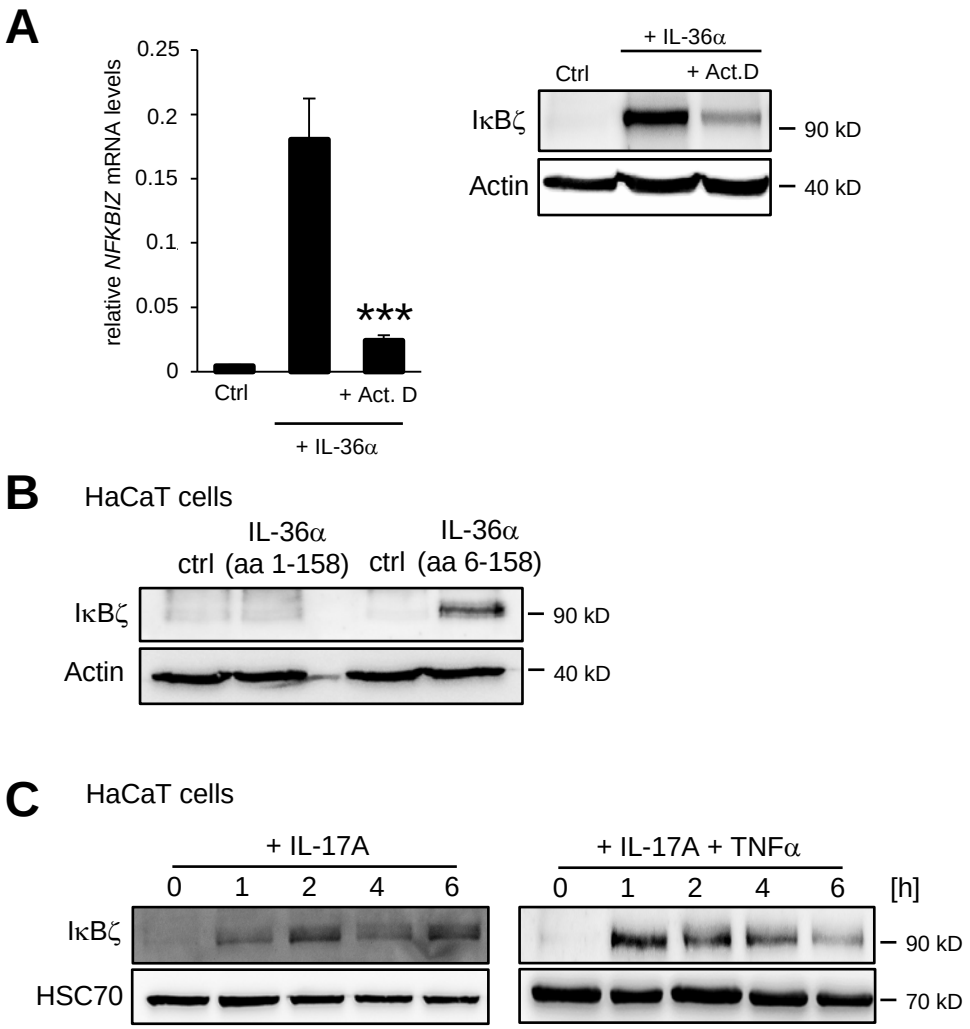

Fig. S1. Induction of IκBζ protein expression by full-length and truncated IL-36α as well as by IL-17A and TNFα. (A) IκBζ is transcriptionally induced by IL-36α. HaCaT cells were pre-treated for 30 min with 100 ng/mL of active IL-36α followed by the addition of 5 µg/mL actinomycin D or a DMSO control for 30 min. *NFKBIZ* mRNA levels were analyzed by qPCR and normalized to *RPL37A*. IκBζ protein levels were detected by Western blot in parallel. **(B)** IκBζ is not induced by full-length IL-36α. HaCaT cells were stimulated for 24 h with 2 µg/mL biologically inactive full-length IL-36α (aa 1-158) or 200 ng/mL truncated IL-36α (aa 6-158), followed by immunoblot analysis. **(C)** IL-17A, alone or in combination with TNFα, induces IκBζ. HaCaT cells were treated for the indicated times with 100 ng/mL IL-17A alone (*left)* or in combination with 10 ng/mL TNFα (*right*).

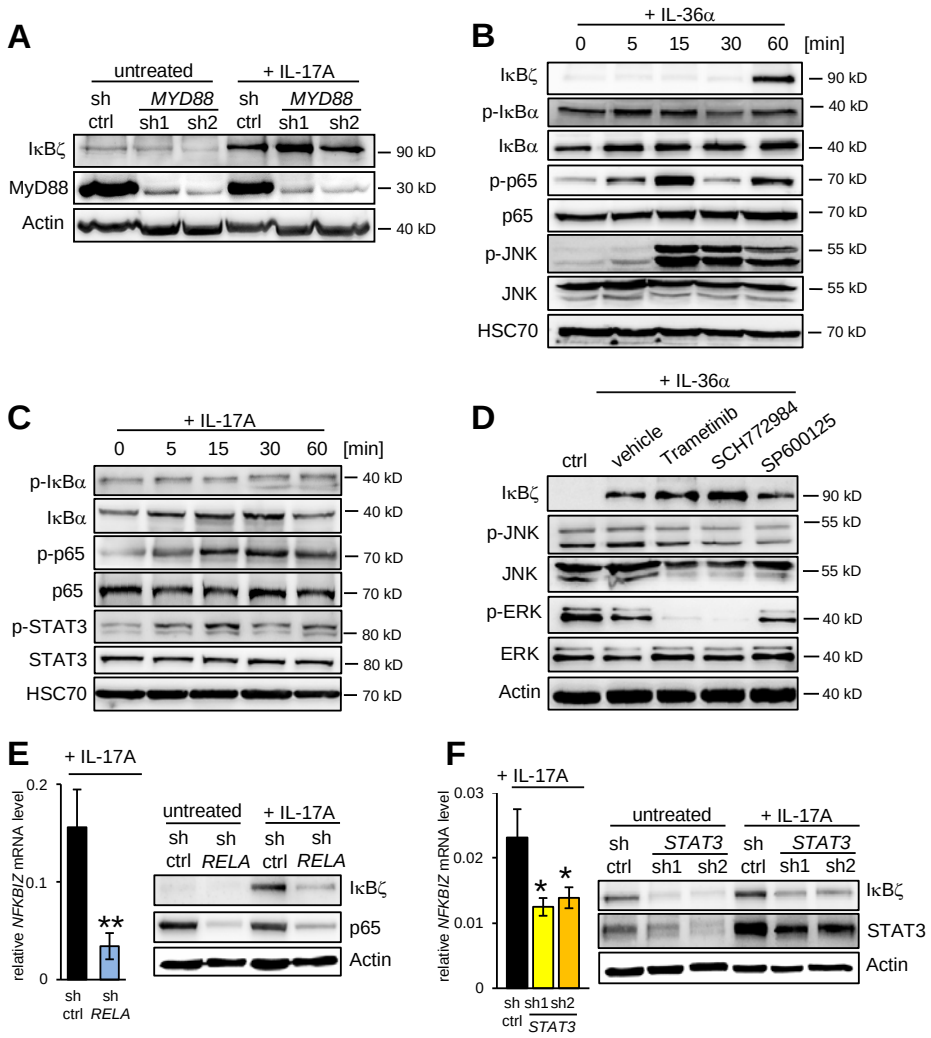

Fig. S2. Mechanism of IκBζ induction by IL-17A. In all experiments, HaCaT cells were stimulated with 200 ng/mL IL-17A. **(A)** HaCaT cells stably expressing a control shRNA (sh ctrl) or two different shRNAs targeting *MyD88* were treated for 2 h with IL-17A and analyzed by Western blotting. **(B)** Upstream signaling of IL-36α-treated primary KC. Cells were stimulated with 100 ng/mL IL-36α for the indicated time. NF-κB activation was detected by staining for the phosphorylated forms of IκBα (p-IκBα at Ser32) and p65 (p-p65 at Ser536). Activation of the MAPK pathway was detected by phosphorylated JNK (p-JNK at Thr183/ Tyr185). **(C)** Immunoblot analysis of IL-17A-treated HaCaT cells. NF-κB and STAT3 activation was detected with antibodies against the phosphorylated forms of IκBα (p-IκBα at Ser32) p65 (p-p65 at Ser536) and STAT3 (p-STAT3 at Tyr705). **(D)** HaCaT cells were either left untreated (Ctrl) or stimulated for 2 h with 100 ng/mL IL-36α together with the vehicle control DMSO, 50 nM Trametinib (MEK inhibitor), 1 µM SCH772984 (ERK1/2 inhibitor) or 10 µM SP600125 (JNK inhibitor). The status of phosphorylated ERK (p-ERK1/2) and p-JNK was measured as a control for kinase inhibition. **(E)** Gene expression and Western blot analysis of IκBζ in control and *RELA* (p65) knockdown cells after 1 h treatment with IL-17A. Knockdown efficiency was controlled by immunoblot detection of p65. *NFKBIZ* mRNA levels were normalized to *RPL37A*. **(F)** Relative mRNA and protein levels of IκBζ in control and *STAT3* knockdown HaCaT cells after 1 h of treatment with IL-17A. Knockdown efficiency of *STAT3* was controlled by immunoblot analysis. mRNA levels were normalized to *RPL37A*.

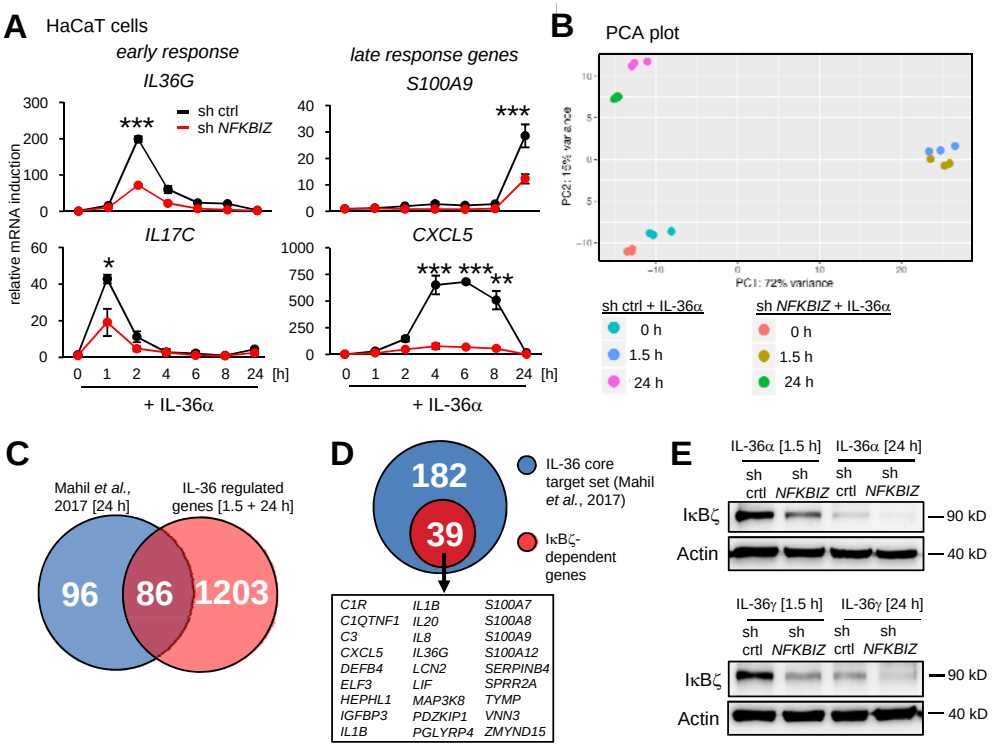

Fig. S3. Characterization of IκBζ-mediated gene expression in keratinocytes. (A) Induction of psoriasis-related gene expression by IL-36α in the presence and absence of IκBζ. Biological triplicates from control and *NFKBIZ* shRNA-transduced HaCaT cells were stimulated with 100 ng/mL IL-36α for the indicated times. Expression of *IL36G*, *S100A9*, *IL17C* and *CXCL5* was analyzed by qPCR and relative mRNA induction was calculated after normalization to the reference gene *RPL37A*. Significance is shown by asterisks (*p < 0.05; ** p < 0.01; *** p < 0.001). **(B)** Principle component analysis (PCA) of IL-36α-modulated gene expression in primary KC expressing a control or *NFKBIZ*-specific shRNA. PCA revealed only minor variances between the triplicate samples, whereas the transcripts of untreated cells or cells treated with IL-36α for either 1.5 h or 24 h were strongly different. Moreover, comparison of the transcript clusters between wildtype and *NFKBIZ* knockdown cells revealed that only a specific subset of IL-36α-regulated genes was affected by IκBζ depletion. **(C)** Venn diagram showing the overlap of IL-36-regulated genes identified in our RNAseq analysis and previously published data (5). A core set of 182 IL-36 target genes defined by Mahil *et al.* (Ref. 5) was compared to our RNAseq data containing the merged sets of IL-36 target genes after 1.5 and 24 h of stimulation. Note that our data set included genes of a late (24 h) and early (1.5 h) stimulation time point which latter was not analyzed by Mahil *et al.* (2017). **(D)** Overlap of the IL-36 core target gene set (Ref. 5) and IκBζ-dependent target genes. Examples of overlapping target genes are depicted below. **(E)** Western blot analysis of the IκBζ knockdown in HaCaT cells expressing a control or *NFKBIZ*-specific shRNA after the indicated times of treatment with IL-36α or IL-36γ.

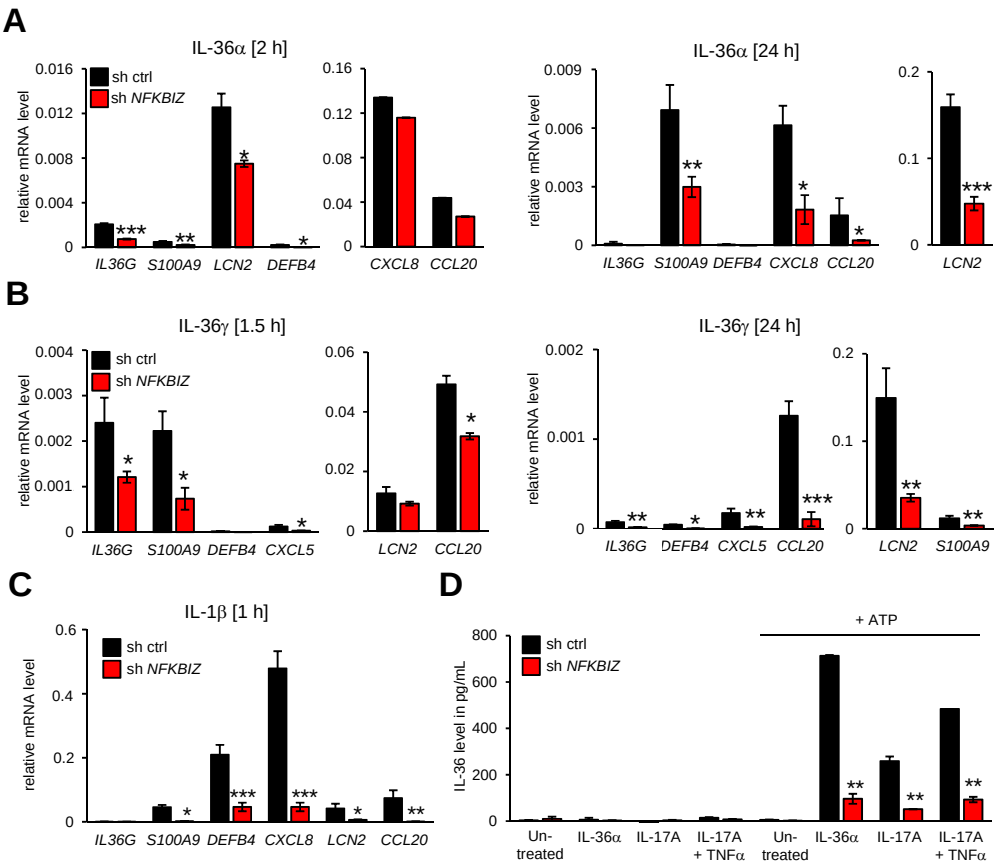

Fig. S4. Characterization of the IL-36/IκBζ axis in keratinocytes. Control and *NFKBIZ* knockdown HaCaT cells (corresponding to Fig. S3E) were treated for 2 and 24 h with 100 ng/mL IL-36α **(A)**, for 1.5 and 24 h with IL-36γ **(B)**, or for 1 h with 100 ng/mL IL-1β **(C)**. Expression of *IL36G*, *S100A9*, *DEFB4*, *LCN2*, *CCL20* and *CXCL5* was analyzed by qPCR and normalized to the reference gene *RPL37A*. **(D)** IL-36 protein levels in cytokine-stimulated HaCaT cells. Control and *NFKBIZ*-depleted HaCaT cells were stimulated for 48 h with IL-36α (100 ng/mL), IL-17A (100 ng/mL) or IL-17A (100 ng/mL) + TNFα (10 ng/mL). 30 min before harvest cells were additionally treated with 5 mM ATP to facilitate IL-36γ release by P2X7 receptor-mediated exosome formation. IL-36γ was determined in the supernatant using an IL-36G ELISA. Significance is shown by asterisks (*p < 0.05; ** p < 0.01; *** p < 0.001).

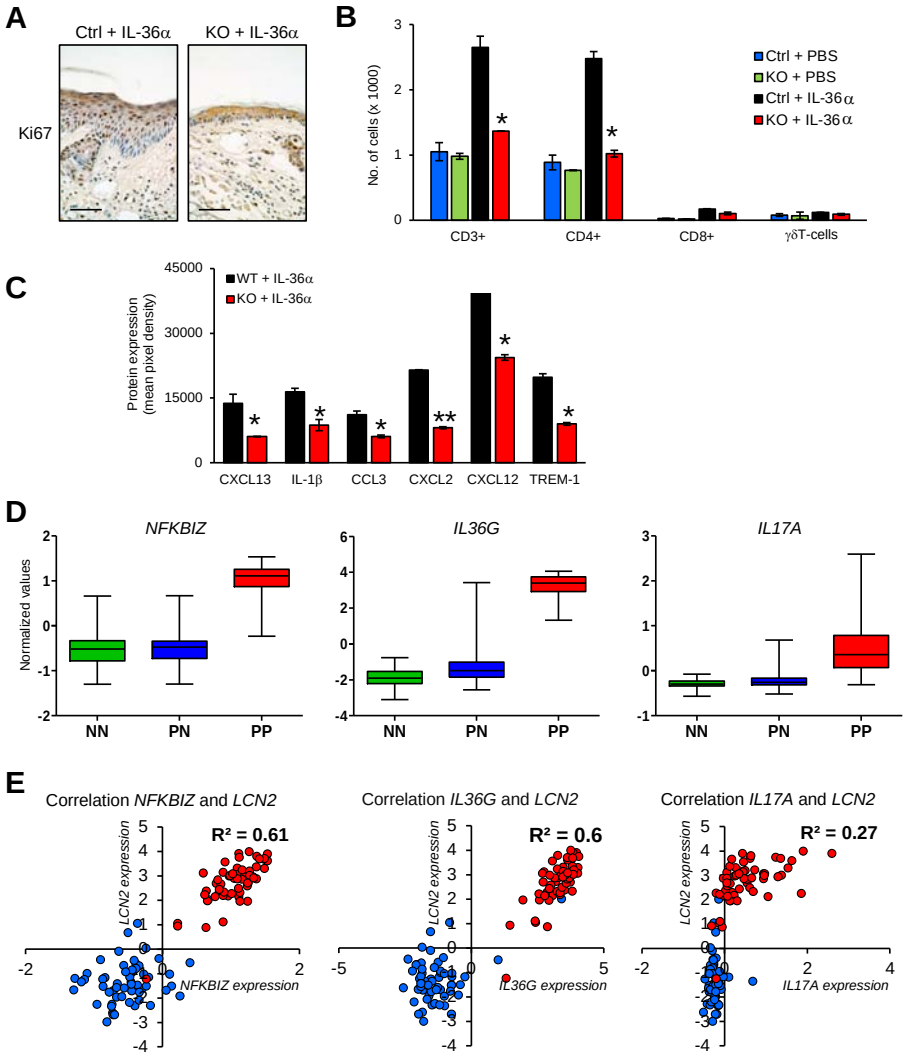

Fig. S5. Further characterization of the IL-36/IκBζ axis *in vivo*. (A) IHC analysis of Ki67 in IL-36α-treated ears as a marker for keratinocyte hyperproliferation. **(B)** Analysis of T-cell subpopulations in PBS and IL-36α-treated ears by flow cytometry. Single cell suspensions were prepared from 3 pooled ears per group and T-cells were identified as CD45+ and CD3+ cells. For further discrimination of T-cell subpopulations cells co-stained with CD4 or CD8. γδT-cells were identified as CD45+, CD3+ and γδ-TCR+. Error bars derive from two independent measurements (*p < 0.05; ** p < 0.01; *** p < 0.001). **(C)** Quantification of secreted cytokines in IL-36α-treated ear tissue. Pooled protein lysates of two ears from either IL-36α-treated control or KO mice were analyzed using a cytokine antibody array. For both samples, equal amounts of protein were used, and equal loading controlled by analyzing reference spots on the membranes. Depicted is the mean pixel density of two dots per cytokine. Significance is shown by asterisks (*p < 0.05; ** p < 0.01; *** p < 0.001; n.s. = not significant). **(D)** Expression data from skin biopsies of 64 healthy patients and 58 psoriasis patients were analyzed from the GEO profile data set GDS4602 (48, 49), using the GEO Dataset Analysis Tool (GDS browser from NCBI). Shown is the mean normalized expression of *NFKBIZ* (ID: 223218_s_at), *IL17A* (ID: 216876_s_at) and *IL36G* (ID: 220322_at) in normal skin (NN) of healthy individuals as well as in uninvolved skin (PN) and psoriatic lesions (PP) from psoriasis patients. **(E)** Normalized expression values from *LCN2* (ID: 212531_at) were plotted against *NFKBIZ*, *IL36G* and *IL17A*.

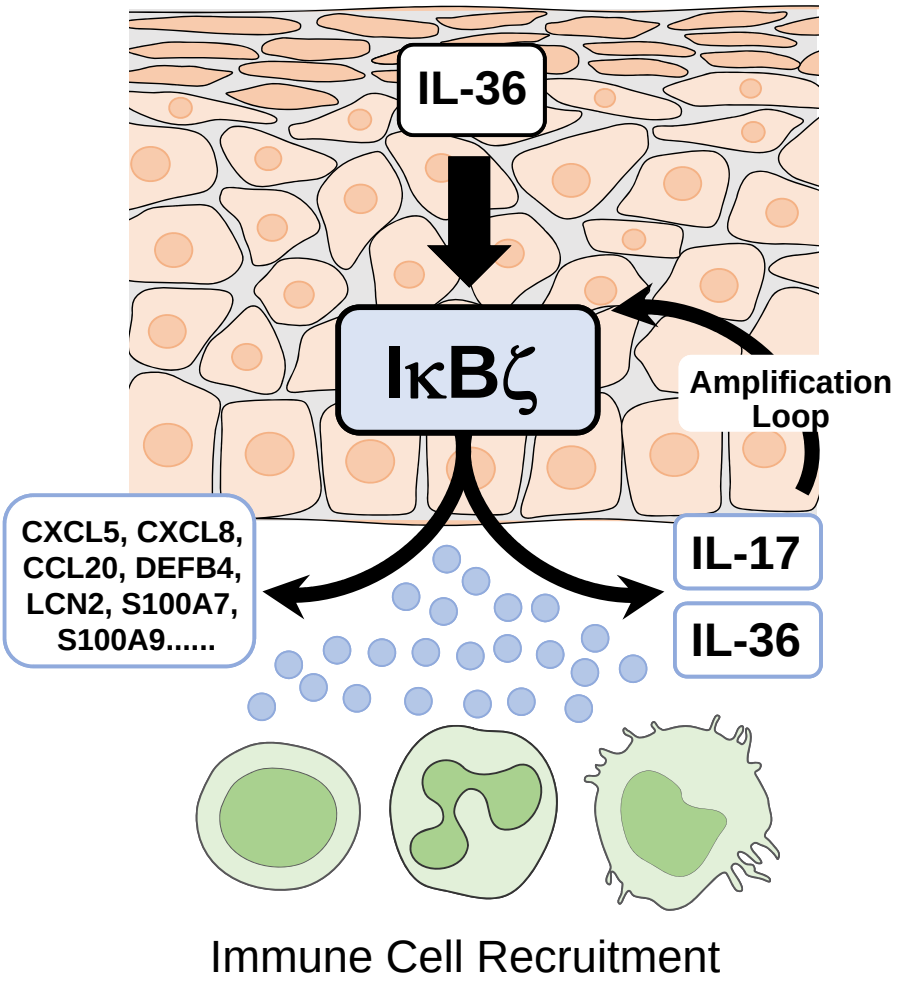

Fig. S6. Simplified model of IL-36-driven IκBζ signaling in keratinocytes. Binding of IL-36 to its receptor triggers the expression of the transcriptional regulator IκBζ, which then transcriptionally upregulates several antimicrobial peptides, cytokines and chemokines involved in the pathogenesis of psoriasis. Among others, induction of IκBζ target genes results in the recruitment and activation of immune cells. Important IκBζ target genes are also IL-17 and IL-36 itself, triggering an amplification loop of proinflammatory IκBζ signaling in keratinocytes.

Table S1. List of genes regulated by *NFKBIZ* knockdown in primary KC after 1.5 h of IL-36α treatment

	Base Mean	log2 fold Change	lfcSE	stat	P value	P value adj.
NTSR1	36.69	3.57	0.47	-7.63	2.26554E-14	2.80042E-11
RMRP	15.62	2.55	0.67	-3.82	0.00013082	0.003760604
DOK7	236.97	2.43	0.35	-6.87	6.54443E-12	4.04476E-09
UBBP4	13.30	2.35	0.60	-3.95	7.91843E-05	0.002581941
MATK	19.32	2.32	0.51	-4.59	4.3557E-06	0.000297611
RAMP1	206.36	2.26	0.35	-6.50	7.95432E-11	3.37984E-08
DUSP9	53.29	2.23	0.41	-5.43	5.74436E-08	9.29835E-06
SYT12	117.45	2.20	0.41	-5.34	9.2756E-08	1.33006E-05
ASCL2	32.82	2.18	0.47	-4.65	3.37294E-06	0.000240115
CRLF1	58.59	2.11	0.38	-5.49	4.07773E-08	7.20064E-06
SPRY4	642.68	2.09	0.22	-9.50	2.00174E-21	9.07253E-18
LYNX1	189.12	2.04	0.40	-5.12	2.99845E-07	3.2616E-05
DUSP2	409.28	2.02	0.35	-5.85	4.97137E-09	1.16544E-06
USH1G	13.45	2.02	0.62	-3.24	0.001212883	0.016508214
KIAA1644	25.47	2.01	0.45	-4.49	7.10439E-06	0.000429326
DEGS2	46.57	1.99	0.46	-4.35	1.38739E-05	0.00072277
PTGES	125.49	1.97	0.34	-5.76	8.25718E-09	1.78211E-06
TMEM105	20.05	1.93	0.46	-4.17	3.09087E-05	0.001334178
CX3CL1	33.79	1.93	0.47	-4.10	4.14642E-05	0.001713643
SNCB	58.08	1.91	0.42	-4.55	5.39648E-06	0.000342878
HAS1	18.97	1.90	0.48	-3.95	7.95946E-05	0.002589111
CPLX1	21.35	1.90	0.48	-3.99	6.55802E-05	0.002306451
STMN3	122.69	1.89	0.37	-5.17	2.33847E-07	2.64968E-05
KRT1	188.81	1.88	0.29	-6.61	3.85818E-11	1.69225E-08
DNLZ	22.01	1.87	0.59	-3.18	0.001486806	0.018753345
GRIA1	19.04	1.87	0.50	-3.73	0.000189181	0.004844251
LRFN1	90.52	1.85	0.38	-4.91	8.97741E-07	7.71716E-05
CITED4	2028.14	1.84	0.30	-6.06	1.36946E-09	4.43346E-07
FOXL1	13.71	1.83	0.54	-3.40	0.000679254	0.011530356
PLLP	142.79	1.79	0.26	-6.85	7.49452E-12	4.43057E-09
PALD1	34.37	1.78	0.40	-4.50	6.93618E-06	0.00042382
CAPN8	90.37	1.75	0.32	-5.44	5.40551E-08	8.96571E-06
GPR153	2211.19	1.75	0.33	-5.33	9.87708E-08	1.39894E-05
SYT8	300.56	1.75	0.30	-5.87	4.30154E-09	1.05144E-06
DCN	19.76	1.74	0.45	-3.85	0.000117377	0.003492291
ENTPD2	328.87	1.74	0.32	-5.53	3.21671E-08	5.91049E-06

SLC22A17	329.90	1.74	0.30	-5.75	9.08664E-09	1.9288E-06
PTGS1	202.11	1.72	0.26	-6.65	2.97177E-11	1.49656E-08
EDN2	26.70	1.71	0.38	-4.49	7.17739E-06	0.000431819
EGFL7	324.81	1.70	0.42	-4.08	4.41959E-05	0.001793826
TNFRSF18	311.45	1.69	0.32	-5.34	9.2929E-08	1.33006E-05
SH3TC1	1053.00	1.69	0.36	-4.65	3.3605E-06	0.000240115
RP11-1055B8.6	15.98	1.67	0.54	-3.11	0.001858448	0.021601366
TP73	23.76	1.67	0.46	-3.61	0.000304315	0.006739047
MROH6	3512.63	1.66	0.33	-5.10	3.34272E-07	3.55086E-05
BGN	16.86	1.66	0.53	-3.11	0.001880921	0.021784395
SLC19A1	1829.84	1.66	0.37	-4.48	7.57219E-06	0.00044571
TH	116.02	1.65	0.33	-4.98	6.23379E-07	5.6133E-05
KLK14	51.87	1.65	0.39	-4.20	2.65412E-05	0.001191025
RP11-1275H24.1	55.10	1.63	0.42	-3.93	8.55968E-05	0.002747145
PTPRU	2427.25	1.63	0.32	-5.07	3.90059E-07	4.05098E-05
NAPRT1	1086.21	1.63	0.31	-5.24	1.57862E-07	2.00602E-05
CDT1	2468.96	1.62	0.32	-4.99	5.94145E-07	5.53328E-05
CPNE5	32.61	1.62	0.36	-4.55	5.3036E-06	0.000338559
ABCA2	528.66	1.62	0.34	-4.77	1.85847E-06	0.000144398
NUDT8	189.96	1.62	0.42	-3.89	0.000102143	0.003156451
GDNF	35.28	1.61	0.34	-4.76	1.94597E-06	0.000150337
FAM132A	82.35	1.61	0.40	-3.99	6.57703E-05	0.002306451
FGFR4	330.38	1.61	0.35	-4.55	5.48997E-06	0.000345589
LINC00173	14.42	1.61	0.59	-2.73	0.00640307	0.046458131
COL5A3	97.34	1.59	0.35	-4.55	5.47311E-06	0.000345589
PLK1	2492.76	1.59	0.27	-5.84	5.31008E-09	1.22375E-06
OLFM2	237.37	1.58	0.33	-4.84	1.27851E-06	0.000105357
EEF1A2	31.73	1.58	0.38	-4.21	2.55856E-05	0.001159625
RP11-770E5.1	17.62	1.58	0.46	-3.44	0.000578136	0.010235564
KCNK5	128.56	1.57	0.28	-5.64	1.73734E-08	3.32713E-06
TONSL	1878.45	1.57	0.34	-4.58	4.57553E-06	0.000303651
WNT7B	1240.12	1.55	0.32	-4.90	9.73165E-07	8.27008E-05
GJC2	76.42	1.55	0.42	-3.67	0.000239484	0.005702741
CTD-2555C10.3	51.20	1.54	0.41	-3.76	0.000172436	0.004535047
GAREML	77.41	1.54	0.30	-5.04	4.63403E-07	4.47349E-05
SLC52A3	439.00	1.53	0.26	-5.88	4.1459E-09	1.04392E-06
HPDL	120.37	1.53	0.29	-5.36	8.16353E-08	1.21613E-05
AC018638.1	21.57	1.52	0.50	-3.07	0.002158634	0.023670122
C15orf39	3127.90	1.52	0.35	-4.37	1.2356E-05	0.000666683
TMEM121	33.87	1.51	0.48	-3.15	0.001652997	0.02019389
PROB1	480.44	1.51	0.33	-4.58	4.60044E-06	0.000303651

PRRT4	127.54	1.50	0.36	-4.12	3.71906E-05	0.001565573
NPAS1	54.44	1.50	0.41	-3.63	0.000286895	0.006501514
GPAA1	6340.25	1.50	0.35	-4.24	2.26669E-05	0.001059113
PROM2	2941.51	1.50	0.32	-4.65	3.28821E-06	0.00023656
C1orf145	18.13	1.50	0.47	-3.18	0.001457413	0.018554718
PLEKHA7	188.14	1.49	0.22	-6.77	1.31768E-11	7.16657E-09
LPHN1	126.92	1.49	0.37	-4.07	4.75998E-05	0.001878553
KCNMA1	121.21	1.49	0.27	-5.47	4.59965E-08	7.81768E-06
LINC00162	35.08	1.48	0.40	-3.69	0.000226536	0.005475789
CTB-102L5.4	34.47	1.47	0.47	-3.15	0.00160817	0.019842369
IRF2BPL	1128.35	1.47	0.29	-5.01	5.44604E-07	5.14235E-05
SLC16A3	3228.38	1.47	0.36	-4.08	4.50465E-05	0.001817499
FASN	96217.62	1.47	0.36	-4.04	5.42499E-05	0.002046291
IGFBP2	5259.48	1.46	0.34	-4.37	1.22969E-05	0.000666137
CBX2	339.33	1.46	0.34	-4.31	1.63281E-05	0.000816227
TAS1R3	76.91	1.46	0.36	-4.10	4.04412E-05	0.001681587
AC079250.1	42.29	1.45	0.39	-3.73	0.000188518	0.004839375
KIF18B	1034.89	1.45	0.24	-5.97	2.4432E-09	6.92087E-07
GALK1	231.14	1.45	0.38	-3.85	0.00012019	0.003544967
CDC42BPG	2591.47	1.45	0.34	-4.25	2.10619E-05	0.000997833
FURIN	11269.18	1.44	0.34	-4.28	1.8625E-05	0.000904443
LRP3	1688.33	1.44	0.36	-4.01	6.11098E-05	0.00222205
MFSD3	1337.78	1.44	0.32	-4.48	7.30959E-06	0.000437835
FLJ27365	1882.10	1.43	0.33	-4.34	1.40193E-05	0.000727079
SH2D2A	301.43	1.43	0.31	-4.60	4.24967E-06	0.000293314
TMEM201	1333.13	1.43	0.37	-3.86	0.00011361	0.003402546
GAS2L1	3357.03	1.42	0.35	-4.09	4.34396E-05	0.00176841
AMN	57.17	1.42	0.40	-3.57	0.000358417	0.0076028
SLC39A4	1011.15	1.42	0.37	-3.83	0.000126202	0.003666611
ZNHIT2	408.48	1.42	0.36	-3.96	7.554E-05	0.002503256
AQP3	2941.08	1.42	0.32	-4.45	8.41513E-06	0.000486896
MMP9	284.79	1.41	0.32	-4.41	1.05104E-05	0.000585699
EFR3B	61.07	1.41	0.29	-4.80	1.57838E-06	0.000124861
N4BP3	1574.65	1.41	0.29	-4.82	1.43298E-06	0.000115291
ICAM1	1169.32	1.41	0.26	-5.48	4.19055E-08	7.30499E-06
RECQL4	1722.72	1.41	0.31	-4.58	4.58649E-06	0.000303651
GCHFR	113.17	1.41	0.37	-3.84	0.000121533	0.003553739
C3	64.73	1.41	0.28	-5.04	4.63898E-07	4.47349E-05
COL18A1	3120.75	1.40	0.33	-4.22	2.47191E-05	0.001127872
TNNI2	23.89	1.40	0.42	-3.34	0.000826532	0.013144283
ARHGAP4	37.37	1.40	0.40	-3.51	0.000452464	0.008864767

TELO2	4341.95	1.40	0.33	-4.19	2.78231E-05	0.001224305
TROAP	553.42	1.40	0.26	-5.36	8.38118E-08	1.22536E-05
MDFI	6269.58	1.40	0.32	-4.34	1.41705E-05	0.000727079
C17orf70	2465.73	1.40	0.35	-4.00	6.23973E-05	0.002238565
ADRA1B	117.18	1.39	0.24	-5.89	3.86772E-09	9.92253E-07
NOTCH3	2944.00	1.39	0.34	-4.05	5.10446E-05	0.001971743
PRR12	2128.98	1.39	0.35	-3.97	7.18753E-05	0.00244527
RP11-509E16.1	36.54	1.39	0.42	-3.34	0.000846042	0.01332845
PDGFB	117.64	1.39	0.30	-4.67	2.95589E-06	0.000216703
BCAM	5055.45	1.39	0.35	-3.96	7.43063E-05	0.002488529
RP11-328M4.2	24.40	1.39	0.37	-3.73	0.000194687	0.00492037
MIDN	3529.69	1.39	0.32	-4.33	1.51615E-05	0.000763523
SLCO4A1	744.48	1.38	0.27	-5.04	4.56923E-07	4.47349E-05
PKMYT1	6033.67	1.38	0.33	-4.13	3.55551E-05	0.00151076
FBXL16	91.25	1.38	0.32	-4.26	2.03352E-05	0.000970165
C1orf233	756.41	1.38	0.36	-3.81	0.000137218	0.00387086
RAVER1	2235.36	1.37	0.37	-3.67	0.000243298	0.005783442
RABL6	5465.28	1.37	0.32	-4.28	1.82986E-05	0.000894986
HPCAL1	1749.61	1.37	0.30	-4.52	6.15698E-06	0.00038402
NME3	779.59	1.37	0.36	-3.85	0.000119222	0.003524046
KCNH3	57.12	1.37	0.37	-3.66	0.000249712	0.005894669
DNASE1L2	101.76	1.37	0.33	-4.08	4.46195E-05	0.00180563
FUOM	535.34	1.37	0.35	-3.87	0.000110039	0.003324876
LINC01023	13.90	1.37	0.49	-2.76	0.005752889	0.04355347
E2F2	110.11	1.36	0.35	-3.92	8.68174E-05	0.002777543
FGFRL1	919.77	1.35	0.31	-4.30	1.69464E-05	0.000844028
GAMT	179.20	1.35	0.38	-3.52	0.000435231	0.008713117
WTIP	959.53	1.35	0.32	-4.24	2.26612E-05	0.001059113
GCAT	389.12	1.35	0.36	-3.74	0.000182912	0.004755364
PDLIM2	2653.01	1.35	0.33	-4.06	4.94549E-05	0.001937864
C16orf59	629.54	1.35	0.34	-3.90	9.58857E-05	0.002990272
RPS6KA4	9670.96	1.34	0.35	-3.87	0.000108537	0.003308931
FAM203A	61.21	1.34	0.35	-3.79	0.000149382	0.004095066
C20orf195	25.04	1.34	0.47	-2.88	0.003981263	0.034283237
RP11-94H18.1	18.24	1.34	0.43	-3.12	0.001833697	0.021530899
TGM3	14.91	1.33	0.49	-2.75	0.005951514	0.044406436
PIDD	958.54	1.33	0.35	-3.77	0.000162192	0.004341182
IGSF9B	119.71	1.32	0.33	-4.02	5.83159E-05	0.002148837
KRT24	13.48	1.32	0.48	-2.77	0.005597304	0.042780518
WDR18	3831.34	1.32	0.35	-3.79	0.000152259	0.004140542
AGRN	39952.14	1.32	0.36	-3.69	0.00022466	0.005454828

RTEL1	57.36	1.32	0.36	-3.63	0.000285977	0.006491527
SCRN2	526.82	1.32	0.30	-4.39	1.13603E-05	0.000617863
DIRAS1	25.22	1.31	0.47	-2.78	0.005478644	0.042293811
PYCRL	1028.07	1.31	0.35	-3.70	0.000211958	0.005259106
ADAM8	9775.55	1.31	0.31	-4.28	1.90483E-05	0.000915193
GPX1	9013.76	1.31	0.35	-3.73	0.000190361	0.004847066
LFNG	1803.78	1.30	0.33	-3.93	8.41492E-05	0.00271132
LAMA5	11199.37	1.30	0.36	-3.57	0.000357171	0.007588206
GPSM1	2890.20	1.30	0.35	-3.70	0.000219024	0.0053532
PIM3	7092.94	1.30	0.32	-4.06	4.89632E-05	0.001924139
CD320	1093.13	1.30	0.36	-3.59	0.000335898	0.007284227
KCNAB2	146.70	1.30	0.31	-4.24	2.28352E-05	0.001063321
POLD1	3651.02	1.30	0.32	-4.03	5.64893E-05	0.002110122
CENPM	436.70	1.30	0.35	-3.75	0.000179517	0.004694911
FCRLB	26.12	1.30	0.47	-2.77	0.005596439	0.042780518
RNF26	2097.26	1.30	0.36	-3.56	0.000375498	0.007854851
H2AFX	5018.73	1.29	0.32	-4.08	4.59253E-05	0.001827923
CAPN15	2199.98	1.29	0.33	-3.88	0.000102903	0.003172729
FSCN1	34967.91	1.28	0.34	-3.75	0.000174741	0.00458678
HR	3930.76	1.28	0.34	-3.76	0.000172075	0.004534317
TMEM238	210.07	1.28	0.34	-3.78	0.000154824	0.004193518
INTS1	11915.94	1.28	0.35	-3.64	0.000272527	0.006306864
PFAS	2113.70	1.28	0.28	-4.48	7.54242E-06	0.00044571
MIR3648	40.25	1.28	0.46	-2.76	0.005848651	0.044016309
SLC4A2	5966.52	1.27	0.36	-3.58	0.00034312	0.007393672
ISYNA1	338.21	1.27	0.33	-3.81	0.000139766	0.003926455
WDR90	2511.18	1.27	0.31	-4.15	3.38966E-05	0.001453919
STX1A	188.68	1.27	0.28	-4.52	6.19671E-06	0.000384733
REEP4	3088.80	1.27	0.33	-3.83	0.000128168	0.003707862
KREMEN2	437.56	1.27	0.32	-3.95	7.85505E-05	0.002578656
GDPD2	24.43	1.27	0.41	-3.10	0.001937903	0.022142576
IMPA2	1886.85	1.27	0.24	-5.38	7.60731E-08	1.16221E-05
UNC93B1	1011.28	1.27	0.32	-3.92	8.99804E-05	0.002845264
PLXNB2	14746.49	1.27	0.31	-4.02	5.7754E-05	0.002137774
PAK6	243.65	1.27	0.35	-3.58	0.000347505	0.007452949
NFKBID	1982.99	1.27	0.32	-4.00	6.46196E-05	0.002288107
TSKU	3249.79	1.26	0.32	-3.94	8.13311E-05	0.002632998
FHOD1	1461.24	1.26	0.30	-4.19	2.80027E-05	0.001228236
PLEC	143550.89	1.26	0.35	-3.62	0.000294712	0.00661254
MMP17	908.43	1.26	0.35	-3.63	0.000285812	0.006491527
TTLL12	9007.03	1.26	0.33	-3.80	0.000142379	0.003975199

RIN1	1375.33	1.25	0.36	-3.45	0.000561586	0.010034017
SRM	8146.16	1.25	0.34	-3.74	0.000187584	0.00483913
LINC00472	20.42	1.25	0.46	-2.74	0.006079827	0.044976826
NUDT16L1	914.77	1.25	0.34	-3.65	0.000266995	0.006226993
MTSS1L	694.87	1.25	0.35	-3.58	0.000345473	0.007432585
DCAF15	1693.72	1.25	0.30	-4.22	2.40036E-05	0.001101457
SLC6A17	46.59	1.25	0.40	-3.08	0.002082431	0.023170877
NRGN	57.27	1.25	0.39	-3.22	0.001275995	0.017089493
MESP2	23.54	1.24	0.46	-2.70	0.006926515	0.048496306
TMEM158	130.00	1.24	0.32	-3.84	0.00012125	0.003553124
FOSL1	13941.72	1.24	0.27	-4.56	5.06496E-06	0.000327944
RELT	1312.93	1.24	0.31	-4.04	5.43148E-05	0.002046291
GNB1L	461.38	1.24	0.35	-3.56	0.00037404	0.007836401
MBLAC1	43.77	1.24	0.33	-3.80	0.000143291	0.003992463
C14orf80	1321.43	1.24	0.34	-3.63	0.000279434	0.006407181
PIGQ	2932.88	1.24	0.37	-3.39	0.000710157	0.011906298
CRISPLD2	128.30	1.24	0.24	-5.05	4.38716E-07	4.41868E-05
GPR3	45.08	1.23	0.33	-3.71	0.000203529	0.00509647
SLC5A5	20.84	1.23	0.43	-2.88	0.003916143	0.034098918
PRSS21	142.03	1.23	0.30	-4.17	3.08373E-05	0.001334178
ASPG	51.03	1.23	0.36	-3.45	0.000564166	0.010053696
FBXW5	5827.71	1.23	0.35	-3.49	0.000477305	0.009080612
C2	25.58	1.23	0.40	-3.05	0.002256431	0.024234356
NPR1	328.31	1.23	0.25	-4.91	9.02426E-07	7.71716E-05
SLC16A5	441.87	1.23	0.31	-3.97	7.22645E-05	0.002450326
EPN1	9428.18	1.23	0.36	-3.44	0.000586778	0.010348154
WNT10A	788.66	1.22	0.26	-4.69	2.75261E-06	0.00020452
EMR2	302.05	1.22	0.18	-6.64	3.22297E-11	1.51113E-08
PIF1	243.31	1.22	0.20	-5.99	2.05776E-09	6.21762E-07
C9orf142	947.16	1.22	0.33	-3.71	0.000208862	0.005191762
RARG	3752.50	1.22	0.31	-3.95	7.86443E-05	0.002578656
INF2	9094.24	1.22	0.34	-3.64	0.000273574	0.006315419
SPRY2	343.56	1.22	0.17	-7.09	1.3528E-12	1.02189E-09
FAM110A	790.49	1.22	0.30	-4.02	5.85485E-05	0.002151577
RP11-21L23.2	41.27	1.22	0.31	-3.88	0.00010579	0.003247022
MFSD2B	325.29	1.22	0.38	-3.21	0.001345697	0.017625853
MPND	178.40	1.22	0.35	-3.44	0.000584384	0.010319309
KLHDC7B	24.69	1.21	0.45	-2.72	0.006493208	0.046862077
CTXN1	284.01	1.21	0.37	-3.24	0.0011925	0.01641136
SAPCD2	236.09	1.21	0.34	-3.52	0.000428185	0.008612481
TMEM180	295.65	1.21	0.33	-3.63	0.00028259	0.006446932

CENPB	5729.18	1.21	0.34	-3.56	0.000373778	0.007836401
CCNF	369.90	1.21	0.27	-4.47	7.91325E-06	0.000461787
PLXNA1	11975.75	1.21	0.31	-3.92	8.89154E-05	0.002818143
CHTF18	2776.72	1.21	0.32	-3.79	0.000151102	0.004126072
SLC6A8	3677.92	1.21	0.34	-3.52	0.000439203	0.008718017
DLX3	218.33	1.21	0.28	-4.31	1.61137E-05	0.000808482
SYTL1	1975.77	1.21	0.30	-4.01	6.02155E-05	0.002206872
TSPAN4	3314.16	1.21	0.33	-3.66	0.000254529	0.005987599
NACC1	4270.71	1.21	0.35	-3.46	0.000550061	0.009880018
FDXR	819.55	1.20	0.34	-3.55	0.000382614	0.007930493
LY6E	11113.91	1.20	0.34	-3.50	0.000465945	0.008986356
TMEM54	192.13	1.20	0.33	-3.68	0.000236449	0.005640787
CDC25B	3436.51	1.20	0.28	-4.33	1.4998E-05	0.000758095
ZNF295-AS1	20.21	1.20	0.44	-2.73	0.00624201	0.045926736
SULT2B1	1498.70	1.20	0.28	-4.25	2.17138E-05	0.001025147
LZTS1	247.60	1.20	0.34	-3.51	0.000452182	0.008864767
SLC25A10	1723.12	1.20	0.36	-3.33	0.000881238	0.01358526
NAT14	542.48	1.20	0.30	-3.95	7.87043E-05	0.002578656
TMEM129	1167.55	1.19	0.31	-3.83	0.000129003	0.003724098
BRAT1	2240.40	1.19	0.34	-3.44	0.000572276	0.010158271
DPP7	2300.92	1.19	0.34	-3.54	0.000405013	0.008243955
BCL9L	9299.58	1.18	0.34	-3.52	0.00043822	0.008718017
ZBTB7B	2370.59	1.18	0.33	-3.59	0.000325255	0.007121569
POLRMTP1	290.54	1.18	0.40	-2.98	0.002858843	0.02800554
DOT1L	2546.66	1.18	0.33	-3.55	0.000389898	0.00803199
ACOT11	204.72	1.18	0.33	-3.55	0.000381463	0.007918697
BCL2L12	1643.39	1.18	0.29	-4.05	5.22739E-05	0.002007819
MMP28	239.03	1.18	0.24	-4.93	8.01708E-07	6.996E-05
DDN	43.77	1.18	0.39	-3.04	0.002404528	0.025188262
CYP1B1-AS1	27.53	1.18	0.38	-3.14	0.001701251	0.020543438
ZNF668	579.01	1.18	0.31	-3.81	0.000140646	0.003943025
SLC25A22	2693.53	1.18	0.34	-3.43	0.00059561	0.010436215
EMC10	386.78	1.18	0.35	-3.32	0.000907026	0.013810567
MNT	2013.89	1.18	0.34	-3.45	0.000559413	0.010008348
TMEM161A	1554.04	1.17	0.34	-3.40	0.000663688	0.011336885
DHRS13	121.14	1.17	0.32	-3.68	0.000234954	0.005624424
NFIC	4031.53	1.17	0.35	-3.35	0.000817746	0.013035047
NDUFS7	1482.17	1.17	0.36	-3.23	0.001224933	0.016589053
ATP5D	3032.23	1.17	0.33	-3.56	0.000366206	0.007731829
TTLL10	214.13	1.17	0.23	-4.98	6.21691E-07	5.6133E-05
TMEM8A	2493.82	1.16	0.34	-3.41	0.000654155	0.011216325

PLXND1	102.71	1.16	0.36	-3.27	0.001086366	0.015375861
ZNF358	252.68	1.16	0.35	-3.37	0.000754833	0.012425503
FOXD2-AS1	55.80	1.16	0.38	-3.06	0.002193656	0.023839395
UNC13D	286.03	1.16	0.40	-2.89	0.003834848	0.033801146
PELP1	3658.21	1.16	0.34	-3.43	0.000600215	0.010489881
EREG	1538.55	1.16	0.22	-5.32	1.0161E-07	1.40979E-05
TBL3	3464.34	1.15	0.35	-3.27	0.001070781	0.015293502
CALM3	3296.49	1.15	0.26	-4.48	7.48667E-06	0.000444525
FAM173A	686.07	1.15	0.33	-3.53	0.000419079	0.008466887
NACC2	1178.86	1.15	0.31	-3.77	0.000162844	0.004350084
PSKH1	662.01	1.15	0.31	-3.73	0.000187914	0.00483913
CNN2	12302.18	1.15	0.33	-3.50	0.000467261	0.008986356
ARHGEF16	955.94	1.15	0.32	-3.57	0.000351208	0.007508458
FBXO46	1182.99	1.15	0.28	-4.04	5.27179E-05	0.002013497
MT2P1	2239.63	1.15	0.27	-4.21	2.57591E-05	0.00116361
EPPK1	8883.83	1.15	0.35	-3.27	0.001066295	0.015261482
C1orf132	53.48	1.15	0.31	-3.69	0.000223139	0.005427575
TCIRG1	2570.29	1.15	0.33	-3.53	0.000420124	0.008475404
MRPS31P2	23.78	1.15	0.40	-2.85	0.004328283	0.03624117
INTS5	1533.46	1.15	0.35	-3.32	0.000904932	0.013807599
EFHD2	4821.89	1.15	0.29	-3.90	9.45193E-05	0.002968082
CARD10	12538.49	1.15	0.33	-3.48	0.000499952	0.009310594
DKFZP761J1410	1237.49	1.15	0.35	-3.30	0.000976658	0.01450839
VPS51	3044.41	1.15	0.33	-3.51	0.000446611	0.008815268
ST6GALNAC4	791.61	1.15	0.37	-3.13	0.001772348	0.021129455
CASKIN2	947.05	1.15	0.35	-3.25	0.001171826	0.016245854
TRMT61A	1714.09	1.15	0.36	-3.20	0.00135727	0.017710947
GNAO1	24.84	1.15	0.41	-2.79	0.005260531	0.041155027
CDHR1	228.93	1.15	0.25	-4.55	5.30121E-06	0.000338559
MT2A	34609.61	1.15	0.27	-4.20	2.68113E-05	0.001199186
COMTD1	1200.86	1.14	0.30	-3.84	0.000121251	0.003553124
SH2D5	6792.14	1.14	0.28	-4.09	4.27068E-05	0.001743797
TMEM109	47.38	1.14	0.37	-3.05	0.002271862	0.024304096
BCAR1	7059.72	1.14	0.33	-3.51	0.000449173	0.008838507
SLC2A4RG	2388.72	1.14	0.33	-3.43	0.00059295	0.010416453
PRODH	200.72	1.14	0.26	-4.36	1.28721E-05	0.000689063
PLA2G4F	832.23	1.14	0.30	-3.76	0.00016776	0.004452725
C2CD4D	31.73	1.14	0.38	-3.00	0.002728715	0.027361611
EFNA3	229.87	1.14	0.33	-3.42	0.000632855	0.01093384
JAG2	5544.67	1.14	0.33	-3.44	0.000575174	0.010196404
HMGA1	25419.87	1.14	0.34	-3.32	0.00091445	0.013855665

TACC3	2981.72	1.13	0.22	-5.27	1.3687E-07	1.78945E-05
ADAM15	13591.22	1.13	0.35	-3.28	0.001021985	0.014830238
SLC25A11	1917.13	1.13	0.32	-3.53	0.000413983	0.00838886
MESDC1	2089.55	1.13	0.28	-4.00	6.44132E-05	0.002287225
TMEM63C	205.57	1.13	0.32	-3.59	0.000337006	0.007296609
POLRMT	2876.10	1.13	0.34	-3.34	0.00082395	0.013118563
FYB	17.80	1.13	0.42	-2.70	0.006863255	0.048223635
CSF1	1501.52	1.13	0.26	-4.34	1.42746E-05	0.000729669
FAM195A	554.06	1.13	0.32	-3.54	0.000399555	0.008157277
LEPREL2	668.88	1.13	0.34	-3.37	0.000760889	0.012510048
MIER2	1206.91	1.13	0.34	-3.35	0.000817466	0.013035047
SF3A2	3907.26	1.13	0.35	-3.24	0.001195644	0.016423036
FBXL18	1375.47	1.13	0.32	-3.47	0.000519056	0.009537305
PPP1R26-AS1	34.87	1.13	0.34	-3.31	0.000932528	0.014052646
MSLN	3178.56	1.13	0.33	-3.42	0.000622658	0.010798827
SREBF1	11755.72	1.13	0.32	-3.50	0.000466607	0.008986356
EPHB6	194.10	1.12	0.38	-2.97	0.003006479	0.028849042
PDDC1	2620.77	1.12	0.30	-3.74	0.0001843	0.004780133
P2RY2	289.17	1.12	0.30	-3.76	0.00017098	0.004522987
HAGHL	511.21	1.12	0.32	-3.48	0.000494722	0.009265476
CCDC85B	6120.98	1.12	0.32	-3.56	0.00037008	0.007797304
PQLC1	4256.82	1.12	0.34	-3.33	0.000868772	0.013500224
HSPBP1	4426.06	1.12	0.33	-3.43	0.000598507	0.010473493
GS1-393G12.12	43.31	1.12	0.37	-3.01	0.002590203	0.026369027
PDLIM7	3714.62	1.12	0.30	-3.77	0.000160882	0.004323151
MYBBP1A	6640.68	1.12	0.32	-3.46	0.000549043	0.009874793
NAB2	1954.12	1.12	0.29	-3.89	9.83776E-05	0.003060961
PHYHIP	134.90	1.12	0.34	-3.26	0.001103067	0.015542387
TNRC18	9129.18	1.12	0.33	-3.36	0.000767287	0.012566419
EXOSC4	636.55	1.12	0.36	-3.07	0.002143543	0.023580707
NECAB3	188.49	1.12	0.33	-3.40	0.000671803	0.011445771
KIAA1875	80.37	1.12	0.33	-3.36	0.000792717	0.012740625
SPHK1	6487.16	1.11	0.32	-3.49	0.000476229	0.009080612
MAFK	659.14	1.11	0.35	-3.15	0.001650963	0.020187177
IFRD2	5528.99	1.11	0.30	-3.71	0.000208407	0.005191762
AGAP3	6981.84	1.11	0.31	-3.56	0.000373948	0.007836401
FAM83H	22302.93	1.11	0.34	-3.26	0.001109241	0.015597054
ZNF865	797.81	1.11	0.31	-3.58	0.000347516	0.007452949
TPRG1	41.60	1.11	0.31	-3.55	0.000379473	0.007914274
PPDPF	6459.78	1.11	0.33	-3.35	0.00081519	0.01302484
ZNF628	501.29	1.11	0.38	-2.94	0.003252789	0.03043921

C1orf86	1716.94	1.11	0.33	-3.33	0.000853183	0.013364898
TTYH3	5900.85	1.11	0.35	-3.12	0.001816749	0.02139627
RHBDF1	1337.58	1.11	0.29	-3.87	0.000106932	0.003267315
MIR429	165.56	1.11	0.32	-3.45	0.000565993	0.010073044
FAM155B	595.11	1.11	0.34	-3.27	0.001083015	0.015375861
IRAK3	56.53	1.10	0.30	-3.64	0.000270825	0.00628396
LLGL1	2596.87	1.10	0.32	-3.47	0.000511825	0.00945555
PCAT6	40.00	1.10	0.39	-2.81	0.005027863	0.039932155
PAQR5	25.84	1.10	0.36	-3.05	0.00232153	0.024660816
FGFR3	2217.87	1.10	0.29	-3.73	0.000191818	0.004875038
EHD1	14554.26	1.10	0.30	-3.72	0.000197978	0.004994262
DGAT1	1640.21	1.10	0.33	-3.33	0.000878068	0.01356715
REXO1	3249.12	1.10	0.35	-3.15	0.001632914	0.020056663
BCL3	2167.42	1.10	0.34	-3.24	0.00118778	0.016379554
TOR4A	1356.01	1.10	0.33	-3.33	0.000872242	0.013538674
BOP1	914.25	1.10	0.33	-3.33	0.000880439	0.01358526
ANO7	37.78	1.10	0.39	-2.80	0.005170873	0.040711269
MAZ	769.32	1.10	0.31	-3.49	0.000479799	0.00909879
RP11-478C19.2	222.05	1.10	0.32	-3.40	0.000668854	0.011410793
PIEZO1	16376.30	1.10	0.33	-3.34	0.000838364	0.013247296
SPPL2B	1421.42	1.09	0.32	-3.43	0.000595051	0.010436215
AURKB	1836.26	1.09	0.25	-4.42	9.78805E-06	0.000552233
COL7A1	25312.35	1.09	0.32	-3.41	0.000641781	0.011066297
MST1R	4253.20	1.09	0.30	-3.69	0.000226272	0.005475789
C1orf159	1403.04	1.09	0.32	-3.41	0.00064215	0.011066297
SECTM1	182.56	1.09	0.33	-3.31	0.00093326	0.014052646
KLF16	1436.81	1.09	0.32	-3.36	0.000787091	0.012719583
MXRA8	320.81	1.09	0.31	-3.53	0.000410814	0.008337063
PPP1R3F	134.69	1.09	0.35	-3.13	0.001737409	0.020795379
ATP13A1	4023.79	1.09	0.33	-3.26	0.001127781	0.015808701
GRWD1	4603.67	1.09	0.34	-3.24	0.001201632	0.01644112
SBNO2	4887.78	1.09	0.32	-3.42	0.000619986	0.010779682
C2orf48	103.98	1.08	0.27	-3.98	6.8751E-05	0.002366601
SPHK2	696.87	1.08	0.37	-2.92	0.003459981	0.03161447
ANGPTL4	367.42	1.08	0.33	-3.25	0.001139777	0.015890257
TGFBR3L	45.45	1.08	0.39	-2.80	0.005059876	0.040116114
CARD14	51.23	1.08	0.31	-3.50	0.000471381	0.009014579
MAPK8IP2	230.07	1.08	0.33	-3.30	0.00098137	0.014551458
RP11-611L7.1	692.21	1.08	0.31	-3.44	0.000588208	0.010359928
PLEKHJ1	1966.51	1.08	0.31	-3.46	0.000541924	0.009798591
CDHR2	57.22	1.08	0.31	-3.52	0.000439146	0.008718017

STAT5A	1472.92	1.08	0.24	-4.43	9.52257E-06	0.000539493
DUS3L	1534.85	1.07	0.31	-3.42	0.000627797	0.010860242
CHCHD10	427.42	1.07	0.27	-3.97	7.0624E-05	0.002418829
FOXK1	2845.90	1.07	0.32	-3.34	0.000846935	0.01332845
RBM38	1224.72	1.07	0.33	-3.29	0.001019701	0.014812904
TMUB1	1648.93	1.07	0.33	-3.22	0.001281995	0.017089493
METRN	1736.04	1.07	0.32	-3.31	0.000937514	0.014073158
ATAD3A	3795.74	1.07	0.32	-3.36	0.00077565	0.012630554
POM121C	1691.66	1.07	0.34	-3.14	0.00170061	0.020543438
RET	117.60	1.07	0.26	-4.07	4.66582E-05	0.001849596
PPAP2C	466.67	1.07	0.35	-3.07	0.002131595	0.023525407
CLUH	17085.03	1.07	0.32	-3.38	0.000721178	0.012046506
ZNF787	1812.98	1.07	0.35	-3.07	0.002112427	0.023389797
UFSP1	33.58	1.07	0.37	-2.86	0.004176185	0.035423326
FBLN2	238.17	1.07	0.30	-3.61	0.0003098	0.006838236
C15orf52	2308.63	1.07	0.21	-4.98	6.41479E-07	5.73828E-05
KIAA1549	284.82	1.06	0.24	-4.40	1.06418E-05	0.0005906
RNASEH2C	387.15	1.06	0.31	-3.49	0.000487566	0.009169339
APRT	2683.25	1.06	0.33	-3.18	0.001477301	0.018673893
PTPN23	3819.87	1.06	0.35	-3.06	0.002247242	0.024183143
PNKP	1789.06	1.06	0.28	-3.78	0.000157581	0.00425125
SLC25A39	8066.04	1.06	0.32	-3.31	0.000938011	0.014073158
CST3	4058.55	1.06	0.27	-3.86	0.000111967	0.003368173
MED16	2091.68	1.06	0.36	-2.97	0.002962883	0.028612441
RP11-465B22.8	1119.09	1.06	0.30	-3.49	0.000490057	0.009203468
C7orf50	3257.85	1.06	0.32	-3.27	0.001086526	0.015375861
PTPRS	928.10	1.06	0.30	-3.55	0.000386977	0.008004449
FAM207BP	33.70	1.06	0.35	-2.98	0.002855121	0.027989243
GIGYF1	2645.31	1.06	0.31	-3.46	0.000538845	0.009779213
LRWD1	1246.36	1.06	0.33	-3.22	0.001279182	0.017089493
NR2F6	1444.93	1.06	0.30	-3.47	0.000517213	0.009516307
SYNGR1	111.23	1.06	0.36	-2.89	0.003794234	0.033598093
TPGS1	272.69	1.06	0.30	-3.50	0.000470441	0.009009271
ARHGEF4	3662.24	1.06	0.24	-4.40	1.09254E-05	0.000599
MT-ND6	36529.48	1.06	0.28	-3.75	0.000179551	0.004694911
FLNC	93.72	1.06	0.34	-3.07	0.002167597	0.023711037
DNM1	119.84	1.05	0.32	-3.28	0.001040037	0.015044024
SORCS2	40.22	1.05	0.36	-2.93	0.003385315	0.031179252
GPC1	9934.83	1.05	0.34	-3.09	0.002025297	0.022758648
RELL2	321.92	1.05	0.31	-3.36	0.000786694	0.012719583
GPR144	36.22	1.05	0.36	-2.89	0.00390999	0.034098918

SLC43A1	128.59	1.05	0.27	-3.95	7.91533E-05	0.002581941
ISOC2	1186.13	1.05	0.33	-3.22	0.001285374	0.017104421
ILVBL	2227.49	1.05	0.34	-3.06	0.002216655	0.024034977
TBX1	92.83	1.05	0.36	-2.93	0.003386906	0.031179252
NINJ1	3040.42	1.05	0.28	-3.82	0.000134146	0.003823852
SIRPB2	34.25	1.05	0.35	-2.99	0.002820388	0.027835316
THEM6	421.31	1.05	0.37	-2.87	0.004099873	0.034906687
PER2	235.79	1.05	0.26	-3.98	6.84185E-05	0.002366601
FANCE	492.62	1.05	0.30	-3.51	0.000440599	0.008732974
DVL1	9114.82	1.05	0.33	-3.19	0.001400847	0.01808862
MT-ND3	22969.29	1.05	0.31	-3.33	0.000865118	0.013489697
PPP1R13L	7732.58	1.04	0.33	-3.20	0.001388635	0.01798684
WDR4	3245.66	1.04	0.27	-3.82	0.000131848	0.003774184
ADAMTSL4	398.75	1.04	0.32	-3.29	0.001001337	0.014655732
CCND1	4598.99	1.04	0.16	-6.40	1.60113E-10	6.59713E-08
ESRRA	2712.01	1.04	0.32	-3.25	0.001134185	0.015833179
SBF1	8431.28	1.04	0.35	-2.99	0.002820995	0.027835316
TMEM79	768.62	1.04	0.32	-3.24	0.001182867	0.016333084
RPUSD1	1953.74	1.04	0.37	-2.78	0.005378559	0.041776627
CYC1	4600.26	1.04	0.27	-3.87	0.000108985	0.003313715
MBD3	3699.81	1.04	0.35	-2.99	0.002781107	0.027642335
ALDH16A1	502.00	1.04	0.37	-2.81	0.004917422	0.039485788
OXLD1	317.07	1.04	0.32	-3.25	0.001152862	0.016044482
PSD4	2859.20	1.04	0.29	-3.61	0.000303131	0.006723774
GIPC1	11654.42	1.03	0.34	-3.03	0.002423959	0.025352749
40057.00	16352.67	1.03	0.31	-3.31	0.000936542	0.014073158
ASPSCR1	874.76	1.03	0.34	-3.06	0.002182058	0.023811751
WDR34	2869.03	1.03	0.33	-3.14	0.001717818	0.020651791
PRR22	131.64	1.03	0.29	-3.57	0.000352591	0.007514392
KLHL26	267.48	1.03	0.33	-3.10	0.001914807	0.022026757
NOC4L	1534.39	1.03	0.35	-2.99	0.002799878	0.027747775
KCTD11	420.33	1.03	0.34	-3.05	0.002260774	0.024261834
RHOT2	4771.50	1.03	0.30	-3.42	0.000623571	0.01080089
CISD3	992.15	1.03	0.32	-3.24	0.001195764	0.016423036
PCNXL3	4860.32	1.03	0.34	-3.01	0.002644579	0.026811754
LRRC45	763.48	1.03	0.32	-3.22	0.001264302	0.017008684
VARS	10713.45	1.03	0.33	-3.07	0.002112197	0.023389797
CTSD	1180.35	1.03	0.34	-3.05	0.002274739	0.024315741
G6PC3	1216.02	1.03	0.34	-3.04	0.002327853	0.024708683
ZDHHC12	2325.25	1.03	0.35	-2.93	0.003383209	0.031179252
SH2D3A	2776.08	1.02	0.26	-3.87	0.000109182	0.003313715

CTD-2228K2.5	67.35	1.02	0.27	-3.85	0.000118466	0.003514569
TM7SF2	870.20	1.02	0.31	-3.30	0.000974377	0.014495193
ENDOG	175.72	1.02	0.35	-2.90	0.003748835	0.033359231
LTBP3	1571.23	1.02	0.32	-3.19	0.001417351	0.018232469
C16orf13	1204.27	1.02	0.33	-3.14	0.001704644	0.020560733
KIF26A	58.65	1.02	0.38	-2.69	0.007120102	0.049464084
DUSP6	602.40	1.02	0.27	-3.72	0.000201177	0.005055857
RP11-54F2.1	213.82	1.02	0.19	-5.42	5.978E-08	9.5627E-06
SIRT6	1393.96	1.02	0.32	-3.16	0.001581123	0.019581242
TMEM38A	104.36	1.02	0.32	-3.19	0.001411108	0.018178666
C20orf27	1964.11	1.02	0.35	-2.88	0.004026182	0.034517023
NCAPH2	2976.95	1.02	0.29	-3.46	0.000535848	0.009740551
EFS	852.73	1.02	0.30	-3.36	0.000790868	0.012738896
PKN3	520.02	1.02	0.29	-3.49	0.000477505	0.009080612
CDH4	1352.87	1.02	0.30	-3.40	0.000685857	0.011598999
PC	3333.94	1.02	0.31	-3.27	0.001086725	0.015375861
BRD4	4559.68	1.02	0.32	-3.16	0.001603292	0.019818149
IMPDH1	4994.38	1.02	0.32	-3.14	0.001673871	0.020361764
PER1	5302.32	1.02	0.35	-2.95	0.003161906	0.029939018
YIF1A	2404.46	1.02	0.34	-3.02	0.002523252	0.026014143
ATP6V0B	4893.20	1.02	0.36	-2.86	0.004255767	0.035834966
RAC3	585.52	1.02	0.36	-2.84	0.004470161	0.037129373
NCLN	10879.70	1.02	0.35	-2.89	0.003852641	0.033840027
UBE2S	1114.82	1.02	0.28	-3.64	0.000277714	0.006400121
CCDC61	401.86	1.02	0.29	-3.47	0.000528961	0.009654066
SULT1A1	165.80	1.02	0.29	-3.55	0.000392242	0.008056373
FOXRED2	555.11	1.02	0.28	-3.57	0.000356003	0.007575227
ARRDC1	3173.95	1.02	0.32	-3.22	0.001281763	0.017089493
CBLC	2056.54	1.01	0.29	-3.46	0.000544338	0.009803122
LAT2	71.13	1.01	0.31	-3.22	0.001271118	0.017061591
ZNF316	1132.30	1.01	0.32	-3.21	0.001341184	0.017585415
MFSD10	7970.37	1.01	0.32	-3.13	0.00177309	0.021129455
LTBR	5083.33	1.01	0.28	-3.57	0.000360655	0.007638353
TRMT2A	1123.20	1.01	0.33	-3.06	0.002231577	0.024098677
B4GALT2	5012.19	1.01	0.33	-3.12	0.001839333	0.021578433
ARHGEF39	68.50	1.01	0.28	-3.61	0.000301518	0.006704671
HOXC11	282.86	1.01	0.23	-4.34	1.40792E-05	0.000727079
ADCK4	807.54	1.01	0.32	-3.15	0.00164014	0.020109099
RAD23A	4718.26	1.01	0.31	-3.29	0.001000817	0.014655732
MEX3A	107.49	1.01	0.29	-3.50	0.000462092	0.008962129
ADCK5	586.51	1.01	0.31	-3.22	0.001264675	0.017008684

ZNF524	341.13	1.01	0.35	-2.88	0.004012855	0.034469661
DCXR	834.38	1.01	0.31	-3.29	0.000998169	0.014655732
RASIP1	675.34	1.01	0.32	-3.12	0.001790454	0.0212431
PGP	820.60	1.01	0.25	-4.08	4.5977E-05	0.001827923
BAK1	2542.84	1.01	0.33	-3.07	0.002125211	0.023510979
AKT1S1	4733.54	1.01	0.33	-3.09	0.001997649	0.022635028
RARA	480.67	1.01	0.32	-3.11	0.001866792	0.021639196
DUSP23	650.19	1.01	0.30	-3.33	0.000866472	0.013490079
C17orf53	532.40	1.01	0.24	-4.12	3.85807E-05	0.001614099
MIR663A	255.94	1.01	0.32	-3.14	0.001688952	0.020467634
AXL	852.90	1.01	0.17	-6.04	1.49893E-09	4.73976E-07
ARFRP1	1872.26	1.01	0.29	-3.42	0.000620761	0.010779682
TIMM17B	1402.80	1.01	0.35	-2.89	0.003896802	0.034051938
WDR24	592.06	1.00	0.33	-3.01	0.002594935	0.026389929
SNAPC4	1998.77	1.00	0.29	-3.45	0.000559083	0.010008348
SEMA4C	557.59	1.00	0.30	-3.38	0.000736496	0.012210955
TMEM175	691.18	1.00	0.30	-3.29	0.000993432	0.014634559
C9orf16	1686.52	1.00	0.33	-3.06	0.002195828	0.023839395
FZR1	2649.62	1.00	0.33	-3.06	0.002228433	0.024098677
RP11-1055B8.7	740.57	1.00	0.35	-2.90	0.003788244	0.033578068
FBXW9	498.76	1.00	0.30	-3.34	0.000850155	0.013363656
RP11-215G15.5	235.10	1.00	0.20	-5.09	3.5582E-07	3.75046E-05
TMEM134	800.21	1.00	0.32	-3.09	0.002021949	0.022758648
PKP3	13159.86	1.00	0.30	-3.29	0.001013192	0.014770654
ZFP36L1	8243.97	1.00	0.25	-4.07	4.7665E-05	0.001878553
NDOR1	1805.92	1.00	0.34	-2.97	0.002978623	0.028682958
GMEB2	1587.34	1.00	0.31	-3.28	0.001043383	0.015076381
ZNF213	746.39	1.00	0.35	-2.87	0.00408169	0.034839129
DRAP1	7103.01	1.00	0.23	-4.33	1.45841E-05	0.000739925
SLC12A4	5020.33	1.00	0.31	-3.28	0.001049434	0.015147718
RP11-1096G20.5	246.66	1.00	0.28	-3.62	0.000293556	0.006597482
COMMD2	435.24	-1.00	0.26	3.84	0.00012252	0.003574915
RP11-2H8.2	35.43	-1.00	0.37	2.70	0.006871068	0.048232271
ARHGEF12	2745.08	-1.01	0.18	5.50	3.88844E-08	6.95672E-06
VLDLR	92.20	-1.01	0.26	3.90	9.49052E-05	0.002969542
PRKRIR	362.13	-1.01	0.26	3.82	0.000134977	0.003831489
MYLIP	97.64	-1.01	0.26	3.82	0.000133327	0.003808513
TNFSF10	247.29	-1.01	0.20	4.92	8.52443E-07	7.38259E-05
AC005224.2	28.82	-1.01	0.36	2.81	0.00498291	0.039753053
CTC-436P18.3	27.08	-1.01	0.36	2.78	0.005383	0.041776627
RP13-631K18.5	36.87	-1.01	0.32	3.12	0.001795383	0.021246149

RFTN1P1	40.55	-1.01	0.32	3.21	0.00134686	0.017625853
AP2B1	3365.29	-1.02	0.20	5.12	3.12266E-07	3.34321E-05
RCBTB1	358.28	-1.02	0.22	4.66	3.20565E-06	0.000233087
ROBO2	70.72	-1.02	0.27	3.85	0.00012054	0.003547569
KRT75	1796.31	-1.02	0.15	6.64	3.09229E-11	1.50164E-08
SLC35B4	248.73	-1.02	0.19	5.26	1.42099E-07	1.82275E-05
OCRL	698.67	-1.02	0.19	5.51	3.64911E-08	6.61559E-06
CTSO	55.38	-1.03	0.35	2.92	0.003462083	0.03161447
ATG4A	64.05	-1.03	0.28	3.66	0.000249422	0.005894669
KRT34	1606.18	-1.03	0.18	5.69	1.28334E-08	2.56611E-06
SLFN5	3131.31	-1.04	0.24	4.26	2.08983E-05	0.000993548
ZNF135	62.19	-1.04	0.33	3.18	0.001469539	0.018632549
SPON1	29.17	-1.04	0.37	2.79	0.005210132	0.040901939
KLF6	16751.19	-1.04	0.16	6.39	1.66308E-10	6.65085E-08
DDX60	1745.46	-1.04	0.31	3.39	0.000701002	0.011796449
RHOQ	33.69	-1.04	0.33	3.20	0.001396257	0.018046484
KDELR3	71.01	-1.04	0.25	4.12	3.79287E-05	0.001591716
TSPYL5	148.08	-1.04	0.25	4.23	2.30956E-05	0.001071778
PIK3CB	563.23	-1.05	0.18	5.91	3.48811E-09	9.12075E-07
YIPF6	487.20	-1.05	0.21	4.97	6.76316E-07	6.01037E-05
RP11-517B11.7	37.17	-1.05	0.38	2.75	0.006035884	0.044773547
SYTL2	46.78	-1.06	0.32	3.29	0.000986963	0.01459073
SNCAIP	40.32	-1.06	0.35	3.01	0.002578651	0.026325829
TAGLN	786.24	-1.07	0.22	4.89	1.01011E-06	8.47805E-05
RASSF6	192.37	-1.08	0.24	4.49	7.01874E-06	0.000426044
KRT15	2745.68	-1.08	0.15	7.35	2.03796E-13	2.13155E-10
TMED2	3722.80	-1.08	0.21	5.23	1.72952E-07	2.09967E-05
C2orf27A	70.51	-1.08	0.28	3.85	0.000116102	0.003461925
PIK3IP1	159.42	-1.09	0.23	4.82	1.41715E-06	0.000114697
RND1	75.76	-1.10	0.25	4.40	1.08094E-05	0.000595043
COG6	258.16	-1.10	0.24	4.67	2.96438E-06	0.000216703
RPS6KL1	37.99	-1.11	0.35	3.18	0.00145262	0.018516646
ZNF165	368.98	-1.11	0.20	5.57	2.5655E-08	4.84488E-06
FAM115A	181.01	-1.11	0.22	4.95	7.49602E-07	6.6184E-05
CENPQ	189.16	-1.12	0.28	4.03	5.62844E-05	0.002108262
LARP6	171.74	-1.12	0.19	5.74	9.50429E-09	1.9288E-06
ANKRD19P	23.58	-1.12	0.39	2.91	0.003622536	0.032533439
RCAN1	2603.32	-1.12	0.18	6.10	1.03261E-09	3.51011E-07
CYP2R1	93.95	-1.12	0.27	4.20	2.71209E-05	0.001203951
LCA5	19.52	-1.12	0.41	2.76	0.005861751	0.044058723
FBXO32	44.10	-1.12	0.31	3.62	0.000295709	0.00662398

TCHH	63.62	-1.12	0.28	3.97	7.27619E-05	0.002461053
ZXDA	109.78	-1.13	0.28	3.98	6.87168E-05	0.002366601
S100A7	119.65	-1.13	0.22	5.20	2.04707E-07	2.39948E-05
RND3	7959.37	-1.13	0.22	5.12	3.03432E-07	3.27442E-05
INA	27.43	-1.13	0.38	3.01	0.002597615	0.026397433
TXNIP	252.13	-1.13	0.25	4.58	4.56995E-06	0.000303651
ZPLD1	36.07	-1.13	0.35	3.23	0.001244177	0.01679948
KCNJ2	68.22	-1.13	0.35	3.21	0.001349603	0.017644757
MGAT4A	41.98	-1.14	0.37	3.08	0.002048242	0.022865311
ASNS	705.06	-1.14	0.22	5.28	1.27181E-07	1.72928E-05
SLC27A6	115.23	-1.14	0.27	4.18	2.9055E-05	0.001270292
NXT2	125.36	-1.15	0.26	4.34	1.4162E-05	0.000727079
CD200	31.00	-1.15	0.36	3.17	0.001536268	0.019216779
EPB41	361.26	-1.15	0.19	6.15	7.55016E-10	2.70157E-07
AC005083.1	24.86	-1.15	0.39	2.93	0.003407772	0.031286616
MAP3K8	627.75	-1.15	0.21	5.41	6.24097E-08	9.75384E-06
APOBEC3G	31.43	-1.16	0.36	3.17	0.001503992	0.018917463
BST2	42.90	-1.16	0.32	3.69	0.000227249	0.005478548
HIST1H2BD	173.66	-1.16	0.20	5.83	5.44439E-09	1.23379E-06
LRRK2	23.77	-1.16	0.42	2.79	0.005230626	0.04099183
BPGM	635.21	-1.17	0.23	5.17	2.38653E-07	2.68179E-05
GALNT5	368.05	-1.17	0.22	5.28	1.29217E-07	1.73956E-05
IL1B	5626.22	-1.17	0.16	7.22	5.29352E-13	4.23388E-10
ERBB2IP	1032.46	-1.18	0.22	5.44	5.40699E-08	8.96571E-06
SNRNP27	114.19	-1.18	0.21	5.48	4.31824E-08	7.4323E-06
MSMO1	4621.80	-1.18	0.24	4.98	6.21501E-07	5.6133E-05
RP11-20B7.1	46.36	-1.19	0.30	3.99	6.50229E-05	0.002296405
FYTTD1	754.82	-1.19	0.26	4.57	4.77388E-06	0.000312629
AC107399.2	21.45	-1.19	0.39	3.06	0.002194606	0.023839395
BEND7	102.89	-1.19	0.24	5.04	4.60455E-07	4.47349E-05
RP11-690G19.3	27.14	-1.19	0.35	3.38	0.000733514	0.012197674
RP11-3L8.3	56.25	-1.20	0.27	4.42	9.99077E-06	0.000559031
ZSCAN31	102.59	-1.20	0.25	4.85	1.21122E-06	0.00010042
RSAD2	192.83	-1.21	0.29	4.23	2.35208E-05	0.001084108
LEPR	128.38	-1.22	0.25	4.84	1.28714E-06	0.000105429
ERO1LB	29.83	-1.23	0.35	3.46	0.000530928	0.009676983
ARL5B	1724.07	-1.23	0.25	4.88	1.05365E-06	8.78928E-05
FAM46A	135.83	-1.23	0.24	5.19	2.12801E-07	2.47303E-05
AC005682.6	20.58	-1.24	0.42	2.97	0.002970335	0.02864372
DISP1	36.85	-1.25	0.40	3.09	0.002013977	0.022721133
STRADB	80.93	-1.25	0.28	4.51	6.63607E-06	0.000408284

SELPLG	36.41	-1.27	0.37	3.45	0.000562561	0.010038252
DNAJB9	219.89	-1.27	0.27	4.74	2.17705E-06	0.000166644
SLC9A2	16.03	-1.27	0.45	2.80	0.005167454	0.040711269
RP11-196G18.22	41.56	-1.27	0.32	3.97	7.19356E-05	0.00244527
HEPHL1	569.61	-1.28	0.22	5.74	9.37452E-09	1.9288E-06
OVCH2	28.82	-1.29	0.37	3.51	0.000446696	0.008815268
BTG4	29.73	-1.29	0.38	3.36	0.000768939	0.012566419
RP11-1020M18.10	109.99	-1.29	0.22	5.87	4.33041E-09	1.05144E-06
PLA2G4C	71.89	-1.29	0.27	4.72	2.37625E-06	0.000180502
ECHDC1	657.12	-1.29	0.22	5.97	2.31761E-09	6.85055E-07
CYFIP2	21.83	-1.30	0.40	3.27	0.001073978	0.015299623
CERKL	25.15	-1.31	0.39	3.38	0.000713863	0.011953695
RAB6B	83.06	-1.31	0.28	4.71	2.4891E-06	0.000188024
RP11-403A21.1	79.28	-1.31	0.27	4.89	1.00606E-06	8.47805E-05
MYO16	331.65	-1.31	0.22	6.06	1.35062E-09	4.43346E-07
DIO2	22.50	-1.32	0.45	2.90	0.003775658	0.033494554
MOXD1	85.44	-1.32	0.26	4.99	5.99805E-07	5.54799E-05
STC2	119.68	-1.32	0.23	5.65	1.60581E-08	3.11918E-06
GPC4	45.74	-1.32	0.30	4.37	1.2644E-05	0.000679529
IL7	66.16	-1.32	0.31	4.24	2.22125E-05	0.001045065
GRIK1	13.80	-1.32	0.49	2.69	0.007148503	0.049586225
PTPRR	15.57	-1.32	0.48	2.75	0.005916566	0.044274511
IMPG1	19.16	-1.33	0.42	3.17	0.001542175	0.019237578
ID4	51.04	-1.33	0.29	4.56	5.05434E-06	0.000327944
SULT1E1	37.89	-1.35	0.35	3.87	0.000109477	0.003315288
ENO2	36.83	-1.35	0.33	4.08	4.5878E-05	0.001827923
APBA1	45.52	-1.35	0.34	4.02	5.70716E-05	0.002126035
FN1	732.37	-1.35	0.19	7.07	1.53616E-12	1.09932E-09
LANCL1	38.30	-1.36	0.39	3.50	0.000457612	0.008927038
IL23A	136.77	-1.38	0.23	5.95	2.70754E-09	7.44259E-07
RP1-93H18.7	16.47	-1.38	0.44	3.13	0.001722921	0.020676574
CCDC115	161.99	-1.39	0.22	6.34	2.31427E-10	8.99061E-08
TMEM217	241.21	-1.39	0.18	7.56	3.93689E-14	4.46083E-11
N4BP2L1	18.71	-1.39	0.42	3.31	0.000947901	0.014194499
HSD11B1	42.67	-1.40	0.31	4.43	9.28077E-06	0.000530213
IL20	265.07	-1.40	0.23	5.97	2.41045E-09	6.92087E-07
RP11-443P15.2	56.88	-1.40	0.33	4.29	1.80294E-05	0.000885001
CCDC126	46.64	-1.40	0.31	4.59	4.49527E-06	0.000303651
RP1-78O14.1	20.49	-1.41	0.41	3.43	0.000603668	0.010536678
CAMK4	16.19	-1.41	0.49	2.88	0.003950799	0.034172405
PLCL2	32.43	-1.41	0.39	3.65	0.000258057	0.006060111

SERINC3	1189.28	-1.41	0.19	7.64	2.14103E-14	2.80042E-11
RP11-439L18.3	15.35	-1.42	0.49	2.89	0.003910237	0.034098918
SOCS3	861.48	-1.43	0.31	4.59	4.48737E-06	0.000303651
CXCL5	283.89	-1.43	0.28	5.16	2.48738E-07	2.77221E-05
ATPAF1	318.40	-1.46	0.20	7.32	2.5558E-13	2.40499E-10
SLC2A10	13.52	-1.46	0.48	3.04	0.002351335	0.02483996
RP11-277P12.20	142.86	-1.46	0.22	6.61	3.73439E-11	1.69225E-08
IGFBP3	871.07	-1.47	0.17	8.44	3.22263E-17	5.47726E-14
RP11-96K19.2	15.89	-1.48	0.54	2.76	0.005763752	0.04358717
VNN3	30.52	-1.50	0.39	3.79	0.000147738	0.004073185
KLHL24	111.36	-1.52	0.25	6.20	5.77507E-10	2.12226E-07
ADORA2BP	24.02	-1.53	0.39	3.96	7.56666E-05	0.002503256
RP1-28O10.1	224.10	-1.54	0.23	6.74	1.57153E-11	8.21852E-09
MIR146A	195.64	-1.54	0.29	5.33	9.99558E-08	1.40113E-05
RRAGD	52.38	-1.54	0.30	5.07	4.04332E-07	4.13361E-05
RP11-568N6.1	29.06	-1.55	0.38	4.05	5.03006E-05	0.001948538
CASP7	286.33	-1.58	0.23	6.97	3.2612E-12	2.21712E-09
FAM171B	67.39	-1.59	0.28	5.74	9.34446E-09	1.9288E-06
CDKL2	19.22	-1.59	0.44	3.60	0.000323486	0.007105713
CADPS2	14.06	-1.61	0.52	3.10	0.001914496	0.022026757
REPS2	29.16	-1.62	0.35	4.57	4.78244E-06	0.000312629
SERPINE3	43.91	-1.64	0.32	5.20	2.03699E-07	2.39948E-05
MSRB3	60.95	-1.65	0.32	5.23	1.69468E-07	2.09408E-05
KB-1460A1.5	17.99	-1.66	0.47	3.50	0.000472202	0.009017595
TEPP	15.98	-1.67	0.46	3.60	0.000319723	0.00703442
TUBA1A	535.97	-1.67	0.18	9.32	1.13575E-20	3.86071E-17
MAP1B	118.14	-1.68	0.23	7.31	2.65315E-13	2.40499E-10
AC104777.2	36.55	-1.68	0.36	4.70	2.5751E-06	0.000193445
SYT14	40.15	-1.72	0.33	5.23	1.70952E-07	2.09408E-05
SOX4	3302.44	-1.72	0.16	11.04	2.49378E-28	3.3908E-24
AC023115.2	14.19	-1.74	0.49	3.57	0.000363481	0.007686239
FZD3	107.90	-1.74	0.24	7.22	5.21551E-13	4.23388E-10
S100A12	22.42	-1.74	0.42	4.20	2.64843E-05	0.001191025
HAS2	15.75	-1.77	0.48	3.73	0.00018957	0.004845076
VIM	471.24	-1.78	0.17	10.51	7.59215E-26	5.16152E-22
NFKBIZ	11511.68	-1.78	0.19	9.23	2.60778E-20	7.09159E-17
KCNJ5	38.35	-1.82	0.35	5.27	1.39448E-07	1.80579E-05
POSTN	29.78	-1.83	0.53	3.47	0.000526519	0.009622418
SPRR2A	433.82	-1.84	0.27	6.80	1.03889E-11	5.88574E-09
BVES	35.85	-1.89	0.36	5.23	1.6806E-07	2.09408E-05
MBD5	562.33	-1.89	0.21	9.06	1.33897E-19	3.03432E-16

LSMEM1	28.35	-1.89	0.45	4.21	2.50722E-05	0.001140155
CXCL6	44.81	-1.90	0.34	5.54	3.02475E-08	5.63391E-06
SPRR3	281.51	-1.92	0.28	6.93	4.32803E-12	2.80229E-09
TLR3	58.90	-1.95	0.31	6.23	4.57619E-10	1.7284E-07
RP11-79H23.3	117.66	-1.96	0.24	8.23	1.92715E-16	2.91149E-13
IL16	141.60	-1.98	0.22	9.02	1.8425E-19	3.57892E-16
UCHL1	25.30	-2.06	0.39	5.24	1.63328E-07	2.05627E-05
SERPINB4	17.44	-2.71	0.52	5.21	1.89325E-07	2.2781E-05
KIAA1683	14.82	-3.01	0.63	4.80	1.58728E-06	0.000124861

Table S2. List of genes regulated by *NFKBIZ* knockdown in primary KC after 24 h of IL-36α treatment

	Base Mean	log2 fold Change	lfcSE	stat	P value	P value adj.
EIF3CL	90.67	4.06	1.13	-3.59	0.000331714	0.008152368
KRT24	31.08	2.91	0.43	-6.75	1.47482E-11	9.70012E-09
CAPN8	61.71	2.09	0.29	-7.25	4.10347E-13	2.983E-10
FAM198B	44.03	1.88	0.31	-5.99	2.03957E-09	5.3152E-07
SLITRK6	45.18	1.75	0.33	-5.33	1.00299E-07	1.57424E-05
STXBP6	13.61	1.73	0.52	-3.29	0.00099468	0.017750032
LIPH	29.41	1.64	0.36	-4.58	4.75827E-06	0.000360893
NTSR1	78.88	1.52	0.25	-6.01	1.90292E-09	5.1979E-07
STAC	26.41	1.44	0.40	-3.59	0.000333048	0.008156136
LINC00887	20.71	1.41	0.41	-3.41	0.000657254	0.013310848
MYH15	30.14	1.36	0.34	-3.97	7.13402E-05	0.002667673
RIC3	117.85	1.36	0.21	-6.38	1.72605E-10	8.13769E-08
DMRTA1	23.41	1.30	0.40	-3.29	0.000992507	0.017734168
DCN	17.44	1.27	0.45	-2.83	0.004682933	0.049665678
SCML2	92.89	1.27	0.24	-5.22	1.74412E-07	2.43331E-05
ITGBL1	28.56	1.27	0.38	-3.33	0.000857423	0.015982091
RP11-298I3.4	17.83	1.24	0.43	-2.88	0.004010271	0.044886435
HSPD1P6	34.86	1.22	0.32	-3.83	0.000128662	0.004094669
PHACTR3	60.59	1.22	0.27	-4.51	6.62191E-06	0.000445448
DIRAS1	33.77	1.16	0.40	-2.91	0.00362251	0.042080834
SDPR	243.29	1.16	0.21	-5.58	2.4665E-08	5.07779E-06
GPR110	497.93	1.15	0.18	-6.43	1.27104E-10	6.5021E-08
SYT8	268.62	1.14	0.21	-5.43	5.61872E-08	9.70073E-06
MAP7D2	48.49	1.12	0.28	-3.97	7.26778E-05	0.002691222
ABCC2	75.47	1.11	0.24	-4.60	4.18993E-06	0.000326957
LINC00589	55.07	1.08	0.28	-3.91	9.18453E-05	0.003187356
SFTA1P	58.81	1.08	0.28	-3.82	0.000130854	0.00414531
PTGS1	511.23	1.07	0.17	-6.19	5.91133E-10	2.04118E-07
CTD-2620I22.1	33.05	1.06	0.36	-2.98	0.002896516	0.035624827
SMOC1	366.80	1.05	0.20	-5.26	1.41323E-07	2.07655E-05
RGS2	307.53	1.04	0.20	-5.24	1.61151E-07	2.31855E-05
PRUNE2	26.42	1.04	0.36	-2.90	0.003700374	0.042733745
SPA17	45.81	1.04	0.29	-3.61	0.000308974	0.007787498
ZNF583	58.68	1.04	0.26	-4.00	6.46924E-05	0.002495898
MYEF2	71.56	1.02	0.25	-4.07	4.72542E-05	0.001977803
ZNF239	91.37	1.02	0.23	-4.41	1.04794E-05	0.000637625
LDHBP2	90.21	1.01	0.24	-4.21	2.59898E-05	0.001277475

AC073254.1	34.29	1.01	0.34	-2.95	0.003227682	0.038665004
PLEKHA7	89.51	1.01	0.25	-3.96	7.50795E-05	0.002750658
LINC00704	101.10	1.01	0.22	-4.48	7.35763E-06	0.000480401
HS3ST2	148.52	1.01	0.22	-4.63	3.69191E-06	0.000298203
SLC16A14	222.42	1.00	0.20	-4.91	8.93763E-07	9.4234E-05
FAM189A2	62.36	-1.00	0.28	3.61	0.000300926	0.007616219
SLIT3	230.67	-1.00	0.22	4.48	7.51757E-06	0.000482943
CFD	43.13	-1.01	0.31	3.30	0.000980138	0.017581391
LY6D	730.05	-1.01	0.16	6.28	3.38131E-10	1.37361E-07
BRSK1	43.25	-1.01	0.31	3.30	0.000973688	0.017511168
HOXC13-AS	55.52	-1.01	0.26	3.84	0.000124073	0.00398533
GYLTL1B	1905.03	-1.01	0.22	4.68	2.87195E-06	0.000241875
HSPG2	11564.52	-1.01	0.27	3.73	0.000187734	0.005368489
POU3F1	92.69	-1.01	0.26	3.84	0.000121601	0.003938646
KCTD11	149.38	-1.01	0.27	3.77	0.000160137	0.004805191
PGLYRP4	148.05	-1.01	0.22	4.70	2.54566E-06	0.000220042
PCOLCE	83.00	-1.01	0.24	4.16	3.2392E-05	0.001511481
TYMP	4581.80	-1.01	0.22	4.52	6.30653E-06	0.000435529
REEP2	76.79	-1.02	0.27	3.78	0.000159338	0.004802299
RP11-178L8.4	76.41	-1.02	0.31	3.30	0.000950581	0.01723022
SDK2	869.43	-1.02	0.24	4.21	2.51133E-05	0.001247714
SMTNL1	26.72	-1.02	0.36	2.85	0.004327679	0.047326918
HELZ2	5813.25	-1.02	0.25	4.17	3.10266E-05	0.001462589
FADS3	1037.55	-1.03	0.19	5.45	5.12252E-08	9.07081E-06
C3	465.87	-1.03	0.16	6.53	6.68566E-11	3.69369E-08
RP11-540O11.1	37.41	-1.03	0.33	3.11	0.001885911	0.026909295
YPEL3	660.07	-1.03	0.20	5.10	3.33169E-07	4.0015E-05
PIK3IP1	498.63	-1.03	0.17	6.15	7.83048E-10	2.35119E-07
CRAT	241.10	-1.04	0.22	4.70	2.549E-06	0.000220042
ADAMTS13	104.37	-1.04	0.24	4.26	2.08188E-05	0.001085092
TAPBPL	180.28	-1.04	0.21	4.93	8.32423E-07	8.84417E-05
COASY	2348.99	-1.04	0.23	4.53	5.87339E-06	0.000411793
ANKRD34A	42.51	-1.04	0.30	3.49	0.000482208	0.010555093
FZD2	82.43	-1.05	0.32	3.33	0.000875477	0.0162528
MTRNR2L10	55.86	-1.05	0.29	3.67	0.000243039	0.006518172
EFNB3	66.44	-1.05	0.26	4.11	3.99571E-05	0.001768869
DMTN	222.27	-1.05	0.26	4.00	6.31471E-05	0.002449964
MT-TY	125.52	-1.05	0.23	4.59	4.36565E-06	0.000338755
CPNE2	431.18	-1.05	0.19	5.41	6.30583E-08	1.04935E-05
RP11-277P12.20	112.18	-1.06	0.23	4.61	3.9345E-06	0.000311937
ENG	106.24	-1.06	0.29	3.68	0.000234302	0.006357919

LGALS9B	181.91	-1.06	0.21	4.99	5.90899E-07	6.63537E-05
SNRNP27	120.27	-1.07	0.21	4.97	6.70389E-07	7.29087E-05
SOCS2-AS1	34.52	-1.07	0.35	3.10	0.001947527	0.027532491
RP11-1212A22.1	57.91	-1.07	0.32	3.36	0.000787142	0.015100013
GPR37	29.64	-1.07	0.35	3.09	0.001989725	0.027928943
C6orf1	1217.75	-1.07	0.23	4.76	1.94035E-06	0.000182314
HAPLN3	266.92	-1.07	0.23	4.70	2.5683E-06	0.000220332
SCN4B	707.59	-1.08	0.17	6.15	7.68511E-10	2.35119E-07
LINC01023	23.73	-1.08	0.37	2.92	0.003497639	0.04097488
BVES	46.92	-1.08	0.30	3.57	0.000355435	0.008582637
FAM171A2	88.86	-1.08	0.34	3.18	0.001468619	0.022740549
RHBDL2	24.91	-1.08	0.38	2.87	0.004165372	0.046210537
SERINC3	1585.24	-1.08	0.16	6.67	2.6143E-11	1.6413E-08
FKBP10	210.72	-1.09	0.25	4.43	9.53804E-06	0.000588122
CORO1A	214.25	-1.09	0.23	4.73	2.2957E-06	0.000207647
NYAP1	89.84	-1.09	0.30	3.65	0.000265543	0.006894125
LGALS7B	931.50	-1.09	0.26	4.17	3.09335E-05	0.001462589
FAM219A	512.66	-1.09	0.24	4.56	5.2364E-06	0.000379077
RAB1B	33.70	-1.09	0.37	2.96	0.003037162	0.036959723
LHX5	28.44	-1.10	0.35	3.13	0.001733432	0.025606591
CRIP2	699.27	-1.10	0.23	4.72	2.36531E-06	0.000210772
RAB6B	86.40	-1.10	0.25	4.38	1.17532E-05	0.000687979
COL5A1	245.29	-1.11	0.25	4.35	1.3793E-05	0.000783986
RHOQ	49.83	-1.11	0.29	3.84	0.000121449	0.003938646
SYDE1	391.62	-1.11	0.25	4.36	1.29345E-05	0.000744382
HOXC4	87.04	-1.11	0.26	4.29	1.80533E-05	0.000977852
ADAMTS4	30.04	-1.11	0.38	2.97	0.003025565	0.03685106
FMNL1	130.10	-1.11	0.25	4.53	5.79198E-06	0.000408157
CCDC115	287.21	-1.11	0.18	6.26	3.95861E-10	1.51879E-07
MARCKSL1	118.24	-1.12	0.30	3.76	0.000171446	0.005049068
TUBA1A	624.18	-1.12	0.18	6.18	6.29244E-10	2.09222E-07
PODNL1	31.93	-1.12	0.36	3.09	0.001986981	0.027918808
LIF	184.44	-1.12	0.25	4.55	5.26953E-06	0.000379077
MAP3K11	1824.36	-1.12	0.24	4.66	3.09117E-06	0.00025566
ACSS1	228.69	-1.12	0.24	4.61	4.04233E-06	0.000317231
SALL4	32.93	-1.12	0.35	3.22	0.001290772	0.020926104
CENPQ	158.67	-1.13	0.21	5.34	9.08296E-08	1.442E-05
ACBD4	285.67	-1.13	0.21	5.39	6.99621E-08	1.13684E-05
PLXND1	91.30	-1.13	0.27	4.25	2.10833E-05	0.001094747
SLC16A8	25.49	-1.14	0.39	2.94	0.003264253	0.038969547
NXPH4	95.49	-1.14	0.30	3.73	0.000189537	0.005397698

FAM214B	1216.79	-1.14	0.22	5.18	2.21473E-07	2.94133E-05
SP6	429.30	-1.15	0.24	4.73	2.26318E-06	0.000207647
SERPING1	400.41	-1.15	0.21	5.54	3.03878E-08	5.91149E-06
SPRED3	43.04	-1.15	0.33	3.50	0.000460265	0.010206017
BLMH	387.27	-1.15	0.17	6.65	2.99076E-11	1.79601E-08
THBS2	802.88	-1.15	0.18	6.36	2.03829E-10	9.08158E-08
CCNJL	26.69	-1.16	0.37	3.11	0.001870603	0.02680162
CTD-2020K17.1	26.53	-1.16	0.36	3.22	0.001270874	0.020748591
SCARB1	2991.83	-1.16	0.23	5.01	5.38841E-07	6.15081E-05
FN1	304.07	-1.16	0.18	6.38	1.76753E-10	8.13769E-08
TMEM132A	3354.91	-1.16	0.23	4.97	6.69016E-07	7.29087E-05
GDPD5	162.98	-1.16	0.26	4.54	5.69741E-06	0.000403552
TMEM191A	68.05	-1.17	0.34	3.48	0.000498525	0.010790008
SYNPO	2585.17	-1.17	0.24	4.88	1.04271E-06	0.000108286
NOTCH4	35.04	-1.17	0.36	3.30	0.000967345	0.017462712
ACE	24.07	-1.18	0.40	2.92	0.003480061	0.040872967
HUNK	27.10	-1.18	0.37	3.19	0.001433596	0.022348565
SV2A	132.35	-1.18	0.25	4.72	2.39885E-06	0.00021239
GPAT2	63.95	-1.19	0.30	3.93	8.63229E-05	0.003065018
IL20	56.19	-1.19	0.32	3.76	0.000166692	0.004956471
FTH1P8	23.31	-1.19	0.39	3.06	0.002214819	0.02984495
SLC17A9	80.11	-1.19	0.25	4.69	2.7174E-06	0.000230262
VWA7	27.89	-1.19	0.37	3.27	0.001079926	0.018668253
APOE	748.01	-1.20	0.22	5.52	3.35329E-08	6.25886E-06
CYP27A1	78.85	-1.20	0.32	3.71	0.000209098	0.005846266
SIPA1	656.02	-1.20	0.23	5.14	2.70849E-07	3.37024E-05
BST2	197.93	-1.20	0.19	6.35	2.18371E-10	9.42544E-08
PPP1R18	4297.35	-1.20	0.23	5.28	1.26839E-07	1.92516E-05
PCSK9	11804.14	-1.21	0.22	5.42	6.06306E-08	1.02993E-05
TMCC2	75.65	-1.21	0.29	4.23	2.38766E-05	0.001199215
SLC39A2	19.35	-1.21	0.41	2.95	0.003220708	0.038614945
POU2F2	1307.38	-1.22	0.19	6.25	4.16135E-10	1.55342E-07
SPNS2	543.97	-1.22	0.23	5.23	1.70651E-07	2.40513E-05
GPR68	577.04	-1.22	0.20	6.03	1.64512E-09	4.73383E-07
MAP1B	410.31	-1.22	0.19	6.48	9.13939E-11	4.85512E-08
CAPS	33.88	-1.22	0.37	3.33	0.000858749	0.015985237
C1R	173.34	-1.22	0.20	6.20	5.65456E-10	2.00258E-07
JDP2	617.13	-1.22	0.18	6.78	1.18876E-11	8.20959E-09
CXCL16	1478.53	-1.23	0.23	5.45	4.93629E-08	8.85455E-06
PLXNA3	1190.72	-1.23	0.22	5.47	4.47546E-08	8.13356E-06
GS1-393G12.12	26.33	-1.24	0.41	3.00	0.002693966	0.034136756

KRT16P2	49.62	-1.24	0.29	4.23	2.30216E-05	0.001169025
CSPG4	501.37	-1.24	0.26	4.72	2.32342E-06	0.000208383
SCAMP5	42.71	-1.25	0.38	3.32	0.000915025	0.016783973
ABCC10	1243.27	-1.25	0.23	5.52	3.3161E-08	6.25886E-06
ACO2	1739.56	-1.25	0.17	7.53	5.18035E-14	5.11078E-11
PAMR1	74.53	-1.26	0.27	4.69	2.71146E-06	0.000230262
FAM195B	32.91	-1.26	0.39	3.25	0.001160528	0.019511564
C6orf15	43.56	-1.26	0.33	3.82	0.000132048	0.004160174
S100A8	8630.75	-1.27	0.22	5.77	7.97492E-09	1.85451E-06
GPR173	31.34	-1.27	0.35	3.58	0.000346392	0.008438046
TXNIP	3456.35	-1.27	0.24	5.29	1.24831E-07	1.91574E-05
HEPHL1	3533.63	-1.27	0.21	6.17	6.80847E-10	2.13724E-07
OSBPL7	212.33	-1.27	0.22	5.72	1.08056E-08	2.40721E-06
ADCY4	34.53	-1.28	0.34	3.74	0.000183712	0.005308437
SEZ6L2	403.34	-1.28	0.25	5.13	2.93584E-07	3.62051E-05
IL23A	73.48	-1.28	0.25	5.16	2.47566E-07	3.14851E-05
FCHO1	211.02	-1.29	0.26	4.96	7.11591E-07	7.67851E-05
ARC	33.63	-1.29	0.36	3.55	0.000380604	0.009007532
KAL1	83.06	-1.29	0.26	4.94	7.9037E-07	8.46247E-05
TSPO	8371.87	-1.29	0.25	5.18	2.18777E-07	2.93374E-05
TNS1	111.45	-1.29	0.30	4.26	2.07814E-05	0.001085092
TUBB3	1857.49	-1.29	0.22	5.84	5.14911E-09	1.24771E-06
PANX2	73.24	-1.30	0.27	4.84	1.32989E-06	0.000133554
RP11-400F19.8	21.40	-1.30	0.45	2.92	0.003516065	0.041155837
SOCS3	157.09	-1.30	0.26	5.03	4.82062E-07	5.54853E-05
AC004463.6	22.13	-1.30	0.41	3.20	0.001362287	0.021577873
CADPS2	17.83	-1.30	0.46	2.84	0.004443628	0.048185798
TMEM92	124.71	-1.31	0.24	5.52	3.33742E-08	6.25886E-06
S100A9	15585.29	-1.33	0.21	6.17	6.69343E-10	2.13724E-07
NKX3-1	20.77	-1.33	0.42	3.16	0.001559432	0.023879019
SLC43A2	569.07	-1.33	0.26	5.17	2.35661E-07	3.07071E-05
LRRC3	171.66	-1.33	0.26	5.07	3.91625E-07	4.62318E-05
SAMD14	18.99	-1.34	0.43	3.11	0.001880611	0.026909295
ZMYND15	46.45	-1.36	0.30	4.48	7.6302E-06	0.000487909
C1QTNF1	1349.56	-1.39	0.22	6.34	2.31811E-10	9.70235E-08
SLC16A11	38.07	-1.39	0.36	3.90	9.44046E-05	0.003243572
SYNGR3	28.03	-1.39	0.39	3.60	0.000313323	0.007868399
CGB7	36.92	-1.40	0.32	4.31	1.64631E-05	0.000902332
GPC4	56.32	-1.40	0.30	4.67	2.94823E-06	0.000246793
TUBB2A	355.53	-1.40	0.19	7.33	2.23646E-13	1.78579E-10
CSF2	39.14	-1.41	0.32	4.37	1.25808E-05	0.000727057

IGFBP6	436.68	-1.42	0.23	6.20	5.552E-10	2.00258E-07
IL36G	383.12	-1.42	0.19	7.37	1.7061E-13	1.47279E-10
ENO2	79.49	-1.43	0.28	5.16	2.44598E-07	3.14851E-05
LGALS7	587.76	-1.43	0.27	5.25	1.48167E-07	2.15419E-05
NACAD	118.79	-1.43	0.26	5.43	5.52136E-08	9.6533E-06
S100A12	54.35	-1.44	0.36	4.00	6.44007E-05	0.002491602
C19orf57	18.77	-1.45	0.46	3.17	0.001531504	0.023608405
S100A7	326.28	-1.45	0.18	7.88	3.29226E-15	4.54727E-12
CORO2B	53.56	-1.45	0.30	4.83	1.38393E-06	0.000135567
AEBP1	212.84	-1.46	0.25	5.96	2.59318E-09	6.63279E-07
APBA1	34.79	-1.46	0.35	4.17	3.08801E-05	0.001462589
PLA2G2F	69.26	-1.47	0.27	5.50	3.75617E-08	6.91736E-06
IL24	170.77	-1.48	0.19	7.67	1.7029E-14	1.96004E-11
PRSS22	410.89	-1.48	0.19	7.68	1.62535E-14	1.96004E-11
UCHL1	35.97	-1.49	0.33	4.50	6.8193E-06	0.000455015
LITAF	2448.79	-1.50	0.14	10.35	4.21026E-25	1.9384E-21
RP13-582O9.5	28.92	-1.50	0.37	4.08	4.55133E-05	0.001934244
CNTNAP1	15.56	-1.50	0.50	3.03	0.002465369	0.031943415
KCND1	80.61	-1.52	0.25	6.00	1.91929E-09	5.1979E-07
SPRR3	227.33	-1.52	0.19	8.23	1.85835E-16	3.20845E-13
LRRC3DN	137.36	-1.54	0.27	5.77	8.0561E-09	1.85451E-06
JAK3	63.63	-1.54	0.30	5.11	3.23868E-07	3.92392E-05
AIM1	3690.16	-1.55	0.15	10.28	9.04763E-25	3.12415E-21
DERL3	126.08	-1.55	0.26	6.02	1.77037E-09	4.99027E-07
PDZK1IP1	566.74	-1.56	0.18	8.60	7.92637E-18	1.82465E-14
ELF3	19.38	-1.57	0.45	3.52	0.000437428	0.00990547
MIR429	16.87	-1.57	0.48	3.25	0.001173527	0.019646978
VNN3	34.10	-1.59	0.35	4.48	7.42522E-06	0.000481489
hsa-mir-1199	26.95	-1.59	0.41	3.88	0.000103197	0.003468021
KAZALD1	15.82	-1.59	0.48	3.35	0.000818648	0.015485891
KCNJ5	195.48	-1.60	0.21	7.65	1.97443E-14	2.09775E-11
DMBT1	32.38	-1.61	0.37	4.33	1.51885E-05	0.000842505
IGFBP4	928.73	-1.62	0.25	6.58	4.58119E-11	2.63647E-08
SLC22A31	38.39	-1.65	0.33	4.99	6.02067E-07	6.70625E-05
SPRR2B	304.78	-1.66	0.20	8.40	4.64465E-17	9.16455E-14
TEPP	62.31	-1.66	0.28	6.00	1.97445E-09	5.24443E-07
CXCL6	31.24	-1.67	0.36	4.59	4.43058E-06	0.000341872
GLI1	29.92	-1.67	0.41	4.07	4.78121E-05	0.001983125
CNTD2	23.15	-1.71	0.43	4.01	6.02711E-05	0.002371695
LCN2	3457.99	-1.72	0.16	10.64	1.94804E-26	1.34532E-22
KRT16P5	79.38	-1.72	0.37	4.62	3.85974E-06	0.000308155

ADAMTS15	29.23	-1.72	0.41	4.24	2.22643E-05	0.001138943
FAM131C	26.24	-1.72	0.40	4.28	1.87246E-05	0.001002417
APH1A	3229.29	-1.79	0.22	8.14	4.06748E-16	6.24222E-13
SPRR2A	1110.16	-1.82	0.20	9.23	2.59764E-20	7.17572E-17
EBF4	21.39	-1.83	0.47	3.91	9.40591E-05	0.003243572
HAS2	17.73	-1.88	0.47	4.04	5.26456E-05	0.002126144
ATP13A2	133.64	-1.90	0.33	5.76	8.20766E-09	1.85843E-06
CHST1	20.40	-1.93	0.48	4.06	4.92054E-05	0.002011045
SERPINB4	27.36	-1.94	0.41	4.73	2.20374E-06	0.000204283
IGFBP3	65.76	-1.99	0.27	7.33	2.32726E-13	1.78579E-10
IL8	89.90	-2.03	0.27	7.45	9.42817E-14	8.68146E-11
C12orf68	31.95	-2.03	0.42	4.82	1.4046E-06	0.000136622
CREB3L1	17.96	-2.31	0.49	4.74	2.11112E-06	0.000197019
CSF3	340.13	-2.49	0.23	10.91	1.04831E-27	1.44793E-23
KM-PA-2	28.98	-3.90	1.30	3.01	0.002654495	0.033822772

Table S3. List of primer sequences for qPCR

Primer	Sequence 5`- 3`	Gene
hgIL36g-F	CTGGAGCCACGATTCAGTCC	*IL36G*
hgIL36G-R	AGGGTCCACACTTGCTGATTC	*IL36G*
hgS100A9-F	GCTGGAACGCAACATAGAGAC	*S100A9*
hgS100A9-R	TGCATTTGTGTCCAGGTCCTC	*S100A9*
hgLCN2-F	AGAGCTACAATGTCACCTCCG	*LCN2*
hgLCN2-R	TTAATGTTGCCCAGCGTGAAC	*LCN2*
hgDEFB4A-F	CCAGCCATCAGCCATGAGGGT	*DEFB4A*
hgDEFB4A-R	GGAGCCCTTTCTGAATCCGCA	*DEFB4A*
hgCXCL8-F	AAGGTGCAGTTTTGCCAAGG	*CXCL8*
hgCXCL8-R	CCCAGTTTTCCTTGGGGTCC	*CXCL8*
hgCCL20-F	TGTCAGTGCTGCTACTCCAC	*CCL20*
hgCCL20-R	GATTTGCGCACACAGACAAC	*CCL20*
hgIL17C-F	CCGGCTTCCCTTACCCTATC	*IL17C*
hgIL17C-R	GGTACTTCCAAGGAGGTTGGG	*IL17C*
hgRPL37a-F	AGATGAAGAGACGAGCTGTGG	*RPL37A*
hgRPL37a-R	CTTTACCGTGACAGCGGAAG	*RPL37A*
hgCXCL5-F	AGCGCGTTGCGTTTGTTTAC	*CXCL5*
hgCXCL5-R	TGGCGAACACTTGCAGATTAC	*CXCL5*
hgNFKBIZ-F	ACACCCACAAACCAACTCTGG	*NFKBIZ*
hgNFKBIZ-R	TGCTGAACACTGGAGGAAGTC	*NFKBIZ*

Table S4. List of primer sequences for generation of luciferase constructs

***NFKBIZ* reporter**	**Primer**	**Sequence 5`- 3`**
w/o STAT3	mutSTAT3-F	GGCGCGCTCTTGCCAGTCCCCAAGAACCA
	mutSTAT3-R	GACTGGCAAGAGCGCGCCCCGCACCCCTC
w/o STAT1/3	mutSTAT1/3-F	ATCCTGTACGGACGCATCCGGAGGAGGGGC
	mutSTAT1/3-R	ATGCGTCCGTACAGGATGAGGCAATGCG
w/o AP1	mutAP1-F	CGCCTCCCTCTGCAGGCCCATCCCTCCAC
	mutAP1-R	AGGGAGGCGGTGGAGGGAACCGGTTGGCC
w/o KLF4	mutKLF4-F	GGTCGGTCGCGCATTGCCTCATCCTGTAC
	mutKLF4-R	GCAATGCGCGACCGACCGGTTGTTTGCCTG
w/o NF-κB	mutNFkB-F	CGCGCGCTGTAAGGGCAGGCAAACAACCGGT
	mutNFkB-R	GCCTGCCCTTACAGCGCGCGGCTTCCAGCCT

References

1. Nemajerova A, et al. (2016) TAp73 is a central transcriptional regulator of airway multiciliogenesis. *Genes Dev* 30(11):1300-1312.
2. Kim D, Langmead B, Salzberg SL (2015) HISAT: a fast spliced aligner with low memory requirements. *Nat Methods* 12(4):357-360.
3. Nair RP, et al. (2009) Genome-wide scan reveals association of psoriasis with IL-23 and NF-kappaB pathways. *Nat Genet* 41(2):199-204.
4. Swindell WR, et al. (2011) Genome-wide expression profiling of five mouse models identifies similarities and differences with human psoriasis. *Plos One* 6(4):e18266
5. Mahil SK, et al. (2017) An analysis of IL-36 signature genes and individuals with IL1RL2 knockout mutations validates IL-36 as a psoriasis therapeutic target. *Sci Transl Med* 9(411).

The CDK4/6-EZH2 pathway is a potential therapeutic target for psoriasis

Anne Müller,[1] Antje Dickmanns,[2] Claudia Resch,[1] Knut Schäkel,[3] Stephan Hailfinger,[1,4] Matthias Dobbelstein,[2] Klaus Schulze-Osthoff,[1,5] and Daniela Kramer[1]

[1]Interfaculty Institute for Biochemistry, University of Tübingen, Tübingen, Germany. [2]Institute of Molecular Oncology, Göttingen Center of Molecular Biosciences (GZMB), University of Göttingen, Göttingen, Germany. [3]Department of Dermatology, Heidelberg University Hospital, Heidelberg, Germany. [4]Cluster of Excellence iFIT (EXC 2180), Image-Guided and Functionally Instructed Tumor Therapies, University of Tübingen, Tübingen, Germany. [5]German Cancer Consortium (DKTK) and German Cancer Research Center (DKFZ), Heidelberg, Germany.

Psoriasis is a frequent, inflammatory skin disease characterized by keratinocyte hyperproliferation and a disease-related infiltration of immune cells. Here, we identified a novel proinflammatory signaling pathway driven by cyclin-dependent kinase 4 (CDK4) and CDK6 and the methyltransferase EZH2 as a valid target for psoriasis therapy. Delineation of the pathway revealed that CDK4/6 phosphorylated EZH2 in keratinocytes, thereby triggering a methylation-induced activation of STAT3. Subsequently, active STAT3 resulted in the induction of IκBζ, which is a key proinflammatory transcription factor required for cytokine synthesis in psoriasis. Pharmacological or genetic inhibition of CDK4/6 or EZH2 abrogated psoriasis-related proinflammatory gene expression by suppressing IκBζ induction in keratinocytes. Importantly, topical application of CDK4/6 or EZH2 inhibitors on the skin was sufficient to fully prevent the development of psoriasis in various mouse models by suppressing STAT3-mediated IκBζ expression. Moreover, we found a hyperactivation of the CDK4/6-EZH2 pathway in human and mouse psoriatic skin lesions. Thus, this study not only identifies a novel psoriasis-relevant proinflammatory pathway, but also proposes the repurposing of CDK4/6 or EZH2 inhibitors as a new therapeutic option for patients with psoriasis.

Introduction

Psoriasis is a mixed autoimmune and autoinflammatory skin disease, affecting 2% to 3% of the population worldwide. Psoriatic skin lesions are characterized by keratinocyte hyperproliferation and a massive infiltration of immune cells, such as neutrophils, macrophages, and Th17 cells (1). The cytokine families IL-17 and IL-36 have been identified as key factors driving the establishment of psoriatic plaques (2). Therefore, state-of-the-art therapies comprise neutralizing antibodies against IL-17 (3, 4), while IL-36 antagonists are currently tested in clinical trials (5). Although psoriasis therapy with neutralizing antibodies is very effective, disadvantages comprise high costs, difficult application routes, systemic side effects such as upper respiratory tract infections, and long-term therapy resistance due to the development of antidrug antibodies (6, 7). Therefore, effective new therapy approaches against psoriasis are needed.

Previously, IκBζ, encoded by the gene *NFKBIZ*, has been identified as a key regulator of transcription in psoriasis (8, 9). IκBζ represents an atypical member of the IκB family that is inducibly expressed and then accumulates in the nucleus, leading to the activation or repression of a selective subset of NF-κB target genes (10). Especially in keratinocytes, IL-17A, alone or even more potently in combination with TNF-α as well as IL-36 cytokines, triggers a NF-κB– and STAT3-dependent transcriptional upregulation of IκBζ expression (9). Subsequently, IκBζ induces a subset of IL-36– and IL-17–responsive target genes in keratinocytes, including *CXCL2*, *CXCL5*, *CXCL8*, *LCN2*, *DEFB4*, or *IL1B*, which all have already been implicated in the pathogenesis of psoriasis (2). How IκBζ regulates these downstream target genes remains elusive. It is assumed that IκBζ recruits epigenetic modifiers, such as TET2 or the SWI/SNF complex, to the promoter sites of its target genes, leading to a change in DNA methylation or nucleosome remodeling (11, 12).

In agreement with its role as a key regulator of psoriasis-related gene expression, IκBζ-deficient mice are completely protected against imiquimod-mediated (IMQ-mediated) or IL-36–mediated psoriasis-like skin inflammation (8, 9). Moreover, human psoriatic skin lesions are characterized by an upregulated expression of IκBζ (8, 9). Altogether, these findings validate IκBζ as an attractive new therapeutic target in psoriasis. As IκBζ lacks any enzymatic activity, it is difficult to develop direct IκBζ inhibitors (13). Therefore, small molecule inhibitors blocking the induction or downstream function of IκBζ could represent an alternative strategy for targeting IκBζ in psoriasis.

CDK4 and CDK6, in complex with cyclin D1, cyclin D2, or cyclin D3, represent well known cell-cycle regulating kinases that can phosphorylate RB, leading to the release of E2F transcription factors and G1-S cell cycle transition (14). Consistently, amplification of CDK4 and CDK6 as well as overexpression of cyclin D proteins are frequently observed events in cancer, leading to the excessive proliferation of tumor cells (15, 16). ATP-competitive CDK4/6 inhibitors, such

Conflict of interest: DK, AM, and KSO filed patent applications for the treatment of psoriasis using CDK4/6 and EZH2 inhibitors at the European Patent Office (19200621.1 and 19200622.9, "Agent for the treatment of psoriasis").

Submitted: October 11, 2019; **Accepted:** July 14, 2020; **Published:** September 28, 2020.
Reference information: *J Clin Invest*. https://doi.org/10.1172/JCI134217.

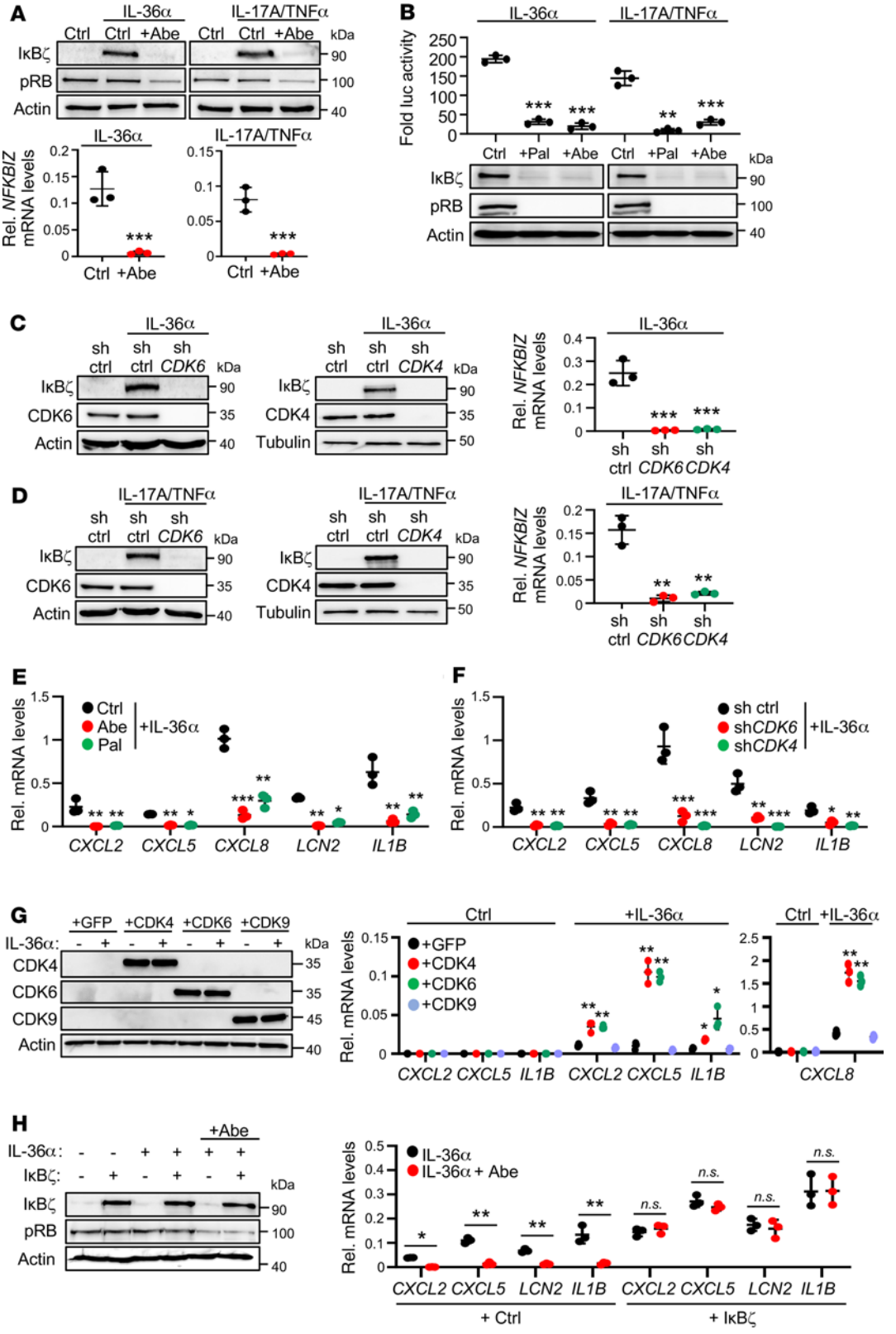
A
IL-36α
IL-17A/TNFα
Ctrl Ctrl +Abe Ctrl Ctrl +Abe kDa
IκBζ
pRB
Actin
90
100
40
Rel. NFKBIZ mRNA levels
***
Ctrl +Abe
B
Fold luc activity
Ctrl +Pal +Abe Ctrl +Pal +Abe
C
sh ctrl
sh CDK6
sh CDK4
CDK6
CDK4
Tubulin
35
50
D
E
Ctrl
Abe
Pal
+IL-36α
Rel. mRNA levels
CXCL2 CXCL5 CXCL8 LCN2 IL1B
F
sh ctrl
shCDK6
shCDK4
G
+GFP +CDK4 +CDK6 +CDK9
IL-36α: - + - + - + - +
CDK9
45
H
+Abe
IκBζ: - + - + - +
IL-36α
IL-36α + Abe
n.s.
+ Ctrl
+ IκBζ

Figure 1. CDK4 and CDK6 regulate the expression of IκBζ and its proinflammatory target genes in IL-36α– and IL-17A/TNF-α–stimulated keratinocytes. (**A**) Human primary keratinocytes were treated for 1 hour with 100 ng/mL IL-36α or 200 ng/mL IL-17A and 10 ng/mL TNF-α. The CDK4/6 inhibitor abemaciclib (Abe) or an ethanol vehicle control (Ctrl) were added in parallel. Phosphorylation of RB (pRB) served as a control for CDK4/6 inhibition, and actin as a loading control. Relative mRNA levels of IκBζ (*NFKBIZ*) were normalized to the reference gene *RPL37A*. (**B**) Luciferase assay of IκBζ (*NFKBIZ*) promoter activity in HaCaT cells that were cytokine-stimulated for 24 hours in the presence or absence of the CDK4/6 inhibitors abemaciclib or palbociclib (Pal). Relative luciferase (luc) activity was normalized to an internal Renilla luciferase control that was transfected in parallel. Endogenous protein levels were analyzed as input controls by immunoblotting (bottom). (**C** and **D**) CDK4 and CDK6 were depleted in primary human keratinocytes by lentiviral transduction of shRNA. Ctrl shRNA– or *CDK4/6* shRNA–depleted cells were treated with (**C**) IL-36α or (**D**) IL-17A/TNF-α, similar as in **A**. (**E** and **F**) Human primary keratinocytes were stimulated with IL-36α as in **A**. (**E**) Cytokine gene expression in CDK4/6 inhibitor–treated cells. (**F**) Relative gene expression levels in IL-36α–treated control or *CDK4/6*-depleted cells. (**G**) Transient overexpression of CDK4, CDK6, or CDK9 in HaCaT cells, treated for 1 hour with 100 ng/mL IL-36α. (**H**) Cytokine gene expression in IL-36α–treated primary keratinocytes overexpressing IκBζ in the presence or absence of abemaciclib. For all analyses, $n = 3 \pm SD$. Significance was calculated using a 1-way ANOVA for multiple groups and a 2-tailed Student's *t* test for comparing 2 groups: $^{*}P < 0.05$; $^{**}P < 0.01$; $^{***}P < 0.001$.

as palbociclib and abemaciclib, have been developed for anticancer therapy and were recently approved for treatment of breast cancer patients (17). Interestingly, common side effects of a CDK4/6 inhibitor therapy constitute neutropenia and leukopenia (17, 18). Moreover, it was found that CDK4/6 inhibition modulates immune cell functions in kinase-dependent or -independent manners (19–22). Mechanistically, it is assumed that these atypical functions of CDK4 and CDK6 derive from their recently discovered role as cofactors for immune regulatory transcription factors (23–25). CDK6, especially, can colocalize at promoter regions of a subset of NF-κB, STAT3, or AP1 target genes, thereby changing the DNA-binding properties or activity of these transcription factors.

We screened for small-molecule inhibitors of IκBζ action in keratinocytes and identified CDK4/6 inhibitors as potent suppressors of IL-36– and IL-17A/TNF-α–mediated IκBζ expression. Mechanistically, CDK4/6 inhibitors suppressed the activity of STAT3, which was identified as a major transcriptional regulator of IκBζ expression in keratinocytes. STAT3 activation was promoted by CDK4/6-mediated phosphorylation of the methyltransferase EZH2, triggering the subsequent methylation of STAT3 and induction of IκBζ expression. Importantly, topical administration of CDK4/6 or EZH2 inhibitors on the skin completely prevented experimental psoriasis by suppressing STAT3 activation and consequently, IκBζ expression in keratinocytes. Moreover, as cyclin D2, cyclin D3, and EZH2 were found to be overexpressed in human psoriatic skin lesions, we propose repurposing CDK4/6 and EZH2 inhibitors for topical skin treatment of patients with psoriasis.

Results

CDK4/6 inhibitors suppress the expression of IκBζ and IκBζ-dependent, proinflammatory genes in IL-36α– and IL-17A/TNF-α–stimulated keratinocytes. IκBζ represents an attractive therapeutic target for psoriasis. However, due to a lack of enzyme activity, direct inhibition of IκBζ is not feasible. Key regulators in psoriasis constitute IL-17 and IL-36 family members (26, 27), which predominantly trigger a proinflammatory response in keratinocytes that is dependent on IκBζ (8, 9). Thus, we screened for small-molecule inhibitors that are able to block induction of IκBζ expression in response to either IL-36α or IL-17A. Previously, it was shown that IL-17–induced IκBζ expression is strongly increased in combination with TNF-α (8, 9). Intriguingly, we found that 2 CDK4/6 inhibitors, abemaciclib (Figure 1A and Supplemental Figure 1A; supplemental material available online with this article; https://doi.org/10.1172/JCI134217DS1) and palbociclib (Supplemental Figure 1B), completely blocked IL-36α– or IL-17A/TNF-α–mediated induction of IκBζ expression in primary human keratinocytes. Moreover, we observed similar effects in response to IL-36γ, IL-1β, or the TLR ligands flagellin and poly(I:C) (Supplemental Figure 1, C and D), thereby revealing a conservation of this pathway in keratinocytes.

To explore whether these effects were due to a CDK4/6 inhibitor-mediated G1 cell cycle arrest, we repeated the experiments in synchronized and single cell cycle phase–arrested keratinocytes. IL-36α treatment triggered IκBζ induction in all phases of the cell cycle; induction was completely suppressed by abemaciclib (Supplemental Figure 1E). Moreover, depletion of *RB* by RNA interference did not influence IL-36–mediated induction or abemaciclib-mediated suppression of IκBζ (Supplemental Figure 1F), thereby clearly indicating that the effect of CDK4/6 inhibitors on IκBζ expression was independent of their ability to trigger cell cycle arrest. Instead, we revealed that CDK4/6-dependent induction of IκBζ was mediated at the transcriptional level, as palbociclib and abemaciclib treatment abrogated the expression of a luciferase construct harboring the *NFKBIZ* (IκBζ) promoter in IL-36α–stimulated HaCaT cells (Figure 1B). Interestingly, also shRNA-mediated depletion of *CDK4* or *CDK6* was sufficient to suppress IL-36α– or IL-17A/TNF-α–dependent expression of IκBζ in human primary keratinocytes, thereby excluding off-target effects of the applied inhibitors (Figure 1, C and D). Accordingly, IκBζ-dependent target genes, such as *CXCL2*, *CXCL5*, or *CXCL8*, were strongly downregulated in IL-36α– and CDK4/6 inhibitor–treated keratinocytes (Figure 1E), as well as in *CDK4*- or *CDK6*-deficient cells (Figure 1F), whereas other NF-κB–dependent but IκBζ-independent genes, such as *NFKBIA* or *TNF*, remained unaffected (Supplemental Figure 1G). Similar effects of pharmacological or shRNA-mediated inhibition of CDK4/6 were obtained in IL-17A and TNF-α–stimulated cells (Supplemental Figure 1, H and I). CDK4/6 inhibitors have the potential to inhibit CDK9 kinase activity, although much higher concentrations are needed (17). To rule out effects deriving from the suppression of CDK9 activity, we transiently overexpressed CDK4, CDK6, or CDK9 in HaCaT cells and analyzed IL-36α–mediated gene expression. Overexpression of CDK4 and CDK6, but not CDK9, could increase IL-36α–mediated, IκBζ-dependent target gene expression in keratinocytes, thereby further confirming the specificity of CDK4 and CDK6 in regulating proinflammatory target gene expression in keratinocytes (Figure 1G).

We hypothesized that CDK4 and CDK6 are not involved in the direct regulation of IκBζ target gene expression but rather trigger the expression of IκBζ, which in turn induces a secondary, IκBζ-dependent gene expression in stimulated keratinocytes.

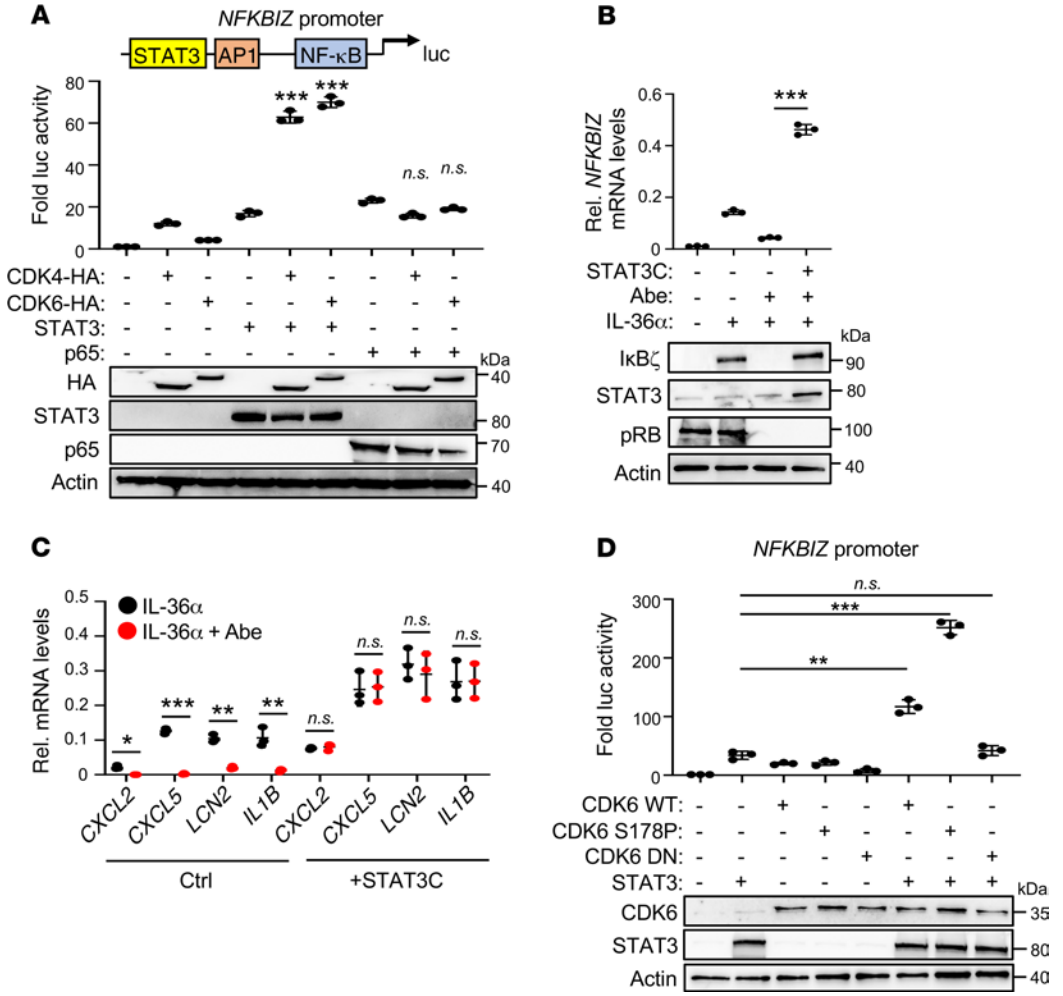

Figure 2. STAT3 mediates CDK4/6-dependent IκBζ induction in keratinocytes. (**A**) Luciferase assay of the *NFKBIZ* promoter in HEK293T cells after transient expression of CDK4, CDK6, STAT3, or p65, alone or in combination. The plasmid amounts for STAT3 (200 ng) and p65 (70 ng) were adjusted to achieve similar luciferase activity in the absence of CDK4/6 expression. Overexpression of the HA-tagged CDK4 and CDK6 proteins was detected using a HA-antibody. (**B**) Primary human keratinocytes with a transient overexpression of hyperactive STAT3 (STAT3C) were treated for 1 hour with 100 ng/mL IL-36α and abemaciclib (Abe). *NFKBIZ* mRNA levels normalized to *RPL37A*. Immunoblot analysis of STAT3C overexpression and CDK4/6 inhibition. (**C**) IκBζ target gene expression in STAT3C-overexpressing primary keratinocytes. Treatment as in **B**. (**D**) Luciferase activity assay of the *NFKBIZ* promoter in HEK293T cells overexpressing STAT3 alone or in combination with WT CDK6 (wt), hyperactive CDK6 (S178P), or a kinase-dead CDK6 mutant (CDK6 DN). For all analyses, $n = 3 \pm SD$. Significance was calculated using a 1-way ANOVA for multiple groups and a 2-tailed Student's *t* test for comparing 2 groups: $^*P < 0.05$; $^{**}P < 0.01$; $^{***}P < 0.001$.

To test this hypothesis, we transiently overexpressed IκBζ in IL-36α– or IL17A/TNF-α–stimulated primary human keratinocytes in the presence or absence of abemaciclib (Figure 1H and Supplemental Figure 1J). In this setup, exogenous overexpression of IκBζ completely abolished abemaciclib-mediated suppression of IκBζ target gene expression, thereby validating CDK4/6-mediated transcriptional upregulation of IκBζ as a prerequisite for CDK4/6-dependent, proinflammatory gene expression in keratinocytes.

CDK4/6-dependent induction of IκBζ expression is mediated by STAT3 in a cyclin-dependent manner. Beside their known involvement in cell cycle regulation, CDK4 and CDK6 have been described to function as transcriptional cofactors for STAT3, NF-κB, or AP-1 (23–25). As we revealed a CDK4/6-dependent induction of IκBζ on the transcriptional level, we next explored the responsible transcription factor. Of note, binding sites for all 3 transcription factors were previously identified at the *NFKBIZ* promoter region (9). Interestingly, expression of both CDK4 and CDK6 increased the STAT3-mediated induction of *NFKBIZ* promoter activity, whereas no synergistic effects could be observed when CDK4 and CDK6 were co-overexpressed with NF-κB p65 or cJun (Figure 2A and Supplemental Figure 2A). In agreement, deletion of the STAT3-binding site abrogated the expression of the *NFKBIZ* luciferase reporter in IL-36α–stimulated, CDK4/6-overexpressing HaCaT cells, whereas deletion of the NF-κB or AP1 motif had only a minor or almost no effect (Supplemental Figure 2B). Finally, transient overexpression of a constitutively active STAT3 mutant (STAT3C) abrogated the effects of CDK4/6 inhibition on the induction of IκBζ (Figure 2B) and IκBζ-dependent target gene expression in IL-36α–stimulated primary keratinocytes (Figure 2C), thereby validating STAT3 as the responsible transcription factor for CDK4/6-mediated effects in keratinocytes.

Previous publications reported that CDK6 acts as a cofactor for STAT3, independently of its kinase function (23). Therefore, we tested if a kinase-dead mutant of CDK6 (CDK6 DN) could

still synergize with STAT3 in driving the expression of the *NFKBIZ* luciferase reporter construct. Surprisingly, the kinase-dead mutant was not able to cooperate with STAT3 anymore, whereas a hyperactive version of CDK6 (CDK6 S178P) further increased the activity of the *NFKBIZ* promoter in a STAT3-dependent manner (Figure 2D). Accordingly, cyclin D2 and cyclin D3, which associate with CDK4/6 to activate their kinase function (14), synergized with CDK4/6 and STAT3 in activating the *NFKBIZ* luciferase promoter, whereas cyclin D1 failed to do so (Supplemental Figure 2, C and D). Moreover, cyclin D2 and cyclin D3 overexpression significantly elevated the expression of *NFKBIZ* and its target genes in IL-36α–stimulated keratinocytes (Supplemental Figure 2, E and F).

Cyclin D2 and cyclin D3 levels are transcriptionally regulated by NF-κB (28, 29). Therefore, we hypothesized that IL-36α or IL-17A/TNF-α stimulation results in a transient NF-κB–dependent upregulation of cyclin D2/D3, thereby explaining the cooperation of CDK4/6 and STAT3 in triggering IκBζ expression. Indeed, we detected a rapid binding of NF-κB p65 to the promoter regions of *CCND2* and *CCND3* upon stimulation of primary keratinocytes with IL-36α (Supplemental Figure 2G). Consequently, IL-36α stimulation led to increased expression of *CCND2* and *CCND3* in a p65-dependent manner (Supplemental Figure 2H), thus validating a NF-κB–mediated transcriptional upregulation of cyclin D2 and cyclin D3 in stimulated keratinocytes. Although p65 failed to cooperate with CDK4/6 in the induction of the *NFKBIZ* promoter directly (Figure 2A), we hypothesized that NF-κB participates in the induction of IκBζ in keratinocytes by transcriptionally upregulating cyclin D2/D3 levels, leading to activation of CDK4/6. In agreement, whereas knockdown of p65/*RELA* abrogated IκBζ expression in IL-36α–stimulated keratinocytes, exogenous overexpression cyclin D2 could fully restore the expression of *NFKBIZ* and its target genes in IL-36α–stimulated primary keratinocytes (Supplemental Figure 2I). Thus, our data imply that IL-36α and IL-17A/TNF-α stimulation of keratinocytes first activates NF-κB, leading to an upregulation of cyclin D2 and D3 levels. Subsequently, CDK4 and CDK6 become activated, leading to a STAT3-mediated induction of IκBζ.

CDK4 and CDK6 phosphorylate EZH2 to induce STAT3-mediated IκBζ expression. Next, we explored the mechanism of how CDK4 and CDK6 regulate STAT3-mediated expression of IκBζ. Of note, in chromatin immunoprecipitation (ChIP) analyses, CDK4 and CDK6 were found to localize to the *NFKBIZ* promoter region, which depended on the presence of STAT3 (Supplemental Figure 3A). Vice versa, knockdown of *CDK6* abrogated the binding of STAT3 at the *NFKBIZ* promoter (Supplemental Figure 3B). We reasoned that this interdependency was due to a CDK4/6-dependent regulation of STAT3 activity in keratinocytes. Accordingly, whereas the putative CDK-dependent phosphorylation site of STAT3 at threonine 727 (T727) remained unaffected (30), phosphorylation of STAT3 at tyrosine 705 (Y705), a prerequisite for STAT3 activation, was completely absent in abemaciclib-treated or *CDK4/6*-deficient cells after stimulation with IL-36α (Figure 3, A and B). As CDK4 and CDK6 are not able to directly trigger Y705 STAT3 phosphorylation, we assumed that CDK4/6-mediated activation of STAT3 might be exerted through an altered availability or activity of a cofactor needed for STAT3 activation in keratinocytes.

Previously, EZH2, a methyltransferase that directs H3K27me3 in conjunction with the PRC2 complex, was found to be important in the differentiation and function of keratinocytes (31–33). Moreover, it was revealed that EZH2 can methylate STAT3 at lysine 49, 140, or 180, thereby modulating STAT3 activity by affecting the subcellular localization or phosphorylation status of STAT3 at tyrosine 705 (34–36). We hypothesized that CDK4/6 might phosphorylate EZH2 in keratinocytes, thus enabling EZH2-mediated methylation and activation of STAT3. Pull-down assays in HEK293T cells validated an interaction of CDK4 and CDK6 with EZH2 (Supplemental Figure 3C). In agreement, EZH2 inhibition by EPZ6438 or shRNA-mediated depletion of *EZH2* inhibited STAT3 activation and induction of IκBζ in IL-36α– or IL-17A/TNF-α–stimulated keratinocytes (Figure 3C and Supplemental Figure 3D). Furthermore, pharmacological inhibition or depletion of *EZH2* effectively prevented IκBζ-dependent target gene expression in IL-36α–treated keratinocytes (Supplemental Figure 3E). Thus, we hypothesized that CDK4/6 phosphorylates EZH2 in keratinocytes, thereby regulating EZH2-dependent activation of STAT3.

In primary human keratinocytes, expression of EZH2 itself was induced by IL-36α (Figure 3D), in line with its previous identification as an NF-κB–regulated target gene (37). Of note, EZH2 harbors 2 potential CDK phosphorylation sites at threonine 345 and 487 (Supplemental Figure 3F), which were previously shown to be phosphorylatable by CDK1/2, thereby modifying EZH2 function (38–40). Indeed, phosphorylation of EZH2 at threonine 345 (T345), but not at threonine 487 (T487) was induced in IL-36α– or IL-17A/TNF-α–treated keratinocytes, whereas abemaciclib treatment or *CDK4/6* depletion completely abrogated this inducible EZH2 phosphorylation (Figure 3D and Supplemental Figure 3G). Moreover, phosphorylated EZH2 (T345) preferentially interacted with STAT3 in HaCaT cells, whereas CDK4/6 inhibition did not only abrogate the phosphorylation of EZH2 but also its interaction with STAT3 (Figure 3E).

These data suggest that CDK4/6-mediated phosphorylation of EZH2 at threonine 345 represents a regulatory switch, leading to the interaction of EZH2 with STAT3 and subsequent STAT3 activation. Accordingly, whereas WT EZH2 synergistically induced the expression of the *NFKBIZ* luciferase promoter in cooperation with CDK4/6 and STAT3, an EZH2 mutant lacking the CDK4/6-directed phosphorylation site (EZH2 T345A) abrogated CDK4/6- and STAT3-mediated *NFKBIZ* promoter-driven luciferase expression (Figure 3F). Furthermore, transient expression of a phospho-mimicking EZH2 (T345D) version could override abemaciclib-mediated suppression of IκBζ induction and IκBζ target gene expression in IL-36α–stimulated primary keratinocytes (Figure 3G), whereas transient overexpression of IκBζ abolished the effects of the pharmacological EZH2 inhibitor (Figure 3H). Finally, also STAT3C overexpression could override target gene expression defects in IL-36α–stimulated, *EZH2*-depleted keratinocytes (Supplemental Figure 3H), thereby validating STAT3 as the main target for suppression of gene expression in EZH2 inhibitor-treated keratinocytes. Therefore, we conclude that IL-36α– and IL-17A/TNF-α–mediated, CDK4/6-dependent induction of IκBζ expression is mediated by phosphorylation of EZH2 at T345, thereby triggering an EZH2-dependent activation of STAT3 in keratinocytes.

CDK4/6-phosphorylated EZH2 mediates STAT3 methylation at K180, leading to IκBζ expression in keratinocytes. As reported before, EZH2 can methylate STAT3 at lysine 49, 140, or 180, thereby changing its transcription factor function or subcellular

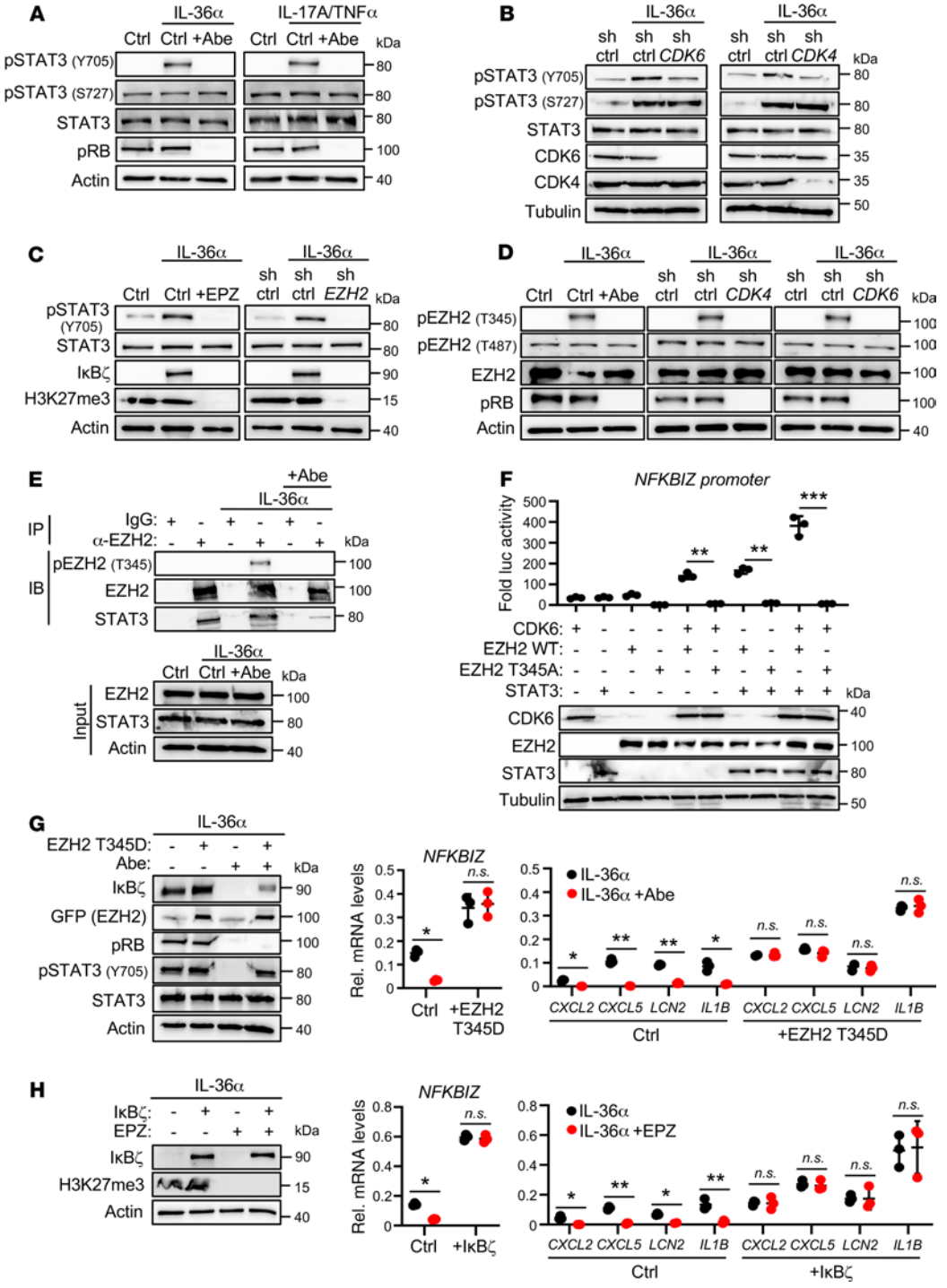

Figure 3. CDK4 and CDK6 phosphorylate EZH2 to induce STAT3 activation. (**A**) STAT3 activity was detected by analyzing the phosphorylation state at tyrosine 705 (Y705) and threonine 727 (T727) of STAT3 in primary human keratinocytes. After overnight starvation, cells were stimulated for 1 hour with IL-36α or IL-17A/TNF-α in the presence or absence of abemaciclib (Abe). (**B**) STAT3 activity in *CDK4*- and *CDK6*-depleted keratinocytes. Stimulation as in **A**. (**C**) Immunoblot detection of phosphorylated STAT3 (Y705) in IL-36α–stimulated keratinocytes, in which EZH2 function was suppressed by the EZH2 inhibitor EPZ6438 (EPZ, 10 μM) or shRNA-mediated knockdown. Detection of H3K27me3 controlled effective EZH2 inhibition or depletion. (**D**) Immunoblot detection of phosphorylated EZH2 at threonine 345 (T345) and threonine 487 (T487) in abemaciclib-treated or *CDK4/6*-depleted keratinocytes following stimulation with IL-36α. (**E**) Coimmunoprecipitation of EZH2 and STAT3 in HaCaT cells treated for 30 minutes with IL-36α in the presence or absence of abemaciclib. An EZH2-specific antibody or IgG was used for pull down of protein complexes. STAT3 and pEZH2 (T345) were detected by immunoblotting. (**F**) Luciferase activity assay of the *NFKBIZ* promoter in HEK293T cells, which transiently overexpress CDK6, WT EZH2 (wt), mutant EZH2 (T345A), or STAT3, alone or in combination. Equal protein expression was detected by immunoblotting. $n = 3 \pm SD$. (**G**) Gene expression in IL-36α– and abemaciclib-treated, primary keratinocytes following transient expression of a phospho-mimicking EZH2 (T345D) mutant. Input controls (left). mRNA levels of *NFKBIZ* and its target genes were normalized to *RPL37A* (right). $n = 3 \pm SD$. (**H**) Overexpression of IκBζ overrides the inhibitory effects of EPZ6438 (EPZ) on IL-36α–stimulated gene expression in primary keratinocytes. $n = 3 \pm SD$. Significance was calculated using a 1-way ANOVA for multiple groups and a 2-tailed Student's *t* test for comparing 2 groups: $^*P < 0.05$; $^{**}P < 0.01$; $^{***}P < 0.001$.

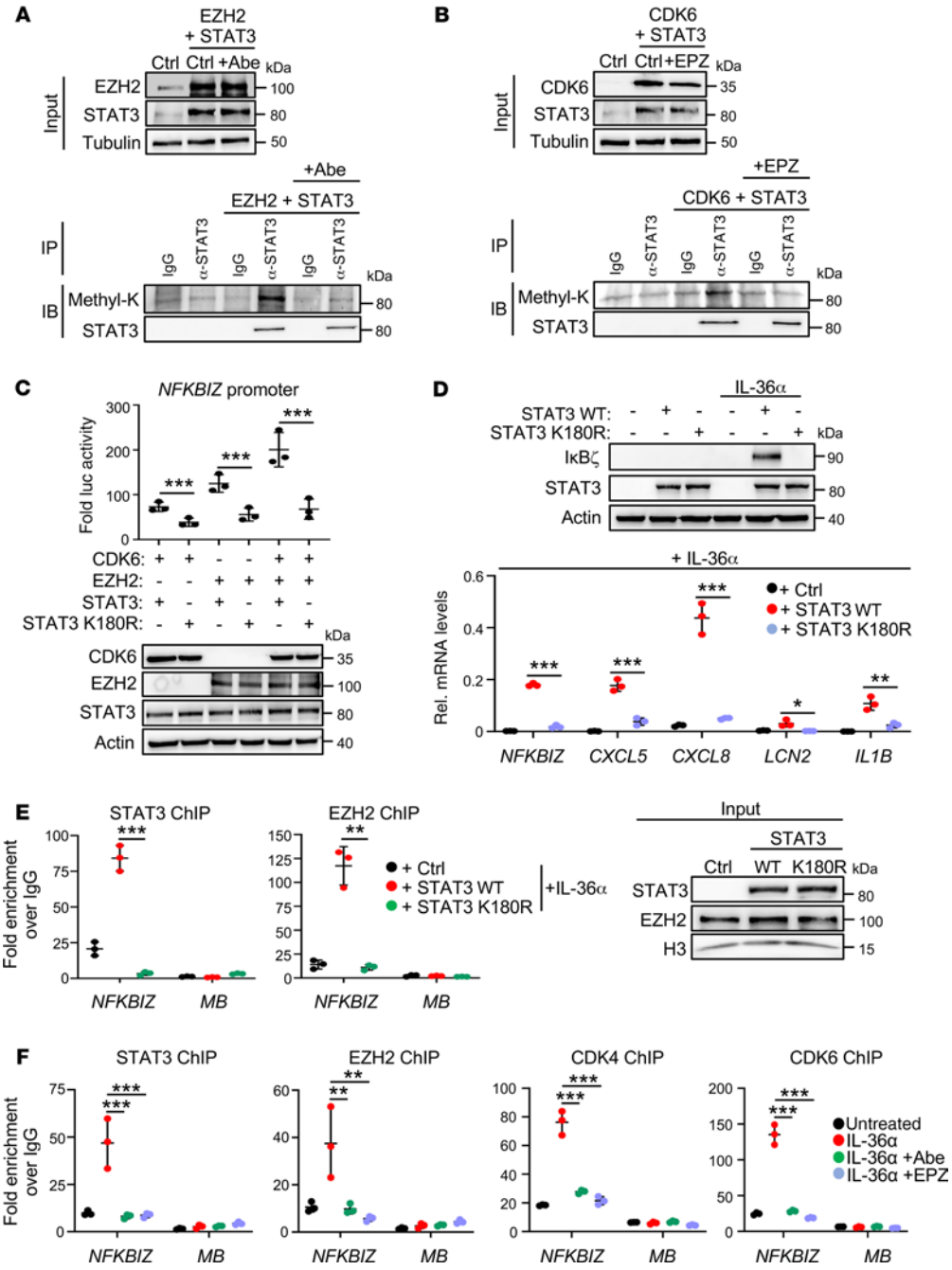

Figure 4. CDK4/6-dependent, EZH2-mediated methylation of STAT3 at lysine 180 induces IκBζ expression in keratinocytes. (**A** and **B**) Detection of methylated STAT3 by coimmunoprecipitation. EZH2 and STAT3 (**A**) or CDK6 and STAT3 (**B**) were transiently expressed in HEK293T cells. After 1 hour of treatment with (**A**) abemaciclib (Abe) or (**B**) EPZ6438 (EPZ), cell lysates were prepared and subjected to immunoprecipitation using a STAT3-specific antibody or control IgG. (**C**) *NFKBIZ* promoter-driven luciferase activity in HEK293T cells, transiently expressing CDK6 and EZH2, alone or in combination with WT (wt) STAT3 or methylation-defective STAT3 mutant (K180R). $n = 3 \pm$ SD. (**D**) Analysis of IκBζ and IκBζ target gene expression in STAT3 wt or STAT3 K180R-expressing HaCaT cells. STAT3 wt or STAT3 K180R constructs were transiently expressed in *STAT3*-KO HaCaT cells, followed by stimulation for 1 hour with IL-36α. $n = 3 \pm$ SD. (**E**) Chromatin immunoprecipitation (ChIP) of STAT3, EZH2, or IgG control in *STAT3*-KO HaCaT cells reconstituted with either STAT3 wt or STAT3 K180R after 30 minutes of stimulation with IL-36α. Fold enrichment at the *NFKBIZ* promoter or at the myoglobin genomic region (*MB*; as negative control) was calculated relative to the IgG control. $n = 3 \pm$ SD. (**F**) ChIP of STAT3, EZH2, CDK4, and CDK6 in IL-36α–stimulated HaCaT cells stimulated for 30 minutes with IL-36α. Shown is the fold enrichment over IgG control. $n = 3 \pm$ SD. Significance was calculated using a 1-way ANOVA for multiple groups and a 2-tailed Student's *t* test for comparing 2 groups: $^*P < 0.05$; $^{**}P < 0.01$; $^{***}P < 0.001$.

localization (34–36). Thus, we immunoprecipitated STAT3 in STAT3- and EZH2-overexpressing HEK293T cells in the presence or absence of abemaciclib, and analyzed the methylation status of STAT3 using a pan-methyl-lysine–specific antibody. Simultaneous overexpression of EZH2 and STAT3 induced methylation of STAT3, as expected, whereas CDK4/6 inhibition abrogated lysine methylation of STAT3 (Figure 4A). Furthermore, lysine methylation of STAT3 was detectable upon

co-overexpression of CDK6 and STAT3, whereas pharmacological EZH2 inhibition abrogated STAT3 methylation (Figure 4B). Thus, CDK4/6 might indeed trigger an EZH2-dependent methylation and activation of STAT3.

EZH2-dependent methylation sites of STAT3 at lysine 49, 140, and 180 were previously identified by mass spectrometric analyses in tumor cells (34–36). Thus, we substituted all 3 lysine methylation sites with arginine residues and tested the STAT3 mutants for their potential to activate *NFKBIZ* luciferase promoter expression. Whereas mutations of STAT3 at K49 and K140 had no effect on the induction of *NFKBIZ* promoter expression, alone or in combination with CDK6 and EZH2 (Supplemental Figure 4A), mutation of lysine 180 (STAT3 K180R), abrogated STAT3-mediated *NFKBIZ* promoter activation (Figure 4C). Thus, we hypothesized that CDK4/6-activated EZH2 methylates STAT3 at lysine 180, which is needed to induce IκBζ expression in stimulated keratinocytes. In agreement, reconstitution of CRISPR/Cas9-generated *STAT3* knockout keratinocytes with WT STAT3, but not with the STAT3 K180R mutant, fully reconstituted IκBζ expression and IκBζ-mediated target gene induction upon IL-36α or IL-17A/TNF-α stimulation (Figure 4D and Supplemental Figure 4B). This correlated with an absence of nuclear translocation of STAT3 K180R in IL-36α–treated keratinocytes (Supplemental Figure 4C), as observed before (34). Accordingly, mutant STAT3 K180R and EZH2 were unable to bind to the *NFKBIZ* promoter region in IL-36α–stimulated keratinocytes (Figure 4E). Thus, whereas IL-36α stimulation triggered WT STAT3 binding to the *NFKBIZ* promoter region together with EZH2 and CDK4/6, inhibition of CDK4/6 (Abe) or EZH2 (EPZ) abrogated the recruitment of this multiprotein complex (Figure 4F). These results therefore suggest that CDK4 and CDK6 phosphorylate EZH2 to induce EZH2-dependent K180 STAT3 methylation, leading to the recruitment of the heteromeric complex to the *NFKBIZ* promoter and subsequent induction of IκBζ and its target gene expression in keratinocytes.

Finally, we wanted to know if cytokines that activate the classical JAK/STAT3 pathway could override CDK4/6- or EZH2 inhibitor-mediated suppression of STAT3 activation. As revealed before (41–43), stimulation of primary keratinocytes with the cytokines IL-6, IL-20, or IL-22, which are upregulated in psoriatic lesions, led to the phosphorylation of STAT3 (Supplemental Figure 4D and refs. 41–43). Of note, neither abemaciclib nor EPZ6438 was able to abrogate STAT3 phosphorylation under these conditions, implying that CDK4/6 and EZH2 specifically control phosphorylation of STAT3 upon stimulation with IL-36α or IL-17A/TNF-α. Importantly, even though IL-6, IL-20, or IL-22 could reestablish STAT3 phosphorylation in IL-36α– and abemaciclib-treated keratinocytes, stimulation with these cytokines failed to restore IκBζ and its target gene expression (Supplemental Figure 4, E and F), nor was it able to reestablish the nuclear translocation of STAT3 in keratinocytes (Supplemental Figure 4G). This finding implies that CDK4/6-EZH2–mediated methylation of STAT3 is distinguished from the activation of STAT3 by the JAK/STAT pathway.

Human and murine psoriatic lesions are characterized by overexpression of cyclin D2, cyclin D3, and EZH2. Our findings suggest that CDK4 and CDK6 mediate the phosphorylation of EZH2 in a cyclin D–dependent manner, leading to STAT3 activation and IκBζ expression. We therefore investigated a potential relevance of this pathway in skin biopsies from patients with psoriasis. Human psoriatic lesions, compared with nonpsoriatic lesions or unaffected skin, were characterized by an upregulation of *CCND2* and *CCND3* (Figure 5A). In contrast, *CCND1* levels were decreased or remained unaffected in lesional skin biopsies. This is in line with our previous observation (Supplemental Figure 2, C and D) that cyclin D1, unlike cyclin D2 and cyclin D3, did not synergize with CDK4/6 and STAT3 in increasing *NFKBIZ* promoter activity or expression of IκBζ and its target genes. In addition, *EZH2* mRNA levels were significantly upregulated in human psoriatic skin lesions (Figure 5B). Immunohistochemistry further demonstrated that, on the protein level, human EZH2, which was only weakly expressed in normal skin, was strongly overexpressed in the basal cell compartment of psoriatic skin lesions, revealing a typical nuclear localization (Figure 5C).

Next, we asked if an upregulation of cyclin D2, cyclin D3, and EZH2 can be also detected in relevant psoriasis mouse models. In the standard model using the TLR7 agonist imiquimod (IMQ), psoriasis-like skin inflammation was triggered by daily application of an IMQ-containing cream on the ears for 6 days, while in a second model daily intradermal injections of IL-36α into the skin of mouse ears were employed for 5 consecutive days. After 6 or 7 days of treatment, not only skin inflammation but also increased expression of *Ccnd2, Ccnd3*, and *Ezh2* mRNA was detectable in both animal models (Figure 5, D and E). Moreover, increased protein levels of cyclin D2/D3 and EZH2 could be detected in the epidermis of IMQ-treated mouse ears (Figure 5F). Thus, in addition to the previously demonstrated overexpression of IκBζ in psoriasis (8, 9), a hyperactive cyclin D-CDK4/6 pathway and elevated EZH2 expression are evident in murine and human psoriatic skin lesions.

Topical application of inhibitors targeting CDK4/6 or EZH2 protects against experimental psoriasis in vivo. IκBζ is one of the key transcriptional regulators in the pathogenesis of psoriasis (8, 9). Due to our finding that CDK4/6 and EZH2 inhibitors suppressed psoriasis-related, proinflammatory gene expression downstream of IL-36α or IL-17A/TNF-α, we next investigated the potential of CDK4/6 and EZH2 inhibitors to block experimental psoriasis in vivo. Moreover, we reasoned that topical application of both inhibitors would be sufficient, as the epidermis constitutes the main target for CDK4/6 and EZH2 inhibition. A prerequisite for efficient takeup of small-molecule inhibitors from the skin are hydrophobicity of these substances. Thus, we selected more hydrophobic inhibitors, such as abemaciclib (for CDK4/6 inhibition) or CPI-169 (44) (for EZH2 inhibition) that are more likely to penetrate the outer skin barrier. Psoriasis-like skin inflammation was induced in the abovementioned psoriasis model by daily application of an IMQ-containing cream on the ears of WT mice for 6 days, before animals were sacrificed and analyzed at day 6 (45). Abemaciclib, CPI-169, and ethanol as vehicle control were applied daily on the ear skin in parallel to IMQ (Supplemental Figure 5A). Whereas IMQ-treated ears exerted ear thickening, along with keratinocyte hyperproliferation and immune cell infiltration, topical application of abemaciclib or CPI-169 strongly suppressed IMQ-induced, psoriasis-like skin inflammation (Figure 6, A and B). Both inhibitors effectively penetrated the skin and inhibited CDK4/6 or EZH2,

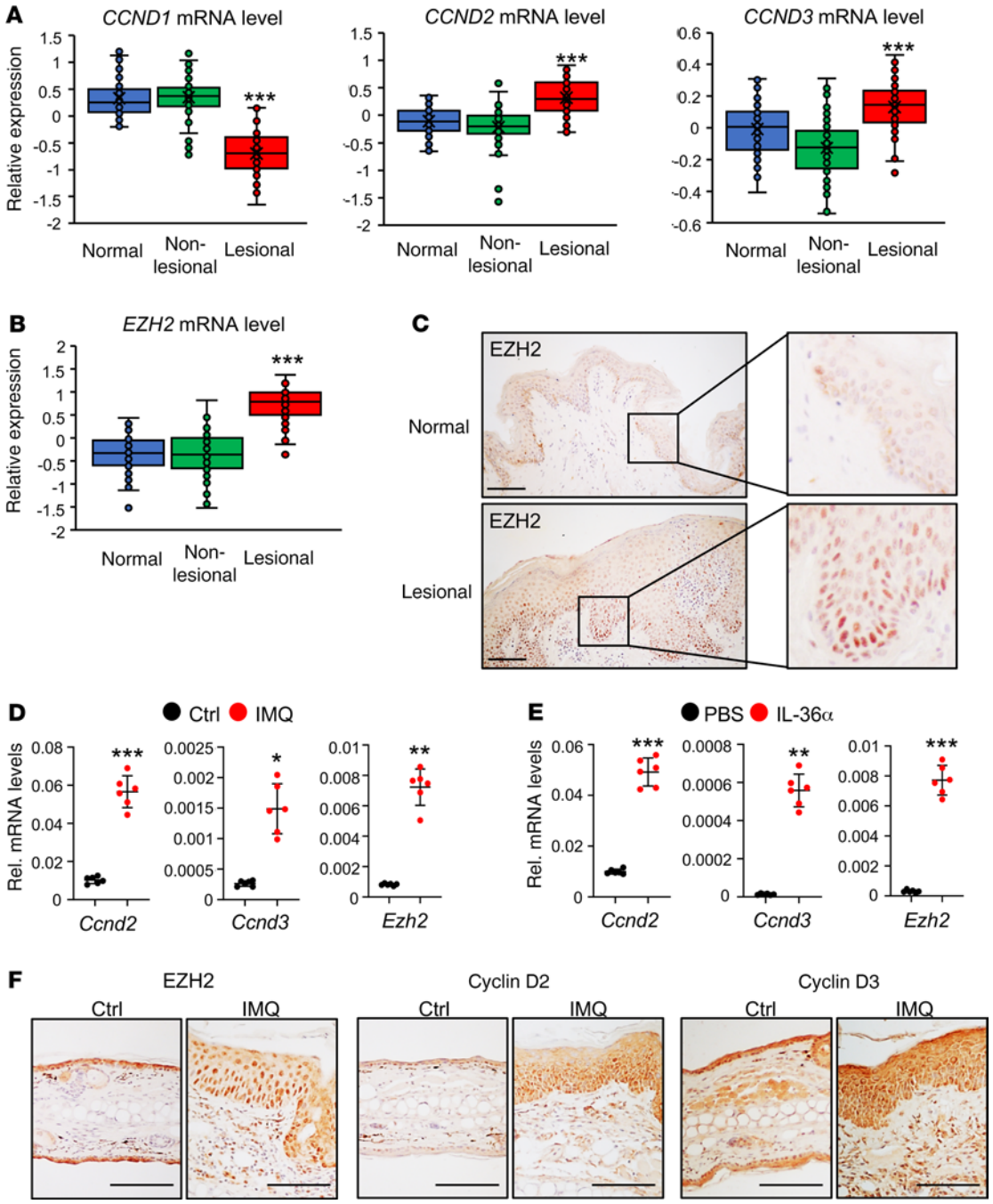

Figure 5. Increased expression of cyclin D2, cyclin D3, and EZH2 in human and murine psoriasis. (**A**) Expression data from skin biopsies of 64 healthy individuals and 58 patients with psoriasis were analyzed from the GEO profile data set GDS4602. Shown are normalized expression values for *CCND1*, *CCND2*, and *CCND3*. *EZH2* mRNA (**B**) and protein levels (**C**) in human skin samples from healthy individuals and patients with psoriasis; retrieved from the same data set as in **A** and **B**. Significance was calculated with a 1-way ANOVA test: $^{*}P < 0.05$; $^{**}P < 0.01$; $^{***}P < 0.001$. Scale bars: 100 μm. (**D**) Analysis of *Ccnd2*, *Ccnd3*, and *Ezh2* mRNA levels in IMQ-treated mice ears at day 6. Values were normalized to *Actin*. $n = 6$ per group ± SEM. (**E**) Analysis of *Ccnd2*, *Ccnd3*, and *Ezh2* mRNA levels in IL-36α–treated mice ears at day 5. $n = 6$ per group ± SEM. Significance was calculated using a 2-tailed Student's *t* test: $^{*}P < 0.05$; $^{**}P < 0.01$; $^{***}P < 0.001$. (**F**) IHC staining of EZH2, cyclin D2, and cyclin D3 in untreated (Ctrl) and IMQ-treated mouse ears at day 6. Scale bars: 40 μm.

as detected by loss of pRB (for CDK4/6 inhibition) or H3K27me3 (for EZH2 inhibition) expression in the epidermis of treated mice (Figure 6C). Moreover, abemaciclib treatment significantly suppressed the infiltration of neutrophils, macrophages, and T cells in IMQ-treated mice (Figure 6D), while topical application of the EZH2 inhibitor CPI-169 fully abrogated immune cell infiltration upon IMQ treatment (Figure 6E). Of note, also the number of infiltrating plasmacytoid dendritic cells (pDCs) and myeloid dendritic cells (mDCs) was significantly suppressed by application of both inhibitors (Supplemental Figure 5B). Importantly, whereas IMQ treatment effectively induced IκBζ expression in the skin, along with phosphorylation of EZH2 at T345

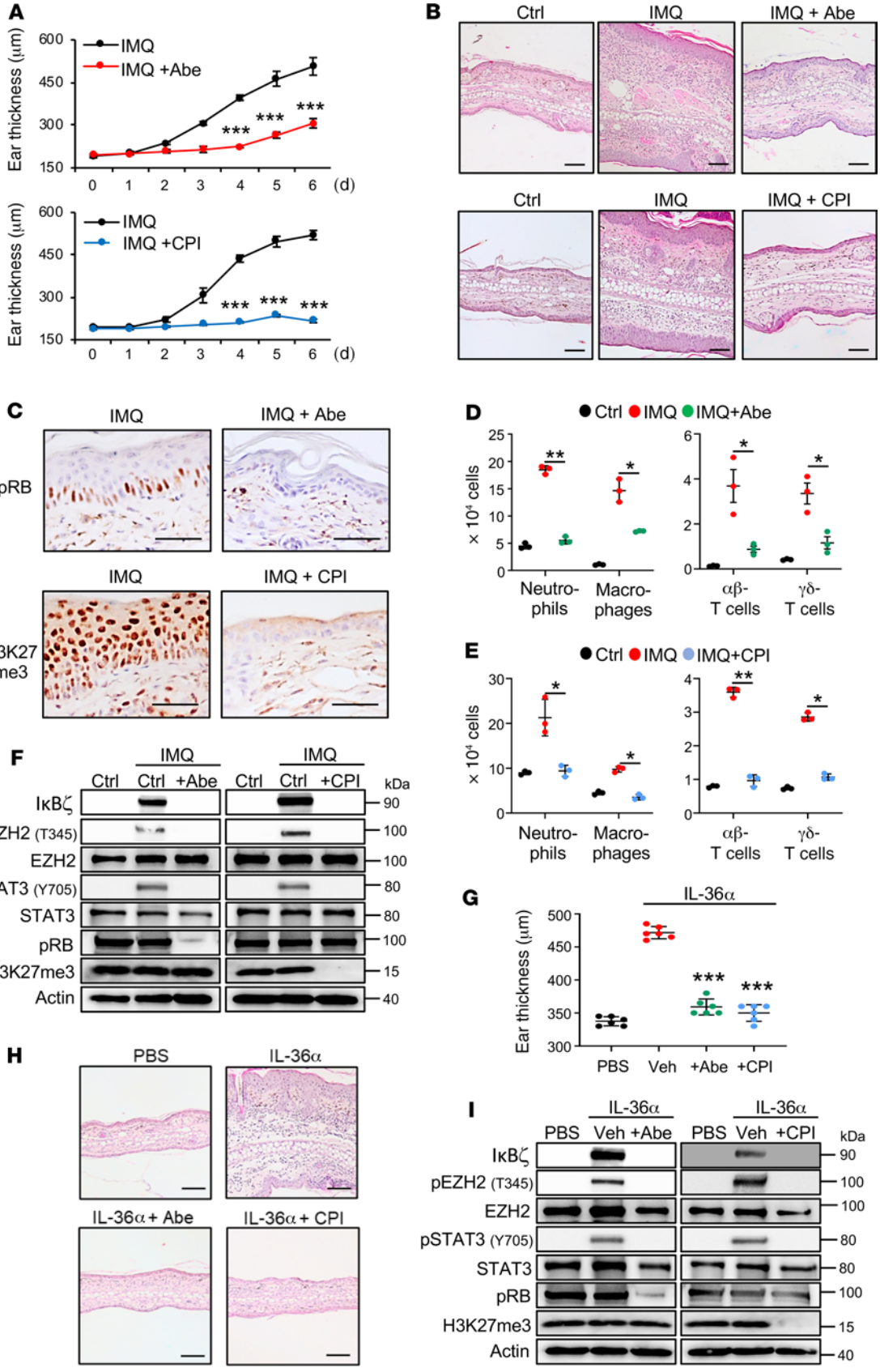
A
Ear thickness (μm)
IMQ
IMQ +Abe
IMQ +CPI
(d)
B
Ctrl
IMQ
IMQ + Abe
IMQ + CPI
C
pRB
H3K27 me3
D
Ctrl IMQ IMQ+Abe
× 10⁴ cells
Neutro-phils
Macro-phages
αβ- T cells
γδ- T cells
E
Ctrl IMQ IMQ+CPI
F
IκBζ
pEZH2 (T345)
EZH2
pSTAT3 (Y705)
STAT3
pRB
H3K27me3
Actin
kDa
G
IL-36α
PBS
Veh
+Abe
+CPI
H
PBS
IL-36α
IL-36α + Abe
IL-36α + CPI
I

Figure 6. CDK4/6 and EZH2 inhibition prevents IMQ- and IL-36–mediated psoriasis-like skin lesions in vivo. (**A**) Ear thickness measurements during topical treatment of mice with IMQ with or without abemaciclib (Abe; 10 μL of a 2% solution) or the EZH2 inhibitor CPI-169 (CPI, 10 μL of a 5% solution). n = 6 mice per group ± SEM. (**B**) H&E staining of untreated (Ctrl), IMQ-, IMQ and Abe–, or IMQ and CPI–treated ears. Scale bars: 100 μm. (**C**) Phospho-RB (pRB) and H3K27me3 staining after 6 days of treatment validated effective CDK4/6 and EZH2 inhibition, respectively. Scale bars: 40 μm. (**D**) Infiltrating immune cells in mouse ears at day 6 of treatment were quantified as follows: Neutrophils: $CD45^+$, $CD11b^+$, $Ly6G^+$; macrophages: $CD45^+$, $CD11b^+$, $F4/80^+$; T cells: $CD45^+$, $CD3^+$, and $\alpha\beta$-TCR^+ or $\gamma\delta$-TCR^+. n = 3 mice per group ± SEM. (**E**) Flow cytometry analysis of IMQ-treated or IMQ and CPI-169–treated mouse ears at day 6. (**F**) Protein levels in untreated (Ctrl) and treated mouse skin tissue at day 6. (**G**) Ear thickness of IL-36α–treated mice at day 5. Ears of mice were daily treated by intradermal injections with 1 μg IL-36α. Control mice received injections with PBS. Additionally, mice received topical treatment with ethanol as control (Veh), 2% abemaciclib (Abe), or 5% CPI-169 (CPI). n = 6 mice per group ± SEM. (**H**) H&E staining of PBS- or IL-36α–treated ears at day 5. Scale bars: 100 μm. (**I**) Immunoblot analysis of IκBζ, EZH2 phosphorylation (pEZH2 T345) and STAT3 activation (pSTAT3 Y705) in treated mouse skin tissue at day 5. pRB and H3K27me3 were analyzed as positive controls for drug action. Significance was calculated using a 1-way ANOVA for multiple groups and a 2-tailed Student's t test for comparing 2 groups: $^*P < 0.05$; $^{**}P < 0.01$; $^{***}P < 0.001$.

and of STAT3 at Y705, topical administration of abemaciclib or CPI-169 completely abrogated these signaling events (Figure 6F and Supplemental Figure 5C). As a positive control, stabilization of the CDK4/6 substrate pRB (46) and EZH2-directed H3K27 methylation were strongly reduced in either CDK4/6 or EZH2 inhibitor-treated mouse skin (Figure 6F). Accordingly, expression of IκBζ target genes, such as *Cxcl2* and *Cxcl5*, and DC- and T cell–derived cytokines, such as *Il17a* or *Il23a*, was significantly downregulated in IMQ- and abemaciclib- or IMQ- and CPI-169–treated skin (Supplemental Figure 5D).

Treatment of mice with the TLR7 agonist IMQ represents a standard mouse model for psoriasis (45). However, IMQ activates immune cells in the first instance, rather than an initial keratinocyte-derived proinflammatory response, as it is likely to happen in human psoriasis pathogenesis. Thus, we additionally investigated the therapeutic effects of abemaciclib or CPI-169 in an IL-36–triggered psoriasis-like dermatitis mouse model (Supplemental Figure 5E). As previously reported (9, 47), repeated intradermal injections of IL-36α into the skin of mouse ears induced ear swelling, and keratinocyte hyperproliferation along with immune cell infiltration (Figure 6, G and H). As a control for drug penetration in the skin of IL-36–treated animals, effective inhibition of CDK4/6 and EZH2 methyltransferase activity was controlled by staining for pRB and H3K27me3, respectively (Supplemental Figure 5F). Similar to the IMQ mouse model, topical application of abemaciclib or CPI-169 effectively blocked keratinocyte hyperproliferation and immune cell infiltration (Figure 6, G and H). Moreover, both inhibitors suppressed IL-36–mediated expression of IκBζ, phosphorylation of EZH2 at T345, and activation of STAT3 (pSTAT3 Y705) in the skin of treated mouse ears (Figure 6I). Accordingly, IκBζ target gene expression and key cytokine expression, such as *Il17a* and *Il23a*, were effectively blocked as well (Supplemental Figure 5G). Thus, inhibition of CDK4/6 or EZH2 in IMQ- or IL-36–mediated psoriasis-like skin inflammation mouse models effectively prevented psoriasis induction in vivo, by suppressing STAT3-mediated induction of IκBζ expression and IκBζ target gene expression.

CDK4/6 and EZH2 inhibitors effectively attenuate already established psoriasis-like skin inflammation in vivo. As CDK4/6 and EZH2 inhibitors could fully prevent the onset of psoriasis in vivo, we next investigated if inhibition of the CDK4/6-EZH2 pathway also attenuates already established psoriatic disease. We therefore first induced psoriasis-like skin inflammation in mice with IMQ and then topically applied abemaciclib or CPI-169 after day 2 of IMQ treatment (Figure 7A). Already, 3 treatments with IMQ effectively induced ear swelling and keratinocyte hyperproliferation. These psoriasis-like symptoms could be fully reversed by starting topical application of abemaciclib or CPI-169 (Figure 7, B and C, and Supplemental Figure 6A). Moreover, psoriasis-related, proinflammatory gene expression as well as infiltration of neutrophils, macrophages, and T cells, which was detectable at the third day of IMQ treatment, were fully resolved by both inhibitors (Supplemental Figure 6B and Figure 7D). Finally, inhibition of CDK4/6 or EZH2 abrogated IκBζ expression as well as phosphorylation of STAT3, as detected by immunoblot analyses of whole skin lysates at day 6 (Figure 7E).

Similar results were obtained by topical application of abemaciclib or CPI-169 on established skin lesions in the IL-36α psoriasis-like mouse model. In this experimental setup, application of both inhibitors at day 4 effectively resolved IL-36α–induced ear swelling, keratinocyte hyperproliferation, and immune cell infiltration as well as psoriasis-associated gene expression, IκBζ expression, and activation of STAT3 (Figure 7, F–I, and Supplemental Figure 6C). Thus, topical application of CDK4/6 and EZH2 inhibitors not only prevented the onset of experimental skin inflammation, but also resolved already established psoriasis-associated symptoms in IMQ- or IL-36α–treated mice. In view of its increased activity in human psoriatic skin and the results obtained in psoriasis-like mouse models, inhibition of this pathway by topical application of CDK4/6 and EZH2 inhibitors could therefore provide a new therapeutic strategy for the treatment of patients with psoriasis.

Discussion

CDK4/6 inhibitors have been developed and approved for the treatment of patients with cancer in order to restrain hyperproliferation of tumor cells (17). Recently, it was found that CDK4 and CDK6 do not only control cell cycle progression by phosphorylation of RB, but also regulate immune cell differentiation and function (20, 21, 48). In this context, CDK4 and CDK6 have been implicated as transcriptional cofactors that activate a subset of NF-κB or STAT3 target genes (23–25). Based on our results in cultured keratinocytes, human skin biopsies, and mouse models, we propose to repurpose CDK4/6 inhibitors for psoriasis therapy. Moreover, our results uncovered a new pathway involving CDK4/6-mediated phosphorylation of EZH2 and EZH2-dependent methylation and activation of STAT3, leading to the inducible expression of IκBζ and IκBζ-dependent target genes in keratinocytes. These findings also suggest the use of EZH2 inhibitors to treat psoriasis.

IκBζ, encoded by *NFKBIZ*, constitutes a risk gene for the development of psoriasis (49). Moreover, we recently reported

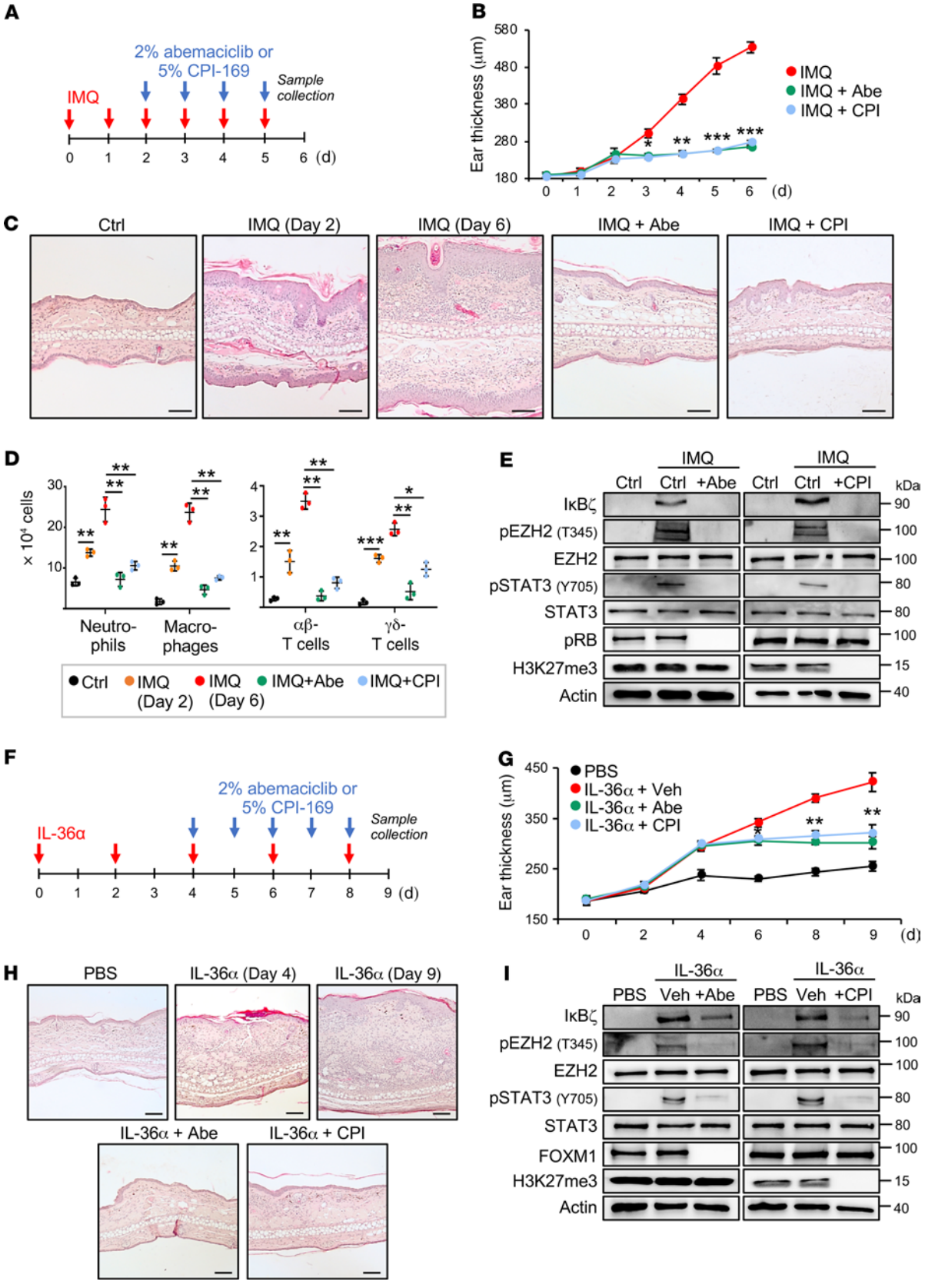
A
2% abemaciclib or
5% CPI-169
IMQ
Sample collection
0 1 2 3 4 5 6 (d)
B
Ear thickness (μm)
580
480
380
280
180
0 1 2 3 4 5 6 (d)
IMQ
IMQ + Abe
IMQ + CPI
C
Ctrl
IMQ (Day 2)
IMQ (Day 6)
IMQ + Abe
IMQ + CPI
D
× 10⁴ cells
Neutro-phils
Macro-phages
αβ-T cells
γδ-T cells
Ctrl
IMQ (Day 2)
IMQ (Day 6)
IMQ+Abe
IMQ+CPI
E
IMQ
IMQ
Ctrl Ctrl +Abe Ctrl Ctrl +CPI
kDa
IκBζ
pEZH2 (T345)
EZH2
pSTAT3 (Y705)
STAT3
pRB
H3K27me3
Actin
90
100
100
80
80
100
15
40
F
2% abemaciclib or
5% CPI-169
IL-36α
Sample collection
0 1 2 3 4 5 6 7 8 9 (d)
G
Ear thickness (μm)
450
350
250
150
0 2 4 6 8 9 (d)
PBS
IL-36α + Veh
IL-36α + Abe
IL-36α + CPI
H
PBS
IL-36α (Day 4)
IL-36α (Day 9)
IL-36α + Abe
IL-36α + CPI
I
IL-36α
IL-36α
PBS Veh +Abe PBS Veh +CPI
kDa
IκBζ
pEZH2 (T345)
EZH2
pSTAT3 (Y705)
STAT3
FOXM1
H3K27me3
Actin
90
100
100
80
80
100
15
40

Figure 7. CDK4/6 and EZH2 inhibitors attenuate established psoriasis-like skin lesions in vivo. All analyses were performed with $n = 6$ mice per group ± SEM. (**A**) Treatment scheme for the therapy using the IMQ mouse model. To explore whether CDK4/6 and EZH2 inhibitors suppress already-established psoriasis-like skin inflammation, mice were first treated with IMQ, followed by the application of 2% abemaciclib or 5% CPI-169 solution starting at the third IMQ application. (**B**) Ear thickness measurements during treatment. (**C**) H&E staining of untreated (Ctrl), IMQ-, IMQ and Abe–, or IMQ and CPI–treated ears. H&E staining shows the prevalence of psoriasis-like symptoms at IMQ day 2 when the inhibitors were applied for the first time. Scale bars: 100 μm. (**D**) Quantification of infiltrating immune cells in mouse ears at day 6. Immune cell subpopulations were quantified as in Figure 6D. $n = 3$ mice per group ± SEM. (**E**) Protein levels in untreated (Ctrl) and IMQ-treated mouse skin tissue in the presence or absence of abemaciclib or CPI-169 at day 6. Mice were treated as in **A**. FOXM1 and H3K27me3 were analyzed as positive controls for drug action. (**F**) Treatment scheme in the IL-36–induced psoriasis mouse model. IL-36–mediated psoriasis-like dermatitis was induced by administration of 1 μg IL-36α at every second day. Control mice received PBS. Starting from day 4 of IL-36α injection, ethanol as Vehicle (Veh), 2% abemaciclib, or 5% CPI-169 were daily applied by topical administration. (**G**) Ear thickness measurements during IL-36α treatment. (**H**) H&E staining of PBS- or IL-36α–treated ears at day 9. Scale bars: 100 μm. (**I**) Immunoblot analysis in IL-36α–treated mouse skin tissue at day 9. Significance was calculated using a 1-way ANOVA for multiple groups and a 2-tailed Student's *t* test for comparing 2 groups: $^{*}P < 0.05$; $^{**}P < 0.01$; $^{***}P < 0.001$.

that IκBζ is overexpressed in human psoriatic lesions, whereas global and keratinocyte-specific IκBζ KO mice are completely protected against psoriasis-like skin inflammation in several psoriasis models (8, 9, 50). Mechanistically, IκBζ is transcriptionally induced in keratinocytes by IL-17 and IL-36, which triggers the expression of psoriasis-relevant target genes encoding for selective chemokines and cytokines and antimicrobial proteins. Deficiency of IκBζ therefore prevents the recruitment of neutrophils and monocytes that are needed for skin inflammation (9, 50). Collectively, our data suggest that interfering with IκBζ expression or function in keratinocytes might be a promising strategy for psoriasis therapy. As IκBζ is crucial for both IL-36 and IL-17 signaling, CDK4/6 inhibitors might be applicable for different subtypes of psoriasis.

Unfortunately, based on a lack of enzyme activity, direct pharmacological inhibition of IκBζ function remains difficult (13). We therefore sought to block the transcriptional induction of IκBζ and identified small-molecule inhibitors of CDK4/6 and EZH2 as potent suppressors of IκBζ expression in keratinocytes. CDK4 and CDK6 have been previously shown to modulate several immune-relevant transcription factors by both kinase-dependent and -independent mechanisms (23–25). In the present study, we clearly demonstrate that STAT3-mediated induction of IκBζ expression is kinase-dependent, as ATP-competitive CDK4/6 inhibitors such as abemaciclib or palbociclib abolished IκBζ expression. Consistent with these findings, a hyperactive but not a dominant-negative version of CDK6 increased *NFKBIZ* promoter activity. Moreover, cyclin D2 and cyclin D3 elevated the expression of *NFKBIZ* and its target genes, supporting the need for CDK4/6 kinase activity.

Despite the requirement of the kinase activity, the involvement of CDK4/6 could be separated from its classical role in cell cycle regulation and phosphorylation of RB. Thus, depletion of RB failed to restore IκBζ expression upon CDK4/6 inhibition. Moreover, IκBζ expression was principally induced by IL-36 stimulation in all phases of the cell cycle, except for G_0-arrested cells that revealed a weaker IκBζ expression. Importantly, although IκBζ expression does not rely on CDK4/6-mediated cell cycle progression, CDK4/6 inhibitors might also have beneficial effects in psoriasis treatment by additionally blocking keratinocyte hyperproliferation, which is a hallmark of psoriasis (2).

In this study, we demonstrate a major role for STAT3 in driving keratinocyte-specific IκBζ expression. IκBζ expression in keratinocytes is predominantly controlled from the proximal promoter 2 of the *NFKBIZ* locus, containing different transcription factor binding sites than the better investigated distal promoter 1 (9). So far, we have not compared the promoter usage in distinct cell types, but we consider it likely that the contribution of the individual promoters and STAT3 to IκBζ expression differs among different cell types. Our experiments show that CDK4 and CDK6 do not directly phosphorylate STAT3 but EZH2, which induces IκBζ and IκBζ-dependent proinflammatory target gene expression in a STAT3-dependent manner. This finding seems surprising at the first glance, since EZH2, as part of the PRC2 complex, is mainly involved in gene repression through trimethylation of H3K27. Recently, however, EZH2 was also found to induce gene expression independently of the PRC2 complex, via interaction with β-catenin or the SWI/SNF complex (51, 52). CDK4/6 phosphorylated EZH2 at T345, thereby inducing an EZH2-dependent methylation of STAT3 at K180, and subsequent induction of IκBζ expression by STAT3. EZH2 phosphorylation at T345 was previously described to be mediated by CDK1 and CDK2, leading to an EZH2-directed epigenetic silencing of genes during G2 phase (39, 53). Thus, even though CDK-mediated phosphorylation of EZH2 at T345 seems to be conserved, its impact on EZH2 function and the choice of methylation substrates might depend on the specific stimulus or cell cycle phase.

Upon CDK4/6-mediated phosphorylation, EZH2 preferentially interacted with STAT3, resulting in STAT3 K180 methylation and enhanced STAT3 activation. Similar observations were made in glioblastoma, where IL-6–induced STAT3 activation is controlled by EZH2-mediated trimethylation of STAT3 at K180 (34). Thus, phosphorylation of EZH2 might induce a switch in EZH2 function from H3K27 trimethylation and transcriptional repression to noncanonical functions, including STAT3 methylation and gene activation. Whether this gene-activating function of EZH2 requires the PRC2 repressor complex or whether it is PRC2-independent remains to be resolved. In addition to its main function in transcriptional repression, non-PRC functions of EZH2 via direct binding to transcriptional regulators have been reported before. For instance, EZH2 was shown to act as a cofactor for transcription factors (such as the androgen receptor, β-catenin, or NF-κB), leading to target gene activation (52, 54, 55). Similar to other nonhistone targets, however, the exact molecular events that link STAT3 methylation to STAT3 activation are currently unknown. In agreement with a previous report (34), our data imply that K180 methylation of STAT3 might be needed for the nuclear import of phosphorylated STAT3.

Regardless of the detailed mechanism of EZH2-mediated STAT3 activation, our study has also important clinical implications. Our

results suggest that targeting of the CDK4/6-EZH2-STAT3 pathway not only suppresses cytokine-mediated induction of IκBζ and proinflammatory target gene expression, but also inhibits immune cell recruitment and skin inflammation. We demonstrate in the IMQ- and IL-36–mediated psoriasis-like mouse models that both CDK4/6 and EZH2 inhibitors completely blocked the development of psoriatic skin lesions. The therapeutic effect of the inhibitors concurred with a suppression of IκBζ expression and a strong inhibition of IκBζ target gene expression, including chemokines (e.g., *Cxcl2*, *Cxcl5*), cytokines (e.g., *Il1f9*, *Il1b*, *Il17a*, *Il23a*), and antimicrobial proteins (e.g., *Lcn2*). In contrast, genes that were not IκBζ-dependent, such as *NFKBIA* and *TNF*, remained unaffected upon CDK4/6 or EZH2 inhibition. These findings further support the view of a rather selective role of IκBζ in the control of immune responses and also indicate that inhibition of IκBζ will be associated with fewer side effects than a broad inhibition of NF-κB by toxic IKK inhibitors.

In line with previous reports showing an upregulated expression of IκBζ in psoriasis (8, 9), we detected an increased nuclear accumulation of EZH2 and elevated cyclin D2 and D3 levels, both in mouse models of psoriasis and in human psoriatic skin lesions. Previous studies also found that mutations in the STAT3 signaling pathway constitute a risk factor for the development of psoriasis (43), while constitutively active STAT3 characterizes the epidermis of human psoriatic lesions (56). Collectively, this suggests that the CDK4/6-EZH2-STAT3 pathway is hyperactive in psoriatic skin lesions. As inhibition of IκBζ blocks multiple signaling pathways in psoriasis, targeting IκBζ might increase overall therapy responses as well as prevent the development of therapy resistance. Due to the clinical availability of hydrophobic CDK4/6 and EZH2 inhibitors, we propose formulation of these inhibitors in, for example, a cream for topical treatment of psoriatic skin lesions. Topical drug administration will also restrict potential side effects and might be especially promising for those patients who have developed resistance to current psoriasis therapies.

Methods

Cell culture and treatment. HaCaT cells were obtained from Petra Boukamp (57) and maintained in DMEM with 10% FCS and antibiotics. Human primary keratinocytes were freshly isolated from foreskin and maintained in CnT-07S medium with gentamycin (CELLnTEC). Recombinant human IL-36α (6995-IL; aa 6-158), IL-36γ (6835-IL; aa 18-169), and mouse IL-36α (7059-ML; aa 6-160) were purchased from R&D Systems. Recombinant IL-17A (catalog 11340174), TNF-α (catalog 11343013), IL-1β (catalog 11340013), IL-6 (catalog 11340064), IL-20 (catalog 11340203), and IL-22 (catalog 11340223) were ordered from Immunotools. Flagellin (vac-fla) and polyI:C (vac-pic) were purchased from Invivogen. In cell culture experiments, all cytokines were used at 100 ng/mL end concentration, except for IL-17A (200 ng/mL) and TNF-α (10 ng/mL). Flagellin was applied at 10 ng/mL and poly I:C was added at a final concentration of 100 ng/mL. The following inhibitors were purchased from Selleckchem: abemaciclib mesylate (LY2835219, S17158), palbociclib isethionate (S1579), EPZ6438 (tazemetostat, S7128), and CPI-169 (S7616). If not otherwise indicated, the inhibitors were used in cell cultures at the following concentrations: abemaciclib (16 μM), palbociclib (50 μM), and EPZ6438 (10 μM). When indicated, cells were starved overnight, before cytokine treatment, by removing cell culture supplements from the growth medium.

Generation of knockdown cells. Lentiviral particles were produced in HEK293T cells using the second-generation packaging system (pMD2.G, 12259; and psPAX2, 12260; Addgene). Keratinocytes were transduced in the presence of 8 μg/mL polybrene, packaging plasmids, and 5 μg of the respective shRNA construct (all from Dharmacon): pLKO.1-puro (sh ctrl); pLKO.1-TRCN0000009876 (sh*CDK4*); pLKO.1-TRCN0000010473 (sh*CDK6*); pTRIPZ-EZH2 (V2THS63066, sh*EZH2*); pLKO.1-TRCN0000040167 (*shRB*); pTRIPZ noncoding ctrl (RHS4743); pLKO.1-TRCN0000020840 (sh*STAT3*); pLKO.1-TRCN0000014683 (sh*RELA*), followed by puromycin selection (1 ng/mL, Invitrogen). For induction of *EZH2* knockdown, pTRIPZ ctrl and pTRIPZ-EZH2–expressing cells were treated for 24 hours with 2 μg/mL doxycycline (AppliChem) before stimulation and harvest of the cells.

Luciferase constructs and reporter assays. Luciferase constructs were generated as described and based on the pInducer20 plasmid (Addgene, 44012) (9). HEK293T cells (1×10^4) were transfected for 24 hours using HeBS buffer and $CaCl_2$ and a mixture of 400 ng firefly luciferase vector and 100 ng TK-Renilla vector. For expression of other proteins, the following concentrations were purchased from Addgene: 70 ng p65 (catalog 106453), 200 ng cJun (catalog 102758), STAT3 (catalog 8706) or EZH2-HA (catalog 24230) constructs, and 500 ng CDK4-HA (catalog 1868), CDK6-HA (catalog 1866), CDK6DN (catalog 1869), cyclin D1-HA (catalog 11181), cyclin D2 (catalog 8958), and cyclin D3 (catalog 10912). Additionally, CDK6 S178P expression construct was a gift from Michael Kracht (University of Giessen, Germany) (58). For transfection of HaCaT cells, 3×10^5 cells were transfected for 4 hours using Lipofectamine 3000 and a mixture of 800 ng firefly luciferase vector, 200 ng TK-Renilla vector, and 4 μg expression or control plasmids according to the manufacturer's instructions (Thermo Fisher Scientific, L3000015). At 36 hours after transfection, luciferase activity was measured with the Dual Luciferase Reporter Assay Kit (Promega, E2980). Expression of the reporter constructs was calculated as the fold induction over unstimulated transfected cells, using data from 3 independent experiments.

Transient overexpression in HEK293T, HaCaT cells, and primary keratinocytes. HEK293T cells (ACC 635, DSMZ Braunschweig, Germany) were transfected using HeBS buffer and $CaCl_2$. HaCaT cells and primary keratinocytes were transfected with Lipofectamine 3000 according to the manufacturer's instructions (Thermo Fisher Scientific, L3000015). Five-microgram expression constructs were incubated with 3×10^5 cells for 4 hours. Thirty-six to 48 hours after transfection, cells were harvested and analyzed. NFKBIZ (catalog 44012), CDK9-HA (catalog 28102), and Flag-STAT3C (catalog 8722) expression constructs were purchased from Addgene and pINTO-GFP-EZH2 T345A and pINTO-GFP-EZH2 T345D were provided by Danny Reinberg (Howard Hughes Medical Institute, New York University Langone Medical Center, New York, New York, USA).

Generation of STAT3 mutants. Mutation of STAT3 at K49, K140, and K180 was performed by site-directed mutagenesis of the human STAT3 pcDNA3 construct from Addgene (catalog 71447), which was previously cloned into the Strep-tagged backbone (pEXPR-IBA103). Substitution of the amino acid was performed with self-designed primers (Supplemental Table 1 and ref. 59).

CRISPR/Cas9 gene editing of STAT3 KO HaCaT cells. The CRISPR/Cas9 one vector system was used to generated *STAT*3 KO HaCaT cells

according to the protocol of Shalem et al. (60). The guide RNA against STAT3 (forward: 5′-CACCGACTGCTGGTCAATCTCTCCC-3′, reverse: 5′-AAACGGGAGAGATTGACCAGCAGTC-3′) was cloned into the Cas9 containing lentiCRISPRv2 containing Cas9 vector (Addgene, 52961), followed by lentiviral transduction and puromycin selection.

Synchronization of HaCaT cells. Synchronization of the cells with a double thymidine block was performed as described (61). After the second thymidine block, cells were released in normal medium. At 0, 4, 10, and 14 hours after release, cells were stimulated with IL-36α and/or abemaciclib for 1 hour. Propidium iodide staining was performed by flow cytometry (LSRII, Becton Dickinson) to detect the cell cycle phase at the time point of cell harvest.

Western blot analysis. Western blot analysis was performed as described (9). The following antibodies were used and purchased from Cell Signaling: anti-IκBζ (catalog 9244), anti-pSTAT3 at Tyr705 (catalog 9145), anti-pSTAT3 at Ser727 (catalog 9134), anti-STAT3 (catalog 12640), anti-p65 (catalog 8242), anti-EZH2 (catalog 5246), anti-pRB (at Ser807/811; catalog 8516), anti-FoxM1 (catalog 5436), anti-H3 (catalog 4499), anti-CDK4 (catalog 12790), anti-CDK6 (catalog 13331), anti-CDK9 (catalog 2316), anti-cyclin D1 (catalog 2978), anti-cyclin D2 (catalog 3741), anti-cyclin D3 (catalog 2936), anti-cJun (catalog 9165), anti-H3K27me3 (catalog 9733), anti-GAPDH (catalog 2118), anti-H3 (catalog 9715) and anti–β-actin (catalog 3700). Anti–α-Tubulin (T9026) was purchased from MilliporeSigma. Anti–β-Gal (sc377257) and anti-GFP (sc9996) were obtained from Santa Cruz Biotechnology. Anti-pEZH2 at T345 (catalog 61242) and anti-pEZH2 at T487 (catalog 12820) were purchased from Active Motif and anti–pan-methyl-lysine antibody was purchased from Enzo (ADI-KAP-TF121-E). For detection of mouse IκBζ, a self-made rabbit antiserum raised against peptides CSAPGSPGSDSSDFSS and CLHIRSHKQKASGQ was applied (50).

Chromatin immunoprecipitation (ChIP). ChIP assays were performed as described (62). After sonification, chromatin was incubated with protein G–coupled Dynabeads (10004D, Invitrogen) and 2 μg STAT3 (Thermo Fisher Scientific, MA1-13042), CDK4 (Cell Signaling, 12790), CDK6 (MilliporeSigma, HPA002637), EZH2 (Diagenode, C15410039), NF-κB p65 (Diagenode, C15310256), or control IgG antibody (Abcam, ab46540) overnight at 4°C. The promoter region of myoglobulin (*MB*) served as an internal negative control (forward: 5′- CTCTGCTCCTTTGCCACAAC-3′, reverse: 5′-GAGTGCTCTTCGGGTTTCAG-3′). ChIP primers corresponding to the promoter region of *NFKBIZ* (forward 5′-GCCTTAACTGGGCTAACAGC-3′, reverse 5′-CTGGCAAGTCCTGGAAGGAG-3′), *CCND2* (forward 5′-GGGAGAGGGAGGAGAGCTAA-3′, reverse 5′-GAGAGGTGAGGGCAGAGAGA-3′), and *CCND3* (forward 5′- GGCAATTACAGCCACATTCC-3′, reverse 5′-GGTGGCAACAGACACTGCTA-3′) were self-designed. Data from 2 independent experiments are presented as the fold enrichment, calculated over the percentage of input from the IgG control ChIP.

Coimmunoprecipitation (CoIP). Cells were lysed by mechanical disruption using a Dounce homogenizer and standard lysis buffer (50 mM Tris-HCl pH 7.5, 150 mM NaCl, 1% NP-40, 1x Protease inhibitor cocktail, Roche). Subsequently, lysates were sonicated for 5 minutes at high power (Bioruptor, Diagenode), followed by preclearing of the lysates with protein A/G PLUS agarose beads (Santa Cruz, sc-2003) for 1 hour at 4°C. Precleared lysates were incubated either with antibodies specific for CDK4 (Cell Signaling, 12790), CDK6 (MilliporeSigma, HPA002637), EZH2 (Cell Signaling, 5246), STAT3 (MA1-13042, Thermo Fisher Scientific) or β-Gal (sc-19119, Santa Cruz) as an IgG control, overnight at 4°C. For endogenous IPs immune complexes were precipitated with protein A/G PLUS agarose beads and eluted by 6× SDS-PAGE sample buffer.

Cytokine array. Cytokine levels were detected from primary human keratinocytes that had been treated for 24 hours with 100 ng/mL IL-36α, using the human cytokine array from R&D Systems (ARY005B) according to the manufacturer′s instructions. Prior to analysis, input lysates were normalized to equal cell numbers. Spot intensity was quantified with the dot blot analyzer from ImageJ and normalized to the reference spots. Relative expression levels are represented as mean pixel intensities.

Gene expression analysis by qPCR. Gene expression analyses were performed as described (9). Relative gene expression was analyzed using self-designed primers ordered at Metabion (Supplemental Table 2). Relative mRNA levels were calculated by normalization to the human reference gene *RPL37A* or the mouse reference gene *Actin* using the 2-ΔΔCt method.

Mice. Experiments were conducted in accordance with the German law guidelines of animal care. Ears of female C57BL/6 mice (8–12 weeks old, Jackson Laboratory) were topically treated for 6 consecutive days with 5 mg Aldara cream (containing 5% imiquimod, 3M Pharmaceuticals) and 10 μL abemaciclib (2% in 10 μL ethanol), 10 μL CPI-169 (5% in 10 μL ethanol), or vehicle control. At day 7, mice were sacrificed and analyzed. In the therapeutic mouse model, IMQ was applied first to establish psoriasis-like skin lesions. Then, starting on the third day of IMQ administration (IMQ day 2), IMQ and the inhibitors were added in parallel until mice were sacrificed at day 6 (IMQ day 6). In the IL-36α–mediated psoriasis model, ears of male C57BL/6 mice (8–12 weeks old, Jackson Laboratory) were treated by intradermal injections of 1 μg murine IL-36α (7059-ML, R&D Systems) or PBS control for 5 consecutive days. For application of abemaciclib (2% in ethanol), CPI-169 (5% in ethanol), or the vehicle control, substances were mixed with Miglyol 812 (Carl Roth) in a ratio of 1:2. Inhibitors were topically applied 6 hours before intradermal injections of IL-36α or PBS. Mice were sacrificed and analyzed at day 6. For treatment of established psoriasis-like skin disease, mice were treated every second day with IL-36α for 8 days, followed by the analysis of the mice at day 9 (IL-36 day 9). Both abemaciclib and CPI-169 were applied daily on the skin, starting from the third IL-36α administration (IL-36 day 4).

Flow cytometry. Sample preparation was performed as described (9). The following anti-mouse antibodies from BioLegend were used: anti-CD45 FITC (catalog 103107), anti-CD11b Pacific Blue (catalog 101223), anti-Ly6G PE (catalog 127607), anti-F4/80 APC (catalog 123115), anti-CD11c Pacific Blue (catalog 117322), anti–MHC-II APC (catalog 107613), anti-CD172a PE (catalog 144011), and anti–Siglec-H PE (catalog 129605). Anti–PDCA-1 APC (17-2092-80) and anti-αβTCR Pacific Blue (catalog HM3628) were purchased from Invitrogen, and anti-γδTCR APC (catalog 17-5711-82) from MilliporeSigma. Acquisition was performed with the LSRII flow cytometer (Becton Dickinson) and live, single cells were gated using the FlowJo (Tree Star) software.

Histology. Ear sections from mice were fixed in 10% formalin (Carl Roth) and subsequently embedded in paraffin. Five-micrometer sections were prepared and incubated with the following antibodies from

Cell Signaling: pSTAT3 (catalog 9145), pRB (catalog 8516), H3K27me3 (catalog 9733) and EZH2 (catalog 5246), cyclin D2 (catalog 3741), and cyclin D3 (catalog 2936). Antigen retrieval was performed in 1 mM EDTA pH 8.0 for pSTAT3, and 10 mM citrate buffer pH 6.0 + 0.5% Triton X-100 for EZH2, H3K27me3, pRB, cyclin D2, and cyclin D3. After incubation with peroxidase-coupled secondary antibodies, sections were stained with DAB substrate.

Analysis of patient data. Gene expression data originated from the GEO data set GSE13355 (63, 64). Prenormalized gene expression values from each sample were directly taken from the GEO profile data set GDS4602. The following reporters were taken for analysis: *EZH2*, ID 203358_s_at; *CCND1*, ID 208711_s_at; *CCND2*, ID 200953_s_at; and *CCND3*, ID 201700_s_at.

Statistics. Results from in vivo experiments are represented as the mean ± SEM. Results from cell culture experiments are represented as the mean ± SD. Significance was calculated using a 1-way ANOVA to compare multiple groups, and a 2-tailed Student's *t* test was applied when 2 groups were compared with each other. A *P* value less than 0.05 was considered significant. Significance is depicted by asterisks as follows: $^{*}P < 0.05$, $^{**}P < 0.01$, $^{***}P < 0.001$.

Study approval. All animal experiments were approved by the Regierungspräsidium, Tübingen, Germany (IB 4/18G, IB 1/19G). Human psoriasis skin samples came from the Department of Dermatology, Heidelberg University Hospital. Experiments were approved by the ethics committee of the University Hospital Heidelberg. Isolation of primary human keratinocytes from foreskin was approved by the local ethics committee of the University Hospital Tübingen.

Author contributions

AM, AD, and CR performed experiments and data analysis. SH, KSO, MD, and DK designed the experiments. KS donated human psoriasis skin samples and helped with the analysis. SH, KSO, MD, and DK wrote the manuscript.

Acknowledgments

We thank Michael Kracht for the CDK6 S178P construct and Danny Reinberg for the EZH2 T345A and T345D constructs. Several expression constructs were obtained from Addgene and provided by the following individuals: Sander van den Heuvel (CDK6, CDK4, CDK6DN), Andrew Rice (HA-CDK9), Kristian Helin (HA-EZH2), Jin Chen (cJUN), George Darnell (p65), Jim Darnell (STAT3C), Jie Chen (STAT3), Philip Hinds (cyclin D2), Bob Weinberg (cyclin D3), Bruce Zetter (cyclin D1), Feng Zhang (lentiCRISPRv2), and Stephen Elledge (pInducer20). We thank Caroline Schönfeld for technical assistance. The study was supported by grants from the Else-Kröner-Fresenius-Stiftung (to DK), the TR/SFB 156 (to DK and SH), the TR/SFB 209 (to SH and KSO), the DFG Excellent Strategy EXC-2180 and the Emmy-Noether program of the Deutsche Forschungsgemeinschaft (both to SH).

Address correspondence to: Daniela Kramer, Interfaculty Institute for Biochemistry, Auf der Morgenstelle 34, 72076 Tübingen, Germany. Phone: 49.7071.2974159; Email: daniela.kramer@uni-tuebingen.de.

1. Nestle FO, Kaplan DH, Barker J. Psoriasis. *N Engl J Med*. 2009;361(5):496–509.
2. Lowes MA, Suárez-Fariñas M, Krueger JG. Immunology of psoriasis. *Annu Rev Immunol*. 2014;32:227–255.
3. McGeachy MJ, Cua DJ, Gaffen SL. The IL-17 family of cytokines in health and disease. *Immunity*. 2019;50(4):892–906.
4. Kurschus FC, Moos S. IL-17 for therapy. *J Dermatol Sci*. 2017;87(3):221–227.
5. Wolf J, Ferris LK. Anti-IL-36R antibodies, potentially useful for the treatment of psoriasis: a patent evaluation of WO2013074569. *Expert Opin Ther Pat*. 2014;24(4):477–479.
6. Wasilewska A, Winiarska M, Olszewska M, Rudnicka L. Interleukin-17 inhibitors. A new era in treatment of psoriasis and other skin diseases. *Postepy Dermatol Alergol*. 2016;33(4):247–252.
7. Jullien D, Prinz JC, Nestle FO. Immunogenicity of biotherapy used in psoriasis: the science behind the scenes. *J Invest Dermatol*. 2015;135(1):31–38.
8. Johansen C, et al. IκBζ is a key driver in the development of psoriasis. *Proc Natl Acad Sci USA*. 2015;112(43):E5825–E5833.
9. Müller A, et al. IκBζ is a key transcriptional regulator of IL-36-driven psoriasis-related gene expression in keratinocytes. *Proc Natl Acad Sci USA*. 2018;115(40):10088–10093.
10. Oeckinghaus A, Hayden MS, Ghosh S. Crosstalk in NF-κB signaling pathways. *Nat Immunol*. 2011;12(8):695–708.
11. Zhang Q, et al. Tet2 is required to resolve inflammation by recruiting Hdac2 to specifically repress IL-6. *Nature*. 2015;525(7569):389–393.
12. Tartey S, et al. Akirin2 is critical for inducing inflammatory genes by bridging IκB-ζ and the SWI/SNF complex. *EMBO J*. 2014;33(20):2332–2348.
13. Annemann M, et al. Atypical IκB proteins in immune cell differentiation and function. *Immunol Lett*. 2016;171:26–35.
14. Sherr CJ, Beach D, Shapiro GI. Targeting CDK4 and CDK6: from discovery to therapy. *Cancer Discov*. 2016;6(4):353–367.
15. Choi YJ, Anders L. Signaling through cyclin D-dependent kinases. *Oncogene*. 2014;33(15):1890–1903.
16. Gong X, et al. Genomic aberrations that activate D-type cyclins are associated with enhanced sensitivity to the CDK4 and CDK6 inhibitor abemaciclib. *Cancer Cell*. 2017;32(6):761–776.e6.
17. Vidula N, Rugo HS. Cyclin-dependent kinase 4/6 inhibitors for the treatment of breast cancer: a review of preclinical and clinical data. *Clin Breast Cancer*. 2016;16(1):8–17.
18. Klein ME, Kovatcheva M, Davis LE, Tap WD, Koff A. CDK4/6 inhibitors: the mechanism of action may not be as simple as once thought. *Cancer Cell*. 2018;34(1):9–20.
19. Goel S, et al. CDK4/6 inhibition triggers anti-tumour immunity. *Nature*. 2017;548(7668):471–475.
20. Amulic B, et al. Cell-cycle proteins control production of neutrophil extracellular traps. *Dev Cell*. 2017;43(4):449–462.e5.
21. Scheicher R, et al. CDK6 as a key regulator of hematopoietic and leukemic stem cell activation. *Blood*. 2015;125(1):90–101.
22. Schaer DA, et al. The CDK4/6 inhibitor abemaciclib induces a T cell inflamed tumor microenvironment and enhances the efficacy of PD-L1 checkpoint blockade. *Cell Rep*. 2018;22(11):2978–2994.
23. Kollmann K, et al. A kinase-independent function of CDK6 links the cell cycle to tumor angiogenesis. *Cancer Cell*. 2013;24(2):167–181.
24. Buss H, et al. Cyclin-dependent kinase 6 phosphorylates NF-κB P65 at serine 536 and contributes to the regulation of inflammatory gene expression. *PLoS ONE*. 2012;7(12):e51847.
25. Handschick K, et al. Cyclin-dependent kinase 6 is a chromatin-bound cofactor for NF-κB-dependent gene expression. *Mol Cell*. 2014;53(2):193–208.
26. Moos S, Mohebiany AN, Waisman A, Kurschus FC. Imiquimod-induced psoriasis in mice depends on the IL-17 signaling of keratinocytes. *J Invest Dermatol*. 2019;139(5):1110–1117.
27. Tortola L, et al. Psoriasiform dermatitis is driven by IL-36-mediated DC-keratinocyte crosstalk. *J Clin Invest*. 2012;122(11):3965–3976.
28. Iwanaga R, et al. Activation of the cyclin D2 and cdk6 genes through NF-kappaB is critical for cell-cycle progression induced by HTLV-I Tax. *Oncogene*. 2008;27(42):5635–5642.
29. Wang Z, Sicinski P, Weinberg RA, Zhang Y, Ravid K. Characterization of the mouse cyclin D3 gene: exon/intron organization and promoter activity. *Genomics*. 1996;35(1):156–163.
30. Shi X, Zhang H, Paddon H, Lee G, Cao X, Pelech S. Phosphorylation of STAT3 serine-727 by cyclin-dependent kinase 1 is critical for nocodazole-induced mitotic arrest. *Biochemistry*. 2006;45(18):5857–5867.
31. Ezhkova E, et al. Ezh2 orchestrates gene expression for the stepwise differentiation of

tissue-specific stem cells. *Cell*. 2009;136(6):1122–1135.
32. Eckert RL, Adhikary G, Rorke EA, Chew YC, Balasubramanian S. Polycomb group proteins are key regulators of keratinocyte function. *J Invest Dermatol*. 2011;131(2):295–301.
33. Wurm S, et al. Terminal epidermal differentiation is regulated by the interaction of Fra-2/AP-1 with Ezh2 and ERK1/2. *Genes Dev*. 2015;29(2):144–156.
34. Kim E, et al. Phosphorylation of EZH2 activates STAT3 signaling via STAT3 methylation and promotes tumorigenicity of glioblastoma stem-like cells. *Cancer Cell*. 2013;23(6):839–852.
35. Dasgupta M, Dermawan JK, Willard B, Stark GR. STAT3-driven transcription depends upon the dimethylation of K49 by EZH2. *Proc Natl Acad Sci USA*. 2015;112(13):3985–3990.
36. Yang J, et al. Reversible methylation of promoter-bound STAT3 by histone-modifying enzymes. *Proc Natl Acad Sci USA*. 2010;107(50):21499–21504.
37. Iannetti A, et al. Regulation of p53 and Rb links the alternative NF-κB pathway to EZH2 expression and cell senescence. *PLoS Genet*. 2014;10(9):e1004642.
38. Zeng X, Chen S, Huang H. Phosphorylation of EZH2 by CDK1 and CDK2: a possible regulatory mechanism of transmission of the H3K27me3 epigenetic mark through cell divisions. *Cell Cycle*. 2011;10(4):579–583.
39. Chen S, et al. Cyclin-dependent kinases regulate epigenetic gene silencing through phosphorylation of EZH2. *Nat Cell Biol*. 2010;12(11):1108–1114.
40. Wei Y, et al. CDK1-dependent phosphorylation of EZH2 suppresses methylation of H3K27 and promotes osteogenic differentiation of human mesenchymal stem cells. *Nat Cell Biol*. 2011;13(1):87–94.
41. Wolk K, et al. IL-22 and IL-20 are key mediators of the epidermal alterations in psoriasis while IL-17 and IFN-gamma are not. *J Mol Med*. 2009;87(5):523–536.
42. Zheng Y, et al. Interleukin-22, a T(H)17 cytokine, mediates IL-23-induced dermal inflammation and acanthosis. *Nature*. 2007;445(7128):648–651.
43. Calautti E, Avalle L, Poli V. Psoriasis: A STAT3-centric view. *Int J Mol Sci*. 2018;19(1):E171.
44. Bradley WD, et al. EZH2 inhibitor efficacy in non-Hodgkin's lymphoma does not require suppression of H3K27 monomethylation. *Chem Biol*. 2014;21(11):1463–1475.
45. van der Fits L, et al. Imiquimod-induced psoriasis-like skin inflammation in mice is mediated via the IL-23/IL-17 axis. *J Immunol*. 2009;182(9):5836–5845.
46. Anders L, et al. A systematic screen for CDK4/6 substrates links FOXM1 phosphorylation to senescence suppression in cancer cells. *Cancer Cell*. 2011;20(5):620–634.
47. Campbell JJ, et al. Efficacy of chemokine receptor inhibition in treating IL-36α-induced psoriasiform inflammation. *J Immunol*. 2019;202(6):1687–1692.
48. Laphanuwat P, Jirawatnotai S. Immunomodulatory roles of cell cycle regulators. *Front Cell Dev Biol*. 2019;7:23.
49. Tsoi LC, et al. Enhanced meta-analysis and replication studies identify five new psoriasis susceptibility loci. *Nat Commun*. 2015;6:7001.
50. Lorscheid S, et al. Keratinocyte-derived IκBζ drives psoriasis and associated systemic inflammation. *JCI Insight*. 2019;4(22):130835.
51. Li J, et al. TRIM28 interacts with EZH2 and SWI/SNF to activate genes that promote mammosphere formation. *Oncogene*. 2017;36(21):2991–3001.
52. Shi B, et al. Integration of estrogen and Wnt signaling circuits by the polycomb group protein EZH2 in breast cancer cells. *Mol Cell Biol*. 2007;27(14):5105–5119.
53. Kaneko S, et al. Phosphorylation of the PRC2 component Ezh2 is cell cycle-regulated and up-regulates its binding to ncRNA. *Genes Dev*. 2010;24(23):2615–2620.
54. Kim J, et al. Polycomb- and methylation-independent roles of EZH2 as a Transcription Activator. *Cell Rep*. 2018;25(10):2808–2820.e4.
55. Lee ST, et al. Context-specific regulation of NF-κB target gene expression by EZH2 in breast cancers. *Mol Cell*. 2011;43(5):798–810.
56. Miyoshi K, et al. Stat3 as a therapeutic target for the treatment of psoriasis: a clinical feasibility study with STA-21, a Stat3 inhibitor. *J Invest Dermatol*. 2011;131(1):108–117.
57. Boukamp P, Petrussevska RT, Breitkreutz D, Hornung J, Markham A, Fusenig NE. Normal keratinization in a spontaneously immortalized aneuploid human keratinocyte cell line. *J Cell Biol*. 1988;106(3):761–771.
58. Sambrook J, Russell DW. Calcium-phosphate-mediated transfection of eukaryotic cells with plasmid DNAs. *CSH Protoc*. 2006;2006(1):pdb.prot3871.
59. Zheng L, Baumann U, Reymond JL. An efficient one-step site-directed and site-saturation mutagenesis protocol. *Nucleic Acids Res*. 2004;32(14):e115.
60. Shalem O, et al. Genome-scale CRISPR-Cas9 knockout screening in human cells. *Science*. 2014;343(6166):84–87.
61. Peña-Diaz J, et al. Transcription profiling during the cell cycle shows that a subset of Polycomb-targeted genes is upregulated during DNA replication. *Nucleic Acids Res*. 2013;41(5):2846–2856.
62. Nemajerova A, et al. TAp73 is a central transcriptional regulator of airway multiciliogenesis. *Genes Dev*. 2016;30(11):1300–1312.
63. Nair RP, et al. Genome-wide scan reveals association of psoriasis with IL-23 and NF-kappaB pathways. *Nat Genet*. 2009;41(2):199–204.
64. Swindell WR, et al. Genome-wide expression profiling of five mouse models identifies similarities and differences with human psoriasis. *PLoS ONE*. 2011;6(4):e18266.

Supplemental information

The CDK4/6-EZH2 pathway is a potential therapeutic target for psoriasis

Anne Müller[1], Antje Dickmanns[2], Claudia Resch[1], Knut Schäkel[3], Stephan Hailfinger[1,4], Matthias Dobbelstein[2], Klaus Schulze-Osthoff[1,5], Daniela Kramer[1,*]

[1] Interfaculty Institute for Biochemistry, University of Tübingen, 72076 Tübingen, Germany

[2] Institute of Molecular Oncology, Göttingen Center of Molecular Biosciences (GZMB), University of Göttingen, 37077 Göttingen, Germany

[3] Department of Dermatology, Heidelberg University Hospital, 69120 Heidelberg, Germany

[4] Cluster of Excellence iFIT (EXC 2180) "Image-Guided and Functionally Instructed Tumor Therapies", University of Tübingen, Germany

[5] German Cancer Consortium (DKTK) and German Cancer Research Center (DKFZ), 69120 Heidelberg, Germany

[*] To whom correspondence should be addressed:

Daniela Kramer, Interfaculty Institute for Biochemistry, Hoppe-Seyler-Str.4, 72076 Tübingen, Germany, phone: +49-7071-2974159, email: daniela.kramer@uni-tuebingen.de

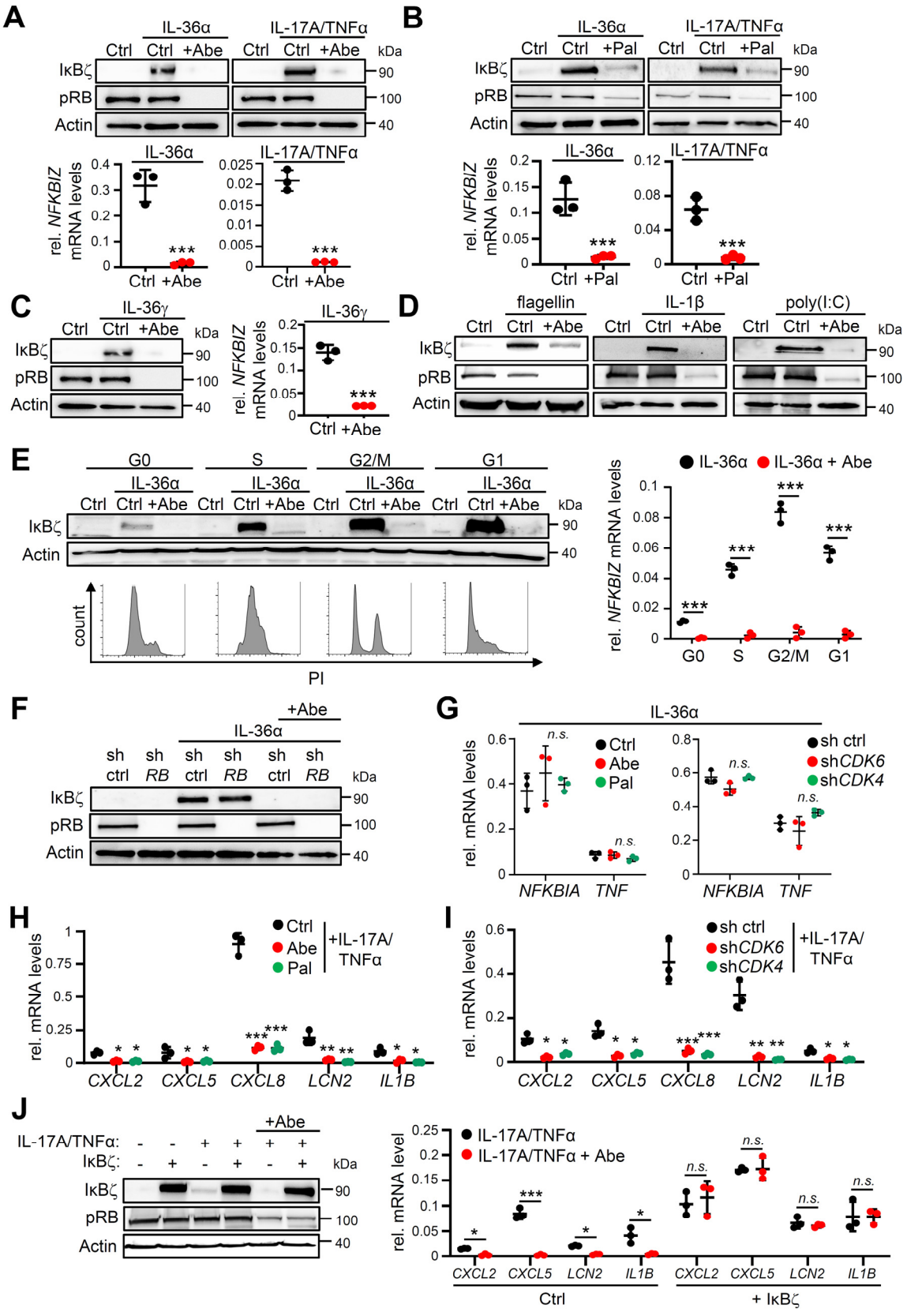

Supplemental Figure 1. Effects of CDK4/6 inhibition on IL-17A/TNFα-stimulated keratinocytes and analysis of possible cell cycle effects.

(A) IκBζ protein and mRNA (*NFKBIZ*) expression in human primary keratinocytes stimulated for 24 h with IL-36α or IL-17A/TNFα with or without abemaciclib (Abe, added for 2 h). Suppression of Rb phosphorylation controlled effective CDK4/6 inhibition. **(B)** IκBζ expression in human primary keratinocytes stimulated for 1 h with 100 ng/mL IL-36α or 200 ng/mL IL-17A and 10 ng/mL TNFα with or without palbociclib (Pal). **(C + D)** IκBζ expression in primary human keratinocytes treated with IL-36γ (100 ng/mL for 1 h) (C), flagellin, IL-1β (both 100 ng/mL for 1h), or poly(I:C) (10 ng/mL for 4 h) in the presence or absence of abemaciclib (D). **(E)** IκBζ expression in synchronized HaCaT cells. Cells were synchronized by double thymidine block. At different times after release (0 -16 h), cells were stimulated in the different cell cycle phases for 1 h with 100 ng/mL IL-36α in the presence or absence of abemaciclib (Abe). The different cell cycle phases at the time of cell harvesting were controlled by PI staining. **(F)** IκBζ protein levels in *RB*-deficient HaCaT cells treated with IL-36α and abemaciclib. **(G)** Expression of IκBζ-independent genes in CDK4/6 inhibitor-treated and *CDK4/6*-depleted keratinocytes. Stimulation as in (B). **(H + I)** Expression of IκBζ target genes in human primary keratinocytes stimulated for 1 h with 100 ng/mL IL-17A and 10 ng/mL TNFα**,** following CDK4/6 inhibition (H) or shRNAs (I). **(J)** Effect of IκBζ overexpression on CDK4/6-controlled cytokine expression in IL-17A/TNFα-stimulated primary keratinocytes. Treatment as in (B). All analyses: $n = 3 \pm$ SD. Significance was calculated using a 1-way ANOVA for multiple groups and a 2-tailed Student's t-test comparing two groups: $^{*}p < 0.05$; $^{**}p < 0.01$; $^{***}p < 0.001$, *n.s.* = not significant.

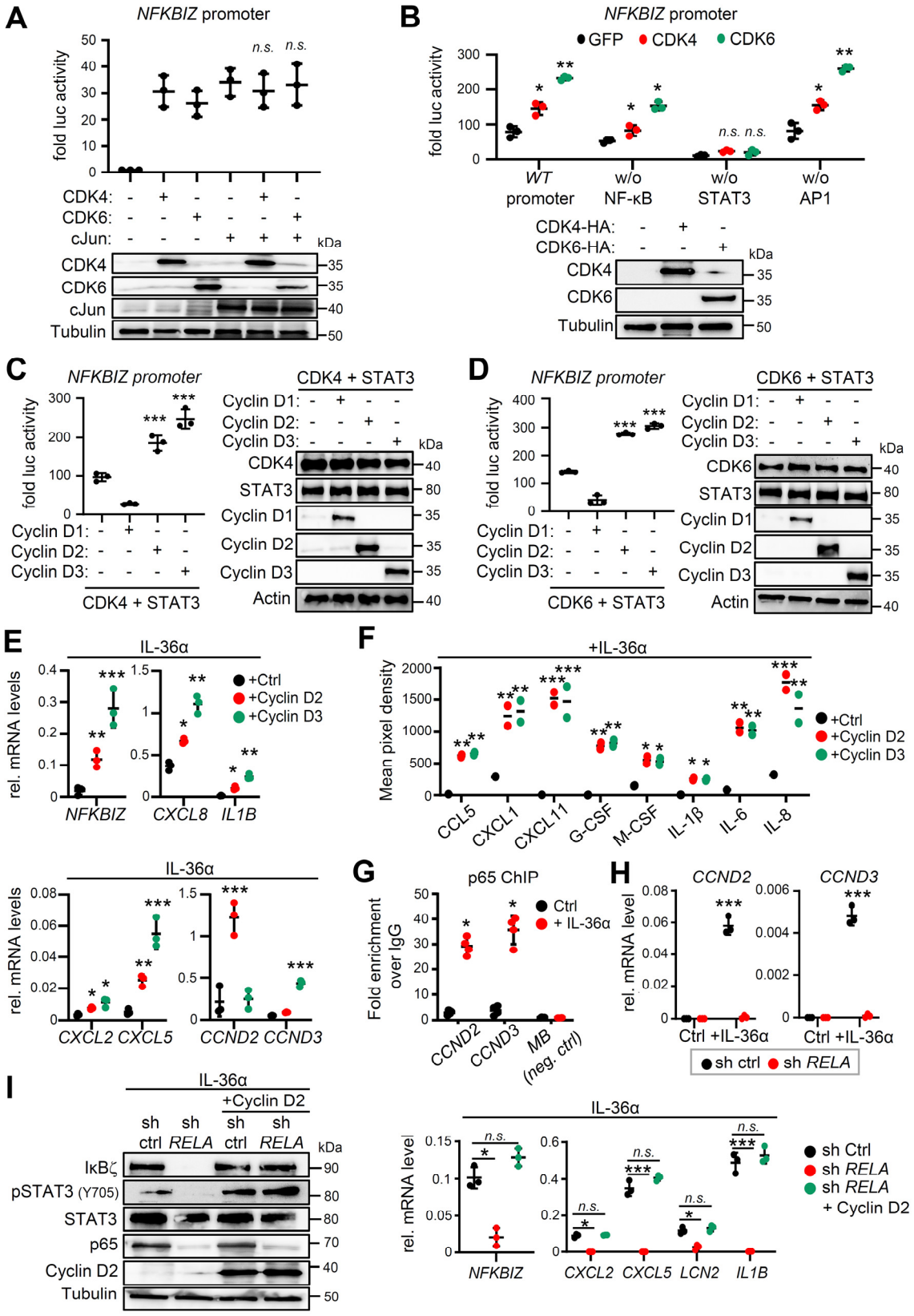

Supplemental Figure 2. CDK4/6 regulate STAT3-mediated IκBζ induction in a cyclin D2/D3-dependent manner. (A) *NFKBIZ* promoter activity in HEK293T cells transiently overexpressing CDK4, CDK6 or cJun, alone or in combination. Relative luciferase activity was

normalized to co-transfected Renilla luciferase control. **(B)** Analysis of the *NFKBIZ* promoter in IL-36α-stimulated HaCaT cells using luciferase constructs that harbor deletions of NF-κB, STAT3 or AP1 binding sites. CDK4, CDK6 or GFP as control were transiently co-overexpressed in parallel. Relative luciferase activity was normalized to co-transfected Renilla control. **(C + D)** *NFKBIZ* promoter activity in HEK293T cells transiently overexpressing STAT3 and CDK4 (C) or STAT3 and CDK6 (D)**,** alone or in combination with cyclin D1, cyclin D2 and cyclin D3 overexpression. **(E)** Gene expression in primary human keratinocytes transiently overexpressing cyclin D2 or cyclin D3. Cells were stimulated for 1 h with 100 ng/mL IL-36α. Relative mRNA levels were normalized to *RPL37A*. (Ctrl = cells overexpressing empty control vector). **(F)** Cytokine levels in supernatants of cells, treated for 24 h with IL-36α, similar as in (E). *n* = 2. **(G)** p65 binding to the *CCND2* and *CCND3* locus in primary human keratinocytes. Cells were treated for 5 min with 100 ng/mL IL-36α. **(H)** *CCND2* and *CCND3* mRNA levels in control knockdown (Ctrl) or *RELA* knockdown cells, treated for 15 min with IL-36α, similar as in (E). **(I)** Transient overexpression of cyclin D2 in control or *RELA*-depleted primary human keratinocytes, treated for 1 h with IL-36α, similar as in (E). Significance was calculated using a 1-way ANOVA for multiple groups and a 2-tailed Student's t-test comparing two groups: *p < 0.05; **p < 0.01; ***p < 0.001, *n.s.* = not significant. All analyses: *n* = 3 ± SD.

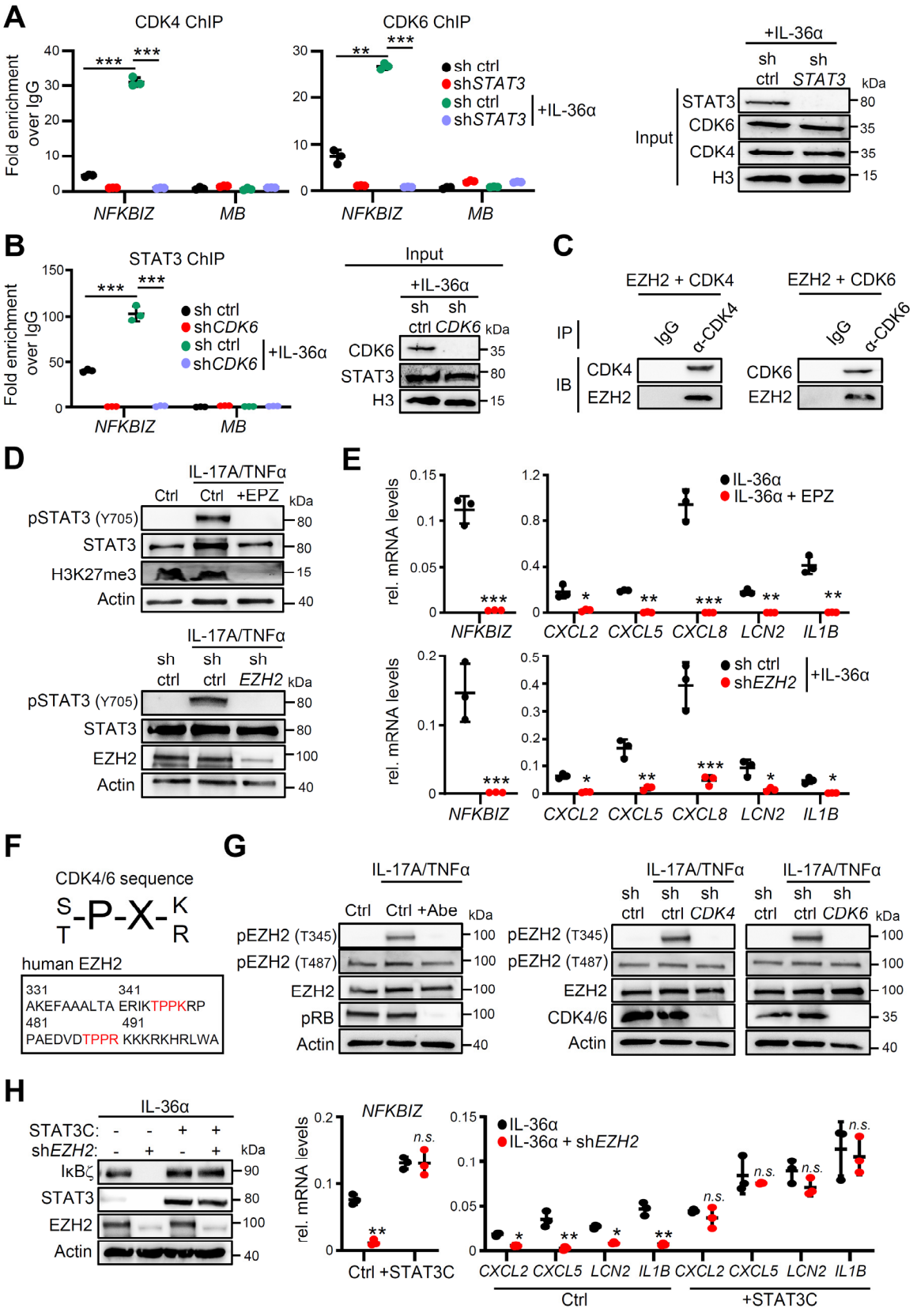

Supplemental Figure 3. Extended analysis of CDK4/6-mediated phosphorylation of EZH2 at T345 that induces STAT3 activation. (A) Chromatin immunoprecipitation (ChIP) of CDK4, CDK6 or IgG (control). Control or *STAT3*-deficient HaCaT cells were treated for 30 min

with 100 ng/mL IL-36α. Relative binding was calculated as the fold enrichment over IgG. (*MB* = myoglobulin promoter; internal negative control). Equal CDK4/6 and STAT3 levels were controlled by immunoblot analysis of the ChIP input. **(B)** STAT3 ChIP in IL-36α-stimulated, *CDK6*-deficient cells. Stimulation and analysis as in (A). **(C)** Detection of CDK4/6 interaction with EZH2 in HEK293T cells. EZH2 was transiently overexpressed together with CDK4 or CDK6. CDK4/6-EZH2 complexes were pulled down using a CDK4- or a CDK6-specific antibody or control IgG. **(D)** STAT3 activity was analyzed by immunoblot detection of phosphorylated STAT3 (Y705) in keratinocytes, treated for 1 h with 100 ng/mL IL-17A and 10 ng/mL TNFα in the presence or absence of active EZH2. Detection of H3K27me3 controlled effective EZH2 inhibition (EPZ = EPZ6438 or *EZH2* shRNA knockdown). **(E)** Gene expression in EPZ6438-treated or *EZH2*-depleted human primary keratinocytes (Treatment: 100 ng/mL IL-36α). mRNA levels were normalized to *RPL37A*. **(F)** CDK4/6 substrate sequence and putative CDK phosphorylation sites of human EZH2 (marked in red). **(G)** Analysis of EZH2 activation by immunoblot detection of T345- or T487-phosphorylated EZH2 in IL-17A/TNFα-treated keratinocytes. Cells were treated as in (D), with or without abemaciclib (Abe) or *CDK4/6*-specific shRNAs. **(H)** Analysis of IL-36α-mediated IκBζ induction and target gene expression in *EZH2*-depleted HaCaT cells, which overexpress a hyperactive STAT3 (STAT3C) version. Treatment: 1 h with 100 ng/mL IL-36α. Significance was calculated using a 1-way ANOVA for multiple groups and a 2-tailed Student's t-test comparing two groups: *$p < 0.05$; **$p < 0.01$; ***$p < 0.001$, *n.s.* = not significant. All analyses: $n = 3 \pm$ SD.

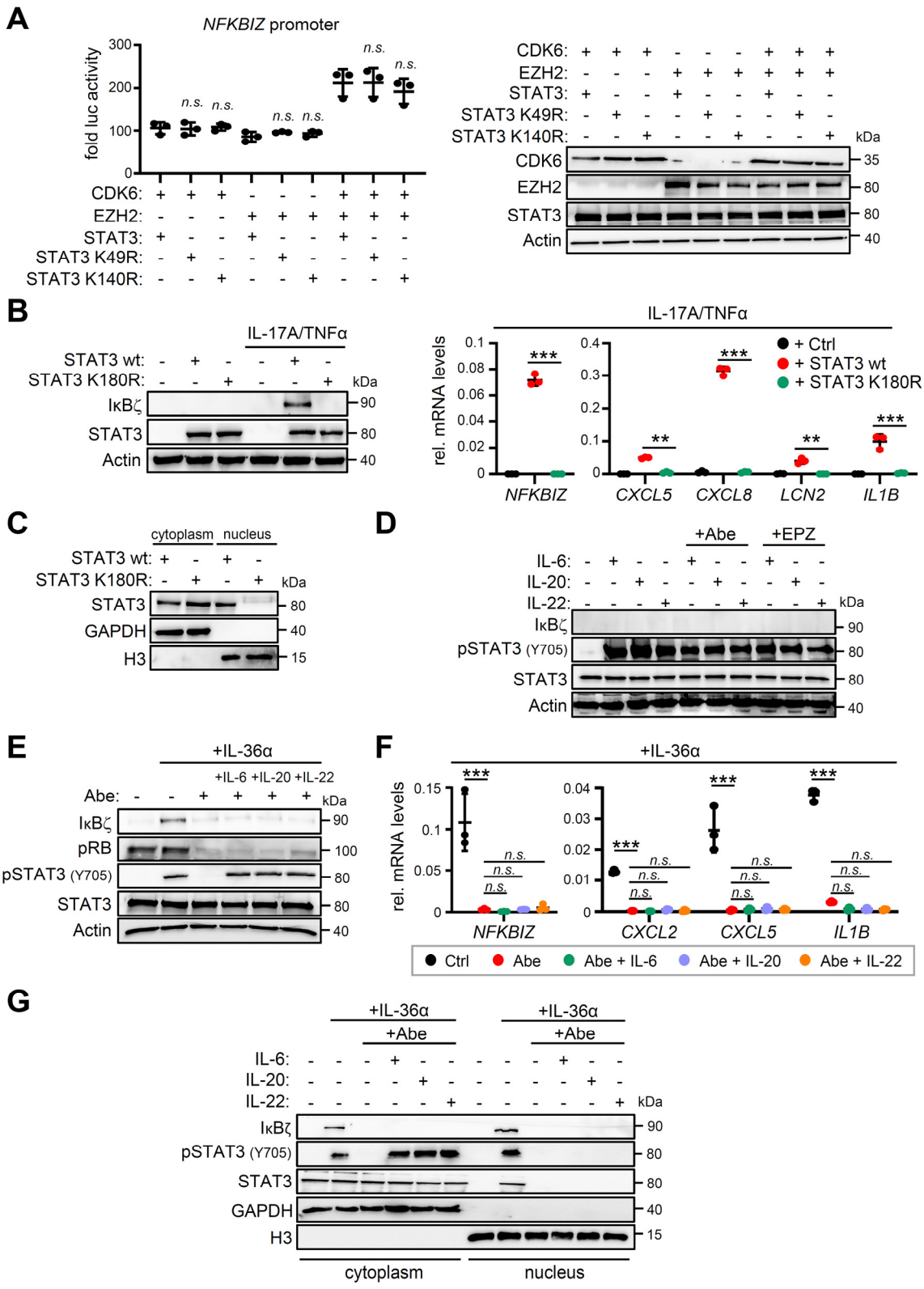

Supplemental Figure 4. Extended analysis of EZH2-mediated methylation of STAT3 in keratinocytes. (A) Analysis of *NFKBIZ* promoter activity in HEK293T cells transiently overexpressing CDK6 and EZH2, alone or in combination with wildtype STAT3 or mutant STAT3 K49R and K140R. Relative luciferase activity was normalized to co-transfected Renilla

control. **(B)** Expression of IκBζ and its target genes in *STAT3* KO HaCaT cells, transiently overexpressing wildtype STAT3 or STAT3 K180R. Cells were treated for 1 h with 200 ng/mL IL-17A and 10 ng/mL TNFα. Relative mRNA levels of *NFKBIZ* and its target genes were normalized to *RPL37A*. **(C)** *STAT3* KO HaCaT cells transiently overexpressing wildtype STAT3 or mutant STAT3 (K180R) were stimulated for 1 h with 100 ng/mL IL-36α, followed by nuclear fractionation of the cells and immunoblot analysis. GAPDH and H3 were used as markers for the cytoplasmic and nuclear fraction, respectively. **(D)** Primary human keratinocytes were treated for 1 h with 100 ng/mL IL-6, IL-20 or IL-22 in the presence or absence of abemaciclib (Abe) or EPZ6438 (EPZ). **(E + F)** Primary human keratinocytes were treated for 1 h with 100 ng/mL IL-36α, in the presence or absence of abemaciclib (Abe), IL-6, IL-20 or IL-22, similar as in (D). **(E)** Immunoblot analysis of IκBζ and pSTAT3 (Y705). Actin served as a loading control. **(F)** mRNA levels normalized to *RPL37A*, treated as in (E) **(G)** Nuclear fractionation of primary human keratinocytes treated as in (E). GAPDH and H3 were used as markers for the cytoplasmic and nuclear fraction, respectively. Significance was calculated using a 1-way ANOVA test: *p < 0.05; **p < 0.01; ***p < 0.001, *n.s.* = not significant. All analyses: $n = 3 \pm SD$.

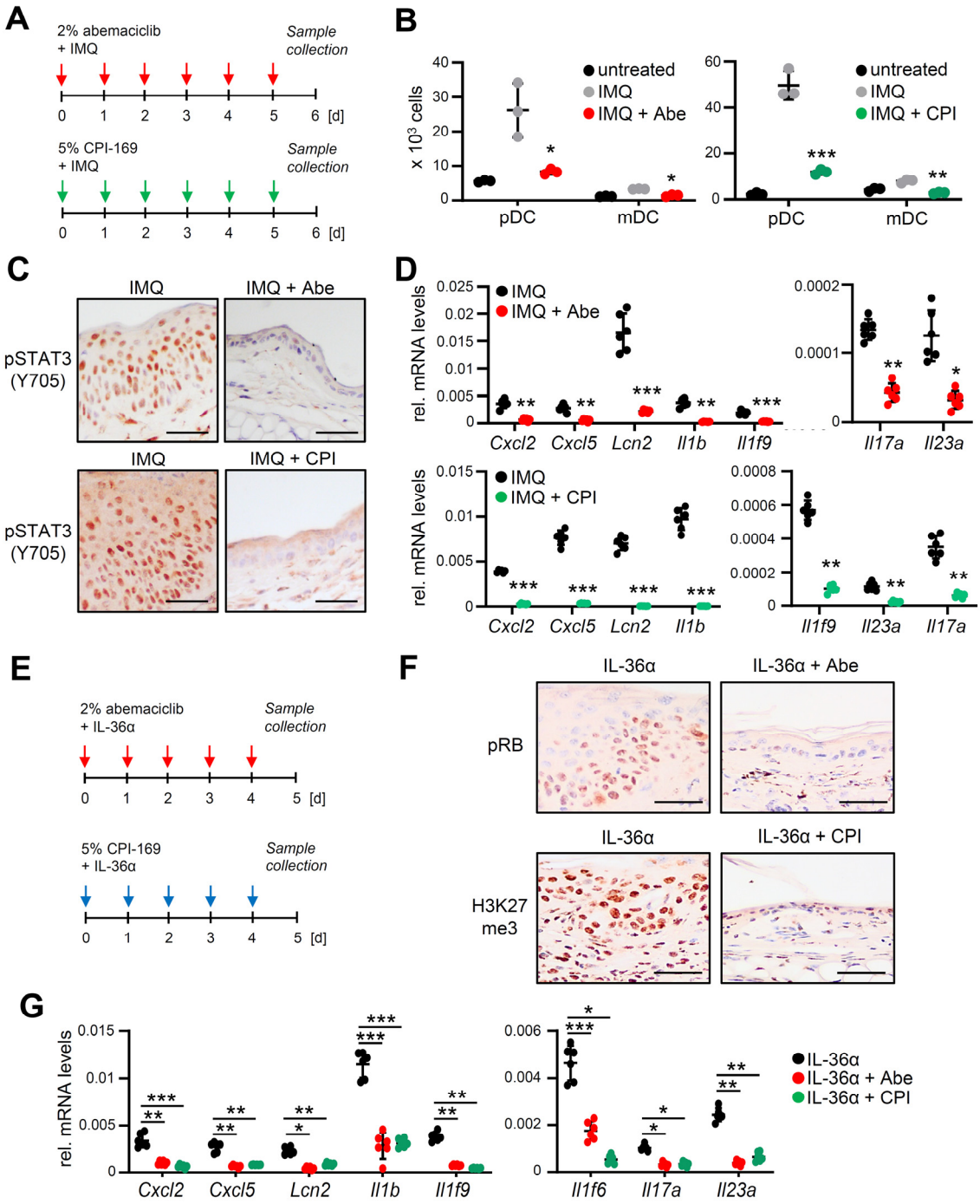

Supplemental Figure 5. Extended analysis of the in vivo effects of CDK4/6 or EZH2 inhibition on psoriasis induction in the imiquimod (IMQ)- and IL-36 mouse models. (A) Treatment scheme for induction of IMQ-mediated, psoriasis-like skin inflammation. Mice received daily topical applications of IMQ-containing Aldara cream and abemaciclib (Abe; 10 µL of a 2% solution) or CPI-169 (CPI, 10 µL of a 5% solution). **(B)** Characterization of infiltrating dendritic cell subsets into the ears of IMQ-treated mice by flow cytometry at day 6. Plasmocytoid dendritic cells (pDC) were detected as CD45$^+$, CD11c$^+$, MHC-II$^+$, PDCA-1$^+$,

Siglec-H$^+$, and myeloid derived dendritic cells (mDC) were analyzed as CD45$^+$, CD11c$^+$, MHC-II$^+$, CD172a$^+$. *n* = 6 ears per group ± SEM. **(C)** IHC staining of phosphorylated STAT3 at Y705 (pSTAT3) in the epidermis of treated mice at day 6. Scale bar: 40 μM. **(D)** Gene expression analysis of IκBζ target genes in IMQ-, IMQ/Abe- and IMQ/CPI-treated skin samples at day 6. Relative mRNA expression was normalized to *Actin*. **(E)** IL-36α treatment scheme with topical application of abemaciclib or CPI-169 as in (A). 1 μg murine IL-36α or PBS control was intradermally injected into one ear of the mice for five consecutive days. **(F)** IHC staining in ear skin sections of PBS or IL-36α-treated mice at day 5. pRB and H3K27me3 served as a marker for effective inhibition of CDK4/6 and EZH2, respectively. Scale bar: 40 μM. **(G)** Expression of IκBζ target genes in IL-36α-, IL-36α/Abe- and IL-36α/CPI-treated skin samples of IL-36α-treated mice at day 5. All analyses: *n* = 6 per group ± SEM. Significance was calculated using a 1-way ANOVA test for multiple groups and a 2-tailed Student's t-test comparing two groups: *p < 0.05; **p < 0.01; ***p < 0.001.

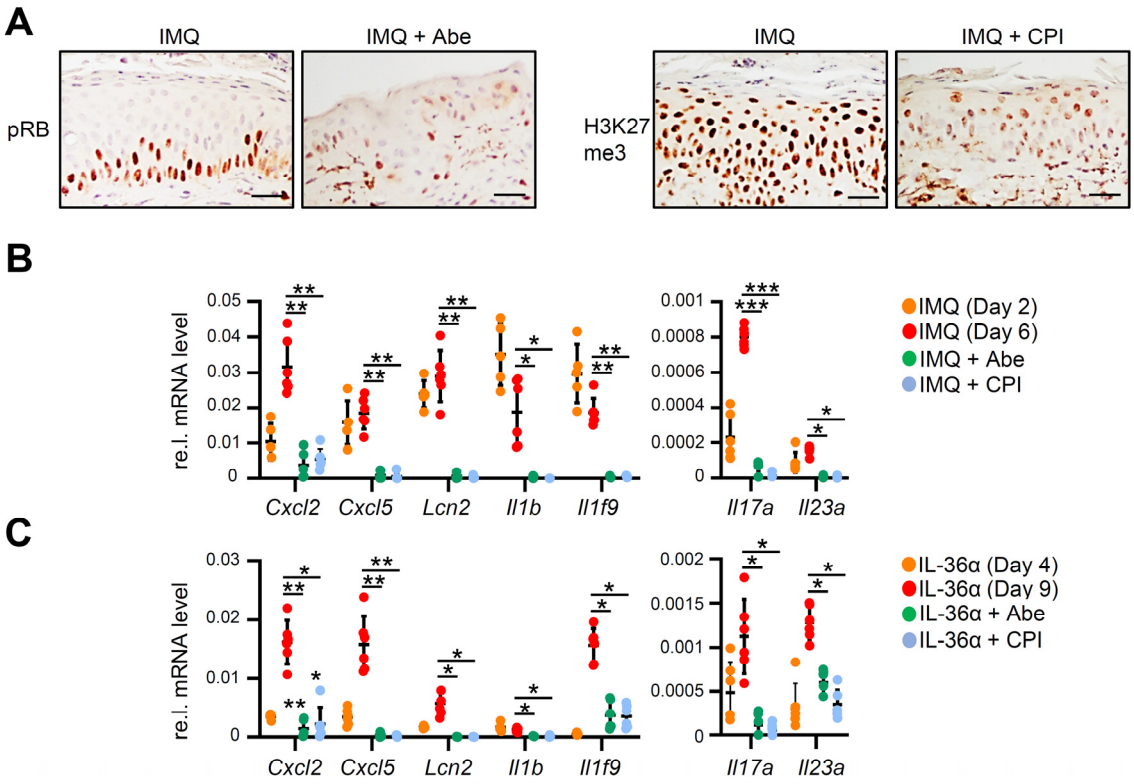

Supplemental Figure 6. Extended analysis of the in vivo effects of CDK4/6 or EZH2 inhibition on already established IMQ- and IL-36-mediated psoriasis-like skin inflammation. (A) IHC staining of pRB (marker for CDK4/6 inhibition) and H3K27me3 (marker for EZH2 inhibition) at day 6 of IMQ treatment. **(B)** Gene expression analysis of IMQ-treated animals either at day 2 (starting time point of inhibitor treatment, IMQ day 2) or at day 6 (24 h after the last inhibitor application, IMQ day 6). Relative mRNA levels were normalized to *Actin*. **(C)** Gene expression analysis of IL-36α-treated animals either at day 4 (starting time point of inhibitor treatment, IL-36α day 4) or at day 9 (24 h after the last inhibitor application, IL-36α day 9). Relative mRNA levels were normalized to *Actin*. All analyses: *n* = 6 per group ± SEM. Significance was calculated using a 1-way ANOVA test: *p < 0.05; **p < 0.01; ***p < 0.001.

Supplementary Table S1. Primers used for silent mutagenesis of STAT3.

K49R forward	GACTGGGCATATGCAGCCAGCAGAGAGTCACATGCCACG
K49R reverse	CACCAACGTGGCATGTGACTCTCTGCTGGCTGCATATGC
K140R forward	CGTAGTGACAGAGAGGCAGCAGATGTTG
K140R reverse	GGTTGTAGACGACGGAGAGACAGTGATG
K180R forward	AACTACAAAACCCTCAGGAGCCAAGGAGACATGC
K180R reverse	GTACAGAGGAACCGAGGACTCCCAAAACATCAAC

Supplementary Table S2. Gene expression primer.

Human_CXCL2_forward	TGATTTCACAGTGTGTGGTCAAC
Human_CXCL2_reverse	TCTCTGCTCTAACACAGAGGG
Human_CXCL5_forward	AGCGCGTTGCGTTTGTTTAC
Human_CXCL5_reverse	TGGCGAACACTTGCAGATTAC
Human_CXCL8_forward	AAGGTGCAGTTTTGCCAAGG
Human_CXCL8_reverse	CCCAGTTTTCCTTGGGGTCC
Human_LCN2_forward	AGAGCTACAATGTCACCTCCG
Human_LCN2_reverse	TTAATGTTGCCCAGCGTGAAC
Human_IL1B_forward	TCAGCCAATCTTCATTGCTCAAG
Human_IL1B_reverse	GGTCGGAGATTCGTAGCTGG
Human_NFKBIZ_forward	ACACCCACAAACCAACTCTGG
Human_NFKBIZ_reverse	TGCTGAACACTGGAGGAAGTC
Human_NFKBIA_forward	AAGTGATCCGCCAGGTGAAG
Human_NFKBIA_reverse	CTCACAGGCAAGGTGTAGGG
Human_TNF_forward	CAAGGACAGCAGAGGACCAG
Human_TNF_reverse	CCG GATCATGCTTTCAGTGC
Human_RPL37A_forward	AGATGAAGAGACGAGCTGTGG
Human_ RPL37A _reverse	CTTTACCGTGACAGCGGAAG
Human_CDK4_forward	TCTCGAGGCCAGTCATCCTC
Human_CDK4_reverse	GCAGTCCACATATGCAACACC
Human_CDK6_forward	GGTACAGAGCACCCGAAGTC
Human_CDK6_reverse	CTCCTGGGAGTCCAATCACG
Human_EZH2_forward	CTGCTTCCTACATCGTAAGTGC
Human_EZH2_reverse	GTGAGAGCAGCAGCAAACTC
Human_CCND2_forward	AGCTGTGCATTTACACCGAC
Human_CCND2_reverse	CATGCTTGCGGATCAGAGAC
Human_CCND3_forward	ACTGGCTCTGTTCGGATGC
Human_CCND3_reverse	AGCGCTGCTCCTCACATAC
Human_RELA_forward	AGGCTATCAGTCAGCGCATC

Human_RELA_reverse	AGCATTCAGGTCGTAGTCCC
Mouse_Cxcl2_forward	CGCCCAGACAGAAGTCATAGC
Mouse_Cxcl2_reverse	CTTTGGTTCTTCCGTTGAGGG
Mouse_Cxcl5_forward	CCCTACGGTGGAAGTCATAGC
Mouse_Cxcl5_reverse	GAACACTGGCCGTTCTTTCC
Mouse_Lcn2_forward	AATGTCACCTCCATCCTGGTC
Mouse_Lcn2_reverse	ACTGGTTGTAGTCCGTGGTG
Mouse_Il1b_forward	AGCTGAAAGCTCTCCACCTC
Mouse_Il1b_reverse	GCTTGGGATCCACACTCTCC
Mouse_Nfkbiz_forward	AACTCGCCAAGAGACCAGTG
Mouse_Nfkbiz_reverse	AGAGCCACTGACTTGGAACG
Mouse_Il1f6_forward	GCCTGTTCTGCACAAAGGATG
Mouse_Il1f6_reverse	ACAGCGATGAACCAACCAGG
Mouse_Il1f9_forward	GTCAGCGTGACTATCCTCCC
Mouse_Il1f9_reverse	TGGCTTCATTGGCTCAGGG
Mouse_Il23a_forward	CAGCTCTCTCGGAATCTCTGC
Mouse_Il23a_reverse	TGTCCTTGAGTCCTTGTGGG
Mouse_Il17a_forward	GCCCTCAGACTACCTCAACC
Mouse_Il17a_reverse	TTCCCTCCGCATTGACACAG
Mouse_Actin_forward	AGGAGTACGATGAGTCCGGC
Mouse_Actin_reverse	GGTGTAAAACGCAGCTCAGTA
Mouse _Ccnd2_forward	CTCACGTGTGATGCCCTGAC
Mouse _ Ccnd2_reverse	TGTTCAGCAGCAGAGCTTCG
Mouse _ Ccnd3_forward	TTGCATCTATACGGACCAGGC
Mouse _ Ccnd3_reverse	GAGACAGGCGGTGCAGAATC
Mouse_Ezh2_forward	ACTGCTTCCTACATCCCTTCC
Mouse_Ezh2_reverse	ACGCTCAGCAGTAAGAGCAG

Acknowledgements

At this point, I would like to thank everyone who supported me during my Ph.D. thesis.

First, I would like to thank my doctoral supervisor Prof. Dr. Klaus Schulze-Osthoff for the opportunity to complete this thesis under his supervision.

For her advice and guidance of my Ph.D. I would like specially to thank Dr. Daniela Kramer. In particular, the constructive exchange and the frequent discussions on a professional and personal level have always been a great help to me and have always influenced and encouraged me positively. Additionally, I would also like to thank you for proofreading my thesis. This thesis would not have been possible in its current form without your support. Thank you so much!

Special thanks also to Claudia Resch, who helped me enormously with thousands of histological sections and stains and patiently endured several new attempts at embedding.

Furthermore, I would like to thank Stephan Hailfinger, who was always on hand with advice and action, and the entire working group for the friendly working atmosphere, many valuable suggestions, and constant willingness to help that have contributed significantly to the success of this work.

I wish to thank all my co-authors for their help and commitment to the projects.

I would also like to thank my family, friends, and fellow students who also supported and motivated me in difficult times. This support has contributed to the success of this thesis.

Contributions

"IκBζ is a key transcriptional regulator of IL-36–driven psoriasis-related gene expression in keratinocytes " Proceedings of the National Academy of Sciences USA 2018;115(40): 10088-93.

Project planning of this publication was started by Daniela Kramer. The RNAseq results were obtained by Daniela Kramer and the bioinformatic analysis by André Hennig. The intradermal application of IL-36 in mice was performed by Daniela Kramer. The histology was performed by Claudia Resch. Stephan Hailfinger and Klaus Schulze-Osthoff supported the project with advice in critical points. The manuscript was written by Daniela Kramer and revised by Stephan Hailfinger, Klaus Schulze-Osthoff and me.

" The CDK4/6-EZH2 pathway is a potential therapeutic target for psoriasis" J Clin Invest. 2020;130(11):5765-5781.

The aim of research was pointed out by Daniela Kramer and me. The histology was performed by Claudia Resch. The manuscript was written by Daniela Kramer under revision of Matthias Dobbelstein, Stephan Hailfinger, Klaus Schulze-Osthoff and me.